NASA TECHNICAL MEMORANDUM

NASA TM-78267

SKYLAB REACTIVATION MISSION REPORT

By Systems Analysis and Integration Laboratory, Science and Engineering Directorate

March 1980

NASA

George C. Marshall Space Flight Center
Marshall Space Flight Center, Alabama

TECHNICAL REPORT STANDARD TITLE PAGE

1. REPORT NO.	2. GOVERNMENT ACCESSION NO.	3. RECIPIENT'S CATALOG NO.
NASA TM-78267		

4. TITLE AND SUBTITLE	5. REPORT DATE
Skylab Reactivation Mission Report	March 1980
	6. PERFORMING ORGANIZATION CODE
7. AUTHOR(S)	8. PERFORMING ORGANIZATION REPORT #
William B. Chubb, Editor	
9. PERFORMING ORGANIZATION NAME AND ADDRESS	10. WORK UNIT NO.
George C. Marshall Space Flight Center Marshall Space Flight Center, Alabama 35812	11. CONTRACT OR GRANT NO.
	13. TYPE OF REPORT & PERIOD COVERED
12. SPONSORING AGENCY NAME AND ADDRESS	Technical Memorandum
National Aeronautics and Space Administration Washington, DC 20546	14. SPONSORING AGENCY CODE

15. SUPPLEMENTARY NOTES

Prepared by the Systems Analysis and Integration Laboratory, Science and Engineering Directorate.

16. ABSTRACT

On July 11, 1979, Skylab impacted the Earth's surface. The debris dispersion area stretched from the South Eastern Indian Ocean across a sparsely populated section of Western Australia. This report discusses in some detail the events leading to the reentry of Skylab, together with a final assessment of the Skylab debris impact footprint. Also included are detailed evaluations of the various Skylab systems that were reactivated when control of Skylab was regained in mid-1978 after having been powered down since February 4, 1974.

17. KEY WORDS	18. DISTRIBUTION STATEMENT
	Unclassified-Unlimited

19. SECURITY CLASSIF. (of this report)	20. SECURITY CLASSIF. (of this page)	21. NO. OF PAGES	22. PRICE
Unclassified	Unclassified	387	NTIS

ACKNOWLEDGEMENT

This report was prepared from information, analysis and reports provided by government and industry sources. Significant contributions were made by Systems Dynamics Laboratory, Systems Analysis and Integration Laboratory, Electronics and Control Laboratory, Structures and Propulsion Laboratory and the Space Science Laboratory all of the George C. Marshall Space Flight Center; and the IBM Corporation and the McDonnell Douglas Corporation.

SKYLAB REACTIVATION MISSION REPORT

APPROVAL: Herman E. Thomason

Dr. Herman Thomason
Skylab Reactivation Project Engineer
Systems Analysis and Integration Laboratory
Marshall Space Flight Center

TABLE OF CONTENTS

LIST OF FIGURES

LIST of TABLES

SKYLAB REACTIVATION MISSION REPORT

SECTION 1

MISSION SUMMARY

1.Ø INTRODUCTION

On July 11, 1979, Skylab impacted the Earth surface. The debris dispersion area stretched from the South Eastern Indian Ocean across a sparsely populated section of Western Australia. This report discusses in some detail the events leading to the reentry of Skylab together with a final assessment of the Skylab debris impact footprint.

1.1 Background

On February 9, 1974, Skylab systems were configured for a final power down and Skylab was deactivated. Prediction of solar cycle 21 activity, the solar cycle predicted to begin in 1977, indicated that the final attitude in which Skylab was left, the gravity-gradient attitude, would result in a potential storage period of 8 to 1Ø years. However, in the fall of 1977 it was determined that Skylab had left the gravity gradient attitude and was experiencing an increased orbital decay rate. This was a result of greater than predicted solar activity at the beginning of solar cycle 21. This increased activity increased the drag forces on the vehicle. Skylab was now predicted to reenter the Earth's atmosphere in late 1978 or early 1979 unless something was done to reduce the drag forces acting upon it. It was necessary to make a decision to either accept an early uncontrolled reentry of Skylab or to attempt to actively control Skylab in a lower drag attitude thereby extending its orbital lifetime until a Shuttle mission could effect a boost or deorbit maneuver with Skylab.

In order to verify what options could be accomplished with the on-board Skylab systems, a small team of NASA engineers went to the Bermuda Ground Station to establish communications and interrogate Skylab systems. On March 6, 1978, the Airlock Module (AM) command and telemetry (TM) systems were commanded on from the Bermuda Ground Station. The reception of the AM TM carrier at Bermuda was proof that the on-board AM systems had

responded to the commands. For the next several days, the AM electrical power system was properly configured and the AM batteries charged whenever the simultaneous conditions of ground station coverage at Bermuda and solar energy availability permitted. Subsequently AM power was transferred to the Apollo Telescope Mount (ATM) systems and the operational status of the ATM systems was determined. On March 11, 1978, power was applied to the ATM Attitude and Pointing Control System (APCS) bus which in turn supplied power to the primary Apollo Telescope Mount Digital Computer (ATMDC)/Workshop Computer Interface Unit (WCIU). Power was maintained on the APCS bus for approximately 5 minutes and the receipt of ATMDC telemetry data at Bermuda was confirmed. The receipt of this data indicated that the primary ATMDC/WCIU hardware and attendant software were operational and cycling. On March 13, 1978, engineers concluded the interrogation test on Skylab. The resulting data indicated no discernible degradation of the Skylab systems during its 4 years of orbital storage. Aided with this data, the knowledge that Skylab was in an unstable tumble prompted investigation into schemes which might extend the orbital lifetime of Skylab.

The first option investigated was to use the on-board Thruster Attitude Control System (TACS) to maintain a quasi-stable tumble of Skylab. However, it was soon determined that this option would not extend Skylab lifetime sufficiently to correspond to the operational readiness of the Space Shuttle for a possible reboost or deorbit mission. The only alternative left was to reactivate and continuously control the Skylab in a minimun drag attitude. In order to accomplish this the End On Velocity Vector (EOVV) minimum drag attitude control scheme was developed and used after the initial Skylab reactivation on June 11, 1978. Skylab remained in this low drag EOVV control orientation until January 25, 1979, when the vehicle was commanded to a high drag Solar Inertial (SI) orientation.

With the active control of Skylab in mid-1978 in a low-drag attitude to minimize its rate of decay, it was decided to accelerate the development of an orbital retrieval system that might be accommodated on an early flight of the Space Shuttle, thus increasing chances of rendezvousing with Skylab. The rate of orbital decay, however, continued to increase due to increased solar activity. Skylab's on-board systems also showed signs of deterioration and there were increasing concerns over the Space Shuttle's schedule. For these reasons, the concept of Skylab recovery was terminated in December 1978. At that time, it was decided to reorient and control the vehicle in a solar inertial attitude which was the normal vehicle orientation for original Skylab mission operations.

As Skylab's altitude decreased, the magnitude of the aerodynamic torques on the vehicle increased. Studies indicated that vehicle control in the solar inertial orientation would no longer be possible below about 140 n.m. due to these increased aerodynamic torques and the limited control authority available from the vehicle Control Moment Gyros (CMGs). Aerodynamicists and control engineers at the Marshall Space Flight Center (MSFC), while investigating vehicle orientations which produced minimal disturbance torques on the vehicle, found certain orientations where the summation of these disturbance torques was zero. These attitudes were called Torque Equilibrium Attitudes (TEA). On June 20, 1979, with the vehicle at approximately 142 n.m., Skylab was reoriented and controlled to a high drag TEA attitude. It was controlled in this attitude until just prior to reentry on July 11, 1979, when the vehicle was commanded to tumble in order to reduce its drag and decrease the possibility of impacting high population density centers.

1.2 Purpose

The purpose of this report is to review the Skylab Reactivation mission and associated Skylab Subsystem Operations from the time it was decided to interrogate Skylab Systems in March of 1978 until impact July 11, 1979.

SECTION 2

MISSION DESCRIPTION

2.0 INTRODUCTION

This section contains a description and summary of the most significant events in the Skylab Reactivation Mission from the interrogation tests in March, 1978 until Skylab reentry on July 11, 1979. It gives a brief description of the operating modes, significant flight events and Skylab attitude control maintenance considerations.

2.1 OPERATING MODES

The Skylab vehicle was maintained in several different operating modes during the Skylab Reactivation Mission. The Solar Inertial (SI) mode had been a part of the first ATMDC flight program and was the major operating mode during the original mission. When initial plans were made to extend the orbital lifetime of Skylab, the End-On-Velocity-Vector (EOVV) Mode was developed because of its minimum drag characteristics. After plans for a reboost/deorbit mission were abandoned, the Torque Equilibrium Attitude (TEA) mode was developed to control the vehicle as the orbit decayed toward reentry. Only the SI and TEA Modes were used for control subsequent to January 25, 1979. A brief description of the EOVV, SI and TEA control modes follows.

2.1.1 End-On-Velocity-Vector (EOVV) Mode

The EOVV mode was a minimum drag attitude with the relatively small surface areas of the front or back ends of Skylab being pointed approximately along the velocity vector. This mode was a modification of the Z Local Vertical (ZLV) mode (vehicle "Z" axis along the local vertical) that was used during the original Skylab Mission. In the EOVV mode, the vehicle coordinate axes were offset slightly from the ZLV axes to align the vehicle principle axes with the ZLV axes. The vehicle was then rolled such that its solar arrays pointed toward the sun near orbital noon for maximum power collection and attitude reference updating. Desaturation of CMG momentum was done with gravity gradient torques and was continuously active around the orbit.

There were two subsets of the EOVV mode, EOVV A and EOVV B. The EOVV B mode can be thought of as a backward EOVV A mode. The EOVV A mode had the Skylab Command Module docking port pointed along the velocity vector while the EOVV B mode had the aft end of the workshop pointed along the velocity vector. The EOVV B mode was developed to prolong the life of CMG #2 by allowing maximum solar impingement on CMG #2 spin bearings for negative sun angles. For the same reason, EOVV A was utilized when the vehicle experienced positive solar angles.

The EOVV mode was used in the first part of the Skylab Reactivation Mission to reduce the vehicle rate of descent as much as possible. It was hoped that the orbital life of Skylab could be extended until a reboost/deorbit mission could be launched by the Space Shuttle. The effect of the EOVV mode on the descent rate is illustrated by the altitude profile in Figure 2-1. There was a noticeable slowing down of the Skylab fall when EOVV was entered June 11, 1978. It was estimated that if Skylab had remained in EOVV that reentry could have been delayed until at least April of 1980.

2.1.2 Solar Inertial Mode (SI)

In the SI Mode (Figure 2-2), the Skylab solar arrays were maintained perpendicular to the sun during the daylight portion of the orbit for maximum power collection. During the night portion of the orbit, momemtum desaturation maneuvers were performed to decrease any undesired accumulation of CMG momentum. This mode had been used extensively and was the major operating mode of the original Skylab mission. The SI Mode was a minimum maintenance mode of operation with very little commanding required under normal conditions. Late in the reactivation mission SI maintenance increased due to large aerodynamic torques encountered at the lower altitudes.

The SI Mode was used after January 25, 1979, primarily as a low maintenance holding pattern mode for vehicle control while preparations were made for entering the TEA control mode.

The atmospheric drag on the vehicle in the SI Mode changed as the vehicle revolved around the orbit from minimum drag at orbital noon and midnight to maximum drag at the sunset/sunrise terminators. This placed the average drag on the vehicle approximately midway between minimum and maximum. The effect of this drag can be seen in the altitude profile of Figure 2-1. A noticeable increase in the descent rate was observed when the SI Mode was entered on January 25, 1979.

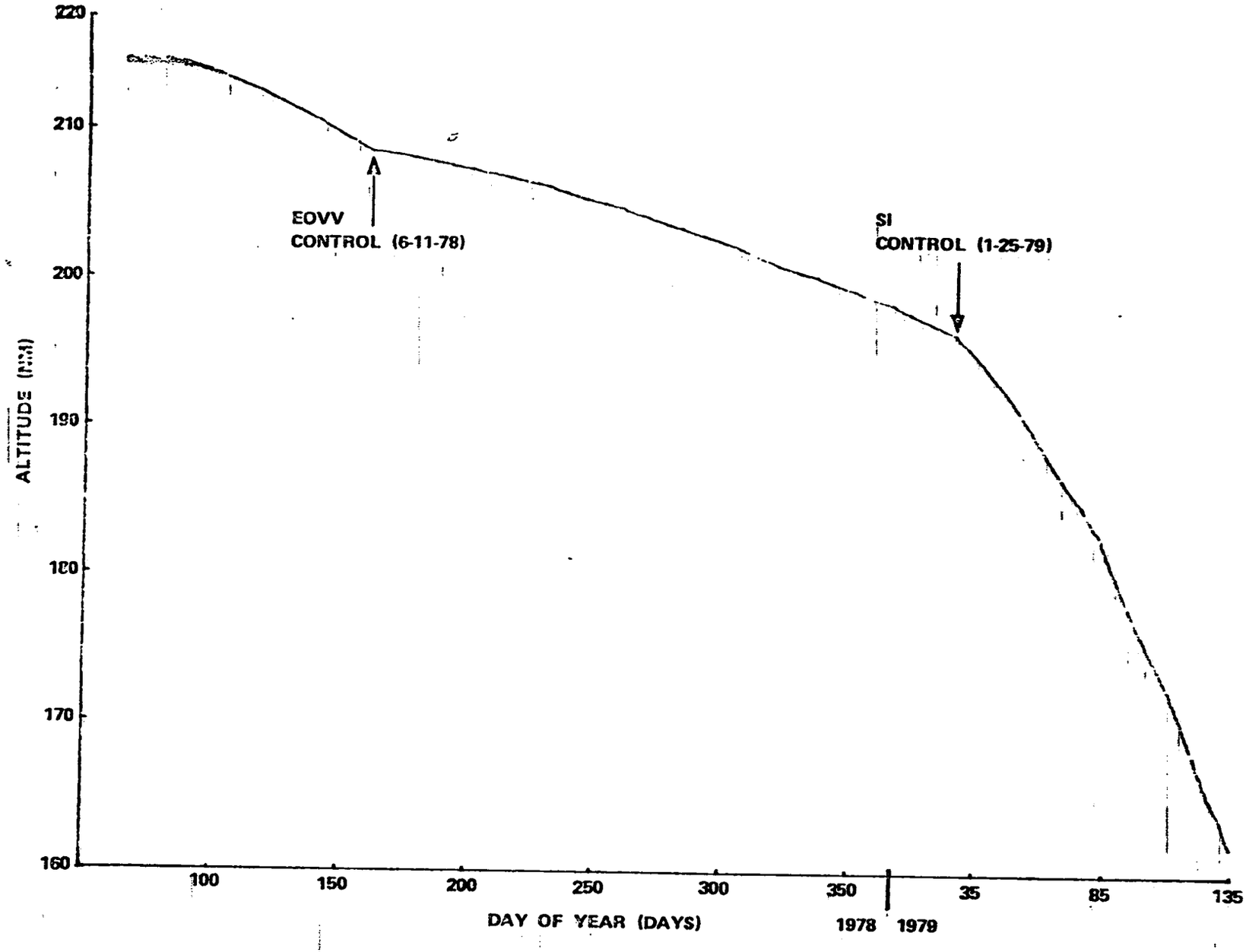

FIGURE 2-1 SKYLAB ALTITUDE HISTORY FROM MARCH, 1978 TO MAY, 1979

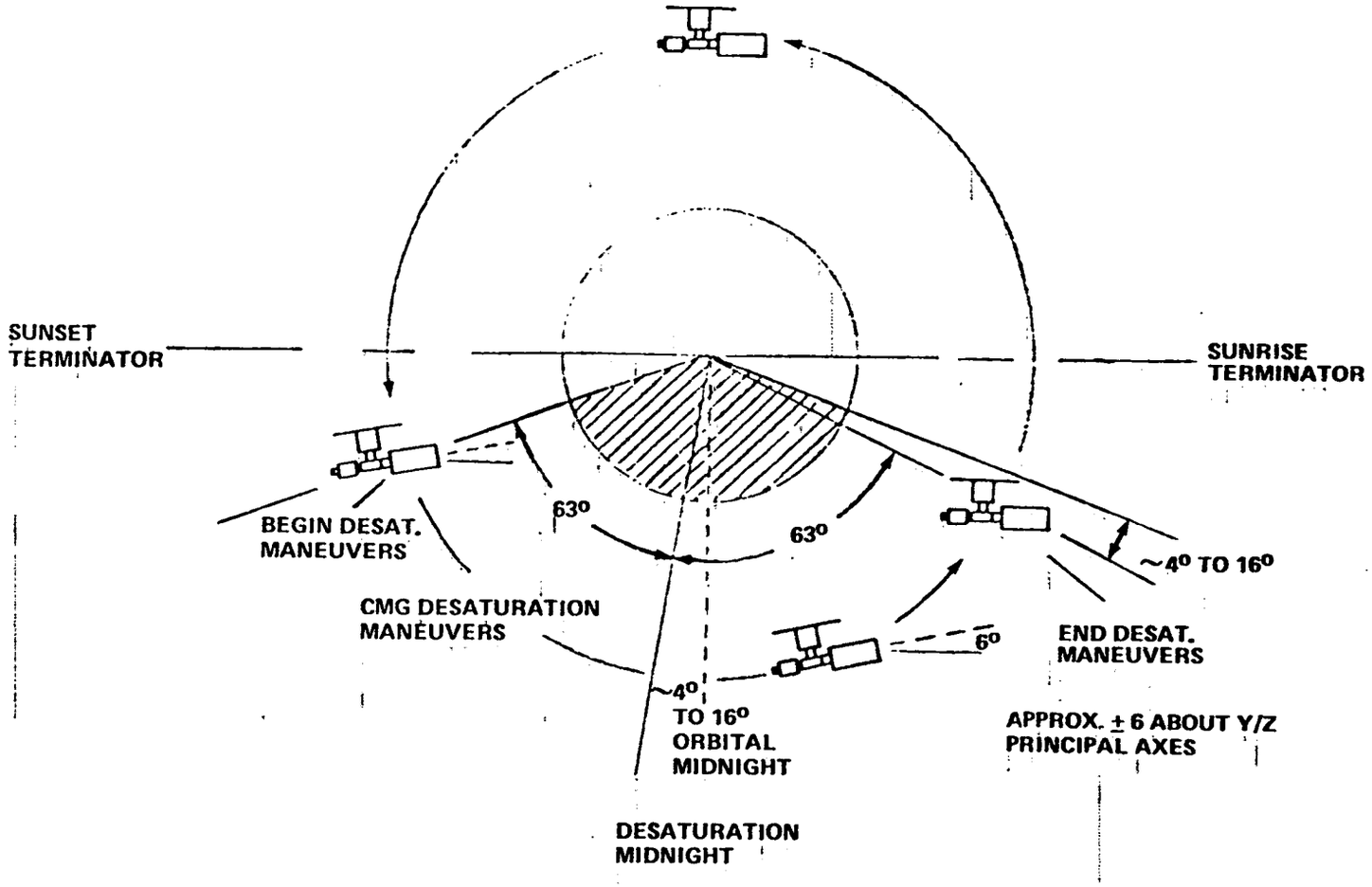

FIGURE 2-2 SOLAR INERTIAL ORIENTATION

2.1.3 Torque Equilibrium Attitude (TEA)

TEA Control was a mode in which gravity gradient torques counterbalanced aerodynamic torques. This was the only mode that could maintain attitude control below altitudes of about 140 n.m. There were many TEA control attitudes that were identified for the Skylab vehicle but only a few were useable because of solar power collection constraints. These attitudes also existed only over certain ranges of altitudes so that procedures for acquiring a particular TEA attitude had to consider the vehicle altitude and predicted rates of descent as well as total vehicle power generating capability in the selected attitude.

There were two TEA attitudes that were available for control during the final days of the reactivation mission. One was T121P (Figure 2-3) in which the longitudinal axis of the vehicle was nearly perpendicular to the orbital plane resulting in a high aerodynamic drag on the vehicle. This was the TEA attitude that was actually used from June 20, 1979 until the vehicle was tumbled just prior to reentry on July 11, 1979. The other attitude available was T275 (Figure 2-4) which was similar to an EOVV attitude (the long axis of the vehicle lying along the velocity vector) and had a low aerodynamic drag. If necessary, it was planned to shift the reentry orbit of Skylab by maneuvering from the T121P to the T275 attitude thus decreasing the drag on the vehicle and shifting the predicted Skylab reentry point to a later orbit.

The TEA Mode was a modification of the original Skylab Z axis (ATM solar viewing axis) along the local vertical (ZLV) mode. The TEA Mode was activated by first commanding an offset ZLV maneuver to the desired TEA attitude. If an exact TEA attitude was not obtained, the vehicle would experience small aerodynamic and gravity gradient torques. The momentum state of the CMG's would gradually approach saturation as the CMG's generated torques to keep the vehicle in control while under the influence of these external disturbance torques. Skylab computer logic sensing this unbalanced torque environment would command the vehicle to a different attitude from that predicted based on its update of a revised torque equilibrium attitude. CMG desaturation was accomplished by maneuvering the vehicle to an attitude near the newly estimated torque equilibrium position such that the external torque field acted on the vehicle in a manner to desaturate the CMG's moving them away from their momentum saturation limit. The desaturation maneuvers were computed every 300 seconds using a 3 by 3 matrix (referred to as the SLOPE MATRIX) which related momentum errors to attitude errors about the TEA attitude.

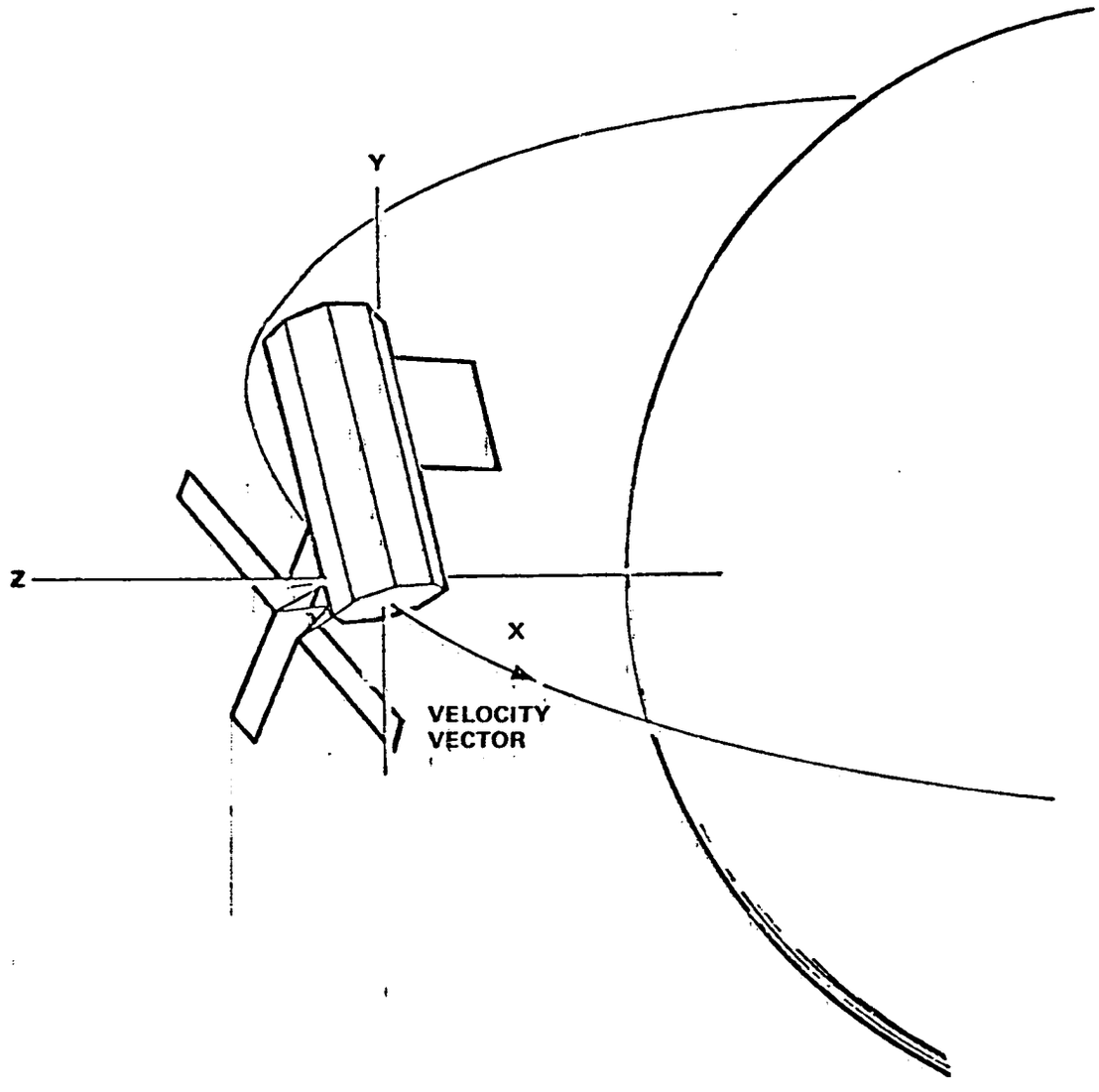

FIGURE 2-3 T121 TORQUE EQUILIBRIUM ATTITUDE (TEA 121 P)

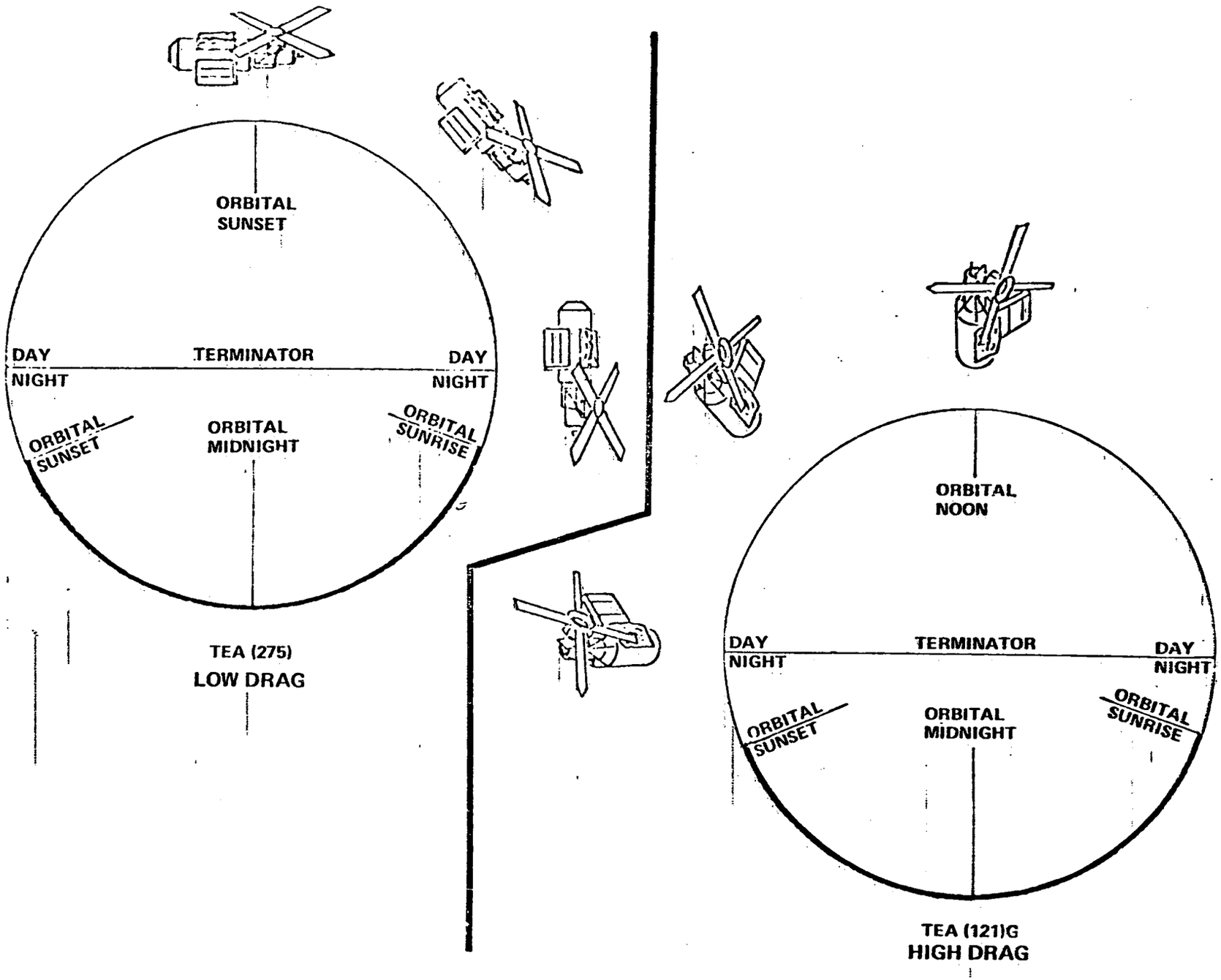

FIGURE 2-4 TEA (275) AND (121)G TORQUE EQUILIBRIUM ATTITUDE

Since T121P was a near maximum drag attitude and because the atmosphere was rapidly becoming more dense, the Skylab descent rate increased significantly after TEA acquisition on June 20, 1979. This is shown in Figure 2-5 by the altitude profile for the later part of the reactivation mission.

2.2 SIGNIFICANT FLIGHT EVENTS

The significant Skylab flight events are listed in Table 2-1. The initial entry in this table, the March interrogation test on March 11, 1978, is considered the beginning of the Skylab Reactivation Mission and the last event, Skylab reentry on July 11, 1979 is the end of the mission. These events are also shown on Figure 2-6 which illustrate the time spent in each of the various operating modes during the Skylab Reactivation Mission lifetime.

2.2.1 March Interrogation Test

In March, 1978 a team of NASA engineers went to the STDN ground station at Bermuda with the intent of establishing the operational status of Skylab systems and, additionally, obtaining data which could help determine the vehicle attitude motion. The STDN ground stations command uplink capability, having been changed since the primary mission, was no longer directly compatible with the Skylab command decoder. A work-around was developed whereby a limited number of predetermined Skylab commands were pre-assembled and only these commands were available for uplink to Skylab. This command capability limitation remained throughout the Skylab Reactivation Mission.

On March 6, 1978 at 21:50 GMT, communication with the Skylab Airlock Module (AM) command and telemetry systems was reestablished. After 2.5 minutes of operation, a loss of signal was observed which was later attributed to the vehicle rotating its transmitting antenna out of the line of sight of the ground station. Upon acquiring the signal the second time, a loss of modulation on the AM telemetry downlink had occurred. Between March 6 and March 10, trouble-shooting tasks on the AM telemetry system were successfully performed and charging of the AM batteries was initiated.

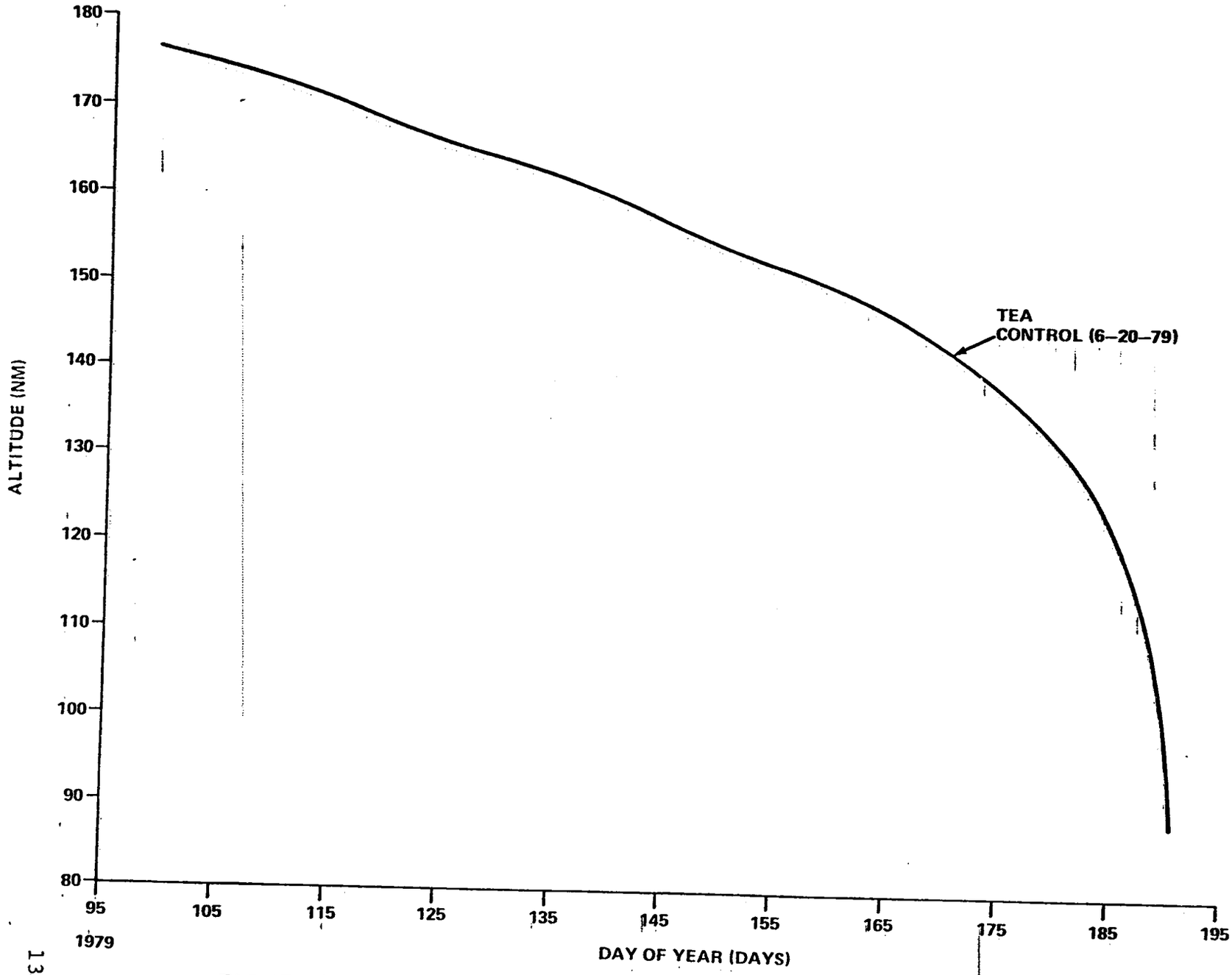

FIGURE 2-5 SKYLAB ALTITUDE HISTORY FROM APRIL, 1979 TO JULY, 1979

Table 2-1. Significant Flight Events of the Skylab Reactivation Mission

DATE	EVENT
March 11, 1978	Initial ATMDC Interrogation
May 31, 1978	"P" patch implemented (FF80 buffers 1-3)
June 1-5, 1978	"Q" patch implemented (FF81 buffers 1-8)
June 9, 1978	Initial solar inertial acquisition
June 11, 1978	Initial EOVV acquisition
June 11, 1978	FF81 buffer 9 implemented
June 26, 1978	FF81 buffer 10 implemented
June 28, 1978	Retreat to solar inertial
July 6, 1978	Second EOVV acquisition
July 9, 1978	Loss of attitude reference
July 19-20, 1978	SI acquisition from unknown attitude
July 24, 1978	FF81 buffer 10A implemented
July 25, 1978	Third EOVV acquisition
August 12, 1978	FF81 buffer 11 implemented
September 8, 1978	FF81 buffer 12 implemented
September 11, 1978	FF81 buffer 13 implemented
September 20, 1978	FF81 buffer 14 implemented
November 3, 1978	FF81 buffer 15 implemented
November 4, 1978	EOVV A to EOVV B acquisition
December 3, 1978	FF81 buffer 16 implemented
December 19, 1978	Decision made to discontinue Skylab reboost/deorbit plans
January 25, 1979	EOVV B to SI acquisition
January 30, 1979	FF81 buffer 17 implemented
May 19-20, 1979	TEA Control Patch implemented (FF81 buffers 18-22)
June 20, 1979	TEA Control Acquisition from SI
June 22, 1979	FF81 Buffer 23 implemented
June 24, 1979	TEA Control Reacquisition
July 11, 1979	Reentry

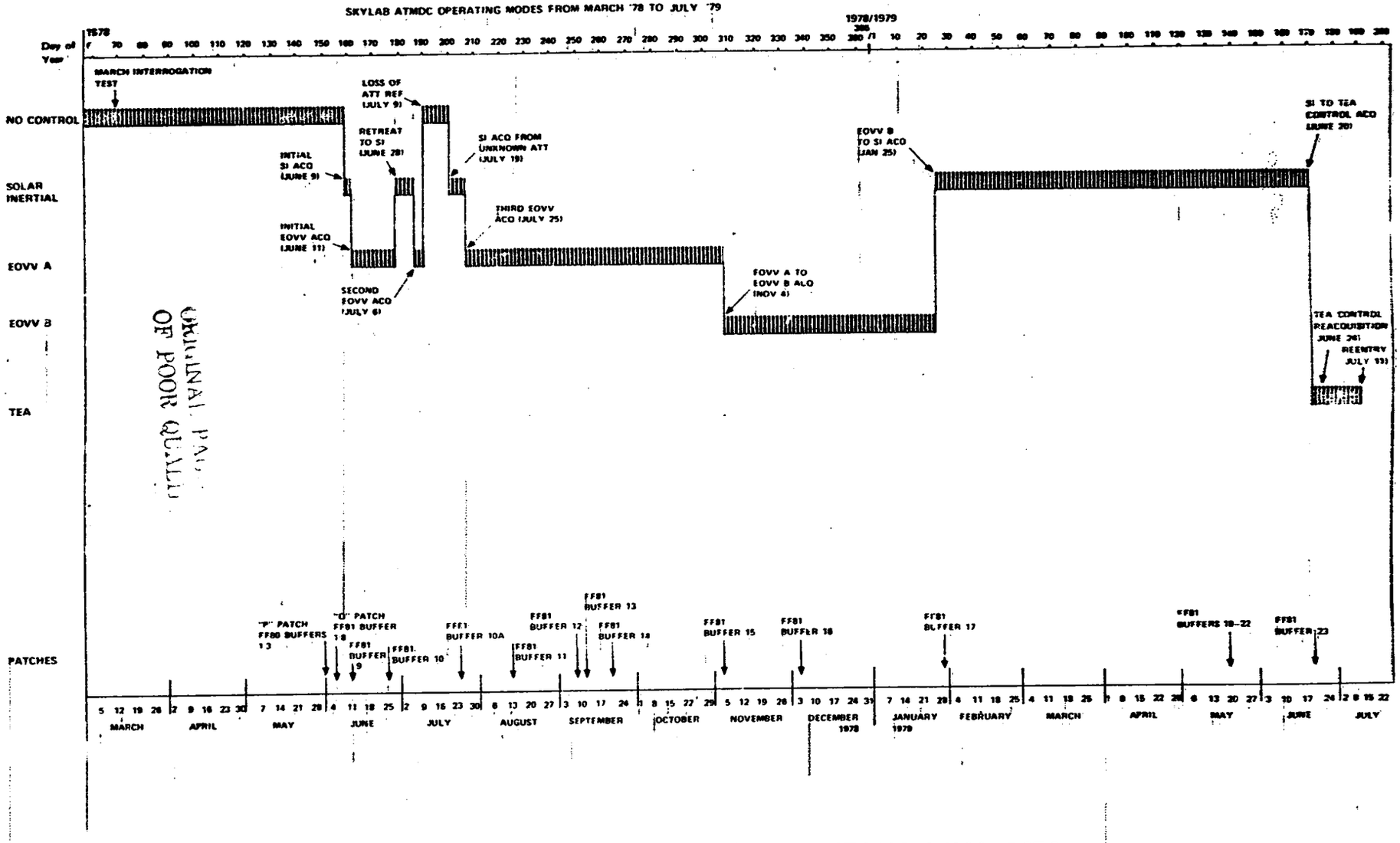

FIGURE 2-6 SKYLAB ATMDC OPERATION MODES FROM MARCH , 1978 TO JULY, 1979

An operational configuration of the AM command, telemetry and electrical power systems was established for the AM by March 10, 1978. Either an electrical short in an AM TM measurement group or a failure in the -24 volt side of DC-DC Converter #1 caused the loss of AM TM modulation. AM TM modulation was established using DC-DC Converter #2.

On March 11, 1978 at 20:34 GMT power was transferred from the AM power system to the ATM power system. The ATM command and telemetry systems were successfully commanded on at 20:35 GMT thereby establishing a two-way communication link between the ground station and the ATM systems. The stage was now set to interrogate the operational status of the Skylab APCS.

At 20:36 GMT on March 11, 1978, power was transferred to the APCS bus and the receipt of ATMDC TM data at Bermuda confirmed that the ATMDC was cycling. ATMDC TM data indicated that the ATMDC and WCIU internal temperatures at power on as measured by thermistors were -15.9°C and -26.2°C, respectively. Power was maintained on the APCS bus for approximately 5 minutes and no anomalies were observed. Subsequent analysis of the ATMDC TM data indicated the following:

1) Both acquisition sun sensors operational

2) Rate gyro Y2 failed

3) Rate gyros X1 and X2 saturated (Ø>1.Ø deg/sec)

4) Rate gyros Y1,Z1,Z2 operational

5) ATMDC flight software parameters, discrete inputs (DI's) and discrete outputs (DO's) were as expected.

ATMDC data indicated 5 of the 6 "six-pack" rate gyros were operational. The saturated X1, X2 rate gyros confirmed earlier predictions that the vehicle was spinning about the X axis greater than 1 degree/second (1.7 deg/sec predicted). Insufficient power and ground station coverage did not permit proper warm up of the CMG bearings therefore the CMG system was not interrogated. The TACS system was not excercised because of the limited supply of nitrogen gas and the desire not to perturb the attitude motion of Skylab which was becoming somewhat predictable. In summary, the Skylab APCS appeared to be operational.

On March 13, 1978 at 20:19 GMT, Skylab systems were configured for shut-down with the objective of reestablishing communications with Skylab at a later date. The interrogation

tests had been highly successful and the operational status of on-board systems exceeded all expectations.

2.2.2 Initial Attitude Control Acquisition

On June 9, 1978, attitude control of Skylab was acquired for the first time since Skylab had been powered down in February, 1974. This section describes the events that occurred prior to and during this attitude control acquisition.

2.2.2.1 Preparation

Between March and June of 1978, the primary ATMDC onboard Skylab was periodically turned on to monitor the APCS rate gyros to determine the vehicle rates. The X axis (roll) rate gyro input was saturated which indicated that Skylab's roll rate was greater than one degree per second. NORAD determined that the X axis was near perpendicular to the orbital plane inclining about 3½ degrees. By monitoring the battery charging cycles, it was determined that the roll rate was approximately 1.7 degrees per second. The Y and Z axes rates (pitch and yaw) together with NORAD data and battery charging measurements showed that the vehicle motion was in a type of wobble about the X axis indicating a conical motion, see Figure 2-7. Using this information, a plan was developed to obtain control of the Skylab.

The first task that had to be accomplished was to charge Skylab's AM and ATM batteries. This was accomplished by NASA flight controllers over a period of weeks. After charging the batteries, the ATMDC was powered on in late May, 1978 and the primary ATMDC flight program was modified by uplinking eleven (11) memory load buffers using the Skylab DCS. The first three (3) buffers updated the flight program from FF5Ø to FF8Ø and the remaining eight (8) buffers implemented the new end-on-velocity-vector (EOVV) maneuver capability. Updating the ATMDC with the EOVV logic was completed on June 5, 1978. On June 6, the CMG #2 and #3 bearing heaters were turned on to warm up the bearings in preparation for CMG wheel spin-up on June 8, 1978. Prior to turning on the CMGs, they were caged such that the CMG torque experienced during spin-up would slow the vehicle roll

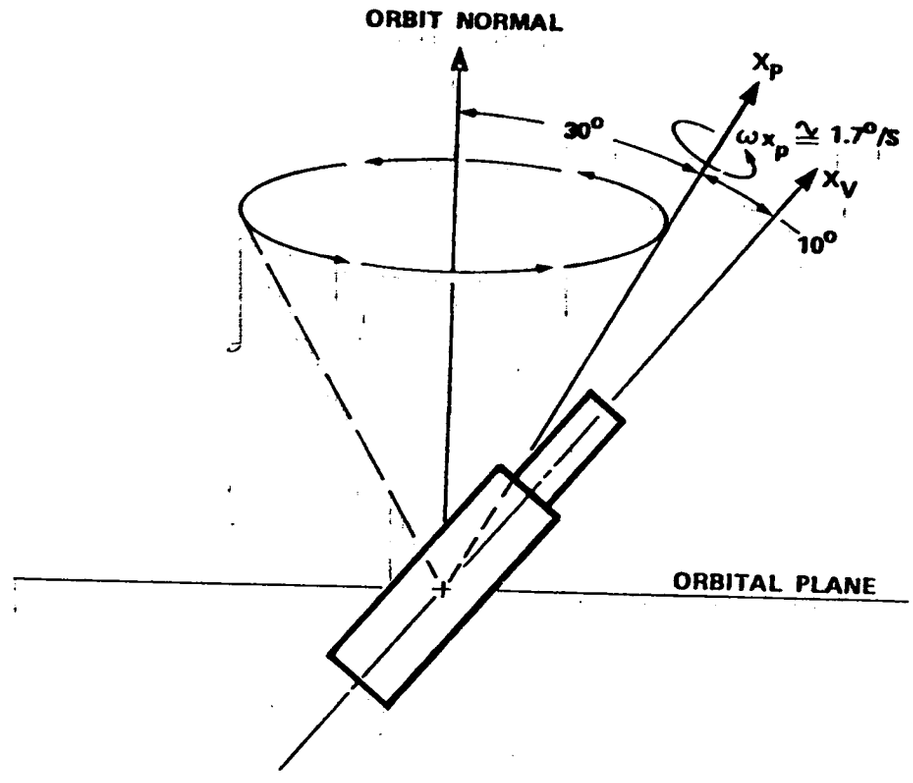

FIGURE 2-7 VEHICLE MOTION PRIOR TO SKYLAB REACTIVATION

rate and thereby reduce the TACS impulse required for attitude control acquisition. After approximately 11 hours the CMGs were up to the nominal spin rate of 8800 rpm.

Prior to solar inertial acquisition, the ATMDC flight program was configured as follows:

1) Software switchover was inhibited

2) Rate gyros 1 & 3 were selected for control in each axis with RG redundancy management inhibited

3) VREF redundancy management was inhibited

4) CMG redundancy management was inhibited

5) Sun sensor averaging was enabled

6) Sun sensor redundancy management was inhibited

7) Computer timing for navigation was selected

Everything was now ready for acquiring attitude control of Skylab. All pertinent commands issued to the APCS system during the initial attitude control acquisition phase of the reactivation mission are shown in Table 2-2. These commands cover the period starting from the initial preparation on May 30, 1978 until after EOVV was determined to be performing correctly and TACS control was inhibited on June 14, 1978.

2.2.2.2 Solar Inertial Acquisition

The target date for the initial solar inertial acquisition was selected to be one day prior to when the sun angle relative to the orbit plane (beta angle) passed through zero degrees. The procedure that was developed called for the EOVV acquisition to take place the day following SI acquisition. From a control standpoint, a zero beta angle was desirable because this was when the ZLV attitude was nearly aligned with the EOVV attitude. This enabled EOVV to be initiated with a minimum of commanding and maneuvering thereby simplifying the procedure. The sun passed through zero beta approximately once every three to four weeks, see Figure 2-8. The June 10 date was considered the earliest zero beta day for all preparations to be complete.

The stage was therefore set to capture the vehicle on June 9, 1978. A total of 19 station passes using Bermuda, Madrid and Goldstone stations--the only stations configured for Skylab systems were scheduled to occur over a period of approximately 16 hours and eleven Skylab orbits, see Figure 2-9. On the first pass the primary computer was powered on at 4:09:15 GMT and a navigation update was issued at 4:12:30 GMT. This navigation update had an error of 15 seconds in the time of midnight because the computer had been powered up 15 seconds later than scheduled. This error had negligible effect on the performance of the vehicle and was considered insignificant.

On the second orbit of June 9, TACS control was enabled and vehicle data was monitored for a suitable opportunity to command solar inertial acquisition. When the ACQSS readings and electrical power measurements showed that the Skylab solar panels were near perpendicular to the sun, the strapdown reference was initialized to (0,0,0,1) and the solar inertial mode was commanded. These commands, issued at 5:46 GMT, placed the vehicle under TACS control and stopped the vehicle rotation rates.

Table 2-2

TIME	SITE	PASS	COMMAND
(May 30, 1978)			
150: 12: 05: 05	BDA	152	Turn on X axis rack rate gyros
150: 12: 05: 19	BDA	152	Turn on Y axis rack rate gyros
150: 12: 08: 27	BDA	152	Select RG 1 and 3 for X axis
150: 12: 08: 57	BDA	152	Inhibit X axis RGRM
150: 12: 09: 26	BDA	152	Select RG 1 and 3 for Y axis
150: 12: 09: 49	BDA	152	Inhibit Y axis RGRM
150: 12: 10: 25	BDA	152	Reset alert discrete outputs
150: 12: 11: 05	BDA	152	Reset caution and warning discrete outputs
150: 13: 41: 28	BDA	154	Turn on Z axis rack rate gyros
150: 13: 43: 15	BDA	154	Select RG 1 and 3 for Z axis
150: 13: 46: 18	BDA	154	Inhibit Z axis RGRM
150: 13: 54: 27	MAD	155	Select standby APCS mode
150: 13: 54: 39	MAD	155	Set TACS thrust = 70 newtons
150: 13: 56: 38	MAD	155	Set TACS pulse width = 320 ms
150: 13: 57: 31	MAD	155	Inhibit X axis SSRM
150: 13: 58: 29	MAD	155	Inhibit Y axis SSRM

TIME	SITE	PASS	COMMAND
150: 13: 59: 22	MAD	155	Select ACQ SS #2 for sun presence
(May 31, 1978)			
151: 09: 42: 34	MAD	160	Implement "P" patch, buffer 1
151: 11: 23: 32	MAD	162	Implement "P" patch, buffer 2
151: 15: 59: 45	BDA	165.5	Implement "P" patch, buffer 3
(June 1, 1978)			
152: 03: 43: 00	MAD	170	Implement FF81 buffer 1
152: 06: 44: 28	BDA	173	Implement FF81 buffer 2
152: 13: 21: 27	BDA	175	Implement FF81 buffer 3
152: 15: 10: 55	MAD	177	Implement FF81 buffer 4
152: 19: 48: 59	BDA	179	Implement FF81 buffer 5
(June 2, 1978)			
153: 07: 22: 08	BDA	184	Implement FF81 buffer 6
153: 14: 12: 49	MAD	186	Implement FF81 buffer 7
(June 5, 1978)			
156: 22: 13: 02	GDS	194	Implement FF81 buffer 8
(June 6, 1978)			
157: 10: 19: 37	MAD	196	Turn on CMG bearing heaters
(June 7, 1978)			
158: 04: 35: 36	MAD	208	Turn on CMGIA heaters
158: 06: 06: 27	MAD	209	T1 patch loaded

TIME	SITE	PASS	COMMAND
158: 06: 07: 56	MAD	209	Telemeter memory load buffer
158: 06: 09: 42	MAD	209	T2 patch loaded
158: 06: 10: 56	MAD	209	Telemeter memory load buffer
(June 8, 1978)			
159: 11: 24: 04	BDA	234	Begin spinning up CMGs
159: 11: 27: 58	BDA	234	Set gimbal rate limit = 1 degree/second
159: 11: 34: 00	MAD	235	CMG cage
(June 9, 1978)			
160: 04: 09: 15	MAD	247	Primary computer turned on
160: 04: 12: 30	MAD	247	Navigation update
160: 04: 12: 52	MAD	247	Set maneuver time = 0
160: 05: 45: 11	MAD	248	Enable TACS
160: 05: 45: 49	MAD	248	Select rate gyro 1 and 3 in Z axis
160: 05: 46: 02	MAD	248	Inhibit Z axis rate gyro redundancy management
160: 05: 46: 15	MAD	248	Initialize strapdown, select solar inertial mode (Begin vehicle spin down)
160: 07: 14: 55	BDA	248.5	Set maneuver time = 4 minutes
160: 07: 15: 44	BDA	248.5	Select attitude hold TACS mode

TIME	SITE	PASS	COMMAND
160: 07: 25: 01	MAD	249	Command attitude maneuver: X = -30 , Y = 0 , Z = 0 (Begin X axis maneuver)
160: 07: 25: 54	MAD	249	Select attitude hold TACS mode (Complete X axis maneuver)
160: 07: 27: 08	MAD	249	Command attitude maneuver: X = 0 , Y = 20 , Z = 0 (Y axis maneuver)
160: 07: 29: 23	MAD	249	Select attitude hold TACS mode
160: 08: 46: 28	BDA	250	Command attitude maneuver: X = 0 , Y = 14 , Z = 0
160: 08: 46: 47	BDA	250	Set maneuver time = 0
160: 08: 50: 23	BDA	250	Initialize strapdown, command solar inertial (Y axis maneuver complete)
160: 08: 52: 39	BDA	250	Implement T2 patch (start rate only control in Z axis)
160: 08: 54: 10	BDA	250	Set TACS pulse width = 120 ms
160: 09: 00: 14	MAD	251	Load T1 patch into memory load buffer
160: 09: 01: 32	MAD	251	Telemeter memory load buffer
160: 09: 04: 10	MAD	251	Display sum check constant on single memory location display
160: 09: 05: 12	MAD	251	Initialize strapdown

TIME	SITE	PASS	COMMAND
160: 10: 25: 14	BDA	252	Initialize strapdown
160: 10: 25: 50	BDA	252	Set maneuver time = 60 minutes
160: 10: 30: 07	BDA	252	Initialize strapdown
160: 10: 42: 03	MAD	253	Initialize strapdown
160: 11: 49: 43	GDS	254	Initialize strapdown
160: 11: 50: 18	GDS	254	Implement T1 patch (End rate only control in Z axis
160: 11: 51: 24	GDS	254	Display maneuver time
160: 11: 51: 54	GDS	254	Set TACS pulse width = 320 ms
160: 11: 52: 26	GDS	254	CMG cage
160: 11: 53: 15	GDS	254	CMG cage
160: 11: 55: 45	GDS	254	Select attitude hold TACS mode
160: 11: 56: 05	GDS	254	Command attitude maneuver: X = 0 , Y = 0 , Z = 180
160: 12: 12: 30	MAD	256	Update CMG momemtum bias: X = 16% 3H, Y = 0% 3H, Z = 6% 3H
160: 13: 25: 57	GDS	257	Set maneuver time = 0
160: 13: 27: 04	GDS	257	Initialize strapdown
160: 13: 27: 18	GDS	257	Select solar inertial mode
160: 13: 33: 25	GDS	257	Enable CMG control
160: 13: 33: 55	GDS	257	Enable gravity gradient dump

TIME	SITE	PASS	COMMAND
160: 13: 38: 43	BDA	258	Set maneuver time = 9 minutes
160: 16: 41: 40	GDS	261	Computer auto enable command (CMG #3 turned off by spurious command)
160: 16: 47: 33	GDS	261	Enable CMG control
160: 16: 56: 26	BDA	262	CMG #2 on, RM inhibited
160: 16: 56: 50	BDA	262	CMG #3 on, RM inhibited
160: 16: 57: 37	BDA	262	CMG #1 VREF, RM inhibited
160: 16: 58: 08	BDA	262	Enable CMG control
160: 18: 17: 05	GDS	263	CMG #3 servo amp on
160: 18: 17: 38	GDS	263	CMG #3 control enabled
160: 19: 54: 29	GDS	264	Set CMG gimbal rate limit = 2 deg/sec
(June 10, 1978)			
161: 03: 11: 43	MAD	265	Reset caution and warning discrete output
161: 03: 12: 07	MAD	265	Reset alert discrete output
161: 04: 48: 04	MAD	266	Set CMG gimbal rate limit = 1 degree per second
161: 09: 26: 59	BDA	268	Navigation update
(June 11, 1978)			
162: 03: 51: 33	MAD	278	Navigation update
162: 03: 52: 15	MAD	278	Set maneuver time = 28 minutes
162: 06: 48: 21	BDA	280	Inhibit CMG control

TIME	SITE	PASS	COMMAND
162: 06: 48: 48	BDA	280	Select ZLV mode
162: 06: 50: 42	BDA	280	Command maneuver bias (12.2 , Y = 10.7 , Z = 1.0)
162: 06: 51: 24	BDA	280	CMG cage
162: 06: 53: 30	BDA	280	Set $K_M Z$ = 0 (inhibit Z axis strapdown update)
162: 06: 54: 49	BDA	280	Enable X and Y axis EOVV strapdown update
162: 06: 55: 47	BDA	280	Set maneuver time = 10 minutes
162: 07: 06: 10	MAD	281	Display SNBRSSP (Past value of the root sum square of the Acq. SS outputs)
162: 08: 27: 22	BDA	282	Enable CMG control
162: 08: 27: 52	BDA	282	Enter EOVV
162: 11: 34: 59	GDS	286	Set η_{YL} = 12 degrees
162: 11: 52: 24	MAD	288	Select ACQ SS #2 in Y
162: 11: 53: 29	MAD	288	Inhibit Y axis ACQ SS RM
162: 13: 06: 48	GDS	289	Load buffer 9 into memory load buffer
162: 13: 10: 07	GDS	289	Telemeter memory load buffer
162: 14: 44: 51	GDS	291	Implement buffer 9
162: 14: 46: 45	GDS	291	Select ACQ SS #1 and #2 for Y axis
162: 14: 47: 15	GDS	291	Inhibit Y axis ACQ SS RM
162: 15: 01: 07	BDA	292	Set $K_M Z$ = .1 (Enable Z axis update)

TIME	SITE	PASS	COMMAND
162: 17: 57: 58	GDS	295	Display η_Y
162: 19: 35: 37	GDS	296	Inhibit TACS
(June 12, 1978)			
163: 02: 54: 10	MAD	297	Navigation update
163: 12: 09: 28	GDS	308	Display interrupt enable mask
163: 13: 46: 53	GDS	310	Enable TACS control
163: 13: 47: 36	GDS	310	Y rate gyro #1 bias = -2 lsb's
163: 13: 48: 18	GDS	310	Y rate gyro #3 bias = -2 lsb's
163: 13: 57: 07	BDA	311	Load interrupt inhibit restore patch
163: 13: 58: 27	BDA	311	Telemeter memory load buffer
163: 18: 35: 02	GDS	315	Y rate gyro #1 bias = +2 lsb's
163: 18: 35: 44	GDS	315	Y rate gyro #3 bias = +2 lsb's
163: 18: 36: 24	GDS	315	Inplement interrupt inhibit patch
163: 18: 37: 32	GDS	315	Set $e_{TN} = 2.5$
163: 18: 38: 34	GDS	315	Display η_Y
(June 13, 1978)			
164: 03: 26: 39	MAD	317	Display interrupt enable mask
164: 03: 29: 19	MAD	317	Set Δt_d = 150.5 seconds
164: 03: 31: 29	MAD	317	Load interrupt inhibit restore patch

TIME	SITE	PASS	COMMAND
164: 03: 33: 05	MAD	317	Telemetry memory load buffer
164: 05: 03: 19	MAD	318	Implement interrupt inhibit restore patch
164: 05: 03: 45	MAD	318	Display $K_{\mu Z}$
164: 05: 05: 14	MAD	318	Set maneuver time = 5 minutes
164: 08: 05: 27	BDA	321	Set $K_{\mu Z}$ = .2
164: 14: 25: 08	GDS	330	Set: erb= -.05 H
164: 14: 25: 40	GDS	330	η_{TL} = .15 radians
164: 14: 26: 20	GDS	330	Δe_{TL2} = .24609 H
164: 14: 27: 09	GDS	330	η_{ym} = .15 radians
164: 14: 27: 36	GDS	330	$K_{\mu Z}$ = 1.9/
(June 14, 1978)			
165: 07: 07: 00	BDA	338	Inhibit TACS control

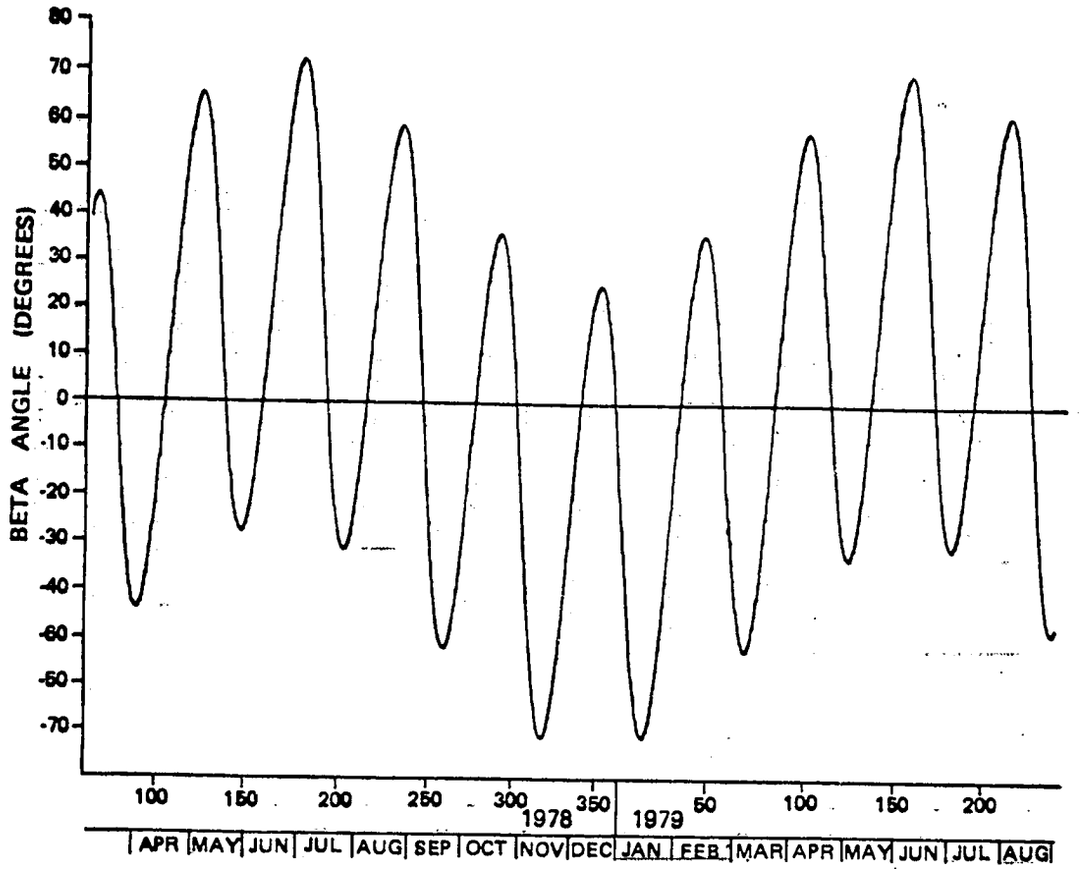

FIGURE 2-8 BETA ANGLE VERSUS DAY OF YEAR

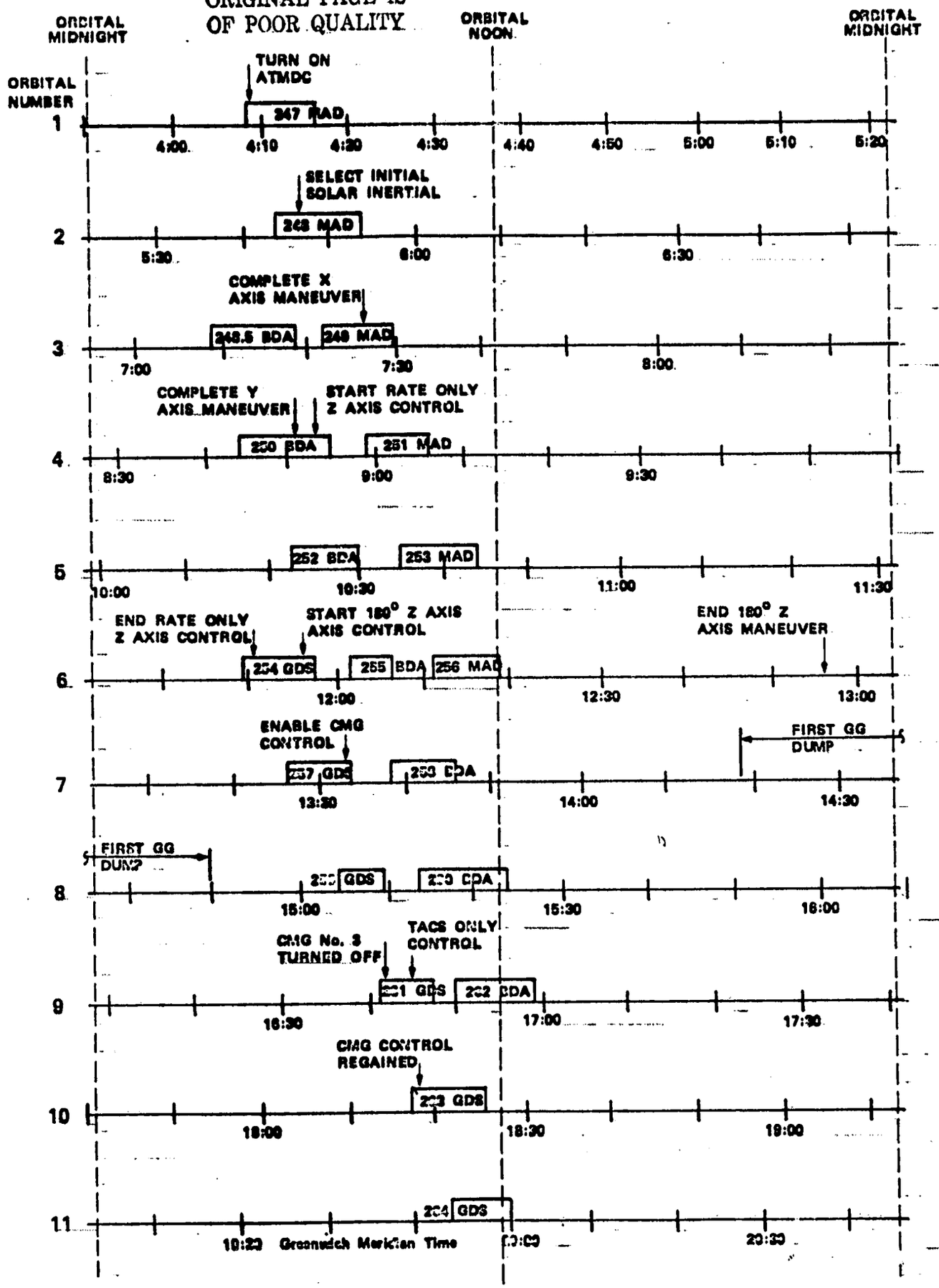

FIGURE 2-9 STATION COVERAGE FOR INITIAL SOLAR INERTIAL ACQUISITION ON

Since the vehicle was in the SI mode, the attitude errors of the X and Y axes would be updated by the ACQ SS readings. If this occurred properly, the solar inertial attitude would be established for X and Y axes and no further maneuvering would be required for these axes. However, when the vehicle rates were stopped, the vehicle was outside the linear range of the ACQ SS. If the ACQ SS's are outside their linear range when operating in TACS only control, it is possible to perform strapdown corrections with an opposite polarity and thereby increase the attitude error.

This was what happened in the Y axis. The strapdown reference in the X axis was updated correctly but the Y axis attitude error was increased until the absolute value of the Y ACQ SS reading was less than 0.8 degrees (See Reference 4 for the specifications of the ACQ SS strapdown corrections). The readings became less than 0.8 degrees when the Y axis was approximately 20 degrees away from the sun. When the Bermuda station was acquired at 7:08 GMT (pass 248.5) the vehicle position was 0 degrees in X and -20 degrees in Y.

The vehicle had been out of station coverage since the Madrid station had lost contact at 5:53 GMT and there was no way at that time to have known for certain the Skylab's position. Therefore, the first maneuver was to establish the X axis position. At 7:25 GMT, a -30 degree maneuver about X was commanded. This maneuver was terminated a few seconds later when ACQ SS data showed that the X axis was already near zero.

With the X reference determined, the next step was to establish the Y position. The ACQ SS data showed that the Y axis was at a negative angle from the SI attitude and therefore a positive 20 degree maneuver was commanded. Just before LOS occurred, the maneuver was stopped by commanding the attitude hold TACS mode. When AOS for the next station occurred, it was seen that the Y axis was still several degrees from the SI attitude. At 8:46 GMT an additional 14 degree maneuver about Y was commanded and when ACQ SS data showed the Y axis was near zero, the strapdown reference was initialized and the SI mode was commanded. This command, which occurred at 8:50 GMT, caused the solar panels to lock on the sun and with the ACQ SS's now in their linear range, strapdown correction was now assured.

The next step was to establish the Z axis attitude reference. This was done by implementing a special ATMDC flight program patch (labeled the T2 patch) to change the TACS control gains in the Z axis. These gains were set so that the Z axis would be in a "rate only" type of control. This allowed the gravity gradient torques acting on the vehicle to cause the X axis to fall into the orbital plane. However, it was possible for the vehicle to fall either forward or backward, depending upon its

X axis orientation with respect to the orbit plane. This meant that if the vehicle fell in a direction other than that desired, the positive X axis would be 180 degrees away from the desired orientation.

At 8:52 GMT, the T2 patch was implemented and the gravity gradient torques began pulling the X axis into the orbital plane. Shortly afterwards, it could be seen that the X axis was falling in the wrong direction and that a 180 degree maneuver about Z would be required after the end of the rate only control. The strapdown reference was re-initialized periodically while the vehicle fell to keep the Z axis attitude error small. By 11:50 GMT, the X axis was sufficiently near the orbital plane to end rate only control. This was done by restoring the TACS control gains to their original values with the T1 patch. At 11:55 GMT, the 180 degree maneuver in Z was commanded. At the completion of this maneuver, the vehicle was at the solar inertial attitude.

The next step was to enable CMG control and gravity gradient dump of the CMG momentum. To ensure a desirable momentum state, the CMGs were caged to nominal momentum prior to enabling CMG control. By caging the CMGs during the 180 degree Z axis maneuver, the caging was accomplished with a minimum of TACS usage. The CMG momentum biases were uplinked and at 13:33 GMT, CMG control and GG dump was enabled. The first GG dump occurred during the following orbital night period. This completed the first phase of the initial attitude control acquisition. The vehicle was in the solar inertial attitude with GG dump performing properly.

2.2.2.3 CMG #3 Servo Off Command

When the Goldstone station was acquired at 16:41 GMT, all systems were nominal. Prior to this pass, it had been decided to invoke the mission rule (Reference 2) which allows computer switchover to be enabled while operating in the solar inertial mode. At 16:42 GMT, the command to enable auto computer switchover was transmitted to the vehicle. The octal code for this command was a 30077. Because of a problem with switch selector #3, it issued an additional command which was sent to the hardware (an octal code 30057) and commanded CMG #3 servo power off.

With CMG #3 servo power off, its gimbal angle positions were frozen and the CMG could not be used for control. Because CMG redundancy management was inhibited, the flight program could not detect that CMG #3 had no control capability. This resulted in a large attitude error in the X axis and when this error

reached 20 degrees, the flight program switched to TACS only control.

While this was happening, the flight data was being analyzed to determine exactly what had gone wrong. When the flight program switched to TACS only control the first time, it was not known then that CMG #3 servo power was off. Therefore, CMG control was quickly re-enabled. Immediately, the X axis attitude increased again to 20 degrees and the flight program switched again to TACS only control. By this time it had been discovered that the servo power was off. It was hoped that the servo power could be restored by issuing the following DCS commands to the flight program: CMG #2 on with redundancy management inhibited, CMG #3 on with redundancy management inhibited and CMG #1 VREF selected with redundancy management inhibited. These commands were issued and CMG control was re-enabled. These commands failed to produce the desired results because a previous spurious command from switch selector #3 had inhibited the capability of the computer subsystem to activate power to the CMG subsystem. (i.e. CMG Auto Shutdown Enable/Inhibit Command). The X axis attitude error again increased to 20 degrees causing a third switch to TACS only control. By this time LOS of the station occurred and the next station acquisition was not scheduled until over an hour later at 18:17 GMT.

It should be noted that a considerable amount of TACS fuel is used whenever the control system switches to TACS only control due to a 20 degree attitude error. The flight program TACS control law tries to remove this 20 degree error as quickly as possible. This is much more costly from a TACS standpoint than maneuvering 20 degrees over some defined maneuver time. It was estimated that approximately 1000 lbf-sec of TACS was used each time the system switched to TACS only.

Figure 2-10 shows the TACS usage for the Skylab Reactivation mission. A large part of the 9569 lbf-sec that was used during June 9-11, 1978 was expended following the three switches to TACS only control. The program switched to TACS only control one other time during the reactivation mission and this occurred on July 19, 1978. On July 24 a program patch was implemented (FF81 buffer 10A) which prevented any further automatic switch to TACS only control.

While the Skylab vehicle was out of site coverage between 16:59 and 18:17 GMT, the problem with CMG #3 was throughly analyzed. A plan was developed to bring the CMG back on line and to re-establish CMG control. At 18:17 GMT commands were issued which turned CMG #3 servo power back on and reenabled CMG control. These commands performed as expected and CMG control of the vehicle was regained.

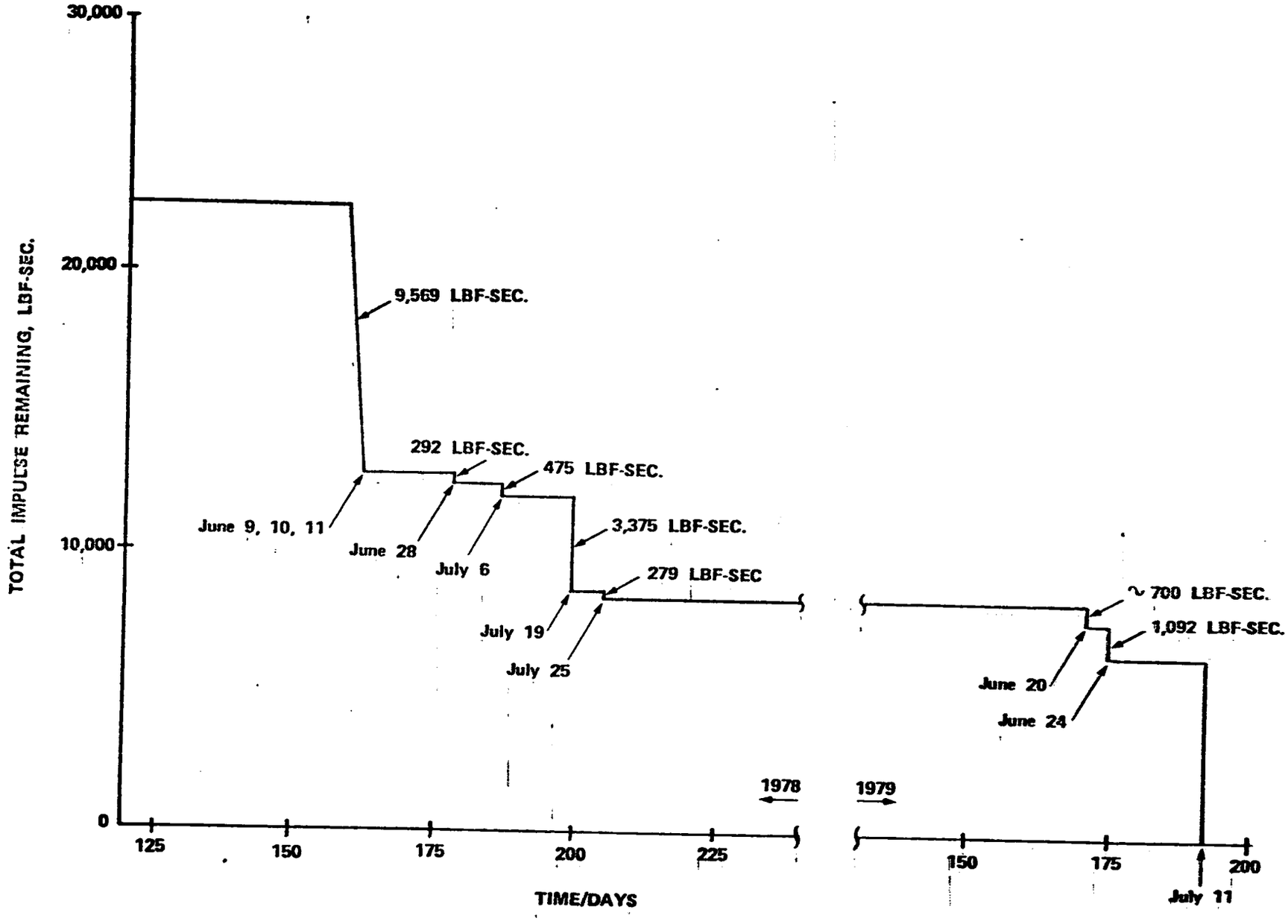

FIGURE 2-10 TACS USAGE DURING THE SKYLAB REACTIVATION MISSION

2.2.3 Initial EOVV Acquisition and Maintenance

The date to enter the EOVV control mode had been originally scheduled for June 10, 1978 because the sun angle was near zero degree on this day. Because of the problems with CMG #3 it was decided to postpone the EOVV acquisition until June 11. The beta angle had increased to 5 degrees on June 11 but this would have little effect on EOVV acquisition.

The station passes that were available on June 11 were similar to those on June 9, see Figure 2-11. Twenty station passes were scheduled covering almost 16 hours and 11 Skylab orbits.

2.2.3.1 Initial EOVV Entry

The entry into EOVV was a two step function. First, an offset ZLV maneuver would be commanded to place Skylab into a near EOVV attitude. Second, the select EOVV attitude command would be issued to initiate the EOVV mode.

At 6:49 GMT on June 11, 1978, the select ZLV mode command followed immediately by the offset ZLV bias commands was sent via the Bermuda tracking site to Skylab. Skylab, under control of the ATMDC flight program, began maneuvering to the commanded attitude. At 6:51 GMT the CMGs were caged so that the EOVV mode would be entered with a satisfactory momentum state. Next orbit, when Skylab came back in range of Bermuda at 3:24 GMT, Skylab was in the proper attitude to enter the EOVV mode. The CMG control mode was then enabled and the select EOVV mode command was sent to Skylab at 8:28 GMT. After the EOVV attitude was acquired, a dramatic change occurred in the orbit decay rate as shown in Figure 2-1.

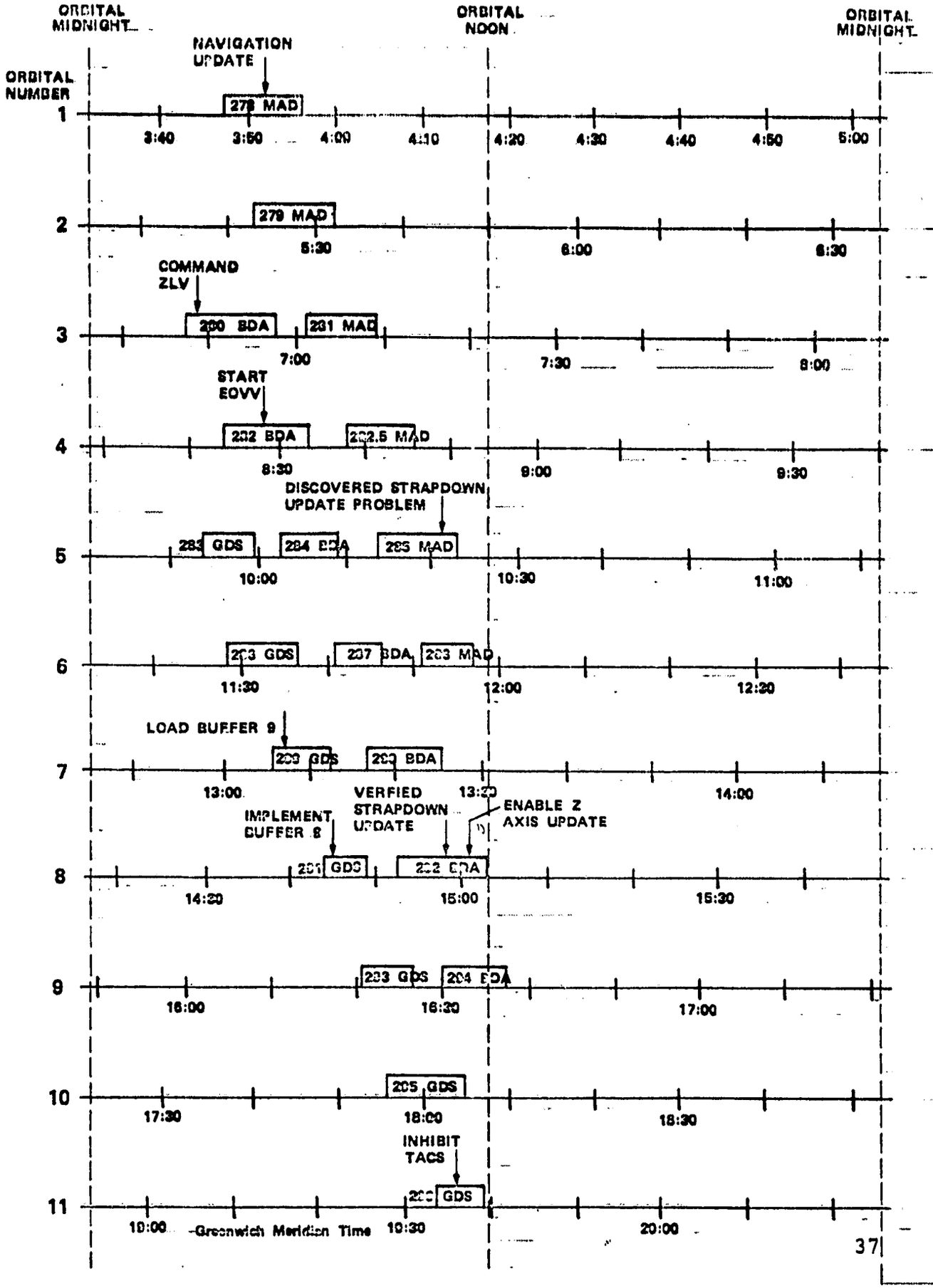

FIGURE 2-11 STATION COVERAGE FOR EOVV ACQUISITION ON JUNE 11, 1978

2.2.3.2 Initial Parameter Tune Up

After entering EOVV, several parameters were expected to need adjustment to keep the EOVV control logic within certain bounds. The first measurement that was monitored was strapdown update. Early in EOVV operation, by observing a variable (SNBRSSP) using the single word display feature of the flight program, it was observed that the strapdown update was occurring prematurely. SNBRSSP is a multipurpose variable that was designed to be used both as a flag, indicating when strapdown update had occurred, and as a computed variable, SNBRSSP = Root Sum Square of $\gamma_{e,x}$ and $\gamma_{e,y}$ (RSS).

SNBRSSP was initialized to its maximum value (+180 deg.) when the sun presence discrete was off and when the sun presence discrete came on again the value of RSS was checked against 5.7 degrees. If it were less than 5.7 degrees, then SNBRSSP was set equal to RSS. RSS would continue to be stored into SNBRSSP as long as it was smaller than SNBRSSP. When RSS became greater than SNBRSSP, the strapdown update was executed. According to the acquisition sun sensor specification, 6.0 degrees was the top of the linear region for the acquisition sun sensor (ACQ SS) and subsequent ACQ SS readings would be smaller until the Y axis swept across or near the sun disc at which time strapdown update should occur. Due to ACQ SS #1 reading lower than expected, RSS was less than 5.7 degrees when the sun presence discrete came on. Thus the strapdown update occurred immediately even though the sun angle was approximately 9 degrees. This error caused the strapdown to be in error by about 3 degrees. To solve this problem, a program patch to change the test limit to 5 degrees instead of 5.7 degrees was generated, verified, and implemented in the primary ATMDC within a span of 4.5 hours.

After solving the problem with strapdown update, the rate gyro integrals were monitored and it was determined that a scale factor error was showing up in all three axes. To compensate for the errors, it was decided to use the updatable drift compensation terms rather than patch the flight program to allow scale factor updates on all gyros. This seemed to be an acceptable plan since the scale factor errors were small and the rate change between Y and Z was slow. The rate gyro drift compensation was determined in the X and Y axis by the strapdown quaternion elements QV11 and QV12 just prior to the strapdown update. The Z axis compensation was determined by the value of μ_2.

2.2.3.3 EOVV Maintenance

While the rate gyro compensations were being monitored and updated, EOVV performance was also being monitored. After several hours of EOVV control, it was observed that the Z axis control (η_{zw}) was continuing to be limited by the flight program. Several more hours of monitoring found the same conditions to exist and it appeared as though EOVV would have to be aborted by returning to SI to regain control of momentum using the gravity gradient dump routine. Several EOVV parameters were changed to allow the CMG's to dump more Z-axis momentum and try to stay in EOVV. The parameters that were changed are listed below:

$K_{\mu Z}$ from .1 to .2
e_{rb} from Ø to Ø.5 H
η_{zL} from .1 to .15 radians
Δe_{TLZ} from .17 to .24609 H
η_{ym} from .1 to .15 radians
$K_{\eta z}$ from 2.85/ to 1.9/

Following these data changes, EOVV control performance improved significantly and the decision to return to SI was cancelled.

During the early EOVV monitoring experience, it became evident that the availability of the elements of the strapdown update quaternion (ΔQ) would help detect the need for updating the rate gyro biases and some of the EOVV parameters. Therefore, SWCR 4001 was generated and patch buffer #10 was built. This change allowed the flight program to save and telemeter the ΔQ quaternion.

2.2.4 EOVV RETREAT TO SI

After operating in the EOVV control mode for approximately 17 days, Skylab was returned to the solar inertial attitude on June 28, 1978 because of momentum management problems in EOVV. Large momentum errors and Z axis attitude errors were first observed at 179:09:23 GMT and the decision was made to enable TACS control to assist the CMG control system. After one orbit, 100 lb-sec of TACS impulse had been used without resulting in a significantly improved CMG momentum state, therefore, the decision was made to return to the solar inertial attitude. An additional 192 lbf-sec of TACS impulse was required to achieve steady state solar inertial operations. A summary of the command history during this period is summarized in Table 2-3.

The initial supposition of the problem was that the CMGs had encountered gimbal stop problems which activated the CMG outer gimbal drive logic in the flight program to reposition the CMG gimbals. This action would generate attitude errors which in turn could corrupt the desired system momentum state. However, subsequent investigations revealed that the postulated CMG gimbal stop problem was more likely an effect rather than the cause and that the strapdown reference error about the sunline was more likely the origin of the momentum management problem. It is more probable that strapdown reference errors introduced control errors which resulted in abnormal momentum states which then could lead to CMG gimbal stop encounters. Following is a brief explanation of the strapdown errors that led to this problem.

Table 2-3. Pertinent APCS Commands for the Retreat to SI on June 28, 1978.

TIME (GMT)	SITE	PASS	COMMAND
(June 28, 1978)			
179: 06: 19: 54	BDA	477	Set Z1 rate gyro bias = -3 lsb's
179: 06: 21: 00	BDA	477	Set Z3 rate gyro bias = -3 lsb's
179: 07: 45: 38	GDS	478	Update TACS thrust = 44 newtons
179: 09: 23: 17	GDS	480	Enable TACS Control
179: 11: 01: 26	GDS	481	Set maneuver time = 45 minutes
179: 11: 03: 20	GDS	481	Select solar inertial mode
179: 12: 37: 40	GDS	482	Update CMG momentum bias
179: 12: 38: 11	GDS	482	Set Y1 rate gyro bias = 0
179: 12: 38: 48	GDS	482	Set Y3 rate gyro bias = 0
179: 19: 49: 40	MAD	482.1	Set Z1 rate gyro bias = 0
179: 19: 50: 20	MAD	482.1	Set Z3 rate gyro bias = 0
179: 19: 51: 10	MAD	482.1	Reset caution and warning discrete outputs
179: 19: 51: 40	MAD	482.1	Reset alert discrete outputs
180: 00: 39: 44	MAD	482.6	Inhibit TACS control

The EOVV strapdown reference update scheme maintained an accurate reference in the X and Y axis by using the acquisition sun sensor to update these axes once per orbit. The Z axis strapdown reference was also updated once per orbit based upon the per orbit change of the orbital Z system momentum; the direction of change being an indicator of the Z axis strapdown reference error. At this time the major source of strapdown errors was thought to be a result of rate gyro scale factor errors. Rate gyro drift bias compensation was being used to compensate for these errors depending upon the apportionment of orbit rate in the Y and Z axes.

The inertial reference maintained onboard Skylab was by definition relative to the orbit plane and the position of the sun with respect to the orbit plane. The onboard software used this definition to compute the local vertical reference system in which the EOVV control equations were defined. Since the orbit plane and sun both move relative to a true geocentric inertial reference, the onboard strapdown reference definition is a quasi-inertial reference system. Even though it was known that the strapdown reference was a quasi-inertial reference, it was believed that the strapdown updating scheme could compensate the movement of the inertial reference. However, a detailed investigation following the problem that occurred on June 28 revealed that this effect was particularly pronounced at high sun angles and exceeded the capability of Z axis strapdown update scheme. In addition a pronounced change in the derivative of the Z axis drift caused by this effect occurs when the sun angle relative to the orbit plan (β) passes through an extremum. This was exactly the situation when the momentum management problem occurred on June 28. The sun angle had just peaked at 73 degrees and had started decreasing. The Z axis reference drift rapidly decreased and was not correspondingly compensated with decreased rate gyro drift bias which in turn led to a large Z axis strapdown reference error.

After this effect was well understood, a strapdown update bias term (e_{rb}, see Section 2.3.1.) was successfully used to compensate for the Z axis drift due to orbit plane and sun motion.

2.2.5 Second EOVV Acquisition From SI

Skylab was controlled in the SI attitude between June 28 and July 6, 1978 to allow time to understand the problems that had been encountered in EOVV and to allow the beta angle to decrease to where EOVV operation would be easier to control. On July 6, the vehicle was maneuvered back to the EOVV mode. The pertinent APCS commands for there procedure are shown in Table 2-4 and station coverage is shown in Figure 2-12.

Table 2.4 Pertinent APCS Commands for the Second EOVV Acquisition

TIME (GMT)	SITE	PASS	COMMAND
(July 5, 1978)			
186: 20: 44: 30	BDA	530	Set ηym = .1 radian
186: 20: 46: 25	BDA	530	Set Δe_{TL2} = .165
186: 20: 47: 30	BDA	530	Set $K\eta_Z = 2.85/\pi$
186: 20: 48: 25	BDA	530	Set maneuver time = 30 minutes
186: 23: 49: 29	GDS	533.1	Inhibit gravity gradient dump
186: 23: 51: 16	GDS	533.1	Enable TACS
(July 6, 1978)			
187: 00: 14: 00	MAD	535	Select ZLV mode
187: 00: 14: 17	MAD	535	Command Maneuver bias (X = 45.7, Y = 6.5, Z = -2.6)
187: 00: 15: 19	MAD	535	Set maneuver time = 10 minutes
187: 01: 23: 29	GDS	535.1	Command maneuver bias ($X = 0^o$, $Y = 0^o$, $Z = 0^o$)
187: 01: 24: 22	GDS	535.1	Inhibit CMG control
187: 01: 24: 55	GDS	535.1	Begin CMG caging
187: 01: 26: 38	GDS	535.1	RG drift compensation, Y1 = 3 lsb's
187: 01: 27: 05	GDS	535.1	RG drift compensation, Y3 = 3 lsb's
187: 01: 27: 25	GDS	535.1	RF drift compensation, Z1 = -2 lsb's
187: 01: 27: 46	GDS	535.1	RG drift compensation, Z3 = -2 lsb's
187: 01: 28: 06	GDS	535.1	RG drift compensation, Z2 = -2 lsb's
187: 01: 36: 30	BDA	535.2	Enable CMG control
187: 01: 36: 49	BDA	535.2	Inhibit TACS control
187: 01: 37: 07	BDA	535.2	Enter EOVV
187: 01: 37: 16	BDA	535.2	Command maneuver bias ($X = 12.2^o$, $Y = -10.7^o$, $Z = 1.0^o$)

Table 2.4 Pertinent APCS Commands for the Second EOVV Acquisition (Continued)

TIME (GMT)	SITE	PASS	COMMAND
187: 01: 37: 34	BDA	535.2	Enable TACS control
187: 03: 14: 08	BDA	535.5	Set $K\mu Z = .2$
187: 04: 51: 03	BDA	535.7	Set $\eta ym = .15$ radians
187: 04: 52: 24	BDA	535.7	Set $K\eta z = 1.9/\pi$
187: 04: 53: 31	BDA	535.7	Set $e_{TL2} = .24609$
187: 07: 51: 46	GDS	535.91	Inhibit TACS
187: 09: 29: 59	GDS	535.92	Set $e_{TN} = 2.8242$
187: 09: 31: 22	GDS	535.92	Set $e_{rb} = .02$
187: 21: 21: 42	BDA	540	RG drift compensation, Y1 = 2 lsb's
187: 21: 22: 41	BDA	540	RG drift compensation, Y3 = 2 lsb's
187: 21: 23: 41	BDA	540	RG drift compensation, Z1 = -3 lsb's
187: 21: 24: 38	BDA	540	RG drift compensation, Z2 = -3 lsb's
187: 21: 25: 35	BDA	540	RG drift compensation, Z3 = -3 lsb's
(July 7, 1978)			
188: 05: 26: 34	BDA	543.9	RG drift compensation, Z1 = -4 lsb's
188: 05: 27: 31	BDA	543.9	RG drift compensation, Z2 = -4 lsb's
188: 05: 28: 29	BDA	543.9	RG drift compensation, Z3 = -4 lsb's
188: 05: 29: 44	BDA	543.9	Set $e_{tn} = 2.5$
188: 15: 51: 55	BDA	544	Set $e_{tn} = 2.4$
188: 17: 23: 12	MAD	545	Set $e_{rb} = 0$

STATION ACQUISITION PERIODS FOR SKYLAB

DATE	7-6-78
DAY NUMBER	187
BETA ANGLE	45.1546 DEGREE
1 REV DELTA TIME	01:32:14 GMT
ORBITAL MIDNIGHT	00:26:04
ORBITAL SUNRISE	00:41:23
NIGHT TO DAY TERM	00:49:03
ORBITAL NOON	01:12:09
DAY TO NIGHT TERM	01:35:12
ORBITAL SUNSET	01:43:01

STA	PASS	AOS	LOS	MAX. ELV.
MAD	535	00:09:10	00:18:19	70.3°
GDS	535.1	01:23:28	01:31:56	45.3°
BDA	535.2	01:36:17	01:41:43	2.5°

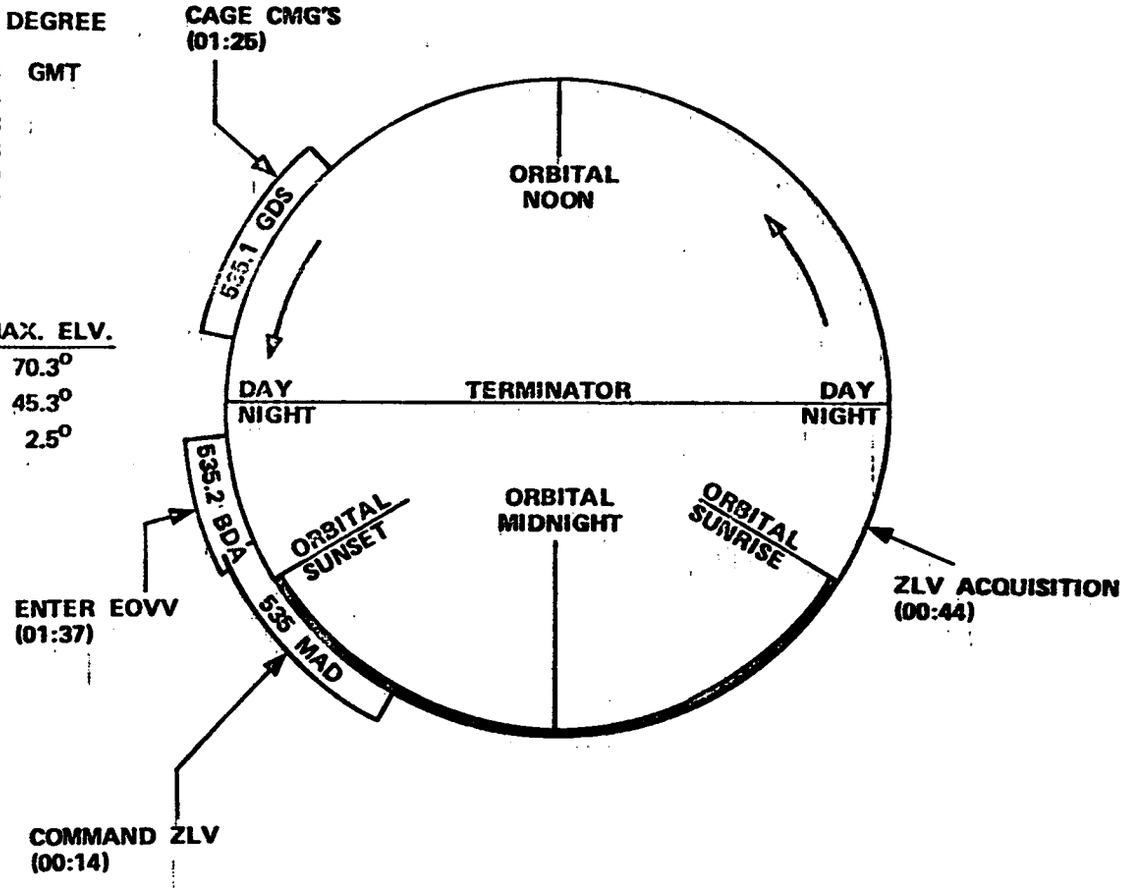

FIGURE 2-12 STATION COVERAGE FOR EOVV ACQUISITION ON JULY 6, 1978

Skylab was first maneuvered to an offset ZLV attituded using a maneuver time of 30 minutes. These commands were issued at 00:14 GMT on July 6 and the commanded attitude was attained at 00:44 GMT. Then at 1:23 GMT the Skylab was commanded to make a 10 minute maneuver of zero degree attitude change. This was done so that the CMGs could be caged while Skylab was performing in a rate only control mode under TACS control, which is a minimum TACS usage cage procedure. At 1:25 GMT, the CMG cage command was issued.

At 1:37 GMT, after the caging operation had been completed, TACS control was inhibited and Skylab was commanded into the EOVV control mode. Eighteen seconds later, the EOVV biases were uplinked and TACS control was reenabled. TACS control had been inhibited to prevent TACS usage until the flight program had received the correct EOVV biases. The total amount of TACS used for EOVV acquisition including the ZLV maneuver and the CMG cage was 475 lbf-sec.

2.2.6 Loss of Attitude Reference

On July 9, 1978 Skylab was operating in the EOVV Mode with all systems functioning normally. This was the situation observed over the Madrid tracking station at 17:00 GMT. However, at the 20:12 GMT pass over Madrid, contact with Skylab was lost. It was determined that the ATM batteries had all automatically tripped at low voltage causing loss of vehicle attitude reference and control. Skylab had previously been placed in a new power configuration with the AM batteries not on line due to two unexplained battery charger failures in that system. The ATM power system and AM solar arrays were not sufficient to carry the load in the EOVV mode causing the ATM batteries to automatically trip off.

Contact with Skylab on subsequent passes was established through the AM and initial recovery operations using the CMGs spinning at partial speed were unsuccessful. After the unsuccessful recovery attempt, a slow roll about the X axis (2.5 rolls/orbit) was induced on Skylab to obtain sun on the solar arrays while plans could be formulated to reacquire attitude control of Skylab. In a favorable solar environment, the integrity of the electrical power system (EPS) could be restored and made ready for reacquisition.

2.2.7 SI Acquisition From Unknown Attitude

On July 19 and 20, 1978 control of the Skylab vehicle was regained by acquiring the solar inertial mode from an unknown attitude. This section describes the events which supported this reacquisition of attitude control. The pertinent APCS commands issued during this time period are shown in Table 2-5.

2.2.7.1 Preparation

On July 11, Skylab was in a random attitude with CMGs stopped and little illumination of the solar arrays. Telemetry showed that vehicle angular rates were small. On July 13, the vehicle was rolling approximately two revolutions per hour and was getting sufficient power for the ATM battery charging. On July 17, the Skylab roll rate was 23 minutes per roll (approximately four revolutions per orbit). Charging of the Electrical Power System Batteries was initiated. By July 18, the batteries were sufficiently charged to spin up the CMGs. At 23:50 GMT, July 18, the CMGs were caged and spin up was initiated. On July 19, CMG spin up was near complete and all systems were ready for

solar inertial acquisition. The station passes that were scheduled to support the solar inertial acquisition are shown in Figure 2-13. Nineteen station passes were scheduled to cover 14 hours and 10 orbits of operations.

Table 2-5. Pertinent APCS Commands for the SI Acquisition From Unknown Attitude

TIME (GMT)	SITE	PASS	COMMAND
(July 18, 1978)			
199: 12:57: 00	MAD	645	Inhibit CMG Control
199: 12: 58: 03	MAD	645	Enable TACS Control
199: 23: 49: 32	GDS	659	CMG 2 Wheel On
199: 23: 49: 44	GDS	659	CMG 3 Wheel On
(July 19, 1978)			
200: 13: 34: 35	MAD	665	Set maneuver time equal to zero
200: 16: 34: 33	BDA	668	Cage CMGs
200: 18: 22: 28	MAD	672	Initialize strapdown
200: 18: 22: 40	MAD	672	Initialize strapdown
200: 18: 22: 50	MAD	672	Initialize strapdown
200: 18: 23: 11	MAD	672	Select solar inertial mode
200: 18: 23: 42	MAD	672	Enable CMG control
200: 18: 27: 28	MAD	672	Select attitude hold CMG mode
200: 19: 33: 29	GDS	673	Select solar inertial mode
200: 19: 56: 49	MAD	675	Maneuver time = 60 minutes
200: 19: 57: 04	MAD	675	Select attitude hold CMG mode
200: 19: 58: 00	MAD	675	Command attitude maneuver ($X = 0^{o}$, $Y = 0^{o}$, $Z = -179^{o}$)
200: 19: 59: 26	MAD	675	Reset caution and warning discrete outputs
200: 20: 00: 12	MAD	675	Reset alert discrete output
200: 21: 11: 31	GDS	676	Set maneuver time = 0
200: 21: 11: 55	GDS	676	Initialize strapdown
200: 21: 12: 13	GDS	676	Select solar inertial mode
200: 21: 12: 38	GDS	676	Set maneuver time = 60 minutes
200: 21: 26: 04	BDA	677	Navigation update
200: 21: 26: 37	BDA	677	Select attitude hold CMG
200: 21: 28: 26	BDA	677	Command attitude maneuver ($Y = 0^{o}$, $Y = 0^{o}$, $Z = -20^{o}$)
200: 21: 28: 52	BDA	677	Display single memory location: 0096

Table 2-5. Pertinent APCS Commands for the SI ACquisition From Unknown Attitude (Continued)

TIME (GMT)	SITE	PASS	COMMAND
200: 22: 49: 22	GDS	678	Set maneuver time = 0
200: 22: 49: 38	GDS	678	Initialize strapdown
200: 22: 49: 54	GDS	678	Select solar inertial
200: 22: 50: 28	GDS	678	Enable gravity gradient dump
200: 22: 51: 01	GDS	678	Enable auto CMG reset
(July 20, 1978)			
201: 00: 28: 51	GDS	680	Enable CMG control
201: 00: 41: 49	BDA	681	Select attitude hold CMG mode
201: 02: 03: 10	GDS	682	Set CMG gimbal rate limit = 2 degrees/second
201: 02: 03: 32	GDS	682	Set maneuver time = 0
201: 02: 03: 52	GDS	682	Select solar inertial mode
201: 02: 04: 37	GDS	682	Inhibit TACS control
201: 02: 05: 37	GDS	682	Enable X axis RGRM
201: 02: 06: 03	GDS	682	Enable Y axis RGRM
201: 02: 06: 24	GDS	682	Enable Z axis RGRM
201: 02: 06: 46	GDS	682	Reset caution and warning discrete output
201: 03: 40: 45	GDS	683	Enable TACS control
201: 03: 41: 03	GDS	683	CMG Nominal H Cage
201: 03: 44: 12	GDS	683	Inhibit TACS control
201: 14: 08: 36	MAD	687	Set gimbal rate limit = 1 degree/second

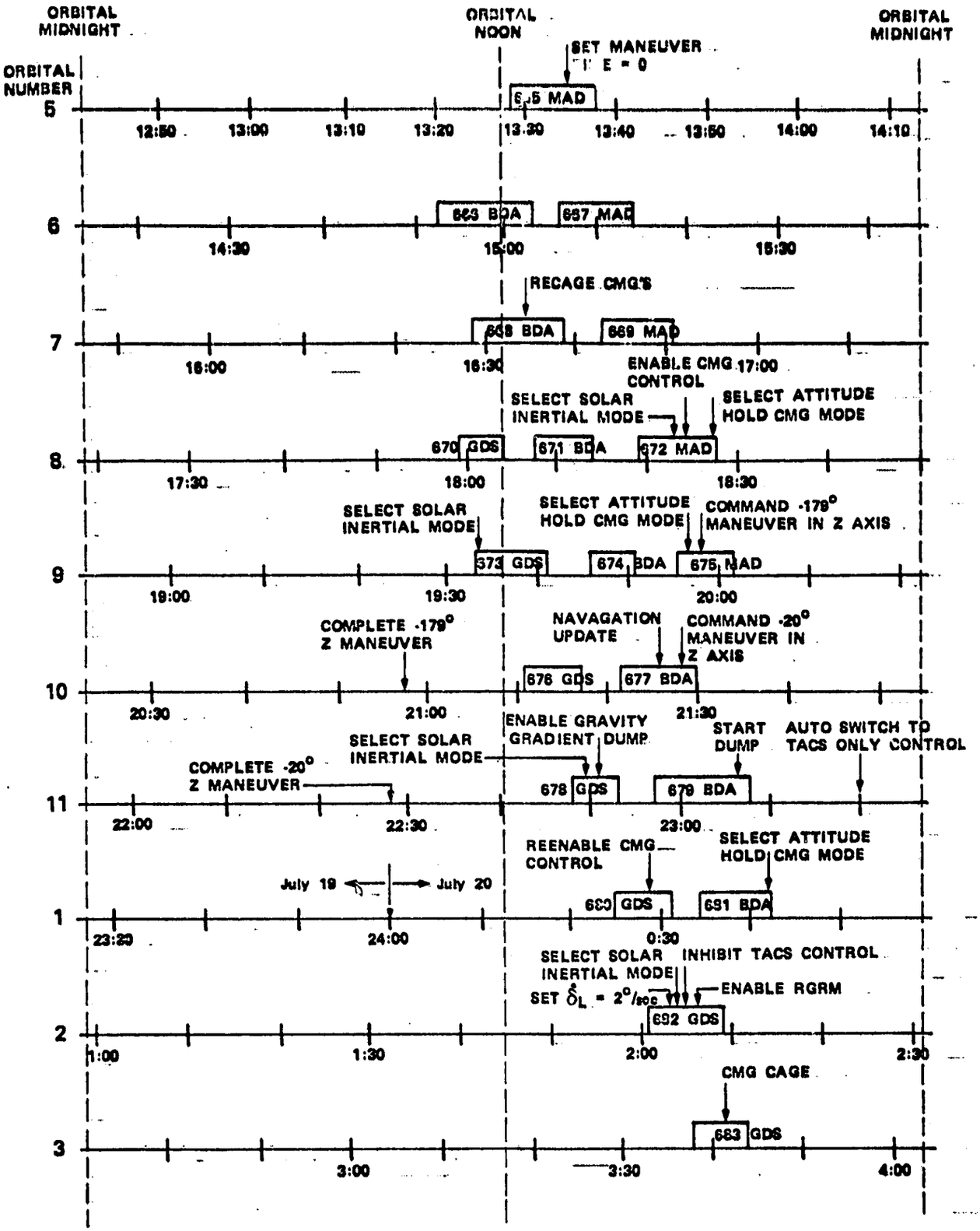

FIGURE 2-13. STATION COVERAGE FOR SOLAR INERTIAL ACQUISITION ON JULY 19 AND 20, 1978

2.2.7.2 Solar Inertial Acquisition

At 13:35 GMT, July 19, (pass 665) the Skylab maneuver time was set to zero in preparation for solar inertial acquisition. The ACQ SS and power system data was then monitored for an opportunity to initiate SI acquisition. This data would indicate when the solar panels were in the field of view of the sun at which time the SI mode would be commanded. However, since the vehicle was rotating about once per 23 minutes and the average station pass was only 8 minutes long, it could be several orbits before the solar panels would be pointing toward the sun over a station pass.

In order to conserve power during CMG spin up. the ATMDC computer was turned off just prior to the last station LOS of each orbit. This allowed the CMGs to drift off the caged position which affected the vehicle spin rate and also resulted in a bad momentum state. At 16:35 GMT, the CMGs were recaged and the ATMDC remained powered up until just prior to reentry on July 11, 1979.

In the eighth orbit of July 19, three station passes were scheduled. AOS of the first pass occurred at 17:59 GMT and LOS of the last pass was at 18:28. This gave 29 minutes of almost continuous coverage except for short gaps between passes. It was almost certain that the vehicle could be captured during these passes.

At 18:22 GMT the sun was inside the linear region of the ACQ SS and the strapdown reference was initialized. As the sun approached zero degrees the strapdown reference was initialized two more times. Then at 18:23 GMT, just after the sun passed through zero degrees in the X axis, the solar inertial mode was selected and CMG control was enabled. By using TACS, the vehicle rates were diminished to zero causing the X and Y axes to "lock" onto the sun. At 18:27, just prior to LOS, the attitude hold CMG mode was selected to freeze the vehicle attitude. (see page 54.)

The position of the X axis with respect to the orbital plane could be estimated by analyzing the CMG momentum changes over an orbit while the vehicle was held in an inertial attitude. After AOS occurred on the ninth orbit, the momentum data indicated that the X axis was approximately 180 degrees away from the desired orientation. At 19:58 GMT a -179 degree maneuver about Z was commanded.

During the next orbit, further analysis of the momentum data indicated that an additional -20 degree maneuver was needed in the Z axis. This maneuver was commanded at 21:28 GMT. Later,

maneuver was unnecessary and that the X axis was actually at the desired attitude prior to the maneuver. This additional -20 degrees was partly responsible for the momentum problems discussed in the following section.

At 22:50 GMT, the solar inertial mode was reselected and gravity gradient dump was enabled. The CMG momentum appeared to be in reasonable condition and, to save TACS fuel, it was decided not to command a CMG cage. The solar inertial acquisition maneuvers nominally when LOS occurred at 23:08 GMT. The solar inertial acquisition maneuvers were almost complete. If all went well, all that remained was to monitor the momentum dump for a few orbits and acquire EOVV the next day. As it turned out, however, some unexpected events occurred prior to the next AOS.

2.2.7.3 CMG Momentum Problems

When AOS occurred at 00:25 GMT on July 20, the flight controllers and system engineers were expecting to see a nominally operating Skylab. Instead, the flight program had executed an automatic switch to TACS only control and the TACS system had used 272 MIB firings and 138 full-on firings for a total of approximately 2000 lbf-sec of TACS fuel. At that time there was no way to have known what had happened so the most reasonable action to take was to reenable the CMGs and select the attitude hold CMG mode while the problem was being analyzed. There were only two more station passes remaining until the Skylab would be out of station coverage for more than seven hours, so an explanation of what happened and a solution to the problem needed to be formulated quickly.

The exact cause of the switch to TACS only control was still not known by the next AOS. However, the Skylab would have to be returned to the SI mode with the dump operating if control was to be maintained through the seven hour period in which there was no ground station coverage. The SI mode was therefore reselected at 2:04 GMT. The gimbal angle rate limit ($\dot{\delta}_L$) was increased to 2 degrees per second in order to give the CMGs more control capability. TACS control was then inhibited to prevent another automatic switch to TACS only control. It was resolved that a rate gyro failure could have produced the observed results and therefore, rate gyro redundancy management (RGRM) was enabled in all three axes.

The Skylab was operating satisfactory when the Goldstone station (pass 683) was acquired at 3:38 GMT. This was the last pass for over seven hours and the CMGs were caged to give them the best chance to remain in control over this period. TACS was

saved. When the Madrid station (pass 684) was acquired at 10:54 GMT, all systems were nominal. Also by this time, the cause of the problem had been discovered.

The automatic switch to TACS only control occurred just after the start of the first GG dump when the X axis attitude error reached 20 degrees. The large attitude error was caused by a phenomena that is referred to as the X-axis momentum siphoning effect. This phenomena had occurred twice during the regular Skylab mission and is described in Section 2.3.2.4 of Reference 1. The X-axis momentum siphoning of July 19, 1978 was brought about by the accumulative effects of three conditions prior to the first dump. First, the Z axis reference was approximately 20 degrees in error which caused more than usual momentum to accumulate. Second, a single sample dump was being executed which does not compensate for the presence of a momentum ramp component. Third, the CMGs had not been caged prior to the dump and therefore were not in the best possible momentum state.

A simulation was made on the AS-II simulator with all flight parameters identical to those of the Skylab vehicle just prior to the dump. The simulation results revealed what had happened after Skylab lost the Bermuda station (pass #679) at 23:08 GMT. Figure 2-14 shows the total momentum and the X axis momentum, attitude error and rate. Because of the X axis momentum siphoning, the X attitude error began to increase and when it reached 20 degrees the flight program switched to TACS only control. Further simulations showed that if this switch to TACS only had been inhibited, the vehicle would not have lost control and the X axis attitude error would have been driven back to zero before the dump was complete.

At this point it was decided to delay the EOVV acquisition and to modify the flight program to prevent any further automatic switch to TACS only control. This requirement was then specified by SWCR #40002 and FF81 buffer 10A was programmed to incorporate the requirement. At 16:12 GMT on July 24, buffer 10A was implemented into the flight program.

2.2.8 Third EOVV Acuqisition From SI

The third EOVV acquisition from solar inertial was very similar to the second EOVV acquisition (See Section 2.2.5). This maneuver was made on July 25, one day following the implementation of buffer 10A. The pertinent APCS commands issued to support the third EOVV acquisition are shown in Table 2-6.

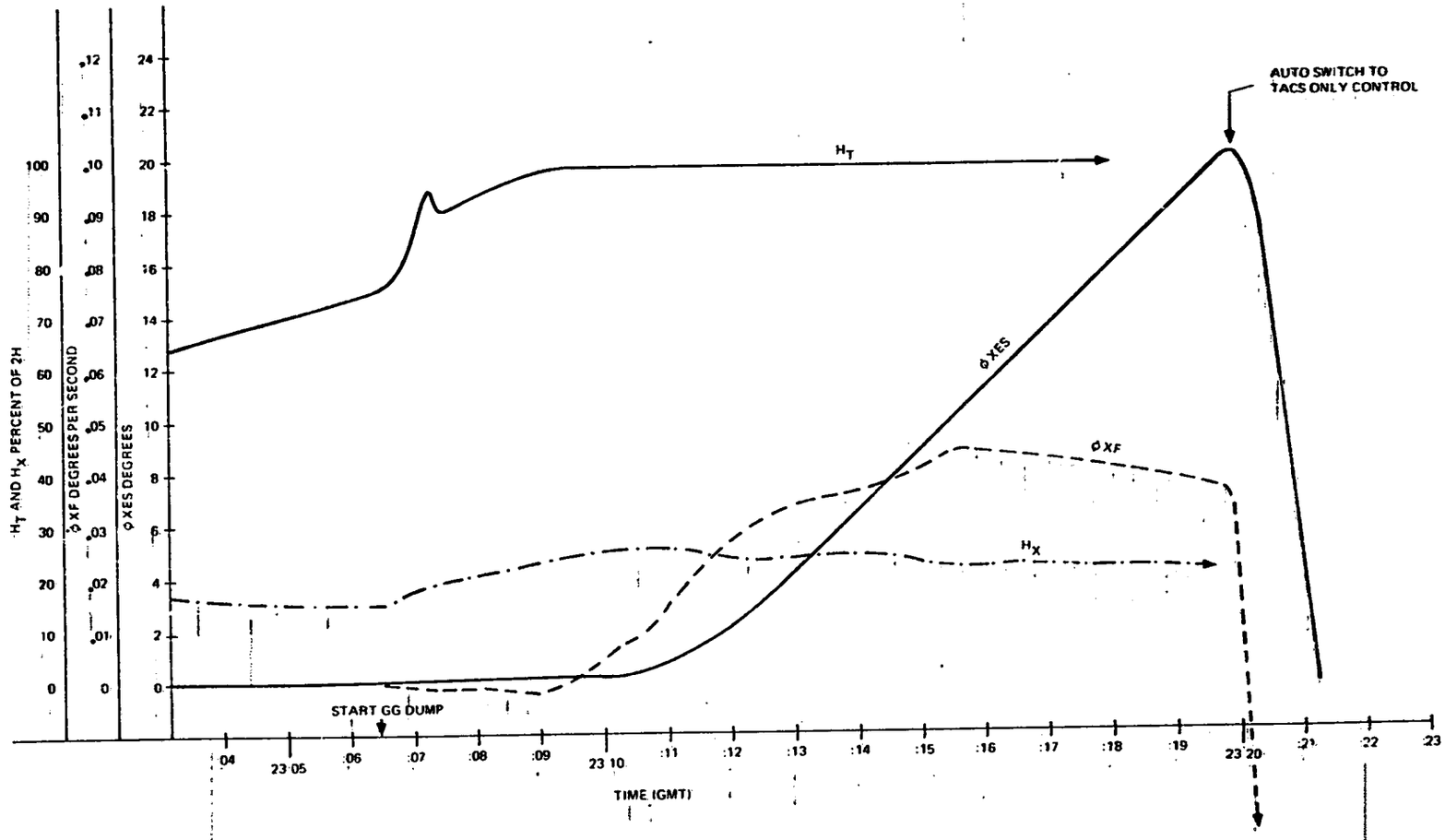

FIGURE 2-14 PLOT OF THE SIMULATED TOTAL MOMENTUM (H_T), X AXIS MOMENTUM (H_X), X AXIS RATE (ϕXF) AND X AXIS ATTITUDE ERROR (ϕXES) DURING THE X AXIS MOMENTUM SIPHONING OF JULY, 19, 1978 (DOY 200)

Table 2-6. Pertinent APCS Commands for the Third EOVV Acquisition From SI

TIME (GMT)	SITE	PASS	COMMAND
(July 24, 1978)			
205: 11: 46: 45	MAD	764	Uplink FF81 buffer 10A
205: 13: 07: 22	BDA	765	Set η_{ym} = .1 radian
205: 13: 08: 14	BDA	765	Set $K\mu_Z$ = 0
205: 13: 09: 16	BDA	765	Set Δe_{TL2} = .16406
205: 13: 10: 16	BDA	765	Set $K_{\eta Z}$ = 2.85/π
205: 16: 11: 36	GDS	769	Implement buffer 10A
(July 25, 1978)			
206: 09: 11: 02	MAD	783	Navigation update
206: 10: 42: 56	MAD	784	Set maneuver time = 10 minutes
206: 12: 07: 32	BDA	785	Inhibit gravity gradient dump
206: 12: 08: 24	BDA	785	Enable TACS control
206: 12: 10: 11	BDA	785	Select ZLV mode
206: 12: 10: 27	BDA	785	Command maneuver bias (X=29.8, Y=9.9, Z=4.2)
206: 13: 43: 25	BDA	787	Command maneuver bias ($X = 0^o$, $Y = 0^o$, $Z = 0^o$)
206: 13: 43: 49	BDA	787	Inhibit CMG control
206: 13: 44: 08	BDA	787	CMG cage
206: 13: 45: 12	BDA	787	CMG cage
206: 13: 48: 11	BDA	787	Enable CMG control
206: 13: 57: 07	MAD	788	Inhibit TACS control
206: 13: 57: 22	MAD	788	Select EOVV
206: 13: 59: 12	MAD	788	Command maneuver bias ($X = 12.2^o$, $Y = 10.7^o$, $Z = 1^o$)
206: 14: 00: 20	MAD	788	Enable TACS control
206: 15: 21: 28	BDA	790	Set $K\mu_Z$ = .2
206: 15: 34: 59	MAD	791	Single memory display, location 0096
206: 15: 36: 57	MAD	791	Inhibit TACS control

An offset ZLV maneuver was commanded at 10:43 GMT with a maneuver time of 10 minutes. At 13:44 GMT and again at 13:45 GMT, commands were issued to cage the CMGs. These commands were issued after the Skylab had been commanded to make a 10 minute maneuver of zero degree attitude change. This caused the CMGs to be caged while the vehicle was in a rate only TACS control mode, which is minimum TACS usage cage procedure. At 13:57 GMT, TACS control was inhibited and the EOVV mode was selected. The EOVV biases were scheduled to be uplinked immediately following EOVV activation. However, the sequence of commands for the EOVV biases had been improperly labeled with an erroneous mark number. When this was discovered, the bias commands were uplinked one at a time using the mark numbers for the individual commands. The uplink of the bias commands was completed at 13:59 GMT, almost 2 minutes late but soon enough so that the EOVV performance was not adversely affected. TACS control was then reenabled at 14:00 GMT. The erroneous mark number was for a command that used switch selector #3 and since this switch selector had been previously powered down, the erroneous command had no effect on Skylab.

After monitoring EOVV performance for an orbit, TACS control was inhibited at 15:37 GMT. The vehicle then remained in this flight configuration until it was maneuvered 180 degrees on November 4, 1978.

Although there were no serious problems between July 25 and November 3, several patches were uplinked to improve the APCS performance. FF81 buffer 11 was implemented on August 12 to improve the calculation of μ_z and η_y (SWCRs 4003 and 4004). FF81 buffer 12, implemented on September 8, modified switchover capability (SWCR 4008), changed the CMG V_{REF} redundancy management constant (SWCR 4009) provided for an automatic adjustment for e_{TN} (SWCR 4006). The strapdown update logic was improved when FF81 buffer 13 (SWCRs 4005 and 4007) was implemented on September 11, 1978. On September 20, 1978, FF81 buffer 14 (SWCR 4015) was implemented to improve the calculation of the gimbal rate command limiting.

2.2.9 EOVV A to EOVV B Transition

On November 4, 1978 Skylab was maneuvered 180 degrees from its normal EOVV orientation with the MDA pointing toward the positive velocity vector (EOVV A) to a new EOVV orientation with the MDA pointing toward the negative velocity vector (EOVV B). The purpose of this maneuver was to increase the probability for extended Skylab lifetime by providing the most favorable thermal conditions, in EOVV operation, to reduce the stress on CMG 2.

Analysis of Skylab data obtained during EOVV operation up to this time showed a relationship between the occurrence of CMG 2 anomalies, the sun angle, and the operating temperature of CMG 2. This data indicated that the stress conditions on CMG 2 could be avoided or reduced by providing a higher operating temperature environment for CMG 2. The EOVV A orientation provided more solar exposure for CMG 2 at positive sun angles while an EOVV B orientation would provide more solar exposure at negative sun angles (Figure 2-15).

The transition maneuver was scheduled for early November 1978 to coincide with the upcoming positive-to-negative change in sun angle (i.e., sun angle movement from North to South of the orbit plane). A modification to the flight software had to be developed (SWCR-S4016, buffer 15) and was implemented to account for computational differences associated with the EOVV A and EOVV B orientations and to automate maneuver sequencing to support the transition maneuvers.

The transition maneuver sequence was developed and simulated, based on available station coverage (Figure 2-16) to minimize TACS utilization and to provide favorable conditions for initiation of EOVV B operations.

Normal and contingency procedures to support the transition maneuver were developed and executed from 11/2/78 through 11/4/78 with the transition maneuver taking place on 11/4/78 as the sun angle passed through zero. It should be noted that the design and simulation effort enabled the maneuver plan to be executed for no TACS usage, saving this limited resource for future operations. Table 2-7 summarizes the pertinent APCS commands for the EOVV A to EOVV B maneuver.

Skylab remained in the EOVV B attitude from November 4, 1978 until January 25, 1979. During this time all Skylab systems functioned satisfactorily.

One software modification was required during EOVV B operation (SWCR-S4019, buffer 16). Its purpose was to insure that all EOVV momentum sample data was utilized in the orbital Z-axis momentum prediction computations. Different sequencing in EOVV B operations caused some samples to be ignored. Buffer 16 was implemented on December 3, 1978.

The sun angle did swing back positive around the mid-point of the EOVV B operation period (see Figure 2-8). However, its magnitude (~27 degrees) and duration (~20 days) were not sufficient enough for the EOVV A orientation to significantly increase the CMG 2 thermal environment over that obtainable by remaining in the EOVV B orientation; and therefore did not warrant a temporary transition back to the EOVV A orientation.

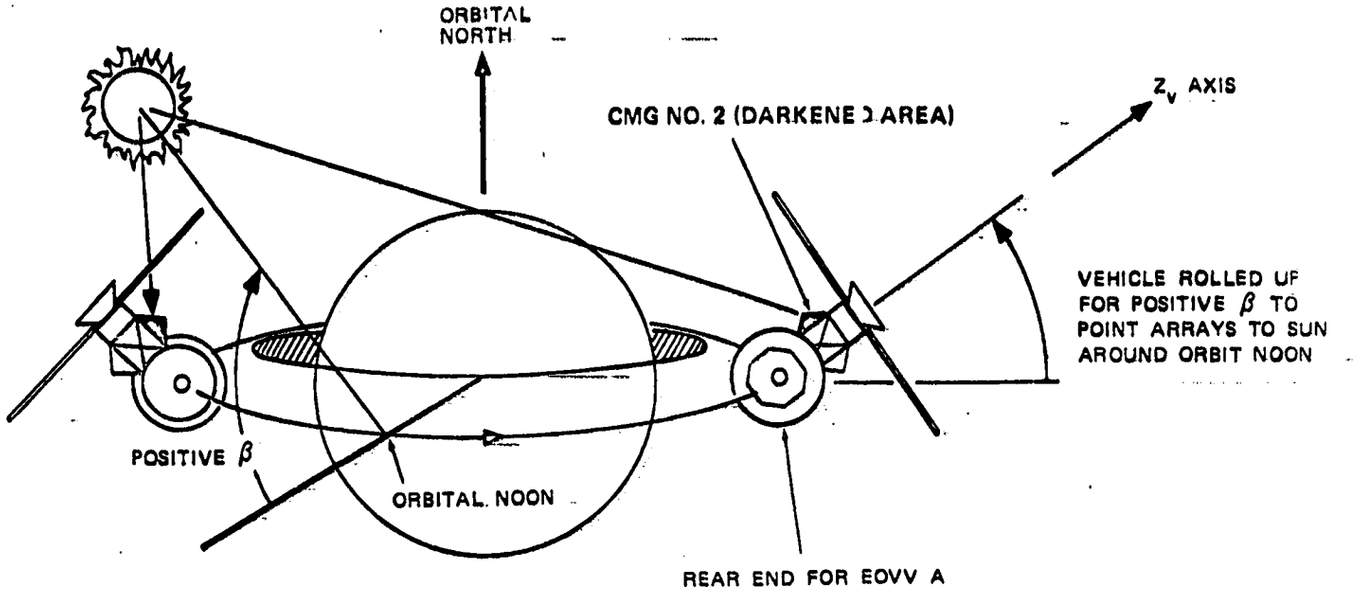

EOVV A ATTITUDE FOR POSITIVE SUN ANGLE (β)

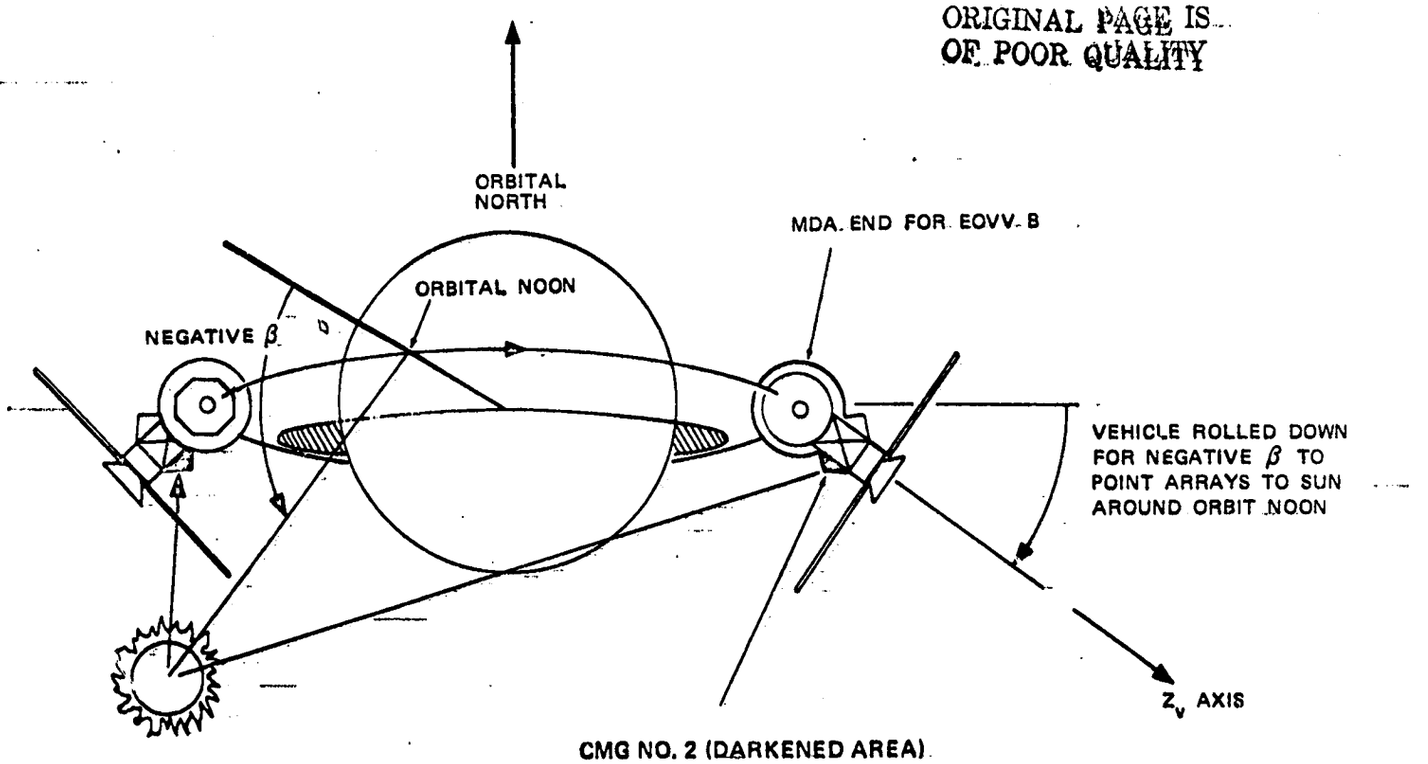

EOVV B ATTITUDE FOR NEGATIVE SUN ANGLE (β)

FIGURE 2-15 EOVV A/B RELATIONSHIP TO CMG NO. 2

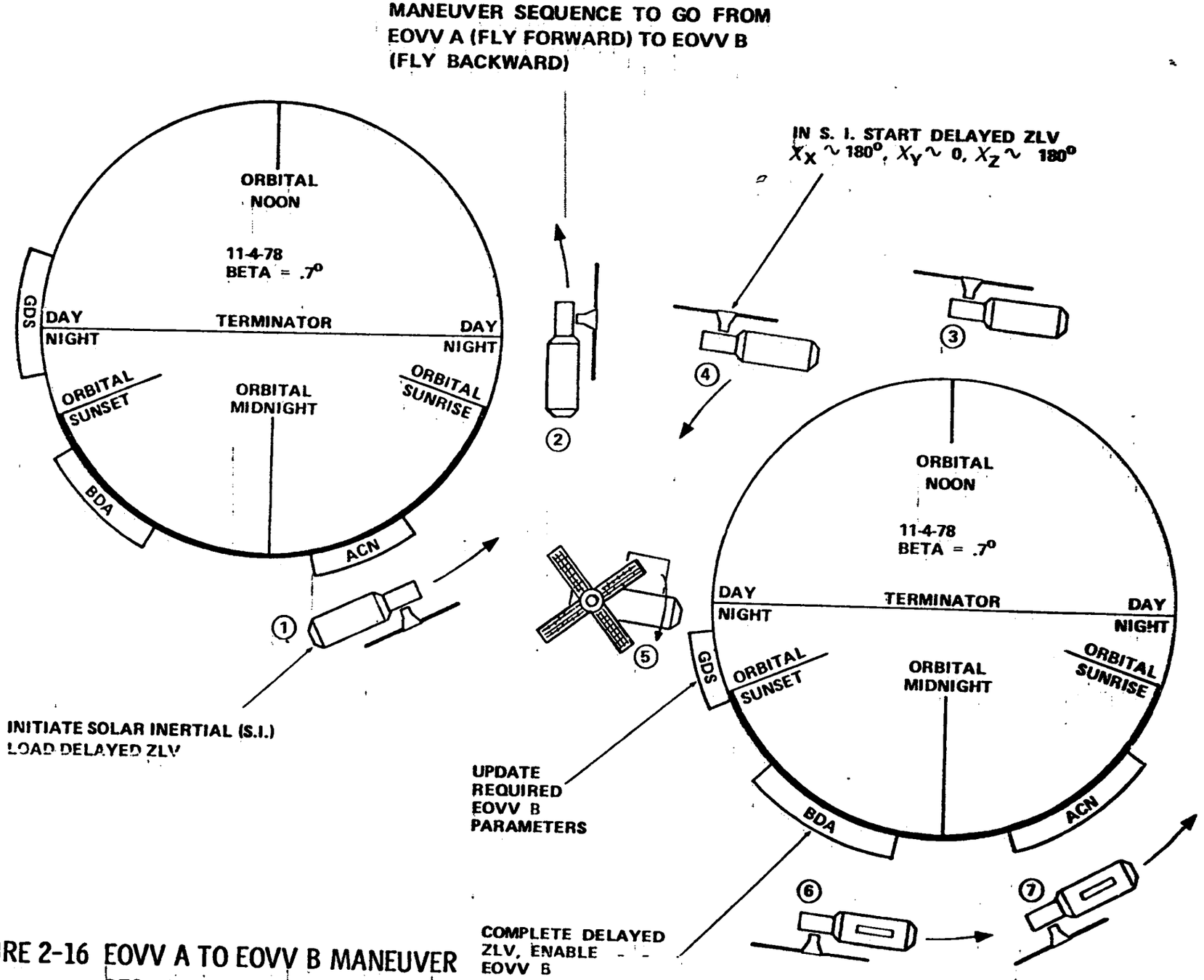

FIGURE 2-16 EOVV A TO EOVV B MANEUVER SEQUENCE

Table 2-7. - Pertinent APCS Commands for the EOVV A to EOVV B Maneuver

TIME (GMT)	SITE	PASS	COMMAND
(November 2, 1978)			
306: 14: 24: 42	ACN	2182	Implement excessive interrupt patch
306: 17: 44: 37	MAD	2184	CMG momentum bias
306: 17: 45: 21	MAD	2184	Enable gravity gradient dump
306: 17: 47: 08	MAD	2184	Display commanded maneuvering time
306: 19: 22: 00	MAD	2185.1	Set maneuver time = 46 minutes
306: 19: 23: 37	MAD	2185.1	Set TACS firing limit = 20 MIBs
306: 19: 25: 14	MAD	2185.1	Display EOVV B flag (loc: 01CE)
306: 20: 45: 15	BDA	2186	Load FF81 Buffer 15
306: 22: 26: 10	BDA	2187	Navigation update
(November 3, 1978)			
307: 01: 25: 03	GDS	2189	Display interrupt enable mask (loc: 0096
307: 01: 52: 30	ACN	2189.1	Implement Buffer 15
307: 03: 01: 47	GDS	2190	Load excessive interrupt patch
307: 09. 51: 17	AGO	2194	Z1 rate gyro bias = 1 LSB
307: 19: 42: 51	BDA	2200	Set erb = -3 LSBs
307: 21: 19: 41	BDA	2201	set $\Delta e_{TN} = 0$
307: 21: 20: 40	BDA	2201	set e_{TL2} min = 0
307: 21: 21: 34	BDA	2201	set e_{TL2} max = .6
307: 21: 22: 41	BDA	2201	Display commanded maneuver time
307: 22: 44: 45	GDS	2203	Enter delayed ZLV command: (Delayed maneuver schedule to begin 308: 01: 41: 53)
307: 22: 45: 32	GDS	2203	Inhibit CMG auto reset
(November 4, 1978)			
308: 00: 20: 48	GDS	2205	Enable switchover to standby mode
308: 00: 22: 24	GDS	2205	Enable TACS Control
308: 00: 34: 30	BDA	2206	X1 rate gyro bias = 0
308: 00: 35: 18	BDA	2206	X3 rate gyro bias = 0
308: 00: 36: 06	BDA	2206	X2 rate gyro bias = 0

Table 2-7 . - Pertinent APCS Commands for the EOVV A to EOVV B Maneuver (Continued)

TIME (GMT)	SITE	PASS	COMMAND
308: 00: 53: 03	ACN	2207	Select solar inertial mode
308: 00: 53: 39	ACN	2207	Set maneuver time = 36 minutes
308: 00: 54: 49	ACN	2207	Display EOVV B flag
308: 01: 58: 48	GDS	2208	Set EOVV B flag
308: 01: 59: 43	GDS	2208	Set $e_{TN} = 0.3$
308: 02: 00: 21	GDS	2208	Set $K\mu_z = 0$
308: 02: 00: 55	GDS	2208	Set $\Delta T_D = 5$ seconds
308: 02: 09: 26	BDA	2209	Y1 rate gyro bias = 0
308: 02: 10: 23	BDA	2209	Y3 rate gyro bias = 0
308: 02: 11: 05	BDA	2209	Y2 rate gyro bias = 0
308: 02: 25: 39	ACN	2210	Inhibit TACS control
308: 02: 28: 22	ACN	2210	Enter EOVV
308: 02: 28: 50	ACN	2210	Attitude Maneuver ($X = -168^{\circ}$, $Y = 169^{\circ}$, $Z = 1^{\circ}$)
308: 03: 49: 39	BDA	2212	Inhibit switchover to standby mode
308: 05: 12: 42	GDS	2213	Set $K\mu z = .2$
308: 05: 13: 40	GDS	2213	Set $\Delta e_{TN} = 0.05$
308: 05: 14: 40	GDS	2213	X1 rate gyro bias = 2 LSBs
308: 05: 15: 33	GDS	2213	X3 rate gyro bias = -2 LSBs
308: 05: 16: 26	GDS	2213	Z1 rate gyro bias = -2 LSBs
308: 05: 17: 36	GDS	2213	Z3 rate gyro bias = 1 LSB
308: 05: 18: 33	GDS	2213	X2 rate gyro bias = 2 LSBs
308: 05: 19: 31	GDS	2213	Z2 rate gyro bias = -2 LSBs
308: 06: 50: 16	GDS	2214	Y1 rate gyro bias = 2 LSBs
308: 06: 51: 15	GDS	2214	Y3 rate gyro bias = 3 LSBs
308: 06: 51: 58	GDS	2214	Enable CMG auto reset
308: 06: 52: 41	GDS	2214	Display interrupt enable mask

2.2.10 EOVV B to SI Acquisition

In concert with the decision of December 19, 1978 to discontinue plans for a Skylab reboost or deorbit mission was the directive to maintain Skylab operations until further specific plans were developed. Presumably these plans would provide for an orderly shutdown of Skylab after first collecting scientific and engineering data from the onboard systems and experiments. Skylab was then committed to remain in the EOVV B attitude as a holding pattern. Subsequently MSFC and JSC were directed to investigate the possibilities of controlling or influencing Skylab reentry. A decision with respect to maintaining Skylab operations had to be made prior to the end of January 1979 because the sun angle (β) would go through zero heading positive at that time. If Skylab remained in the EOVV B attitude past this time, the temperature of the bearings on CMG #2 would drop enhancing the conditions for CMG #2 anomalies. Since the possibility of controlling Skylab reentry could not be positively ruled out, the decision was made by NASA to return Skylab to the solar inertial attitude until a decision could be reached relative to Skylab reentry control. The primary reason for acquiring solar inertial rather switching from EOVV B to EOVV A was the reduced operational maintenance required while in the solar inertial control mode.

Therefore, on January 25, 1979, Skylab was maneuvered from EOVV B to the solar inertial attitude using the delay SI maneuver feature incorporated into the flight software for the Skylab Reactivation Mission. This feature allowed phasing of the maneuver relative to orbit position without regard to station coverage and the maneuver to SI was accomplished without using any TACS impulse. A time history of the DCS commands for this event is presented in Table 2-8.

The aerodynamic drag with Skylab in the solar inertial attitude was dependent upon the sun angle but in all cases was much more than the drag experienced in EOVV. Therefore, with the acquisition of the SI attitude, Skylab's return to earth was accelerated as shown in Figure 2-1.

Following SI acquisition a 5 degree roll maneuver was commanded about the X axis to expose CMG #2 to more sunlight. This maneuver was performed to help prolong the lifetime of CMG #2.

Table 2-8.. Pertinent APCS Commands for the SI Acquisition on January 25, 1979

TIME GMT	SITE	PASS	COMMAND
(January 24, 1979)			
024:15:52:40	GDS	3371	Set e_{rb} = .015625
024:17:41:50	BDA	3372.1	Display commanded maneuver time, DSBTAU (loc 6FDA)
024:17:43:21	BDA	3372.1	Display GG dump half angle (loc 700E)
024:21:01:25	AGO	3374	CMG gimbal rate limit = 1 degree/second
024:21:02:50	AGO	3374	Display CMG gimbal rate limit (loc 01D8)
024:21:05:40	AGO	3374	Navigation update
(January 25, 1979)			
025:05:29:25	MAD	3379	CMG momentum bias
025:05:30:34	MAD	3379	Set TACS firing limit = 40 MIBs
025:05:31:51	MAD	3379	Display TACS firing limit (loc 01CC)
025:05:33:34	MAD	3379	Command delayed solar inertial mode
025:05:34:15	MAD	3379	Display interrupt enable mask (loc 0096)
025:05:35:00	MAD	3379	Enable switch over to standby
025:08:28:44	BDA	3380.1	Enable TACS control
025:09:47:05	-	-	Delayed SI entry
025:10:05:02	BDA	3381.1	X1 rate gyro bias = 0
025:10:05:28	BDA	3381.1	X3 rate gyro bias = 0
025:10:05:54	BDA	3381.1	Y1 rate gyro bias = 0
025:10:06:17	BDA	3381.1	Y3 rate gyro bias = 0
025:10:06:49	BDA	3381.1	Z1 rate gyro bias = 0
025:10:07:23	BDA	3381.1	Z2 rate gyro bias = 0
025:11:34:04	GDS	3381.3	SelectACQ SS1 and 2 for X axis, SSRM enabled
025:11:34:44	GDS	3381.3	Select ACQ SS 1 and 2 for Y axis, SSRM enabled
025:11:55:39	MAD	3381.5	Command maneuver bias (X = 5^{o}, Y = 0^{o}, Z = 0^{o})
025:16:23:02	GDS	3383.2	Inhibit TACS control
025:16:24:41	GDS	3383.2	Inhibit switch over to standby mode
025:18:08:56	BDA	3385	X2 rate gyro bias = 0
025:18:09:55	BDA	3385	Y2 rate gyro bias = 0
025:18:10:49	BDA	3385	Z3 rate gyro bias = 0

2.2.11 Tea Control Acquisition from SI

On May 19 and 20, 1979, the Torque Equilibrium Attitude (TEA) software patch (SWCR 4022, Memory Load Buffers 18 through 22) was uplinked to the ATMDC flight program. This patch provided the capability to maintain attitude control of the vehicle to within a few hours of Skylab reentry. This was possible because in a TEA attitude, aerodynamic torques counterbalanced gravity gradient torques and gyroscopic torques.

The TEA attitude control law was developed after the decision was made to abandon plans for a Skylab reboost/deboost mission. This control law was unique because it was the first spacecraft control scheme which used upper atmospheric aerodynamic torques to desaturate CMG momentum. In the normal SI Skylab Mode, CMG momentum was managed by dumping excess momentum using gravity gradient torques. In a TEA attitude, the aerodynamic torques and gravity gradient torques are equal and opposite. By offsetting the vehicle slightly from this attitude the relative magnitudes of the gravity gradient and aerodynamic torques can be increased or decreased as desired to maintain the CMG momentum at the desired state. The TEA control law was developed, programmed and verified between January and May, 1979.

There were several TEA attitudes and each resulted in different atmospheric drag on the vehicle. The limiting factors in maintaining control were meeting the electric power requirements and being in a dense enough atmosphere to generate the desired aerodynamic torques. Most of the TEA attitudes were unuseable because the Skylab solar arrays could not collect sufficient solar energy to run the various Skylab systems in the specified attitude. Other attitudes could be used only during a range of certain sun angles and below certain altitudes. Two of the usable attitudes, the T275 and T121G are shown in Figure 2-17. The T275 attitude has a smaller projection of surface area into the direction of flight and a corresponding lower atmospheric drag than the T121G attitude. By maneuvering between TEA attitudes the drag on the vehicle could be modulated to slow or speed the desired descent rate of Skylab. This provided the capability to shift the reentry time several orbits if necessary.

Based on early reentry predictions of mid June, 1979, initial procedures were developed to begin TEA operations in the T121G attitude on May 26, 1979. At this time the vehicle altitude was predicted to be approximately 150 n.m. and the sun angle profile such that the T121G attitude would supply sufficient solar power from this point to the predicted reentry. However as the time approached, it became apparent that Skylab was not reentering as fast as predicted and reentry slipped to early July, 1979.

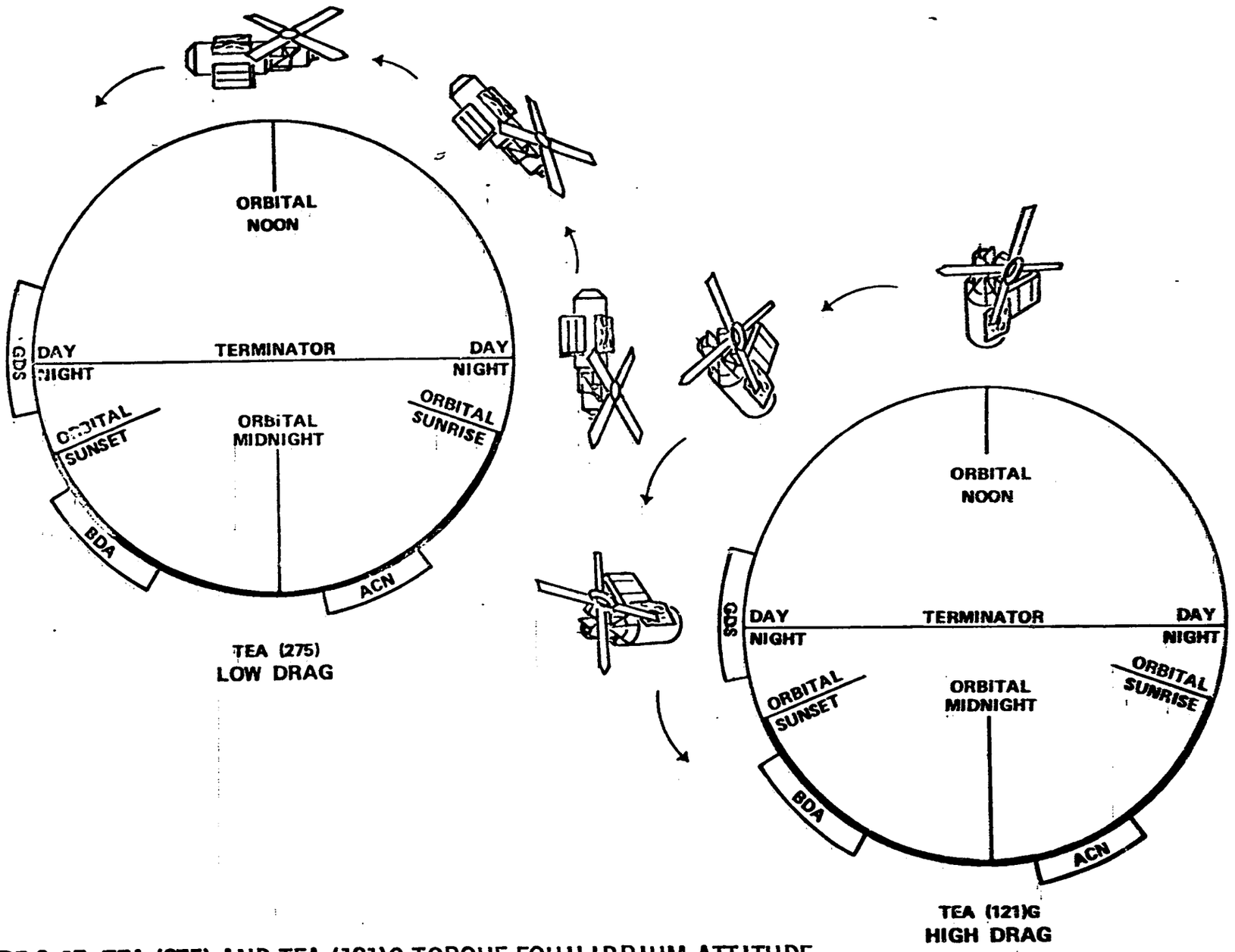

FIGURE 2-17 TEA (275) AND TEA (121)G TORQUE EQUILIBRIUM ATTITUDE

As a result of this delay in reentry, a maneuver from T121G to T121P or T275 would be required to provide sufficient power over the sun angle range from 26 of May to reentry. Because of this and the fact that Skylab would be around 157 n.m. on 26 May, it was decided to delay TEA operations and stay in SI control until late June, 1979. In the June 18-20 time frame, Skylab altitude would be approaching its lower limit for SI control (140 nm) and the sun angle would be such that the T121P (Figure 2-18) attitude would provide sufficient power all the way to reentry.

In addition to requiring only one TEA orientation for solar power, this delay provided additional benefits. More time was available for TEA control analysis; development of procedures for power management, rate gyro bias compensation, TEA parameter updating, and contingencies; and ground controller training.

On May 20, the altitude of the vehicle was approximately 160 n.m. Skylab could be controlled in the SI Mode only until approximately 140 n.m. The Skylab descent rate and expected solar activity indicated that this altitude would be reached near June 18-20. Because of the sun angle at this time, the T121P attitude was the most favorable of the TEA attitudes that were available. This attitude, shown in Figure 2-18 was near perpendicular to the orbital plane and the velocity vector and provide a high atmospheric drag on the vehicle.

The sun angle would allow sufficient power for the T121P attitude through the end of July, which was well past the predicted reentry time. Also, as reentry neared greater atmospheric density would allow the T275 attitude to be useable. It was planned to use the T121P and T275 attitudes for drag modulation during the final 36 hours prior to reentry if the predicted reentry occurred during a highly populated orbit.

On June 17, preparations were begun for the T121P attitude acquisition by uplinking the desired TEA control parameters. (All APCS commands pertinent to the TEA acquisition are shown in Table 2-9). On June 19, the SLOPE matrix was uplinked and sectors 58 and 59 of the flight program were transmitted by memory dump to verify that all TEA variables were correct. Computer timing was then selected in order to prevent computational overflows associated with the sun timing scheme at low altitudes. At 21:23 GMT on June 19, the five degree offset about the axis was removed. All preparations were then complete for the T121P acquisition on June 20.

At 3:24 GMT, June 20, the delayed ZLV commands containing the time to start TEA acquisition and the ZLV offsets were uplinked. At 4:50 GMT, TACS control was reenabled. At 8:17 GMT, the CMG gimbal rate limit was increased to 2 degrees/second to allow for more control authority during acquisition and initial phases of

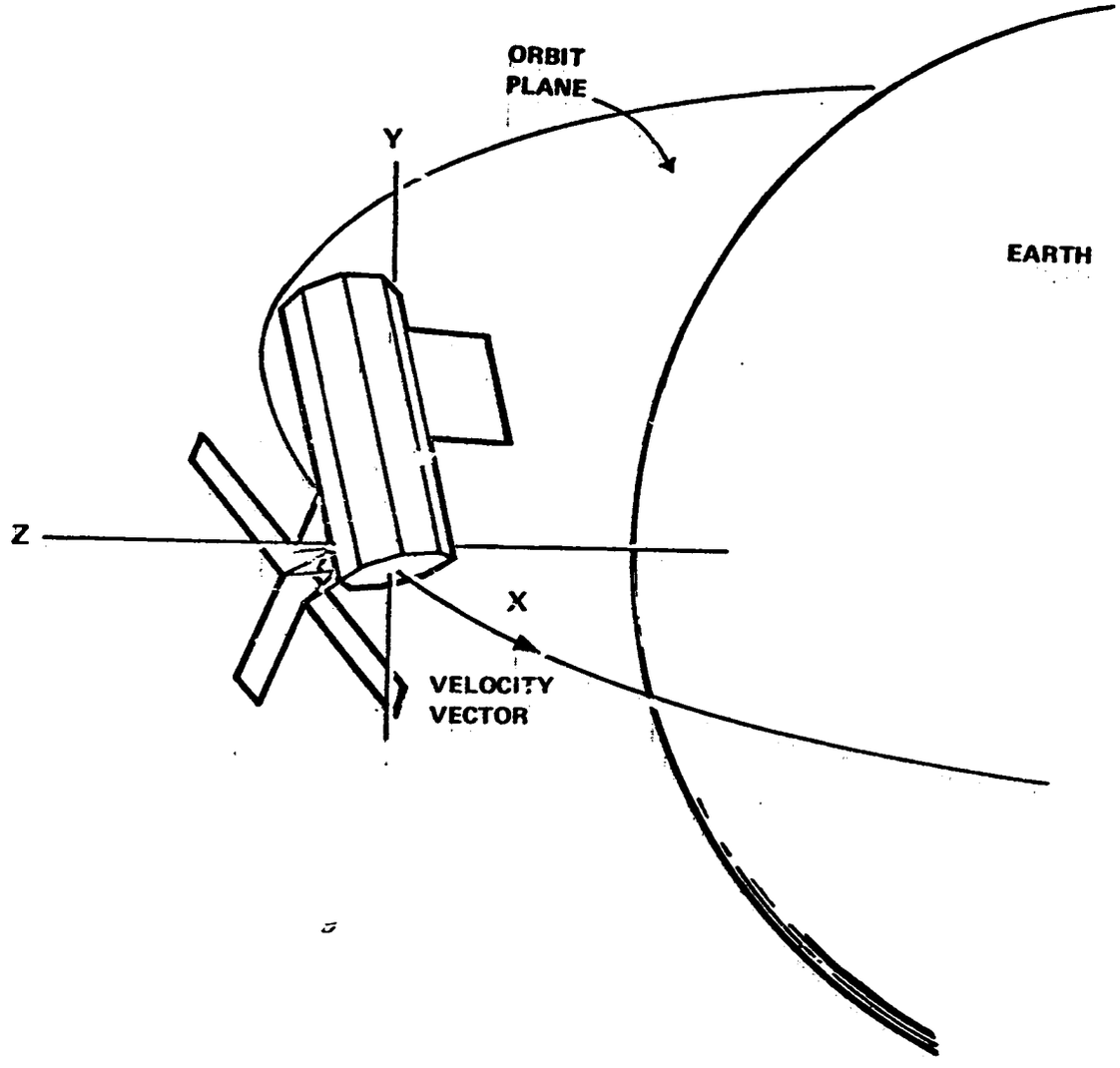

FIGURE 2-18 T121P TORQUE EQUILIBRIUM ATTITUDE

Table 2-9. Pertinent APCS Commands for the TEA Acquisition on June 20, 1979

TIME (GMT)	SITE	PASS	COMMAND
(June 17, 1979)			
168: 00: 19: 53	GDS	4459	Update e_{TLN1}
168: 01: 49: 29	GDS	4460	Update e_{TLN2}
168: 01: 50: 22	GDS	4460	Update e_{TLN3}
168: 01: 50: 50	GDS	4460	Update KDTHX
168: 01: 51: 23	GDS	4460	Update KDTHZ
168: 01: 51: 51	GDS	4460	Update KEF
168: 01: 52: 19	GDS	4460	Update DTHL1
168: 01: 52: 45	GDS	4460	Update DTHL2
168: 04: 57: 45	GDS	4462	Update DTHL3
168: 04: 58: 07	GDS	4462	Update DPHL1
168: 04: 58: 45	GDS	4462	Update DPHL3
168: 04: 59: 29	GDS	4462	Update DEL1
168: 04: 59: 57	GDS	4462	Update DEL2
168: 05: 00: 17	GDS	4462	Update DEL3
168: 05: 00: 41	GDS	4462	Update TDESAT
168: 05: 01: 04	GDS	4462	Update DPH3CL
168: 06: 33: 13	GDS	4463	Update maneuver time
(June 18, 1979)			
169: 00: 13: 04	GDS	4473	Navigation Update
(June 19, 1979)			
170: 00: 11: 03	GDS	4486	Navigation Update
170: 19: 46: 51	GDS	4496.1	Update slope matrix
170: 19: 47: 27	GDS	4496.1	Memory dump (sectors 58 and 59)
170: 21: 19: 56	GDS	4497.1	Select computer timing
170: 21: 23: 06	GDS	4497.1	Remove 5 degree bias in X
(June 20, 1979)			
171: 03: 24: 39	BDA	4500.1	Delayed ZLV commanded

Table 2-9. Pertinent APCS Commands for the TEA Acquisition on June 20, 1979 (Continued)

TIME (GMT)	SITE	PASS	COMMAND
171: 04: 48: 25	BDA	4501	Update ΔMIB
171: 04: 49: 36	BDA	4501	Enable TACS
171: 04: 51: 36	BDA	4501	Navigation Update
171: 06: 21: 44	GDS	4502	Enable switchover to standby
171: 06: 42: 51	GDS	4502	Update Δ MIB
171: 08: 17: 06	AGO	4503	CMG Rate Limit = 2 degrees/second
171: 12: 55: 00	-	-	ZLV Maneuver initiated
171: 13: 00: 53	AGO	4504.1	CMG Cage
171: 13: 14: 04	ACN	4504.2	Update X1 rate gyro drift
171: 13: 14: 28	ACN	4504.2	Update X3 rate gyro drift
171: 13: 14: 55	ACN	4504.2	Update Z1 rate gyro drift
171: 13: 15: 20	ACN	4504.2	Update Z2 rate gyro drift
171: 13: 15: 56	ACN	4504.2	Enable CMG control
171: 13: 16: 21	ACN	4504.2	Enable TEA control
171: 13: 17: 06	ACN	4504.2	Update Δ MIB
171: 13: 17: 51	ACN	4504.2	Update maneuver time
171: 13: 18: 16	ACN	4504.2	Enable TACS
171: 16: 33: 25	MAD	4505	Update X1 rate gyro drift
171: 16: 34: 13	MAD	4505	Update X3 rate gyro drift
171: 16: 35: 00	MAD	4505	Update Z1 rate gyro drift
171: 16: 35: 46	MAD	4505	Update Z2 rate gyro drift
171: 16: 36: 03	MAD	4505	Update maneuver time
(June 21, 1979)			
172: 02: 04: 11	ACN	4511	CMG rate limit = 1 degree/second.

TEA control. The maneuver sequence for going from solar inertial to T121P is shown in Figure 2-19. The delay ZLV maneuver was initiated at 12:53 GMT while the vehicle was outside of site coverage. At 13:01 GMT, shortly after the Santiago station was acquired, the CMGs were caged to the momentum desired for the new TEA attitude. At 13:13 GMT, the maneuver to the TEA attiude was complete.

When the Ascension station was acquired, new rate gyro biases were uplinked. These biases had been previously analyzed and were designed to offset the strapdown reference drift toward a favored direction. The vehicle could be controlled with these biases until the correct rate gyro biases could be computed. Next, CMG control was reenabled to terminate CMG caging and TEA control was initiated.

The total maneuver to TEA control, including the offset ZLV maneuver and CMG cage used approximately 700 lb-sec of TACS fuel. Once TEA control was activated, no TACS was required until reacquisition of TEA control on June 24.

The correct rate gyro biases were computed as a function of the ACQ SS data and the strapdown reference. Procedures had been developed to slightly reorient the T121P attitude so that the ACQ SS's would acquire sun presence. Rate gyro bias information was then computed each orbit and new biases were uplinked as required. The first set of biases following TEA acquisition were uplinked between 16:33 and 16:36 GMT.

Several hours after TEA acquisition, it was noticed that small errors were beginning to accumulate in the TEA reference quarternion (QBL) causing the QBL elements to become unnormalized. An analysis of the flight program showed that this was due to computational drift caused by truncation in the ATMDC. This problem was temporarily solved by developing buffer T14 which reinitialized the QBL quaternion to nominal values. This patch was implemented three times between June 21 and June 22 while a permanent patch was being developed.

The permanent patch, specified by SWCR 4023 and implemented in Buffer 23 was uplinked June 22. This patch renormalized the QBL quaternion approximately once per orbit and corrected the effects of the QBL drift. This was the last software patch implemented into the ATMDC.

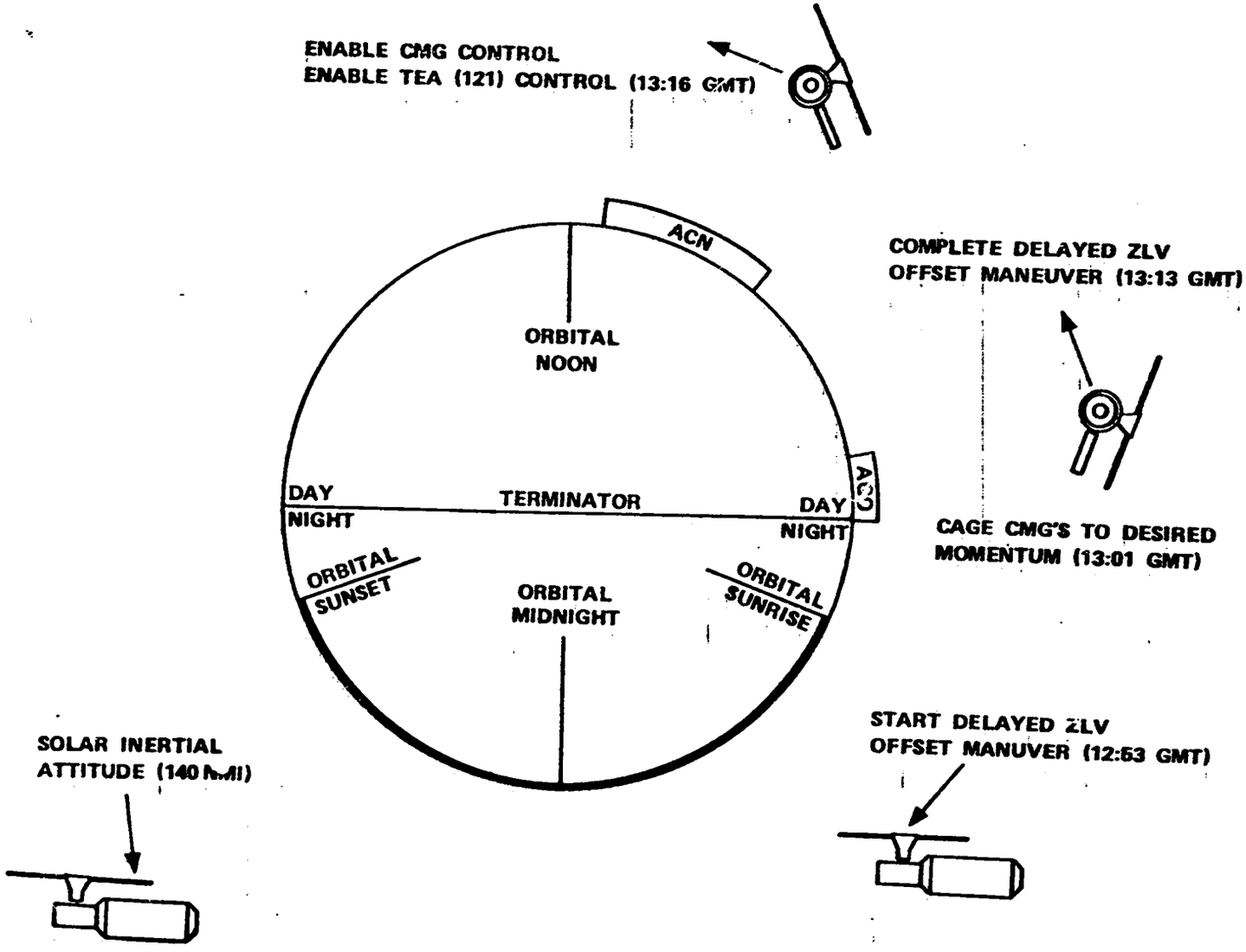

FIGURE 2-19 MANEUVER SEQUENCE TO GO FROM SI TO TEA (121)P ON JUNE 20, 1979

2.2.12 Tea Control Reacquisition

To support the normal maintenance of TEA control, the slope matrix was programmed to receive updates by ground uplink. This was a 3 by 3 matrix relating the momentum errors to attitude errors about the torque equilibrium attitude. This slope matrix was a function of atmospheric density and the TEA attitude. Since atmospheric density was increasing with the vehicle descent, the slope matrix required periodic adjustment.

At 16:13 GMT on June 24, the first slope matrix update since TEA acquisition was uplinked. However, the flight program required that the slope matrix elements be commanded in row order, but it was uplinked from the ground in column order. This meant that the elements in the slope matrix were reversed and the flight program had actually received the transpose of the desired matrix. With an incorrect slope matrix, the vehicle cannot properly manage the CMG momentum and will slowly lose attitude control.

The first pass through the TEA control calculations with the transposed slope matrix occurred after the telemetry station was lost. There was no indication of a problem until the next station acquisition occurred at 17:44 GMT. The telemetry data from this station showed that the CMG momentum was becoming saturated, TEA control parameters were off-nominal, TACS had been used and that, in general, TEA control authority was being lost. An analysis of the DCS commands issued during the previous pass was made and it was discovered that the transpose of the slope matrix had been transmitted.

A contingency TEA control reacquisition procedure had been previously developed for use during the initial TEA control acquisition. Although this contingency procedure was developed assuming that TEA control might be lost due to an offset in the assumed X axis center of pressure, it also applied to the current situation. The commands necessary for the procedure were already resident at the ground stations and were readily available. The reacquisition procedure was executed when the next station coverage occurred over Madrid. (All pertinent APCS commands issued during TEA control reacquisition are shown in Table 2-10).

First, the maneuver time was updated to 20 minutes for the upcoming ZLV maneuver. Next, the CMG rate limit was increased to 2 degrees/second for added CMG control authority. TEA control was then inhibited, the allowable minimum Impulse Bits (MIBS)

Table 2-10. Pertinent APCS Commands for the TEA Control Reacquisition on June 24, 1979

TIME (GMT)	SITE	PASS	COMMAND
(June 24, 1979)			
175: 16: 12: 35	MAD	4557	Slope Matrix Update (elements reversed)
175: 16: 12: 48	MAD	4557	ETLN1 = 0.1
175: 16: 13: 17	MAD	4557	ETLN3 = -0.7
175: 19: 18: 29	MAD	4559	Update maneuver time (20 minutes)
175: 19: 19: 20	MAD	4559	CMG rate limit = 2 degrees/second
175: 19: 19: 32	MAD	4559	Inhibit TEA control
			Update ΔMIB
			Enable TACS
			Enable CMG control
			Select ZLV
175: 19: 19: 53	MAD	4559	Attitude maneuver to desired ZLV offset
175: 19: 20: 19	MAD	4559	Inhibit CMG control
175: 19: 20: 30	MAD	4559	CMG Cage
175: 19: 20: 43	MAD	4559	ETLN1 = 0.0
175: 20: 30: 33	GDS	4560	Slope Matrix Update (Elements corrected)
175: 20: 30: 55	GDS	4560	Enable TACS control
175: 20: 31: 20	GDS	4560	Enable CMG control
175: 20: 31: 42	GDS	4560	Enable TEA control
175: 20: 52: 22	MAD	4560.1	ETLN1 = 0.05
175: 22: 06: 10	GDS	4561	CMG rate limit = 1 degree/second

per half orbit expended by the TACS was increased to 700 MIBs and TACS and CMG control were reenabled to initialize the TACS counters. ZLV was then selected and the desired ZLV offsets were uplinked. This commanded the vehicle to maneuver back to the T121P attitude. Next, CMG control was inhibited and the CMGs were caged to the nominal T121P values.

When the Goldstone station was acquired at 20:29 GMT, the vehicle was back in the T121P attitude with the CMG's in the desired momentum state. The correct slope matrix was uplinked; and TACS control, CMG control and TEA control were then reenabled. An orbit later, it was seen that TEA control was performing properly. The CMG rate limit was then reduced back to one degree/second.

The entire process of losing TEA control and reacquiring TEA control used approximately 1100 lb f-sec of TACS fuel. Although this fuel usage had been unplanned, there was still sufficient fuel remaining for any required maneuvers prior to reentry.

2.2.13 Skylab Reentry

Following acquisition of TEA control, detailed procedures were developed which would provide flight controllers with a limited amount of reentry control capability. Procedures to maneuver Skylab from the high-drag T121P attitude to a low-drag TEA (T275) or ZLV attitude were developed to provide a means of shifting the reentry prediction. By maintaining a low-drag attitude, the orbit lifetime could be extended over that in the T121P attitude. This would make it possible to shift the predicted reentry from an orbit of high population density to one with a lower population density.

Since several factors indicated that TEA control (T121P or T275 and TACS only control could not be reliably maintained below 80 n.m., procedures were also developed to initiate a random vehicle tumble. A random tumble results in a predictable average drag which can be used in reentry predictions. By controlling the time at which the vehicle drag changed due to a tumble, the impact prediction accuracy could be maintained. However, if the tumble occurred at some unknown time due to a loss of TEA or TACS only control, the impact prediction would be degraded.

Beginning on July 9 at 48 hours prior to predicted reentry and each six hours thereafter, NORAD supplied NASA Headquarters, MSFC and JSC with Skylab tracking data and reentry predictions. Communications between these centers was constantly maintained over a telecommunications network loop. Decisions pertaining to

executing procedures for shifting Skylab reentry were made by NASA Headquarters under a set of previously defined groundrules.

The NORAD data received between the 48 and 18 hour-to-go time points indicated that Skylab would reenter during a low population density orbit. The decision at each 6 hour point during this interval was therefore to continue in the T121P attitude as long as the control authority and station coverage permitted. The 12 hour-to-go NORAD data confirmed the previous reentry predictions. Based upon the favorable reentry predictions, the available station coverage, and increasing difficulty in maintaining vehicle control, the decision was made to command a tumble at 07:45 GMT on July 11.

The APCS commands issued in preparation for reentry are shown in Table 2-11. The slope matrix was updated for the last time at 3:35 GMT, July 11 and the last navigation update was issued at 3:38 GMT. At 4:54 GMT, the TACS firing limit was updated to its maximum value in preparation for the tumble. At 6:26 GMT, a delayed SI acquisition command was uplinked with the maneuver indication time corresponding to 7:45 GMT. While maneuvering to SI, the aerodynamic torques increased significantly causing the APCS to fire TACS in an attempt to maintain control. When the TACS was expended control authority was lost and the aerodynamic torques put the vehicle into a tumble.

In order to save battery power and ensure telemetry for the remaining station passes, commands were issued at 8:21 GMT to remove power from the CMGs. Because of spurious commands associated with switch selection 3, the CMG power off commands were later reissued for CMG #1 and CMG #2. At 9:39 GMT the standby mode was selected and at 9:43 GMT the APCS was powered off.

On subsequent passes, the APCS was powered back on to allow flight controllers to receive ATMDC telemetry. When the APCS was powered up for the last time over the Ascension station, ATMDC data showed that the rate gyros were saturated in all three axes which meant that the vehicle rates were greater than 1 degree/second. The power system data indicated that the solar panels were beginning to separate from the vehicle. The Ascension station was lost at 16:06 GMT, and Skylab reentered prior to acquisition of the next ground station.

Table 2-11. Pertinent APCS Commands for Skylab Reentry

TIME (GMT)	SITE	PASS	COMMAND
(July 10, 1979)			
191:17:59:20	BDA	4774	Update slope matrix.
191:18:00:10	BDA	4774	Update maneuver time
191:19:21:33	GDS	4775	Update CMG momentum bias
191:19:22:11	GDS	4775	Memory dump (Sector 56)
191:20:52:43	GDS	4776	Update DTHL1
191:20:53:09	GDS	4776	Update DTHL3
191:20:53:39	GDS	4776	CMG Rate Limit = 2 degrees/second
(July 11, 1979)			
192:03:35:29	ACN	4778	Update Slope Matrix
192:03:37:53	ACN	4778	Navigation Update
192:04:53:44	AGO	4779	Update ΔMIB
192:06:25:37	AGO	4781	Delayed SI commanded
192:07:45:00	-	-	SI Maneuver Initiated (begin tumble)
192:08:20:56	MAD	4783	CMG 1 powered off
192:08:21:11	MAD	4783	CMG 2 powered off
192:08:21:26	MAD	4783	CMG 3 powered off
192:09:38:09	BDA	4784	CMG 1 powered off
192:09:38:47	BDA	4784	Select standby mode
192:09:42:51	BDA	4784	APCS powered off
192:09:52:58	MAD	4784.1	APCS powered on
192:11:11:33	BDA	4785	CMG 2 powered off
192:11:25:00	MAD	4786	APCS powered off
192:15:46:49	BDA	4790	APCS powered on
192:15:49:26	BDA	4790	APCS powered off
192:16:01:31	ACN	4791	APCS powered on
192:16:37:28	-	-	Reentry

2.3 ALTITUDE CONTROL MAINTENANCE

An essential part of the reactivation mission was the activity required to maintain the vehicle in the various attitudes that were operational between SI acquisition on June 9, 1978 and reentry on July 11, 1979. In order to maintain attitude control, the ATMDC telemetry, APCS hardware data and the vehicle environment required considerable analysis. The following sections describe the maintenance required for attitude control of the EOVV, solar inertial and TEA control modes.

2.3.1 EOVV Maintenance

The EOVV operations began on 6/11/78 and after two early anomalies (refer to Sections 2.2.4 and 2.2.6) the EOVV attitude was maintained from 7/25/78 until 1/25/79. The EOVV A attitude (MDA Forward) was maintained continuously from 7/25/78 until 11/4/78 when Skylab was maneuvered 180 degrees to the EOVV B attitude (MDA trailing). The EOVV B attitude was then maintained continuously from 11/4/78 until 1/25/79 when Skylab was maneuvered to the Solar Inertial attitude after it was decided that Skylab could not be saved.

Several ground support operations were required to maintain EOVV. These ground support functions included:

1) software modification to aid EOVV management and provide new operating capabilities;

2) manual attitude correction commands to account for movement of the Solar Inertial reference;

3) adjustment of the desired system momentum reference;

4) rate gyro drift compensation updates to account for varying effects of rate gyro scale factor errors; and

5) generation of navigation parameters which minimized transients induced by periodic updates.

In addition to these functions, infrequent ground updates were also made to a few EOVV parameters to increase or decrease EOVV capabilities, within limits of stability, as a function of the sun angle and to adjust to conditions which existed at the time (i.e., momentum level).

2.3.1.1 EOVV Software Modifications

Memory load buffers 11 through 16 were implemented into the flight software during the EOVV maintenance period. These modifications eliminated computational effects due to cross-coupling and limiting, reduced dependence upon ground support, provided new capabilities, and de-sensitized the onboard system to transients. A summary of the effect these modifications had on EOVV operation is as follows:

1) eliminated X, Y-axis cross-coupling into Z-axis EOVV strapdown updates;

2) eliminated EOVV Y-axis offset errors during limiting.

3) provided automatic adjustment of EOVV nominal momentum

4) compensated EOVV Y-axis offset for strapdown update

5) provided EOVV B capability

6) modified orbit momentum prediction in EOVV B operation

2.3.1.2 SI Movement Correction

The flight software was designed to use the Solar Inertial reference system as its basic attitude reference frame and computed all others, including the local vertical frame upon which the EOVV equations were based, with respect to it. As described in Section 2.2.4, the Solar Inertial reference is not truly inertial but quasi-inertial due to movement of the orbit plane and the sun.

The EOVV control equations were designed to account for this movement. The ACQ SS data was used for strapdown updates about the SI X and Y axis and while orbital Z axis momentum changes were used for updates about the SI Z axis. The ACQ SS provided

an absolute measurement of the X and Y axis SI reference drift. However, the onboard computation of the orbital Z axis momentum change provided a proportional measurement of the Z axis SI reference drift. This measurement was sensitive to various conditions (i.e., rate gyro scale factor, navigation and computation accuracy, overall EOVV performance). In actual operation, the EOVV stabilty limits were exceeded with gains large enough to account for all of the SI reference drift about the Z axis. This was particularly true at large sun angles. However, a built-in capability to manually bias Z axis reference updates was used through the EOVV maintenance period to keep onboard operations within the capability of the EOVV Z-axis strapdown update scheme. These manual biases, or e_{rb} updates, were computed off-line as a function of the estimated SI reference movement and were shown to vary with the sun angle. Figure 2-20 shows a history of the commanded e_{rb} updates. The amplitude and frequency of the e_{rb} update history compares with the changes in sun angle over the same interval of time (Figure 2-4). A few deviations (i.e., around DOY 338) were in response to off-nominal conditions existing at those particular times.

2.3.1.3 Desired Momentum Adjustment

The EOVV control law managed system momentum by generating attitude offset commands, relative to the local vertical reference, to maintain a desired momentum normal to the orbit plane (e_{TN}). Twelve times per orbit (approximately every 30 degrees of orbit), EOVV control equations were excercised to determine the system momentum accumulation normal to the orbit plane. Attitude offset commands were then generated to desaturate or dump the difference between the measured and desired orbital Y momentum.

The theoretical value of orbital Y momentum was constant, for a given EOVV orientation, and was manually initialized following acquisition of the EOVV A and EOVV B orientations. It was necessary, however, to adjust e_{TN} from time to time in order to respond to existing operating conditions (i.e., EOVV performance, rate gyro errors and failures, sun angle). These e_{TN} adjustments were performed manually during the early phases of EOVV operation. However, it was necessary to implement an automatic e_{TN} adjustment capability into the flight software in order to respond to events which could occur during the long gaps in station coverage (7-9 hours).

The automatic e_{TN} adjustment capability was implemented (Buffer 12, SWCR-S4006) on 9/8/79. All e_{TN} adjustments after this date, exclusive of the initial EOVV B value, were made automatically by the flight software. Figure 2-21 shows the values of e_{TN} during EOVV A and EOVV B operation.

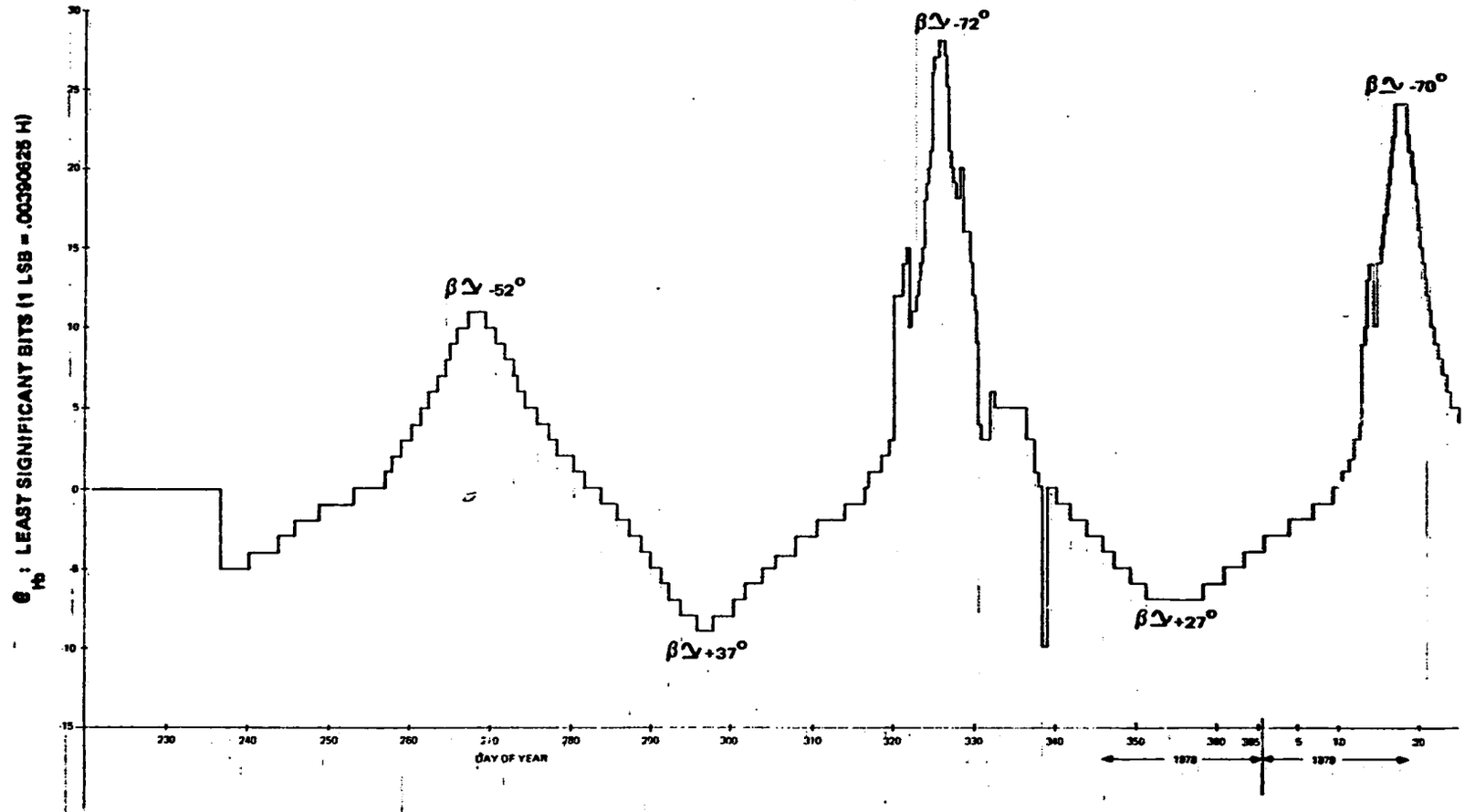

FIGURE 2-20 e_{rb} UPDATES

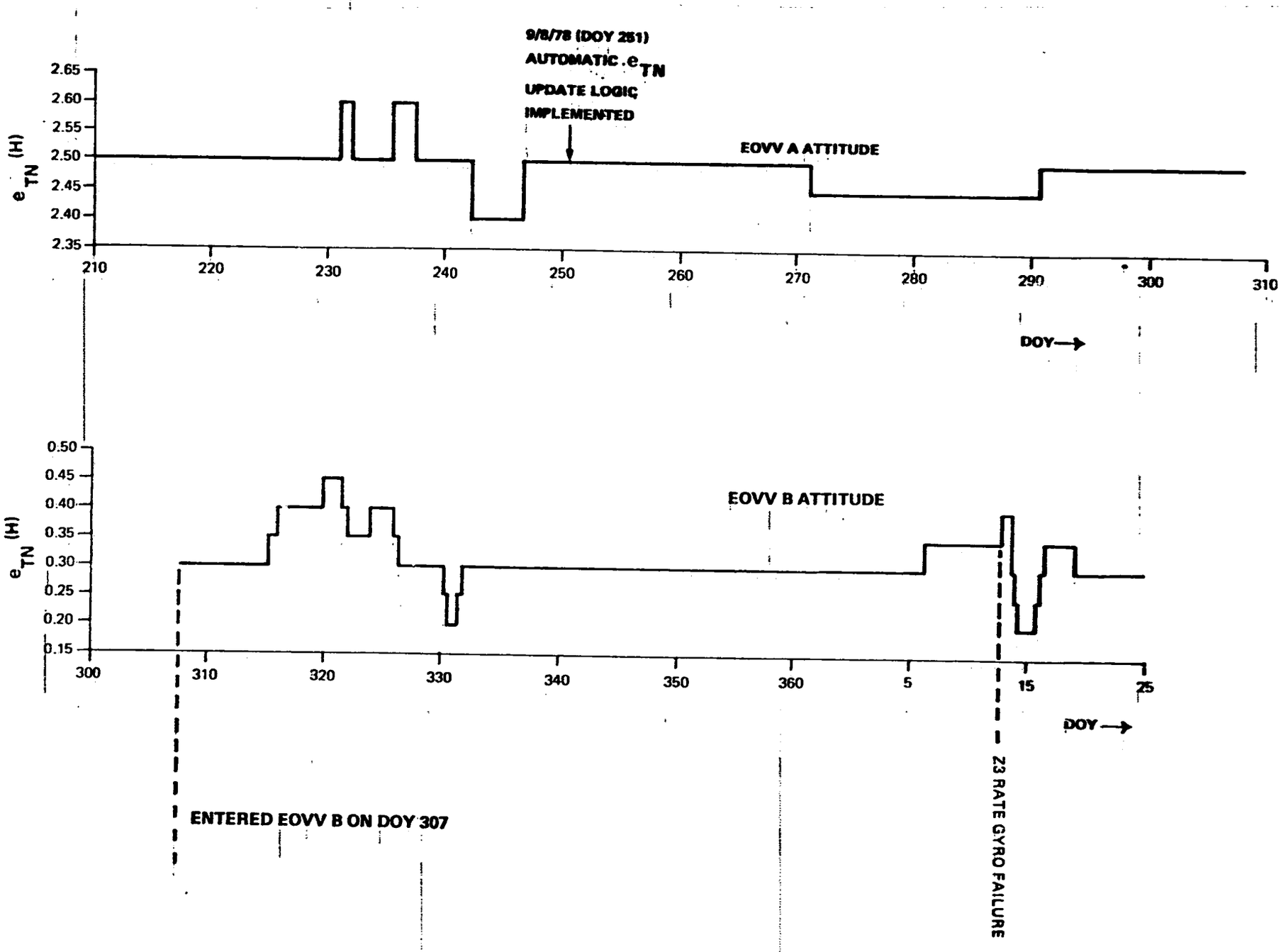

FIGURE 2-21 e_{TN} UPDATES

2.3.1.4 Rate Gyro Drift Compensation

The EOVV control logic operated while vehicle attitude was continuously being maintained relative to the rotating local reference system. The APCS rate gyros were therefore collectively measuring orbit rate. The vehicle Y-axis rate gyros basically sensed a rate component equal to orbit rate times the cosine of the sun angle. Therefore, the Y-axis rate measurement was always of the same polarity: positive for EOVV A and negative for EOVV B operation. The vehicle Z-axis rate gyros basically sensed a rate component equal to orbit rate times the sine of the sun angle. The magnitude and polarity of the Z-axis rate measurement were therefore directly dependent upon the magnitude and sine of the sun angle cycle (see Figure 2-8). The vehicle X-axis maintained a small cyclic offset above and below the orbit plane and therefore, on the average, sensed a zero rate component.

One of the major error sources during EOVV operations was the effect of rate gyro scale factor error on attitude reference drift. These effects were so significant that the rate gyro scale factor errors had to be manually determined and compensated for throughout EOVV operations. The average Y and Z axis rate gyro scale factors were determined, as often as once per orbit, from the EOVV strapdown update and rate integral data telemetered from onboard systems.

After determining the average Y and Z axis scale factor error, the average rate gyro drift, or bias, compensation to counteract the scale factor error was computed. Rate gyro drift compensation was required since the flight software did not provide a readily available capability to directly compensate for scale factor errors. Figure 2-22 shows a history of the average Y and Z axis drift compensation commanded during EOVV operation.

The actual drift compensation commanded for an individual rate gyro was computed to compensate for the measured average scale factor error and, at the same time, to minimize the difference between the rate integrals in that axis.

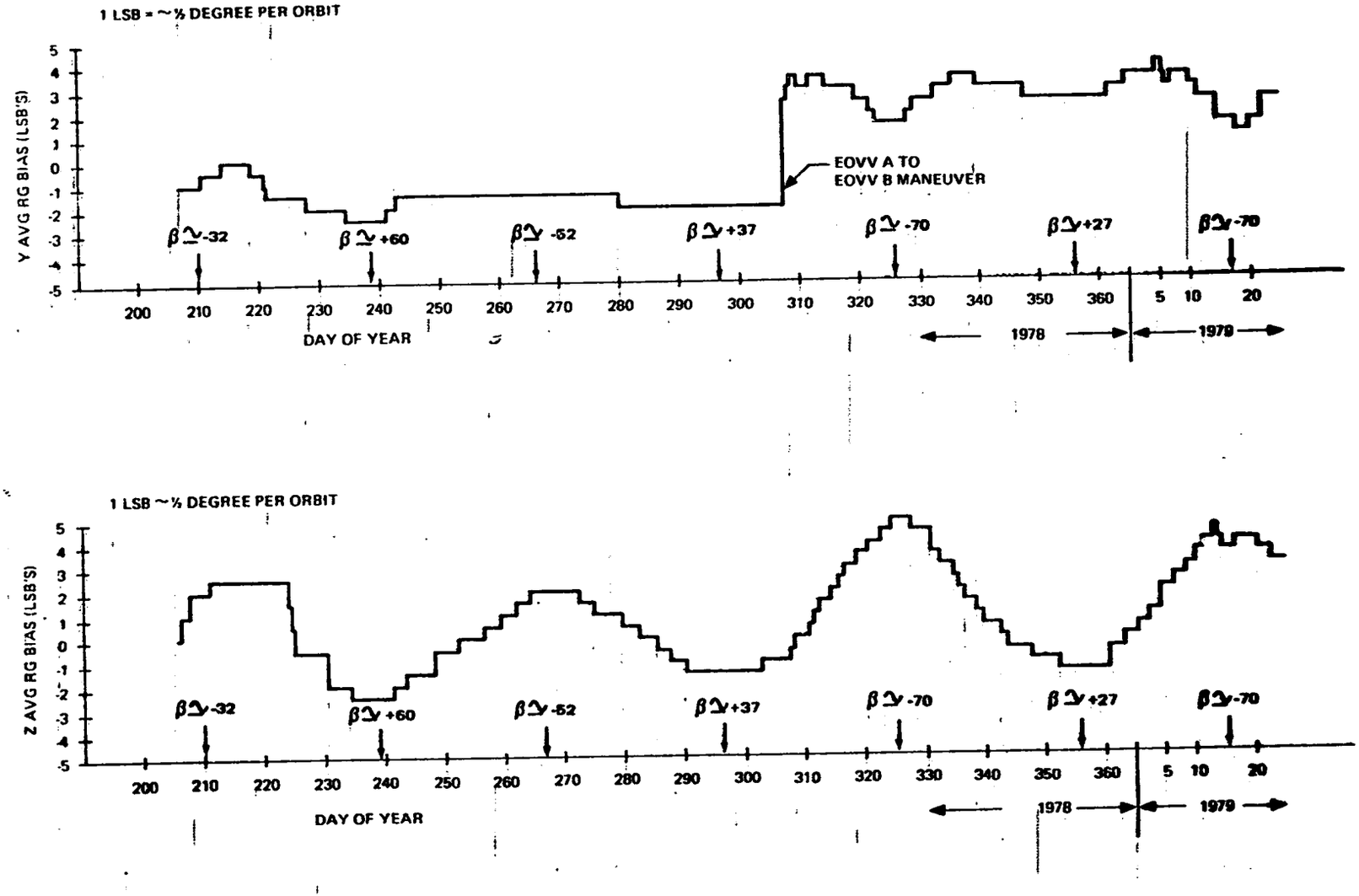

FIGURE 2-22 Y(TOP) AND Z (BOTTOM) AVERAGE RATE GYRO DRIFT BIAS FOR EOVV

2.3.1.5 Navigation Updates

The onboard navigation computations were periodically updated throughout the entire reactivation mission in order to maintain an accurate navigation reference. It was especially important to maintain accurate navigation during EOVV operations. The local vertical attitude reference used in EOVV computations was directly dependent upon navigation data for the time from orbit midnight.

Navigation errors in the time of orbit midnight were directly transferrable to attitude error about orbital north. One degree of attitude error was approximately equal to fifteen seconds error in the time of orbit mdnight.

Navigation updates were commanded, as required, to prevent the error in time of midnight from exceeding ± 60 seconds (± 4 degrees). Initially, these navigation updates were performed to discretely reset the error in time of midnight to zero (discrete update). However, analysis of the navigation error and the update procedure revealed two facts:

1) The navigation error always built up toward the negative 60 second limit (computed midnight lagging actual midnight). This was due to the change in the orbit regression rate resulting from Skylab altitude decay.

2) Discrete updates were resulting in attitude error transients equivalent to the navigation error when the update was performed. This caused perturbations in the EOVV control operation.

Examination of the onboard navigation equations revealed that by biasing one of the navigation update parameters (time between ascending node crossings: T_A) a reversal in navigation error could be induced. By applying a large enough bias an existing error close to the negative 60 second limit could be smoothly ramped toward the positive 60 second limit without causing any attitude transients. Restricting the bias to a reasonable magnitude also ensured that the natural drift due to decay in orbit altitude would overtake the induced drift before the positive 60 second limit would be exceeded.

The smoothed update procedure had an additional effect of reducing the navigation update frequency. The navigation error was allowed to drift across the entire + 60 second error range instead of only across the 0 to -60 second range. Initially

navigation updates were performed once every one or two weeks. This increased to daily updates at the end of the reactivation mission.

2.3.2 Solar Inertial (SI) Maintenance

An important part of Skylab reentry control was the ability to maintain Skylab operating in the SI attitude until the transition to TEA control could be accomplished. Several factors dictated the requirement to remain in the SI mode of control. These were:

1) The time required to develop and construct the TEA control capability.

2) An upper and lower altitude limit, outside of which, TEA control is not possible.

3) The ability to maintain EOVV control to altitudes compatible with TEA control was not probable because of the limited momentum desaturation capability in EOVV control.

4) The ability to successfully acquire the desired TEA control attitudes was directly dependent upon the accuracy of the onboard strapdown reference prior to the maneuver to the TEA attitude. The SI mode provided the most accurate strapdown reference system.

Preliminary analyses indicated control of Skylab in the SI mode could be maintained until the vehicle reached approximately 150 n.m. in altitude. This SI control limit was based upon data which predicted Skylab would reach a 150 n.m. altitude on May 24, 1970, a time which also corresponded to the sur angle passing through the orbital plane (i.e., $\beta = .0$). Subsequent analyses determined that the SI control limit was dependent upon a combination of the sun angle and the atmospheric density; the atmospheric density being directly dependent upon altitude and solar activity. In an aerodynamic torque environment, the maximum control authority was required from the CMG system as the sun angle crossed the orbit plane.

In early April 1979, the solar activity dropped from a $+2\sigma$ value to less than nominal and remained near or below nominal through April and May. This effort reduced the expected orbital decay rate which eventually forced abandoning plans to acquire T121G

TEA control on May 24, 1979. The initial TEA acquisition plans had to be changed because the phasing requirements of sun angle versus altitude required for a successful reentry scenario using T121G TEA control was no longer satisfied. Because of the higher than predicted altitude (157 n.m. vs. 150 n.m.) on May 24, 1979, SI control was maintained through the $\beta = 0$ crossing and the SI control limit was revised to occur between June 18 and June 24 when the sun angle again approached crossing the orbit plane. The altitude projected for Skylab, consistent with this time frame, was 140 to 145 nm.

The design of the momentum management system for SI control used gravity gradient torques to maintain a desired momentum state in the CMG system. Control of the CMG momentum state was effected by a series of maneuvers (called GG dump maneuvers) performed each orbit during the night phase of the orbit and an attitude adjustment (also each orbit) about the sunline (see Reference 3 and 4). These maneuvers and attitude adjustments were computed automatically onboard based upon Skylab operating solely in a gravity gradient torque environment. As the altitude of the Skylab decreased, the influence of the aerodynamic torques on the performance of the SI momentum management system became more pronounced and required CMG bias adjustments in order to maintain adequate control of the CMG momentum and CMG gimbal excursions.

The influence of aerodynamic torques on SI momentum management was first observed within two weeks after acquiring SI on January 25, 1979. The altitude of Skylab was approximately 193 nm when flight controllers observed an unexpected bias offset in the Z axis momentum. This was the first cue to the effects of aerodynamic torques on SI momentum management performance since at that time the existing Skylab simulators did not include aerodynamic models.

The aerodynamic torques experienced by Skylab in the SI attitude were cyclic in nature with a non-zero mean value and had a frequency of one cycle per orbit as compared to the two cycle per orbit frequency of the gradient torques. Depending upon the per axis phasing of the aerodynamic torques relative to the expected gravity gradient torques, the onboard momentum management scheme would interpret the aerodynamic torque component as a bias gravity gradient torque and compensate accordingly. This compensation in turn caused the CMG momentum to operate about a bias value other than that commanded. This condition could lead to CMG gimbal stop encounters if unchecked. A desired set of CMG stop values commandable through the ATMDC DCS, had been established for the primary Skylab mission to minimize CMG gimbal stop encounters. Now, the job was to determine what CMG bias values to command to make the CMG system operate about the set of desired bias values.

Using simulation analyses and observing flight performance, a procedure evolved to determine values for CMG bias commands which forced the momentum management system to keep the CMG gimbals in a favorable operating region. Predicted values for the CMG bias commands versus elapsed time (i.e., predicted altitude, sun angle) were generated to give flight controllers some expectations relative to trends and magnitudes of the commanded bias values. The limits of SI control were rapidly approaching when TEA control was acquired on June 20, 1979.

Control of Skylab in the SI mode was maintained from January 25 to June 20, 1979 with the SI momentum management system operating in an environment for which it was never intended and without using any TACS impulse. The one dominant trait exhibited by simulation results with Skylab operating under these conditions was that if a CMG gimbal stop encounter ever occurred, successful reacquisition of the SI operating mode was highly improbable. Had such an event occurred, active control of Skylab would have most likely been terminated.

2.3.3 TEA Maintenance

The TEA operations began on 6/20/79 and, with only one exception (refer to Section 2.2.12), continued uninterrupted until 7/11/79. At that time Skylab was maneuvered to the Solar Inertial attitude to support reentry operations (Section 2.2.13). A high drag torque equilibrium attitude, referred to as the T121P attitude, was maintained throughout TEA operations (see Figure 2-3). The vehicle X-axis was oriented near the orbit normal with the positive X-axis pointing South. The vehicle Y and Z axes were oriented near the orbit plane so that the ATM and OWS solar arrays were trailing and approximately 45 degrees either side of the vehicle velocity vector.

Several ground support functions were required in order to maintain TEA operations. These ground support functions included:

1) rate gyro drift compensation updates to account for the effects of rate gyro scale factor errors;

2) TEA reference updates to account for small amounts of drift in the attitude reference (also attributed to rate gyro scale factor error);

3) nominal TEA momentum updates to adjust the T121P orientation in order to provide sufficient solar power for Skylab systems;

4) TEA control matrix (Slope Matrix) updates to account for torque equilibrium changes due to nominal TEA momentum updates and altitude decay;

5) TEA momentum error limit updates to provide increased control capability as the orbit altitude decreased; and

6) generation of navigation updates which minimized transients induced by periodic updates.

In addition to these functions, two software modifications were implemented soon after the TEA operations were initiated. Both of these modifications were performed to maintain normalization of the TEA reference quaternion by eliminating computational drift associated with reference updates.

Figure 2-23 shows the altitude and sun angle profiles during TEA operations.

2.3.3.1 Rate Gyro Drift Compensation

The TEA control logic operated while vehicle attitude was continuously being maintained relative to the rotating local vertical reference system. The APCS rate gyros were therefore collectively measuring orbit rate. In the T121P attitude, the vehicle X-axis rate gyros were basically sensing the negative of orbit rate. The vehicle Y and Z axes, being near the orbit plane, were sensing only a small component of orbit rate.

As with EOVV, the effects of rate gyro scale factor errors on attitude reference was a major concern during TEA operations. However unlike EOVV, the T121P attitude did not vary significantly and therefore once the gyro scale factor error and compensation were determined they did not require continued updating.

Once each orbit, while the vehicle attitude was maintained relative to the local vertical, the sun would pass through the X-Z plane of the vehicle. During the early days of TEA operation this sun pass was such that the sun was within the field of view of the ACQ SS. Several times it was even within the ACQ SS linear range.

Although these sun passes did not always occur during real time station coverage, the necessary ACQ SS and onboard attitude reference data was obtained by dumping and processing ASAP recorder data. This data was processed on a Zerox Sigma 5 computer located at MSFC to determine the average scale factor

recorder data. This data was processed on a Xerox Sigma 5 computer located at MSFC to determine the average scale factor error for a given axis and the rate gyro drift compensation required to counteract it. The actual drift compensation commanded for an individual rate gyro was computed to compensate for the measured average scale factor error and, at the same time, to minimize the difference between the individual gyro rate integrals in that axis.

Figure 2-24 shows a history of the rate gyro drift compensation commanded during TEA operations. The initial compensation was commanded just prior to activating TEA operations. A large negative X-axis bias was commanded because TEA control could be lost within one to two orbits if an average bias of this nature were required but not available. If compensation in the opposite direction was needed, which it was, TEA control could remain active until the true compensation was determined.

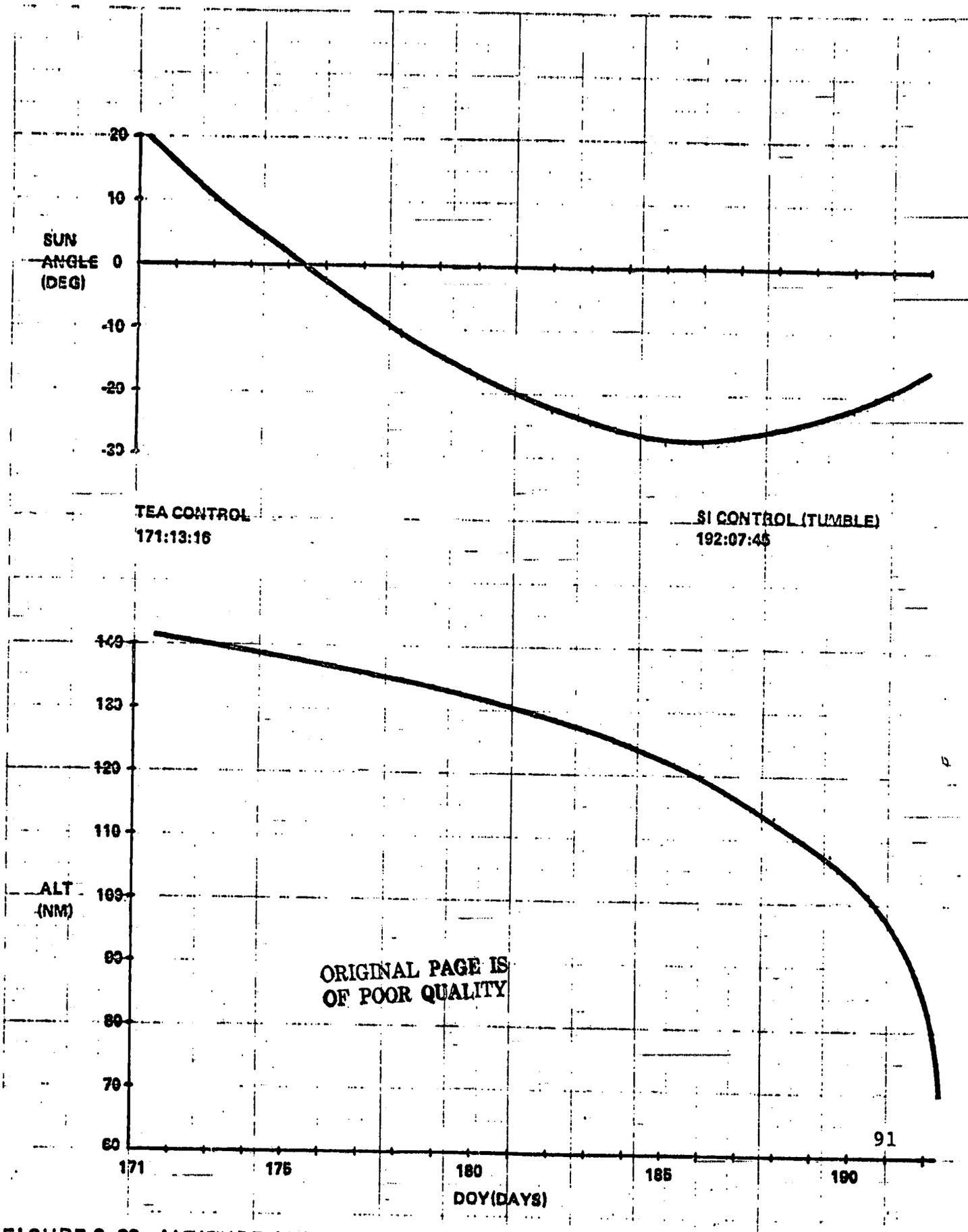

FIGURE 2-23 ALTITUDE AND SUN ANGLE DURING TEA CONTROL

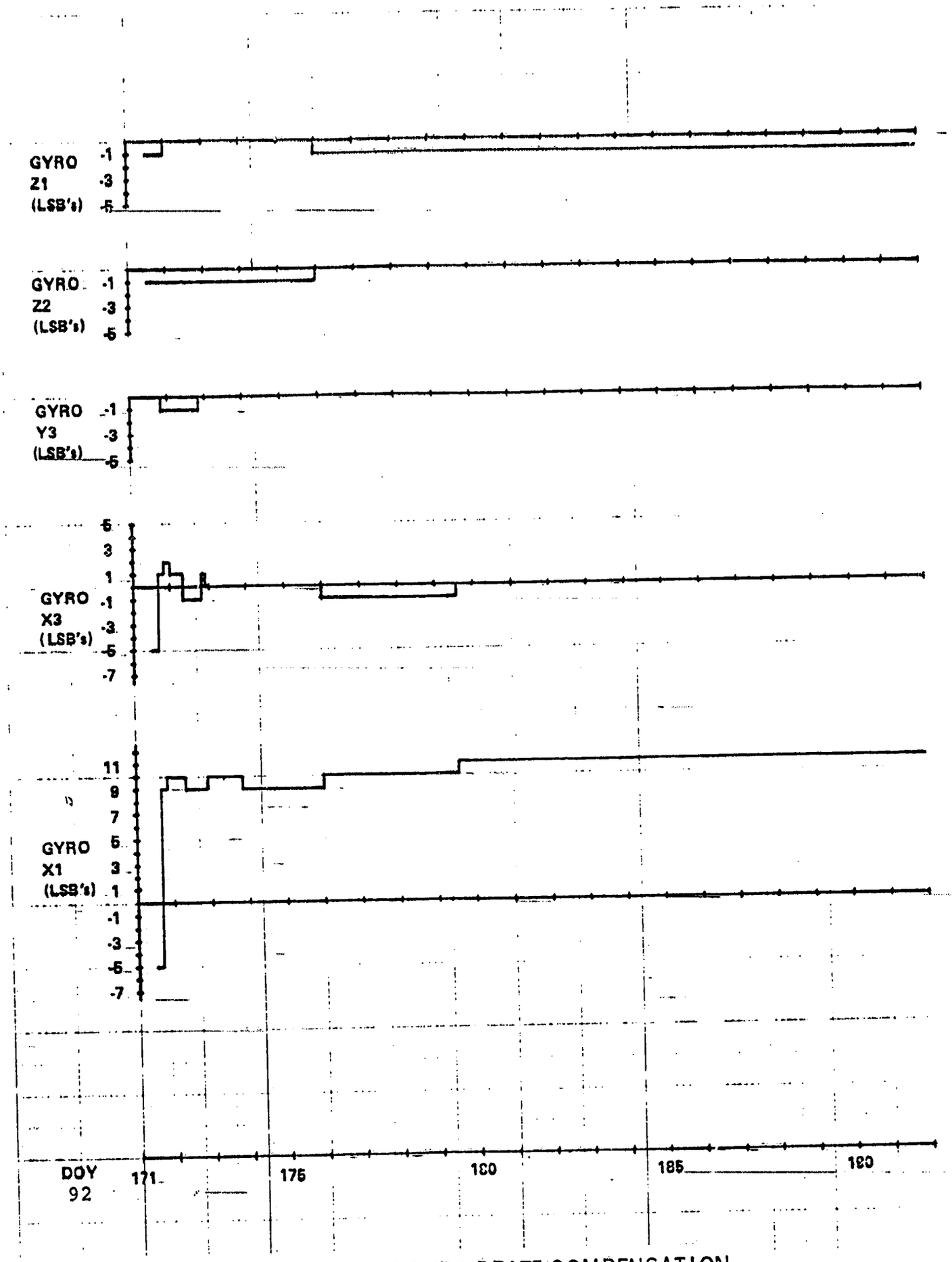

FIGURE 2-24 IEA HISTORY OF RATE GYRO DRIFT COMPENSATION

2.3.3.2 TEA Reference Updates

Throughout the TEA operation period small updates were commanded to adjust the TEA attitude reference. These updates were relative to the local vertical reference system and corrected for small magnitude drifts in the onboard attitude reference quaternions. These drifts were due to: navigation drift within the navigation update limits; and rate gyro scale factor errors below the quantization level of the rate gyro drift compensation command.

The TEA reference updates were generated by comparing the nominal reference profile to a history of the actual TEA reference data. One or more orbits of TEA reference data were required for this operation. This was obtained from up to 3 consecutive orbits of ASAP recorder data. The de-logged data was manually input to a Zerox Sigma 5 computer located at MSFC where it was processed to determine the required update. The resulting update was then commanded to adjust the attitude reference quaternions used for TEA control. Figure 2-25 shows a history of the TEA reference updates.

2.3.3.3 Nominal TEA Momentum Updates

The TEA control law automatically maintained the total system momentum to nominal values specified via DCS command. Every 300 seconds the difference between the actual and the nominal TEA momentum was calculated. This momentum error was translated through a matrix (SLOPE Matrix) which related momentum error to attitude error relative to the torque equilibrium attitude. The resulting attitude errors were used to automatically update the TEA attitude reference such that the momentum error would converge toward zero.

The nominal TEA momentum was defined relative to the local vertical reference system and was updated several times during TEA operations. The X and Z axis updates (e_{TLN1} and e_{TLN3}) were used to tilt the T121P orientation relative to the orbit normal. These adjustments in the T121P attitude were made in unison with changes in the sun angle to provide sufficient solar power for TEA operations and, where possible, to provide ACQ SS data for rate gyro compensation.

Updates in the Y axis (e_{TLN2}) did not effect the T121P orientation but were used to provide a favorable CMG gimbal angle orientation to avoid gimbal stop encounters. Figure 2-26 shows a history of the nominal TEA momentum updates. There were no updates after DOY 182. The power system and rate gyro

compensation needs had settled to the point where it was more important to stabilize the T121P orientation by maintaining a constant value for the nominal TEA momentum.

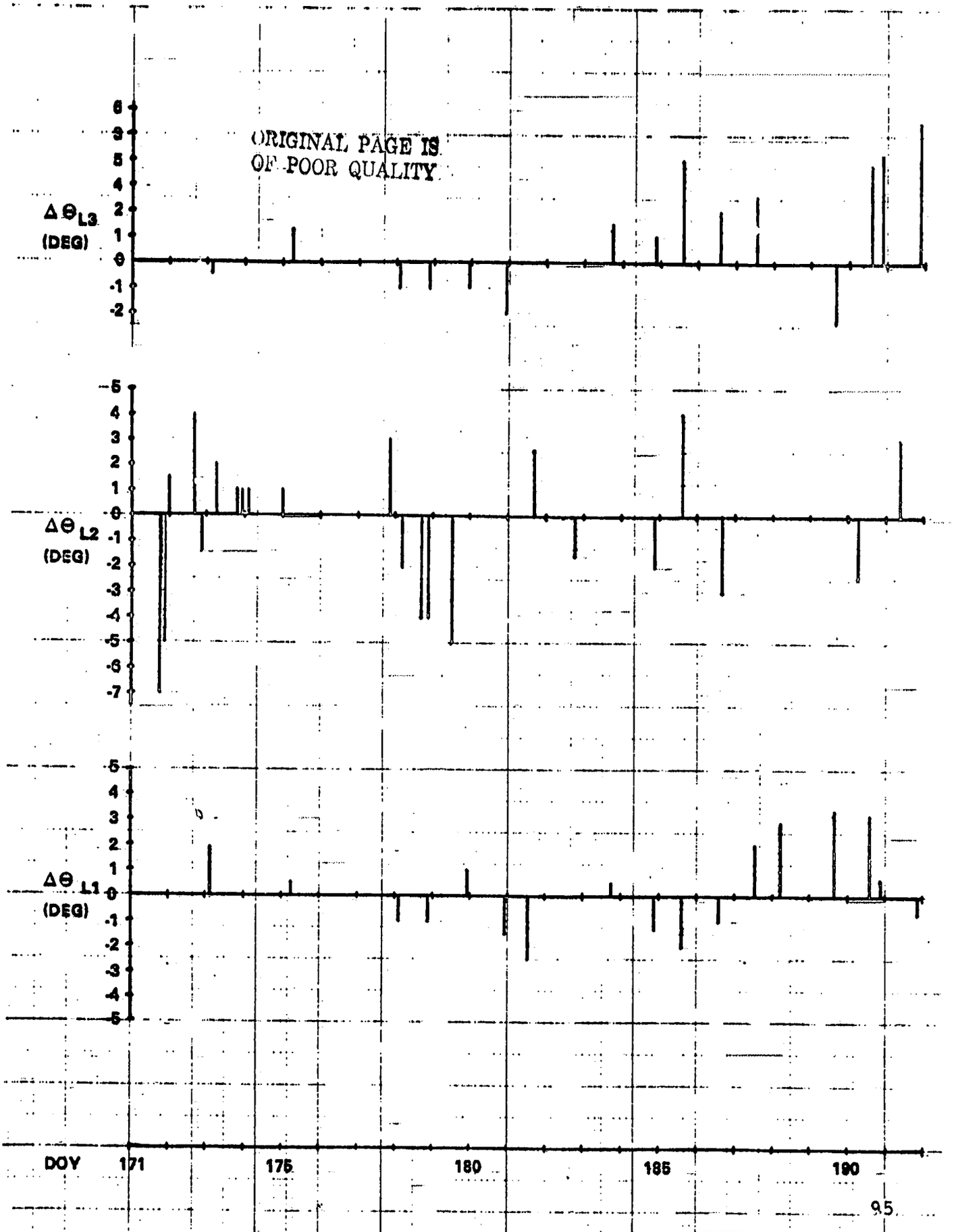

FIGURE 2-25 TEA REFERENCE UPDATE HISTORY

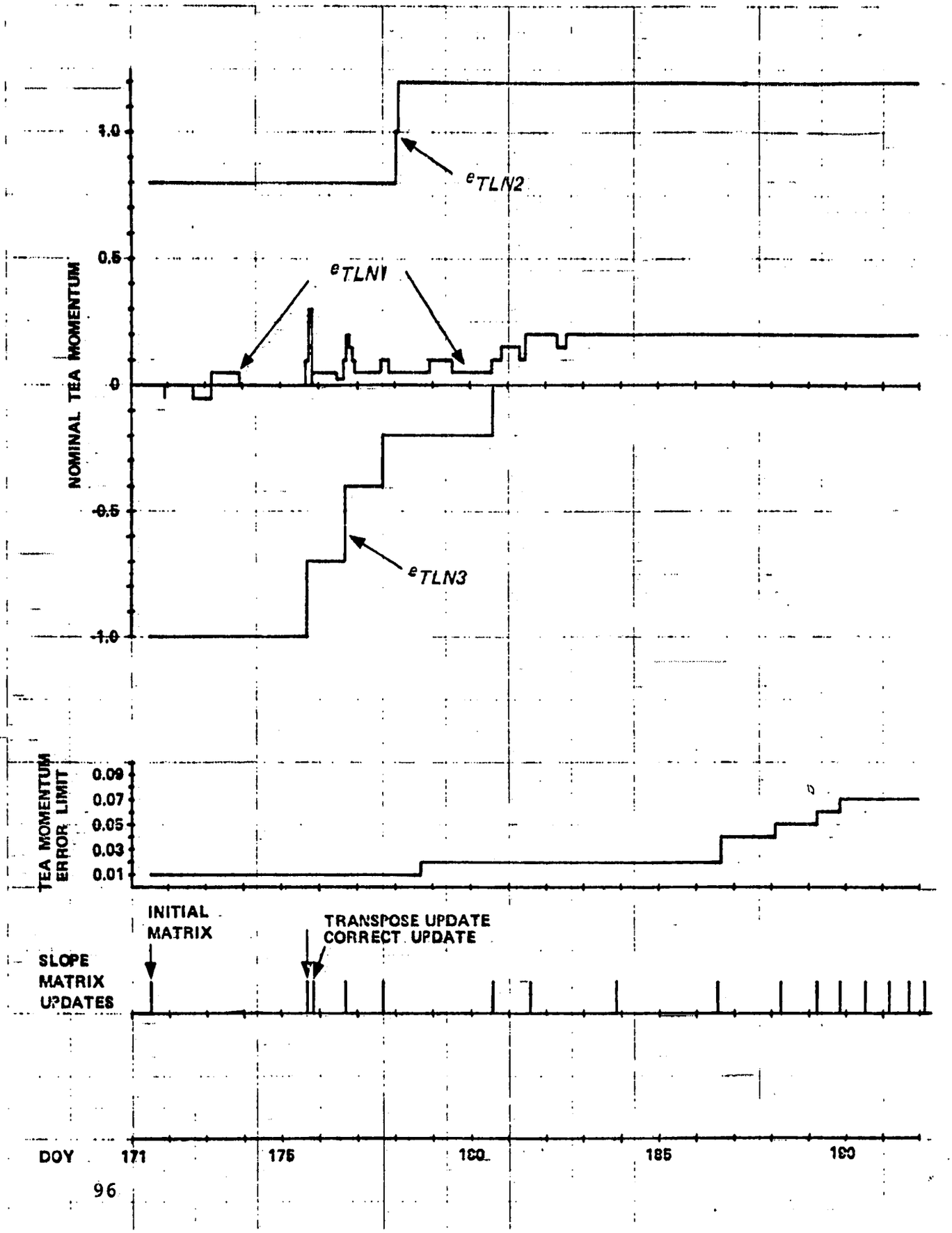

FIGURE 2-26 TEA PARAMETER UPDATE HISTORY

2.3.3.4 Slope Matrix Updates

The TEA control or SLOPE matrix, relating momentum error to attitude error about the torque equilibrium point, was updated several times during TEA operations. The SLOPE matrix was updated with each change in e to account for the shift in the equilibrium attitude. Updates were also made as a function of orbit altitude to account for the increase in aerodynamic torque as altitude decreased. Figure 2-26 shows a history of the SLOPE matrix updates.

The first update on DOY 175 was actually uplinked as the transpose of the desired matrix. This resulted in an attitude control transient as described in Section 2.2.12. The correct matrix was uplinked approximately 3 orbits later after TEA control had been reacquired. Based on observed and predicted control performance, the SLOPE matrixs used from DOY 177 through the first matrix on DOY 191 were all uplinked at one-half gain to desensitize the TEA control operation.

2.3.3.5 TEA Momentum Error Limit Updates

The TEA momentum error limit was updated five times during TEA operations. As shown in Figure 2-26 each update increased the limit. This increase provided greater control authority as the orbit altitude decreased (and aerodynamic torques increased).

2.3.3.6 Navigation Updates

As with EOVV, it was important to maintain an accurate navigation reference during TEA operations. Any navigation error gave a corresponding attitude error about orbit North. Navigation updates were commanded, as required, to prevent the error in time of midnight from exceeding $\pm$ 60 seconds ($\pm$4 degrees). As described in Section 2.3.1.5, the smoothed update procedure was used so that navigation updates did not cause an attitude error transient at the update time. At the end of the mission, navigation updates were being required at least once per day with T biases of 15 seconds.

SECTION 3

ATTITUDE CONTROL

3.0 INTRODUCTION

The actual control of the Skylab attitude to the attitude reference was done exactly as in the original mission. However, only the pointing control system (PCS) of the APCS was used; the experiment pointing control system (EPCS) was disabled.

The major parts of the APCS were the rate gyros, the sun sensors, the star tracker (it had failed during the original Skylab mission), the Apollo Telescope Mount digital computer (ATMDC), the workshop computer interface unit (WCIU), double-gimbaled control moment gyros (CMGs), and cold-gas (compressed nitrogen) thruster attitude control system (TACS).

Six control modes were addressable: 1. STANDBY, 2. SOLAR INERTIAL (SI), 3. EXPERIMENT POINTING, 4. ATTITUDE HOLD/CMG, 5. ATTITUDE HOLD/TACS, and 6. ZLV. EOVV and TEA control were programmed to be substates of the ZLV mode. The basic ZLV (for Z axis along the local vertical) attitude was with the positive Z axis along the local vertical, pointing up, and the positive X axis in the orbital plane, pointing in the direction of the velocity vector. Any angular offset from the basic ZLV attitude (offset identified by the quaternion QAL) could be commanded via a set of three Euler angles (chi's) with a (Y,Z,X) rotation sequence. None of the original APCS capabilities were eliminated by the addition of the EOVV and TEA control methods.

In the following sections EOVV and TEA are mostly discussed in narrative form. Much more detail as well as equation development can be found in Refs. 13 and 14. Sections are also included covering the TACS, CMG, Rate Gyro, sun sensor and ATM digital computer hardware and software systems.

3.1 EOVV AND TEA CONTROL

The problem for both EOVV and TEA was to determine variable reference attitudes such that, on the average, the angular momentum was contained within the two-CMG capability (allowing the CMG's to hold the prescribed attitude reference), while the average reference attitude was consistent with the desired aerodynamic drag. Low drag was desired for EOVV in the hope (at that time) that Skylab could be kept in a high enough orbit long

enough for the Shuttle to carry an orbital retrieval system up to it for boosting Skylab into a higher orbit or for deboosting affording a controlled reentry. The desire for TEA was to find two separate attitudes with a drastically different drag to control the Skylab impact point by switching from a high-drag attitude to a low-drag attitude (or vice-versa) when the impact point prediction was accurate enough to indicate the desired change.

3.1.1.0 EOVV Control (2 CMGs)

Minimizing the drag on Skylab required that the least frontal area was presented to the wind while at the same time holding a GG torque equilibrium (at the altitudes of concern the GG torques were still very dominant and they were therefore used exclusively for momentum control). Keeping the minimum principal moment-of-inertia axis parallel to the wind direction fulfilled this requirement. To have the necessary electrical power from the solar cells as well as strapdown update information from the ACQ SS the Skylab was rolled about the minimum principal moment-of-inertia axis (principal X axis) such that once an orbit the sun-line passed through the center of the ACQ SS.

There were two attitudes which satisfied these requirements: One with the MDA forward, called EOVV A, and one with the MDA backward, called EOVV B. In either case, the MDA had to be pitched down by varying degrees (depending on the beta angle) to align the principal X axis with the orbit tangent.

3.1.1.1 Momentum Control Methods

Control of the angular momentum was split into the control of the momentum component perpendicular to the orbital plane (POP control) and the component in the orbital plane (IOP control). Since IOP control had some effect on POP control, IOP control will be treated first.

3.1.1.2 EOVV IOP Momentum Control

When Skylab was originally designed, it was desirable to minimize the GG torques along the minimum principal moment-of-inertia axis as much as possible since the momentum management scheme (Ref. 15) was least efficient in this axis.

For EOVV control this meant that there were basically no large GG torques available along this axis and furthermore, there would be no change in torques when the principal Y and Z axes were ±45 deg from the orbital plane (tracking of the sun by rolling would make this a frequent occurrence). Therefore, this first order effect had to be abandoned and the actually used momentum control scheme assumed that the Skylab moments-of-inertia were cylindrical, with an average moment-of-inertia difference of ΔI.

The problem was solved by using a second order effect. First, a large cyclic POP torque was generated by "nodding" (pitching) the Skylab in the orbital plane. Cyclic nodding was required to avoid a continuous angular momentum build-up in the POP direction. The cyclic POP torque was then tilted as required (differently for each half cycle) to generate a controllable component in the orbital plane. The second order effect stems from the fact that the IOP torque is proportional to the nodding angle times the tilt angle.

The effectiveness of the IOP momentum control did not depend on the frequency of the nodding. However, other considerations entered: (1) the lower the frequency, the larger the POP momentum swing; and (2) the higher the frequency, the larger the maneuver momentum that has to be exchanged between the vehicle and the CMG system. Since only a limited momentum volume was available with two CMGs and their assoiated gimbal angle stop problems, a nodding frequency of twice orbital frequency was chosen as a viable compromise:

$$\eta_{yn} = -\eta_{ym} \sin(2\Omega_o t) \qquad \text{(E1)}$$

Therefore the IOP momentum control calculations were done every quarter orbit. This had the added advantage that the resolution from the nearly inertial O system to the rotating L system happened in 90 deg intervals allowing indexing of some of the saved momentum samples rather than requiring a full-fledged resolution.

To minimize transients at the quarter orbit sample points the tilting angle was also sinusoidal with twice orbital frequency and its amplitude was the only changing quantity:

$$\eta_{zn} = -\eta_{zm} \sin(2\Omega_o t) \qquad \text{(E2)}$$

where

$$\eta_{zm} = K\eta_z (eZ0 - eA + eR/4)$$

$$K\eta_z = (15H)/(48\eta_{ym}\Omega_o I)$$

eZ0 is the momentum component to be desaturated.

eA is the amplitude

eR is the ramp per orbit

} all e are in units of one H, the momentum of one CMG.

The phasing of the nodding and the tilting angles was the same such that the amplitude was reached half way between sample points.

The sample points were chosen such that one of the samples occurred at the time when the sun was perpendicular to the solar panels. This happened before orbital noon for EOVV A and after for EOVV B (the difference of about 11 deg between the geometric and the principal X axes is the reason). In addition, the nodding rate, being added to the orbital rate, was phased such that it slowed Skylab down when the solar panels were perpendicular to the sun and therefore maximized the power from the solar panels (giving rise to the minus sign in Eq. E1).

The tilting angle amplitude was calculated such that the IOP momentum component which could be affected during the next quarter orbit (it was along the direction of the connecting line between the present sample point and the next one) would be driven to the desired value. The desired value was basically zero, but any constant torque in the L system causes only a cyclic momentum change (with normalized amplitude eA) over one orbit and should not be compensated for. Therefore the momentum attributable to a constant L system torque was subtracted out of the momentum eZ0 to be desaturated over the next quarter orbit.

To recognize a cyclic as well as a ramp momentum change, four past momentum samples were saved. The samples were also used to generate strapdown update information once an orbit.

3.1.1.3 EOVV POP Momentum Control

The torques associated with a rotation about the orbit normal are much stronger than the ones associated with IOP control. Hence the momentum sampling for momentum control has to be done as frequently as possible. However, the transients should have had a chance to settle before the next POP sample is taken. Twelve samples per orbit satisfied both requirements. To further reduce transients, the calculated POP angle (which would have eliminated the momentum offset within the next interval if it were applied fully during interval) was ramped-in such that the angle was achieved at the end of the interval. Since this only reduced the momentum offset by half, the angle was ramped-out during the next interval for a full momentum offset elimination. The ramp due to the newly calculated POP angle was simply superimposed on the rampdown from the previous POP angle (Fig. 3-1). This method still resulted in a constant hang-off, when necessary: the angle change due to the old angle being ramped out was compensated by the ramp-in of the new angle (in flight, constant angle hang-offs were common due to strapdown errors and navigation errors and they were not detrimental, since the momentum control kept the vehicle at the truly desired attitude). A block diagram of the EOVV orbital Y-momentum control scheme is shown in Figure 3-2.

3.1.1.4 EOVV Strapdown Update

Strapdown updates about the vehicle X and Y axes were always furnished by the ACQ SS. To do that the roll angle about the principal X axis was changed by large amounts to compensate for the large beta angle changes (a slow change) and relatively fast smaller corrections were applied to compensate for the nodding and the tilting angles. The overall effect was that the vehicle Z axis nominally traced a cone about orbital north. The difference between where the sun-line was at the closest approach to the ACQ SS center and where it was supposed to be according to the strapdown information gave the strapdown X and Y information.

To gain strapdown update information about the sun-line was more difficult since there was no other sensor available. The selected momentum control method fortunately had the feature that, due to the nodding angle, a misalignment between the ideal orbital plane and the indicated orbital plane generated an IOP momentum ramp.

POP COMMAND SUPERPOSITION

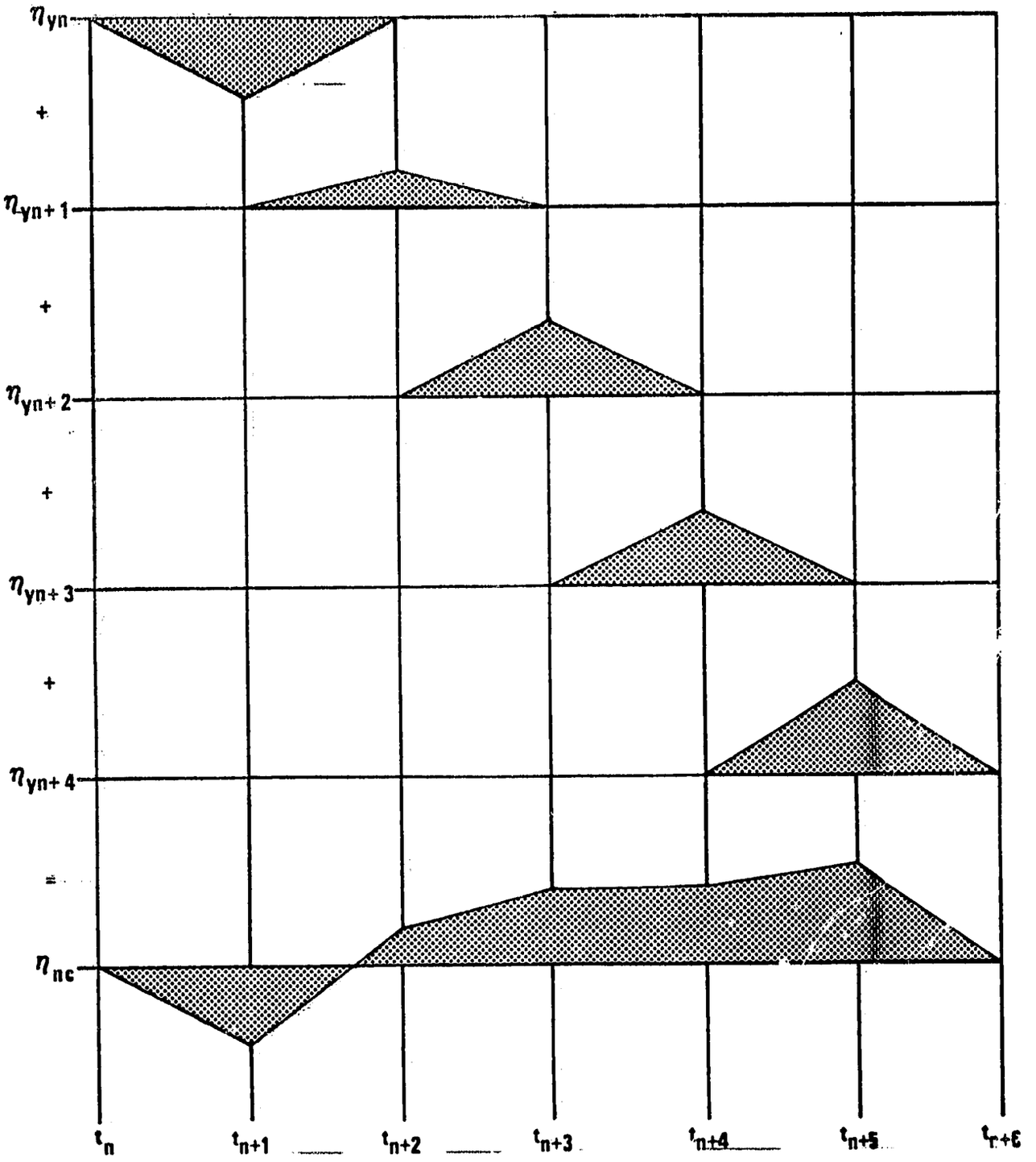

FIGURE 3-1

SKYLAB END-ON-VELOCITY-VECTOR CONTROL

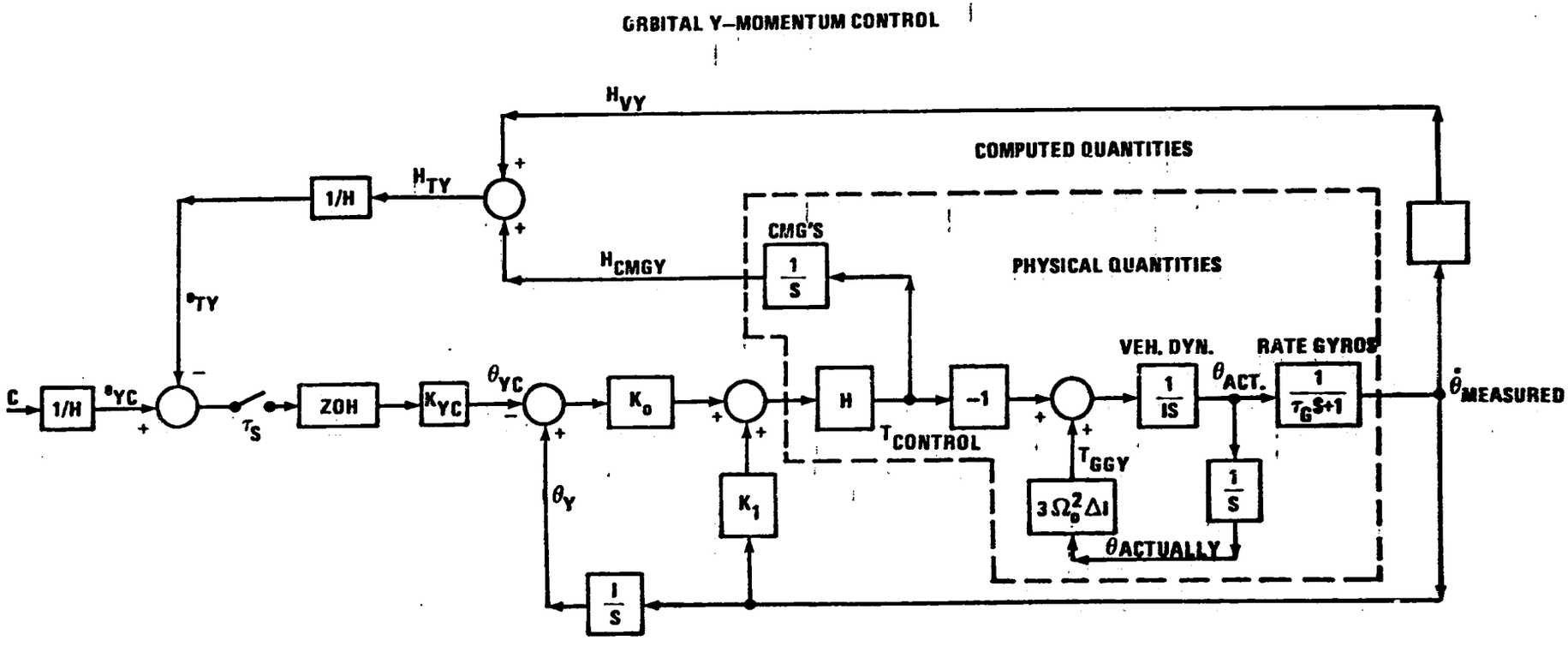

$\tau_S \approx 450\,S$; $K_{yc} = \frac{H}{3\Omega_0^2 \Delta I \tau_S}$; $\Delta I = \frac{1}{2}(I_{PY} + I_{PZ}) - I_{PX}$; K_0 & K_1 ARE NOMINAL CONTROL GAIN

H = 3050 NMS (NOMINAL CMG MOMENTUM); τ_G REPRESENTS RATE GYRO LAG; Ω_0 IS ORBITAL RATE

FIGURE 3-2

The actual strapdown update was done by changing the reference quaterion.

$$QVI = \overline{\overline{\Delta Q}}\ QVI \tag{E3}$$

where the double-bar operator is defined as

$$\overline{\overline{Q}} = \begin{bmatrix} +Q4 & +Q3 & -Q2 & +Q1 \\ -Q3 & +Q4 & +Q1 & +Q2 \\ +Q2 & -Q1 & +Q4 & +Q3 \\ -Q1 & -Q2 & -Q3 & +Q4 \end{bmatrix} \tag{E4}$$

and

$$\Delta Q = [\Delta Q1,\ \Delta Q2,\ \Delta Q3,\ \Delta Q4] = [\underline{\Delta Q},\ \Delta Q4] \tag{E5}$$

with $$\underline{\Delta Q} = 0.5(\underline{s} \times \underline{v} + \mu z\ \underline{s}) \tag{E6}$$

and $$\Delta Q4 = \sqrt{1 - \Delta Q \cdot \Delta Q} \tag{E7}$$

The cross product in Eq. E6 is the ACQ SS update and the last term is the IOP ramp update, where $\underline{v}$ is a unit vector in the sun direction as calculated by the ATMDC and $\underline{s}$ is the measured sun direction unit vector. μz is the angle about the measured sun direction:

$$\mu z = -K\mu z\,(eTLN1 - eTLN1P) \tag{E8}$$

where $K\mu z$ is a gain and (eTLN1 - eTLN1P) is the ramp per orbit (μz is calculated at sample point 1) modified by the ground commanded ramp bias eRB since

$$eTLN1P = eTLN11 + eRB \tag{E9}$$

is calculated right after the μz calculation and therefore is used for the next μz calculation (eTLN1P is modified at every sample point to account for the momentum changes commanded by μZM.

3.1.1.5 ——— EOVV Operation and Performance

The original EOVV equations considered EOVV A only. In EOVV A CMG #2 received more solar radiation when the sun was north of the orbital plane (positive beta angle) and less, when it was south of the orbital plane (negative beta angle). For large negative beta angles the CMG #2 bearing temperatures became critically low (see Section 3.3.3). As a consequence, the EOVV A equations had to be modified during EOVV operation to allow an EOVV B attitude during extended periods of large negative beta angles.

Constant η_{yc} angle hang-offs (caused by strapdown, navigation and other errors) required constant POP momentum hang-offs to generate the necessary commands. Since the range of acceptable POP momentum component was rather limited ($\pm$0.4H from the nominal; the nominal e_{TN} being 2.5H in EOVV A and 0.3H in EOVV B) the nominal POP momentum had to be changed to accept large angle hang-offs (3 deg of POP angle hang-off required 0.1H POP momentum hang-off). This change in nominal momentum was made from the ground at the beginning of the EOVV operation and later was automated on-board to guard against ground inattention, ground system failures, and long telemetry coverage gaps. Momentum excursions outside the specified range caused loss of attitude due to CMG saturation on one occasion (6/28/78) and it was therefore very important to keep the POP momentum bounded.

Strapdown updating about the sun-line was done with information derived from the IOP momentum ramp. Unfortunately, the evaluation of the IOP momentum ramp yielded very noisy readings from one orbit to the next and could only be used with a very reduced gain $K_{\mu z}$. This in turn could lead to large orbit plane misalignments to generate the required strapdown updates to keep up with the $\pm$50 deg rocking of the true orbital plane (due to the precession when viewed with respect to the projection of the sun-line into the orbital plane). The large size of the maximum change per orbit (1.2 deg) was not recognized at the beginning of the EOVV operation and was the cause for loss of attitude on 6/28/78. After that the ideal strapdown update necessary to follow the rocking of the orbital plane was introduced open loop through the quantity called e_{RD} (Eq. E9) and no more problems were experienced.

3.1.2.0 TEA Control

With the decision in December 1978 to discontinue efforts to keep the Skylab in orbit came the decision to terminate the highly successful EOVV mode of operation and to reestablish the solar inertial mode as soon as practical. This would put the spacecraft in an ideal power attitude and greatly reduce ground management of systems. It would also increase the drag on the spacecraft and cause it to reenter sooner. Unfortunately the SI attitude could not be maintained much below 280 km (150 n.m.) since the growing density of the atmosphere would cause the aerodynamics to grow to the point where the storage capacity of the CMGs for angular momentum was inadequate. Since control of attitude to 150 km or below would be required in order to influence reentry and the amount of thruster gas was far too low to consider control with thrusters, another new attitude control scheme had to be developed. Aerodynamic torques are proportional to density and become nearly overwhelming at 150 km and so any attitude control scheme which would work at 150 km would have to accurately take into account the aerodynamic disturbances. Thus it became clear that we must look at the torque equilibrium attitudes (TEAs) if any existed and plan our control schemes about these. Thus the important early questions were: 1. Are there equilibrium attitudes?; 2. If so, is adequate solar power available? An investigation with the mathematical aerodynamic model of the Skylab vehicle indicated there were no aerodynamic trim or equilibrium attitudes but there may be attitudes where aerodynamic, gravity gradient, and gyroscopic torques balance. Indeed, 12 such attitudes were found. Most were not useable as control attitudes since there would be insufficient solar energy available to power the spacecraft and battery power would be completely inadequate for the several weeks required. Only 3 of the 12 TEAs appeared viable if a control scheme could be developed for them. So work began on a TEA control scheme. A candidate scheme was developed which was promising but there were large uncertainties because of lack of confidence in the aerodynamic coefficients. This lack of confidence was due to the lack of test data confirming the aero moment model at these altitudes. As a result there was not a high confidence that the new TEA scheme would work. Later flight performance would show that our models were much better than had been expected. The various mathematical models and tools needed for TEA control are described in the following sections.

3.1.2.1 TEA Bar Angles

For TEA control it was physically most meaningful to use BANK, ATTACK, and ROLL angles to describe the attitude of Skylab with respect to the rotating ZLV system. The first rotation (bank angle) is about the X axis. This axis is, on the average, parallel to the wind direction and a rotation about it does not affect the aerodynamic torques and forces. The second rotation is about the intermediate Y axis and determines the angle of attack the vehicle X axis makes with respect to the wind direction. The third rotation (roll angle) is about the X axis.

3.1.2.2 Torque Equilibrium Attitude

As mentioned previously the aerodynamic coefficients are only a function of the roll angle and the angle-of-attack. Figure 3-3 shows the zero-moment curves for the three components with respect to these angles. As can be seen, there is no set of angles, where all three curves intersect. However, they come close in several areas. To get a true three-axis equilibrium, other external torques are required. Gravity gradient (GG) torques and gyroscopic torques were found to be sufficiently large for all altitudes of concern to create twelve torque equilibrium attitudes (TEAs) altogether. Gyroscopic torques come into play, since the aerodynamic and GG torques are constant with respect to the rotating local vertical coordinate system, and the total angular momentum of the Skylab was selectable within certain limits (imposed by the finite storage capacity of the CMG system). Since the aerodynamic torques do not change (relative to body-fixed axes) when the Skylab is rotated about the relative wind velocity vector and gravity gradient torques do not change in body-fixed axes for a rotation of 180 deg about any axis perpendicular to the local vertical, there is always a pair of TEAs with the same angle-of-attack/roll angle combination, but with bank angles differing by 180 deg, i.e. there were actually only 6 basically different TEAs with respect to the aerodynamic torques and they are indicated in Fig. 3-3 by asterisks. The TEAs are shown for an altitude of 200 km (108 nautical miles) and zero total angular momentum. See Table 3-1.

ZERO TORQUE CONTOURS
ANGLE OF ATTACK VS. ROLL ANGLE

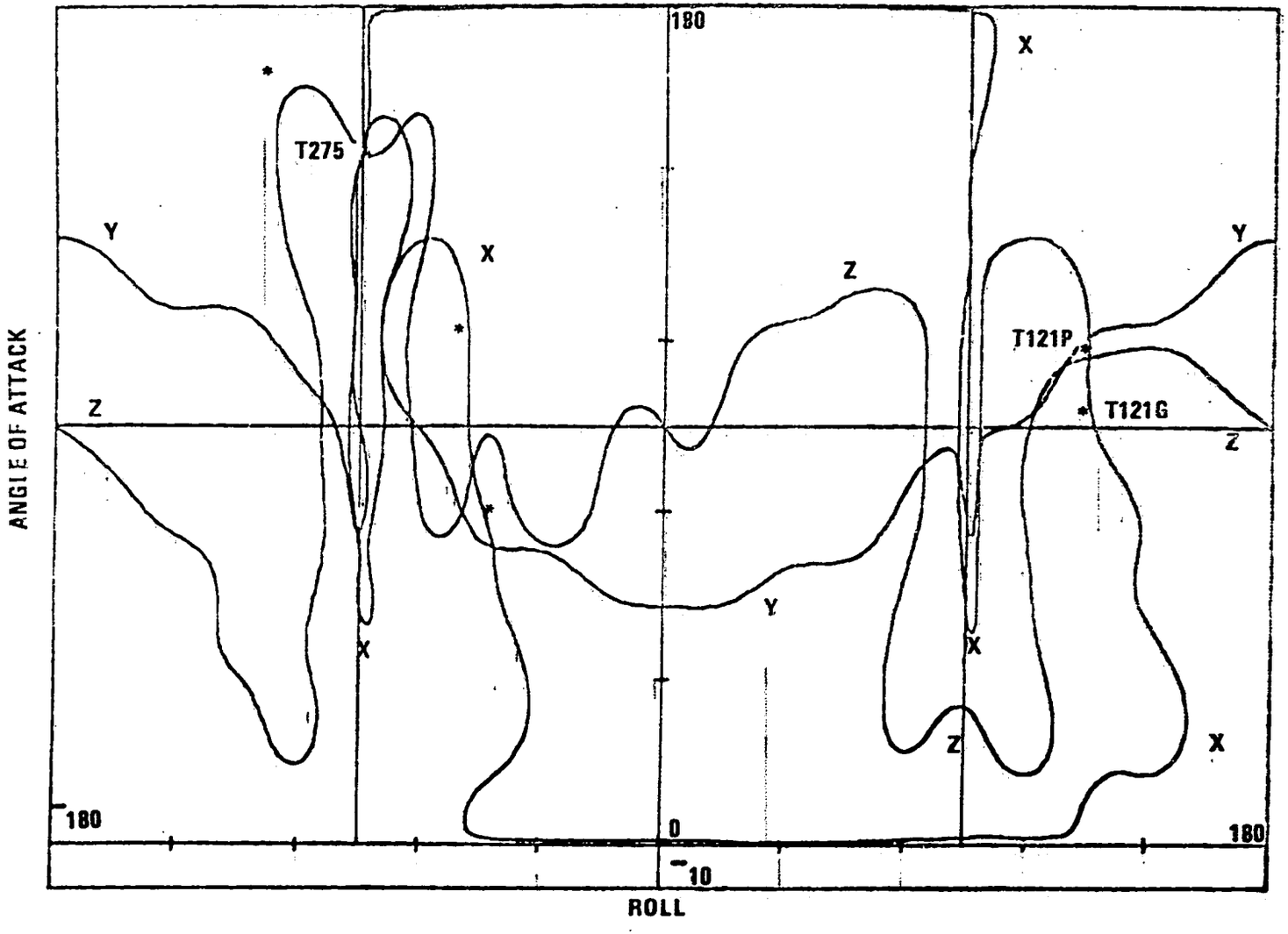

FIGURE 3-3

TABLE 3-1
TEAS FOR δ = 3.11E-10 kg/m^3

(~200 km OR 108 NAUT. MI.)

NO	ID'S	BANK ANGLE	ANGLE OF ATTACK	ROLL ANGLE	CD	BC
1 2	21P/SU ND	− 78.6 +101.4	106.0	+124.9	6.66	132.5
3 4	T121G/UN DS	− 173.2 + 6.8	93.8	+124.0	6.94	127.3
5 6	T275/BU BD	+ 70.2 − 109.4	147.8	1−89.2	3.52	250.5
7 8	BN BS	− 51.4 + 128.6	168.1	− 117.6	2.72	324.9
9 10	DN US	− 11.9 + 168.1	110.6	− 60.7	6.37	138.9
11 12	NU SD	+ 86.4 − 93.6	71.8	− 51.2	7.11	124.2

THE ABOVE TEAS ARE FOR ZERO ANGULAR MOMENTUM AND

A CP OFFSET OF $[+0.06, -0.07, -0.11]^T$ m

From solar panel power considerations a sun-pointing, inertially fixed attitude, as given in the SI mode, was the best and TEA ranged from good to bad. Nine of the TEAs were unuseable when it was established that 28 percent of full sun illumination was required for each orbit, on the average, to supply the needed power (100 percent is the power received when the sun is perpendicular to the solar panels and the vehicle is in an all-daylight orbit, as is the case for high sun elevation angles with respect to the orbital plane). Only the remaining three TEAs were usable, and these only when the optimum angular momentum was used (each of the TEAs exists in a volume of the BAR angle space when the total angular momentum is varied within its available volume). Even then, some of the TEAs did not have enough power for certain beta angles. The three acceptable TEAs were named T121P, T121G, and T275 and they are shown in Figs. 3-4, 3-5 and 3-6 where the point of view is slightly south of the orbital plane and the vehicle is moving from the front lower left to the back upper right. T275 was a low-drag attitude (the ballistic coefficient was approximately 275) with the MDA trailing; T121G and T121P were both high-drag attitudes (the ballistic coefficients were about 121). In T121G the Skylab was approximately in a GG equilibrium attitude with the MDA pointing upward (the same attitude which Skylab had been left in when it was deactivated in early 1974); in T121P the MDA was almost perpendicular to the orbital plane and pointing South. For both T121G and T121P the solar panels were trailing and they were statically stable with respect to aerodynamic torques. T121G was also statically stable with respect to the GG torques (therefore stable in all axes) whereas T121P was in an unstable GG equilibrium. Figs. 3-7 and 3-8 show the variation in T121P for different nominal angular momentum commands; the variation was used to maximize power.

3.1.2.3 TEA Seeking Method

The assumption is made that the total external torque, T , acting on Skylab is changing linearly with the attitude offset, , and that the partial derivatives of the torque with respect to the offset are known.

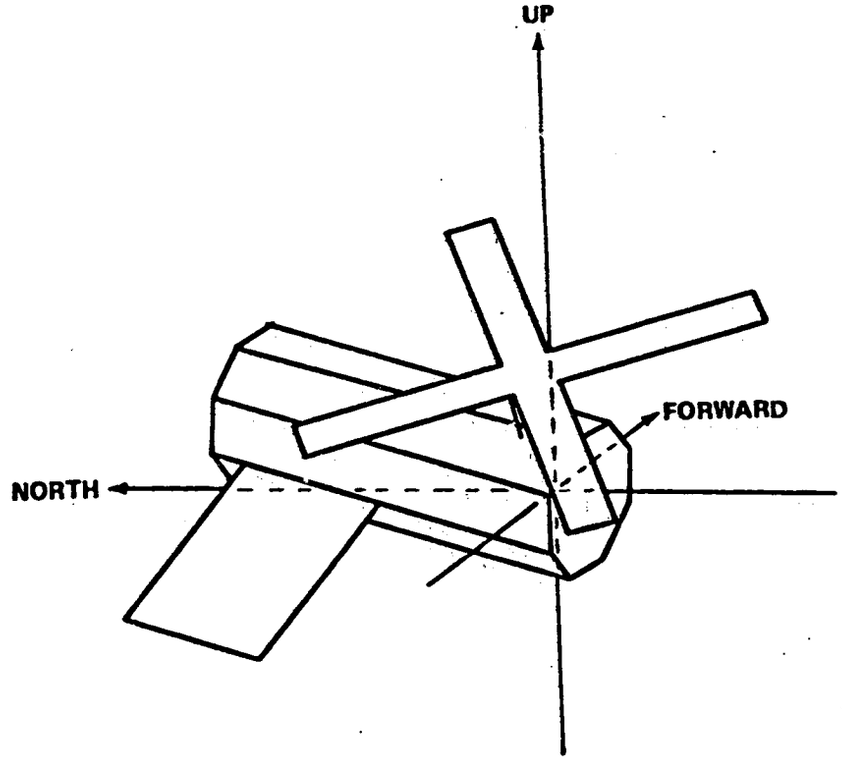

T121P (NO ANGULAR MOMENTUM)
FIGURE 3-4

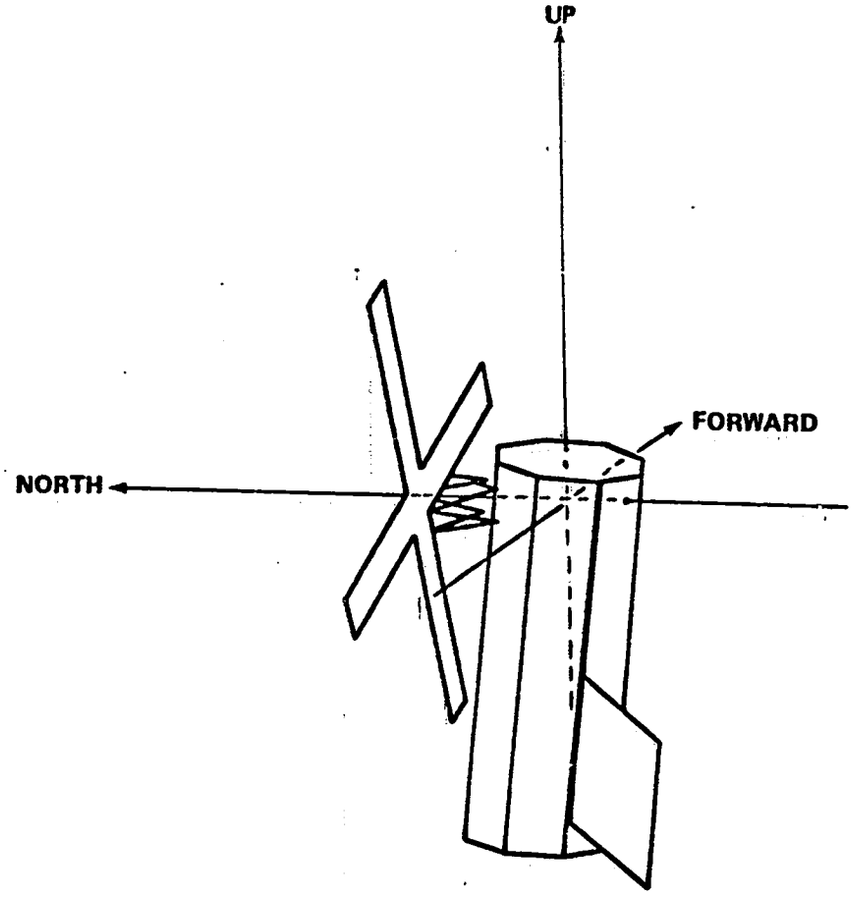

T121G (NO ANGULAR MOMENTUM)
FIGURE 3-5

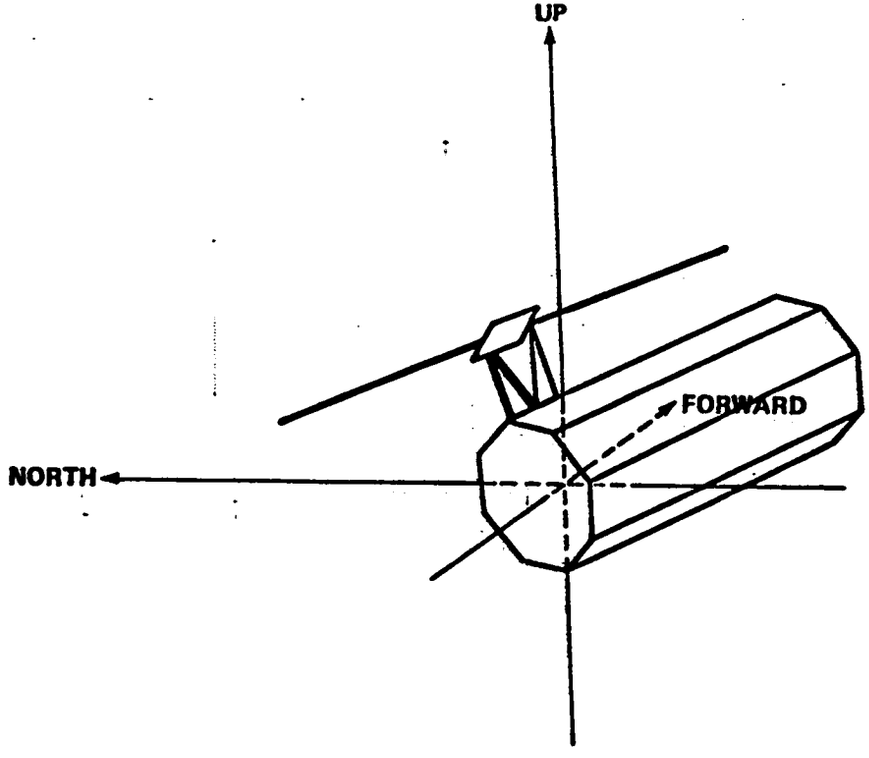

T275 (NO ANGULAR MOMENTUM)
FIGURE 3-6

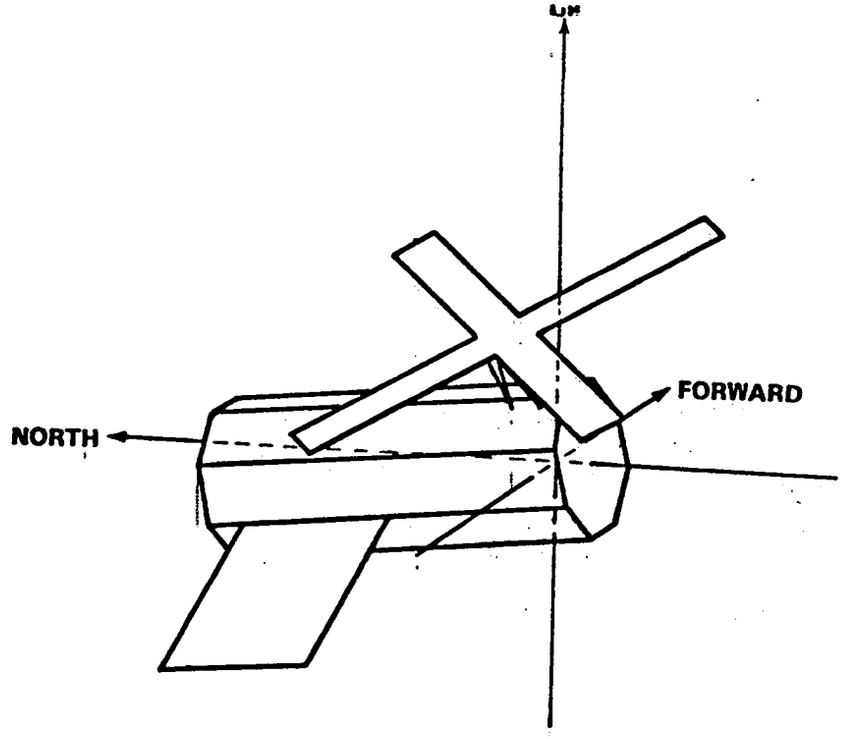

T121P (-1H ANGULAR MOMENTUM IN THE Z AXIS)
FIGURE 3-7

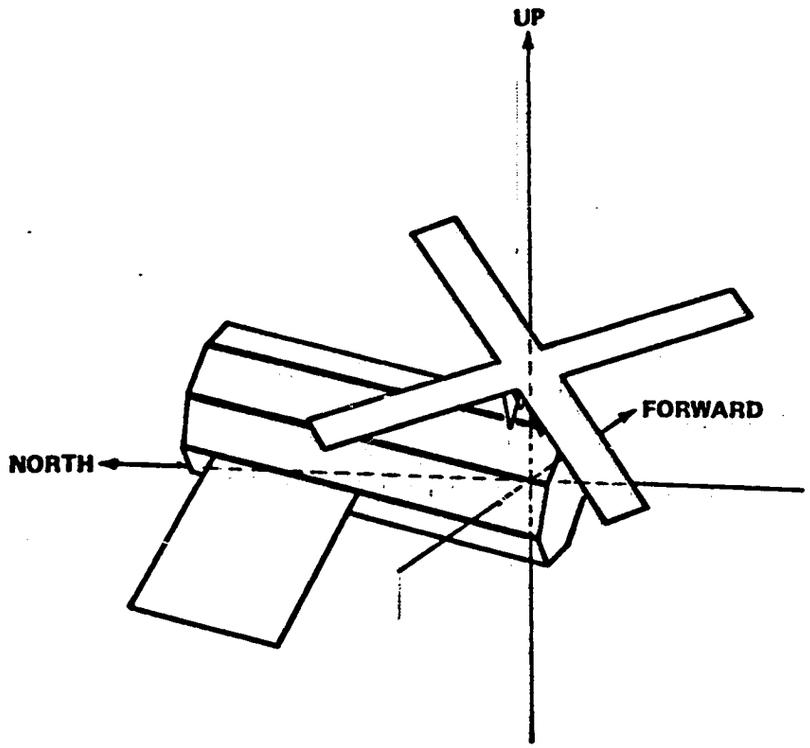

T121P (+0.5H ANGULAR MOMENTUM IN THE X AXIS)
FIGURE 3-8

$$\underline{T}_{ext} = \left[\frac{\partial T_i}{\partial \Phi_j}\right] \underline{\Delta\Phi} \qquad (T1)$$

where

$$\left[\frac{\partial T_i}{\partial \Phi_j}\right] = \begin{bmatrix} \frac{\partial T_1}{\partial \Phi_1} & \frac{\partial T_1}{\partial \Phi_2} & \frac{\partial T_1}{\partial \Phi_3} \\ \frac{\partial T_2}{\partial \Phi_1} & \frac{\partial T_2}{\partial \Phi_2} & \frac{\partial T_2}{\partial \Phi_3} \\ \frac{\partial T_3}{\partial \Phi_1} & \frac{\partial T_3}{\partial \Phi_2} & \frac{\partial T_3}{\partial \Phi_3} \end{bmatrix}$$

Evaluation of the on-board total angular momentum change over the desaturation interval, T_{des}, results in an estimate of the total external torques

$$\underline{T}_{ext} = (\underline{H} - \underline{H}_P)/T_{des} \qquad (T2)$$

where $\underline{H}$ is the present total angular momentum and $\underline{H}_P$ is its past value. The attitude offset from the torque equilibrium attitude, assuming the offset is constant, is then

$$\underline{\Delta\Phi}_{off} = \left[\frac{\partial T_i}{\partial \Phi_j}\right]^{-1} \underline{T}_{EXT} \qquad (T3)$$

Changing the attitude refernce by $-\underline{\Delta\Phi}_{off}$ would, ideally, eliminate a further angular momentum change. However, the previously accumulated angular momentum away from a desired momentum state, $\underline{H}_{nom}$, has to be eliminated during the next desaturation interval by

$$\underline{\Delta\Phi}_{mom} = -\left[\frac{\partial T_i}{\partial \Phi_j}\right]^{-1} (\underline{H} - \underline{H}_{nom})/T_{des} \qquad (T4)$$

The total required attitude change is therefore

$$\Delta\Phi = \underline{\Delta\Phi}_{mom} - \underline{\Delta\Phi}_{off}$$

$$= \frac{-1}{T_{des}} \left[\frac{\partial T_i}{\partial \Phi_j}\right]^{-1} \left\{(H - H_{nom}) + (\underline{H} - \underline{H}_P)\right\} \qquad (T5)$$

This method for attitude change eliminates, ideally, any inital condition within two desaturation intervals. (The parenthetical expressions in Eq. T5 were not combined since these quantities had to be limited separately).

In the Skylab software all angular momentum quantities were normalized by the nominal angular momentum magnitude, H, of one CMG and they were called e. Eq. T5 then becomes

$$\Delta\Phi = [SLOPE](\Delta e_m + \Delta e - \Delta e_p) \qquad (T6)$$

where

$$[SLOPE] = \frac{-H}{T_{des}}\left[\frac{\partial T_i}{\partial \Phi_j}\right]^{-1}$$

$$\Delta e_{nom} = (H - H_{nom})/H$$

Δe_m = limited value of Δe

Δe_p = Past unlimited value of Δe

The reorientation capability of Skylab was limited and therefore $\Delta\Phi$ had to be limited also. To avoid a large momentum offset overcoming a signal due to a momentum change, Δe_m is limited to a value which cannot command more then about 80% of the limit on $\Delta\Phi$.
The actual reference change is done by generating a quaternion

$$\Delta Q_{BL} = \left[\Delta\Phi/2, \sqrt{1-(\Delta\Phi\cdot\Delta\Phi)/4}\right]^T \qquad (T7)$$

and updating the reference quaternion.

$$Q_{BL} = \bar{\Delta Q}_{BL}\, Q_{BL} \qquad (T8)$$

$\bar{Q}$ is defined in equation (E4)

3.1.2.4 TEA Operation and Performance

Nominal flight parameters had to be continuously generated for several days in advance since the conditions tended to change (for example: estimated atmospheric density, estimated CP location, etc.). The data was given to the flight controllers in the form of tables (Tables 3-2 and 3-3 show the data DOY 171.5 through DOY 174.5). Since the altitude decreased slowly and personnel needed time to get used to the TEA operation, the SLOPE was not changed during this time period. ETLN (with components ETLN1, ETLN2, ETLN3 in the L system) is the normalized nominal angular momentum. Z-AXIS BETA is the elevation angle of the vehicle Z axis with respect to the orbital plane. CD and BC are the drag and the ballistic coefficients, respectively. CMG MOM is the angular momentum in the CMG system and it is in percent of 3H. ETSF is the normalized and filtered total system momentum in vehicle components. QBLNOM is the nominal attitude reference quaternion Q AL (a QBL already existed in the flight computer and could be used; therefore the subscripts A and B are equivalent here).

Table 3-4 shows the SLOPE MATRIX UPDATE LOG. The first three columns show the date when the SLOPE was updated (DOY 171 corresponds to 6/20 and DOY 192 to 7/11). The first entry is the start of TEA control rather than the time when the initial SLOPE was loaded. The index in the fourth column is added to facilitate correlation with Table 3-5. Columns 5 through 13 show the components of the SLOPE as indicated by the heading. Table 3-5 shows what data was used to generate the SLOPES. The slope generation parameters for index 2 and 3 are the same; the transpose of SLOPE 3 had been sent up (SLOPE 2) by mistake, whereupon attitude control was promptly lost. SLOPE 3 was sent as soon as attitude control had been regained. SLOPE 13 was used for a higher altitude than the one for which it was calculated, since a 6 hour gap in the ground coverage eliminated an additional slope change and it was considered better to have the proper slope at a lower altitude and take a reduced gain at the higher altitudes.

Figure 3-9 shows the actual BAR angles for DOY 172:03:21 to DOY 172:06:12 versus time in seconds and the predicted BAR angles are shown as horizontal lines. It can also be noted that the BAR angle traces zig-zagged, indicating that the gain was too high. As a consequence the SLOPE gain was later reduced to 0.5 from 1.0, resulting in a much smoother trace. The actual BAR angles are only correct to within the strapdown error, which, due to the availablity of ACQ SS information, was less than a

PARAMETER TABLE 3-2

INDEX	ALTITUDE KM	ALTITUDE NM	DOY	MONTH	DAY	HOUR
1	262.925	141.968	171.50	6	20	12
2	260.825	140.834	172.50	6	21	12
3	259.493	140.115	173.50	6	22	12
4	257.671	139.131	174.50	6	23	12

DOY	ALT	BETA	ETLN 1	ETLN 2	ETLN 3	BANK	ATTACK	ROLL
171.50	141.97	18.20	0.0	0.8	-1.0	-98.05	93.32	114.86
172.50	140.83	13.40	0.0	0.8	-1.0	-98.04	93.22	113.99
173.50	140.11	8.60	0.0	0.8	-1.0	-98.04	93.37	114.89
174.50	139.13	4.10	0.0	0.8	-1.0	-98.04	93.60	114.24

DOY	ALT	BETA	ETLN 1	ETLN 2	ETLN 3	CHIX	CHIY	CHIZ
171.50	141.97	18.20	0.0	0.8	-1.0	-88.22	-112.52	-81.38
172.50	140.83	13.40	0.0	0.8	-1.0	-87.73	-111.95	-81.34
173.50	140.11	8.60	0.0	0.8	-1.0	-88.53	-112.86	-81.28
174.50	139.13	4.10	0.0	0.8	-1.0	-89.70	-114.19	-81.19

DOY	ALT	BETA	ETLN 1	ETLN 2	ETLN 3	Z-AXIS BETA	CD	BC
171.50	141.97	18.20	0.0	0.8	-1.0	8.70	6.55	134.72
172.50	140.83	13.40	0.0	0.8	-1.0	8.65	6.55	134.79
173.50	140.11	8.60	0.0	0.8	-1.0	8.71	6.56	134.68
174.50	139.13	4.10	0.0	0.8	-1.0	8.81	6.56	134.51

PARAMETER TABLE 3-3

DIR COS MATRIX COMPONENTS

ALT	1,1	2,1	3,1	1,2	2,2	3,2	1,3	2,3	3,3
141.97	-0.058	0.912	-0.407	-0.988	0.005	0.151	0.140	0.411	0.901
140.83	-0.056	0.912	-0.406	-0.989	0.006	0.150	0.140	0.410	0.901
140.11	-0.059	0.911	-0.407	-0.988	0.004	0.151	0.140	0.412	0.901
139.13	-0.063	0.910	-0.410	-0.988	0.001	0.153	0.140	0.415	0.899

SLOPE MATRIX COMPONENTS

ALT	1,1	2,1	3,1	1,2	2,2	3,2	1,3	2,3	3,3
141.97	2.038	-0.791	-1.466	2.171	-0.410	1.398	4.271	1.119	1.557
140.83	**********								
140.11	**********								
139.13	**********								

ALT	ETLN 1	2	3	CMG MOM X	Y	Z	GIMBAL ANGLES IG2	OG2	IG3	OG3	ETSF X	Y	Z
142.0	0.0	0.8	-1.0	-19	-15	-40	-16	89	27	105	-0.931	-0.407	-0.780
140.8	0.0	0.8	-1.0	-19	-15	-40	-16	89	27	105	-0.930	-0.405	-0.781
140.1	0.0	0.8	-1.0	-19	-15	-40	-16	89	27	105	-0.930	-0.409	-0.779
139.1	0.0	0.8	-1.0	-19	-15	-40	-16	89	27	105	-0.930	-0.414	-0.777

ALT	ETLN 1	2	3	QBLNOM 1	2	3	4
142.0	0.0	0.8	-1.0	0.0956	-0.2012	-0.6989	0.6796
140.8	0.0	0.8	-1.0	0.0953	-0.2005	-0.6985	0.6803
140.1	0.0	0.8	-1.0	0.0958	-0.2014	-0.6992	0.6793
139.1	0.0	0.8	-1.0	0.0965	-0.2027	-0.7002	0.6777

TABLE 3-4

SLOPE MATRIX UPDATE LOG

DATE				SLOPE MATRIX COMPONENTS								
DAY	HR	MIN	IND	1,1	1,2	1,3	2,1	2,2	2,3	3,1	3,2	3,3
171	13	17	1	2.038	-2.171	-4.271	-0.791	-0.410	1.119	-1.466	1.398	1.557
175	16	14	2	1.975	-1.058	-2.125	-1.719	-0.249	1.513	-3.702	1.244	1.982
175	19	21	3	1.975	1.719	3.702	-1.058	0.249	1.244	-2.125	1.513	1.982
176	15	57	4	2.598	1.309	2.803	-1.421	0.122	1.702	-2.885	2.066	2.925
177	15	43	5	1.664	0.319	0.711	-0.756	0.215	1.101	-1.478	1.218	1.684
180	13	45	6	1.904	0.004	0.072	-0.759	0.215	0.825	-0.973	0.873	0.716
181	13	32	7	1.522	0.137	0.212	-1.010	0.197	0.800	-1.303	0.842	0.683
183	20	52	8	1.088	0.093	-0.130	-0.662	-0.050	0.732	-1.167	0.736	0.736
186	13	50	9	0.784	0.053	-0.024	-0.239	-0.080	0.528	-0.555	0.515	0.379
189	20	21	10	0.378	0.073	-0.056	0.006	-0.193	0.351	-0.246	0.328	0.078
190	13	42	11	0.283	0.079	-0.061	0.046	-0.215	0.319	-0.204	0.294	-0.022
191	4	9	12	0.208	0.084	-0.065	0.075	-0.232	0.295	-0.175	0.269	-0.020
191	17	57	13	0.189	0.189	-0.145	0.236	-0.531	0.539	-0.288	0.482	-0.165
192	3	33	14	0.106	0.204	-0.157	0.276	-0.578	0.541	-0.279	0.480	-0.219

TABLE 3-5 SLOPE GENERATION PARAMETERS

INDEX	SIGMA	GAIN	REF ALTITUDE KM	REF ALTITUDE NM	ETLN X	ETLN Y	ETLN Z	CP X	CP Y	CP Z	REF BAR ANGLES BANK	REF BAR ANGLES ATTACK	REF BAR ANGLES ROLL
1	1	1.0	262.00	141.47	0.0	0.8	1.0	0.00	0.00	0.00	98.05	93.32	114.06
2	1	1.0	255.52	137.97	0.0	0.8	0.7	0.06	0.07	0.16	92.17	92.91	114.02
3	1	1.0	255.52	137.97	0.0	0.8	0.7	0.06	0.07	0.16	92.17	92.91	114.02
4	1	1.0	253.13	136.68	0.0	0.8	0.4	0.06	0.07	0.16	86.93	95.97	115.51
5	1	0.5	250.59	135.31	0.0	0.8	0.2	0.06	0.07	0.16	83.51	98.92	118.03
6	1	0.5	241.78	130.55	0.1	1.2	0.0	0.00	0.00	0.00	80.15	100.16	126.74
7	1	0.5	238.33	128.69	0.2	1.2	0.0	0.00	0.00	0.00	80.09	94.75	126.38
8	0	0.5	229.65	124.00	0.2	1.2	0.0	0.06	0.07	0.11	78.89	94.56	122.36
9	0	0.5	212.33	114.65	0.2	1.2	0.0	0.06	0.07	0.11	79.11	100.03	123.47
10	0	0.5	187.53	101.26	0.2	1.2	0.0	0.06	0.07	0.11	77.38	103.38	124.48
11	0	0.5	179.94	97.16	0.2	1.2	0.0	0.06	0.07	0.11	76.39	104.02	124.71
12	0	0.5	172.64	93.22	0.2	1.2	0.0	0.06	0.07	0.11	75.11	104.50	124.88
13	0	1.0	158.94	86.36	0.2	1.2	0.0	0.06	0.07	0.11	78.73	105.14	125.14
14	0	1.0	152.49	82.34	0.2	1.2	0.0	0.06	0.07	0.11	67.08	105.32	125.22

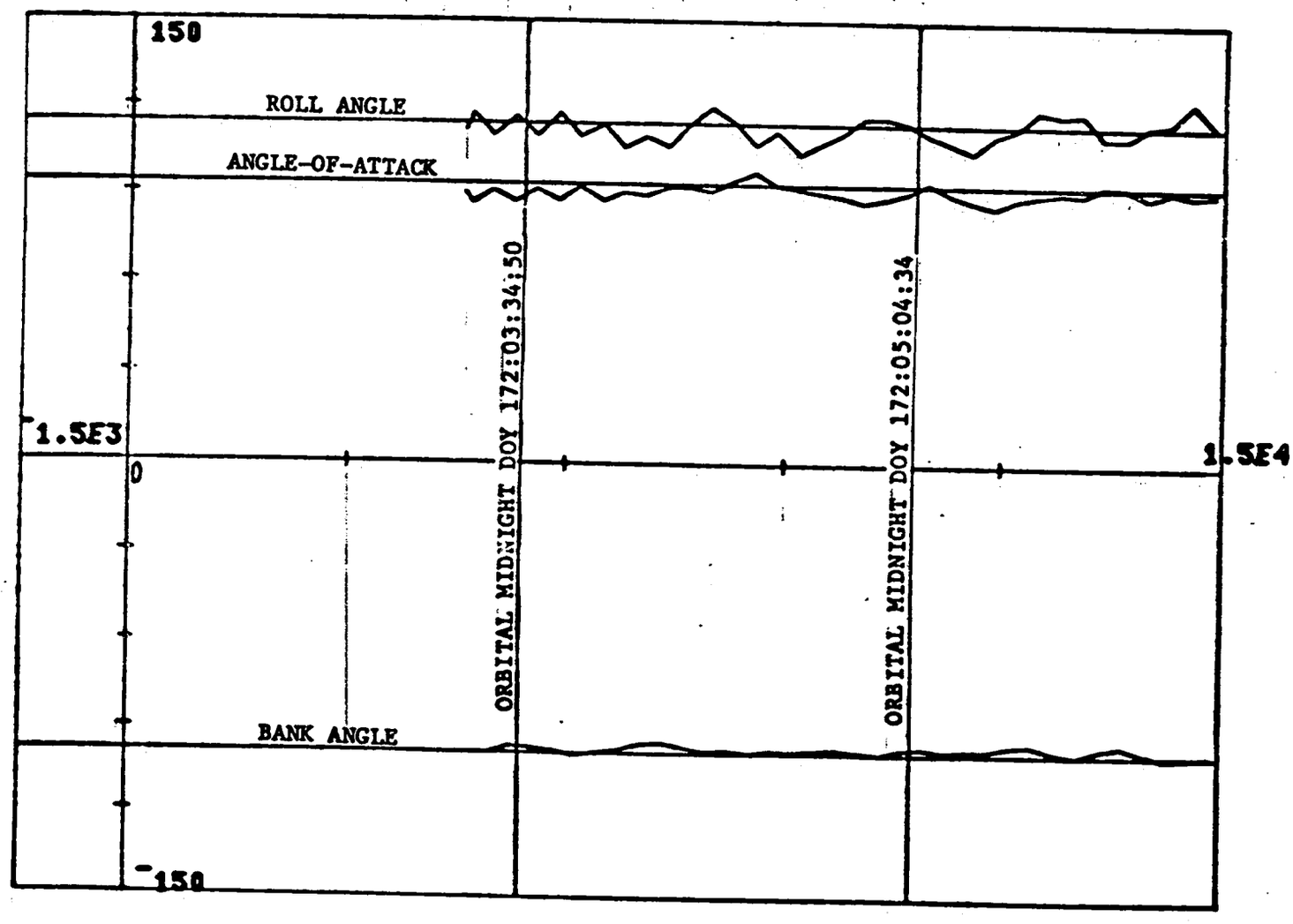
BAR ANGLES (DOY 172:03:21/172:06:12)
150
ROLL ANGLE
ANGLE-OF-ATTACK
ORBITAL MIDNIGHT DOY 172:03:34:50
ORBITAL MIDNIGHT DOY 172:05:04:34
1.5E3
0
1.5E4
BANK ANGLE
-150

FIGURE 3-9

degree. A very good correspondance between the nominal and the actual BAR angles can be seen, indicating that the prediction of the CM and CP locations, as well as the aerodynamic coefficients, was much better than anticipated. The nominal BAR angles were generated assuming that the relative wind velocity is antiparallel to the vehicle velocity vector, but reduced by an amount appropriate for the earth rate. The nominal BAR angles are therefore the nominal average of the actual BAR angles. Some of the good correspondence is due to the fact that changes in ETLN1 were used to influence the roll angle. Initially, a roll angle smaller than nominal was very detrimental since the slope matrix changed drastically such that a roll angle of less than 90 deg was found to be unstable: the actual slope components had changed sign. An initial unfavorable rate gyro bias could have changed the actual roll angle by that much long before the ground would have had enough data to detect and correct for it. To eliminate this possibility, a favorable rate gyro bias compensation was introduced into the software such that if we had had the bad gyro drift, the compensation would have eliminated it. As it turned out, the real rate gyro bias was in a good direction and the compensation had to be changed to the opposite polarity (as always, Skylab seemed to refute Murphy's Law, since anything that could go right, would; also see the last paragraph of this section). The great sensitivity to the rate-gyro introduced drift about orbital north was due to the relatively large negative angular momentum bias in the Z_L axis (ETLN3 = -1H) which then was resolved into the actual X_L axis thereby changing the equilibrium position drastically. This resolution also suggested the (at least temporary) remedy: counteract it with an appropriate amount of momentum bias in the X_L axis.

An overview of the BAR angles for the three weeks of TEA operation is given in Figs. 3-10, 3-11 and 3-12. The bank angle is the lowest trace, the angle of attack is in the middle, and the roll angle is the highest. Each figure shows one week of TEA operation. The horizontal scale is in days, the numbers indicate the start of a day. Only BAR angles from the ASAP tapes are shown, since they were saved in the ground computer.

TEA control was initiated on DOY 171:13:17 GMT (6/20/79) and Skylab impact occurred on DOY 192:16:37 GMT (7/11/79). During the latter half of DOY 171 it can be seen that the average roll angle steadily increased. This was due to the initial rate gyro bias (intentional compensation and basic bias). After corrective action was taken the angles settled close to their predicted values. Figures 3-10 and 3-11 show the BAR angles during the shift in ETLN3 from -1H to 0 between DOY 175.5 and

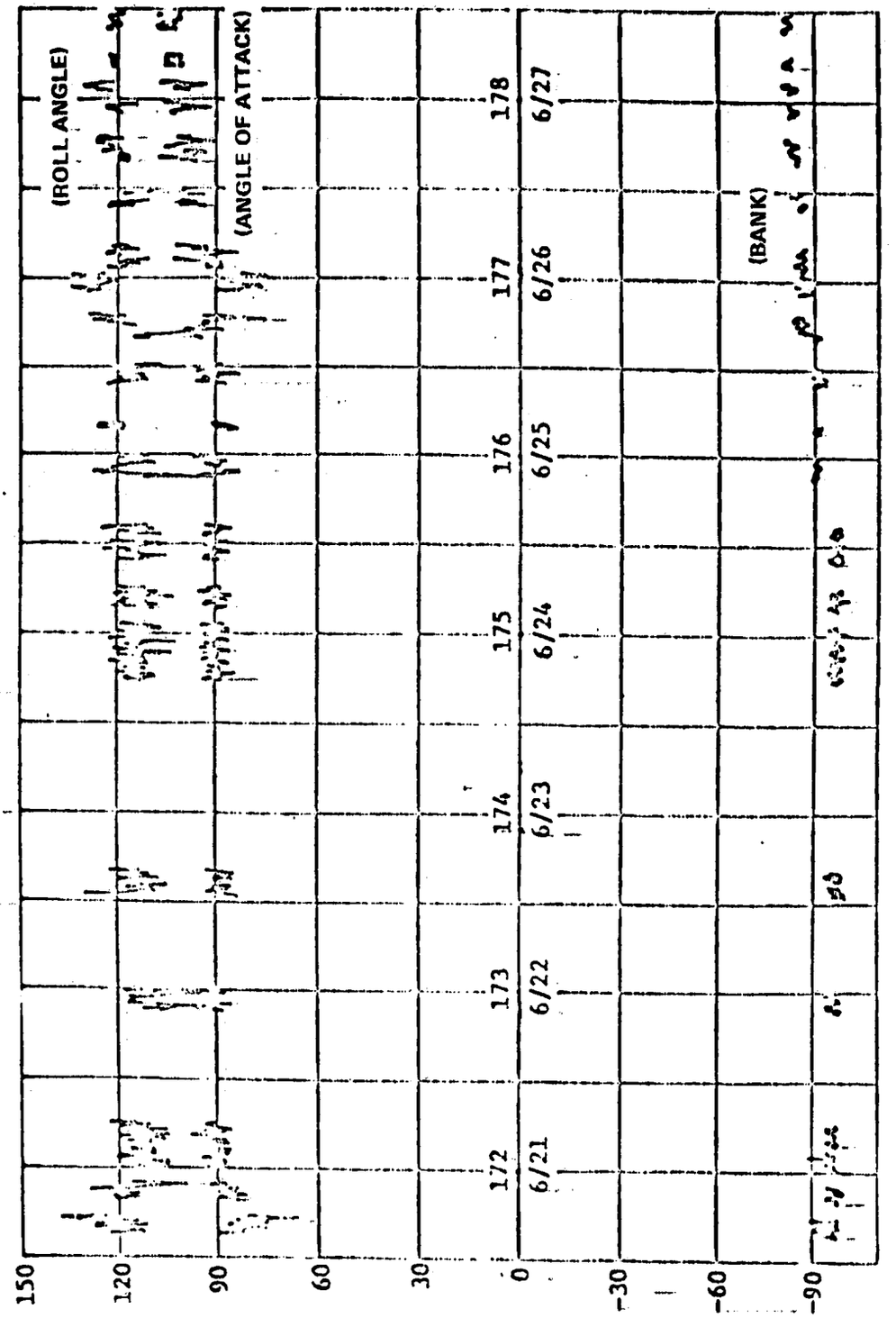

FIGURE 3-10

BAR ANGLES, SECOND WEEK

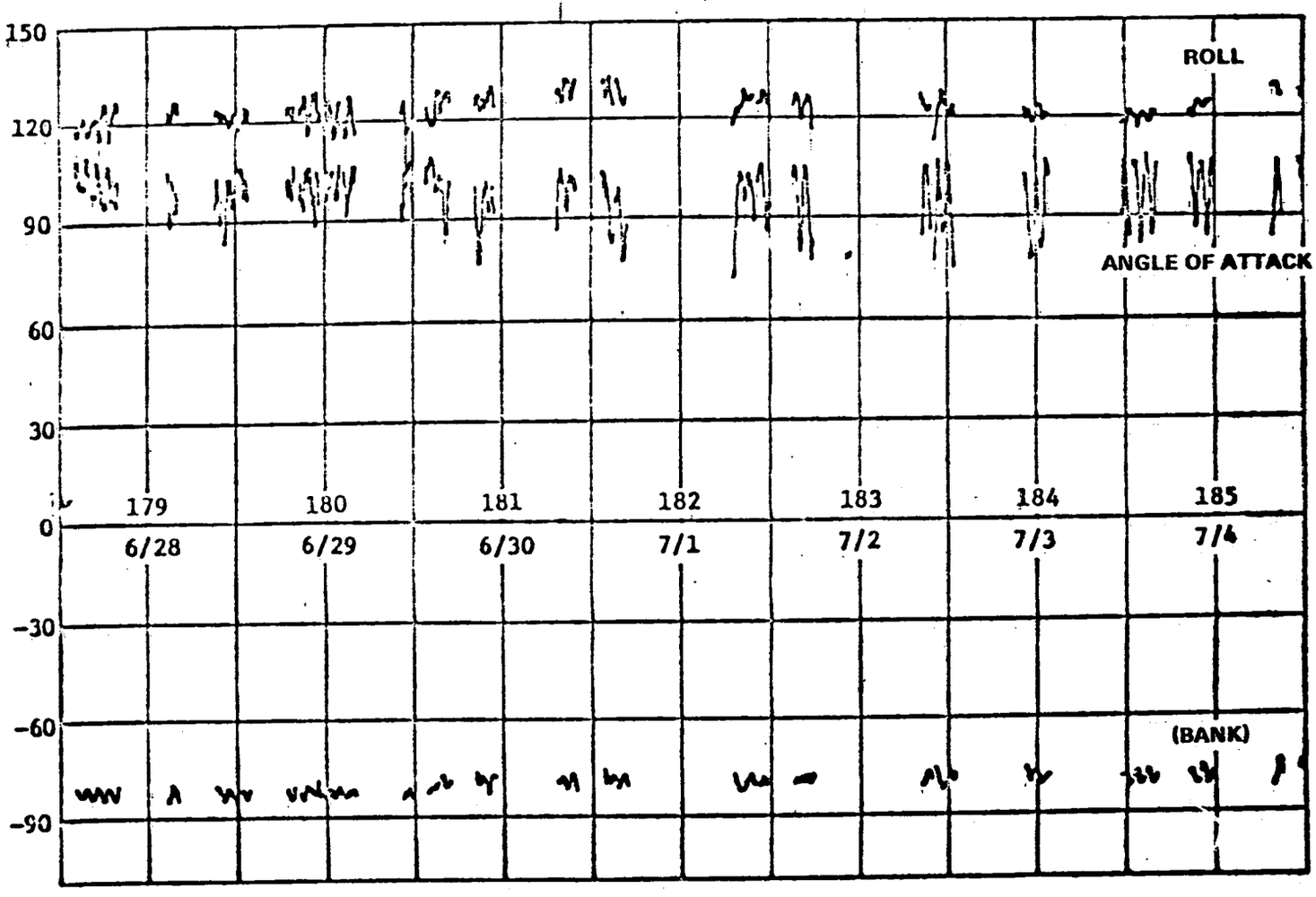

FIGURE 3-11

BAR ANGLES, THIRD WEEK

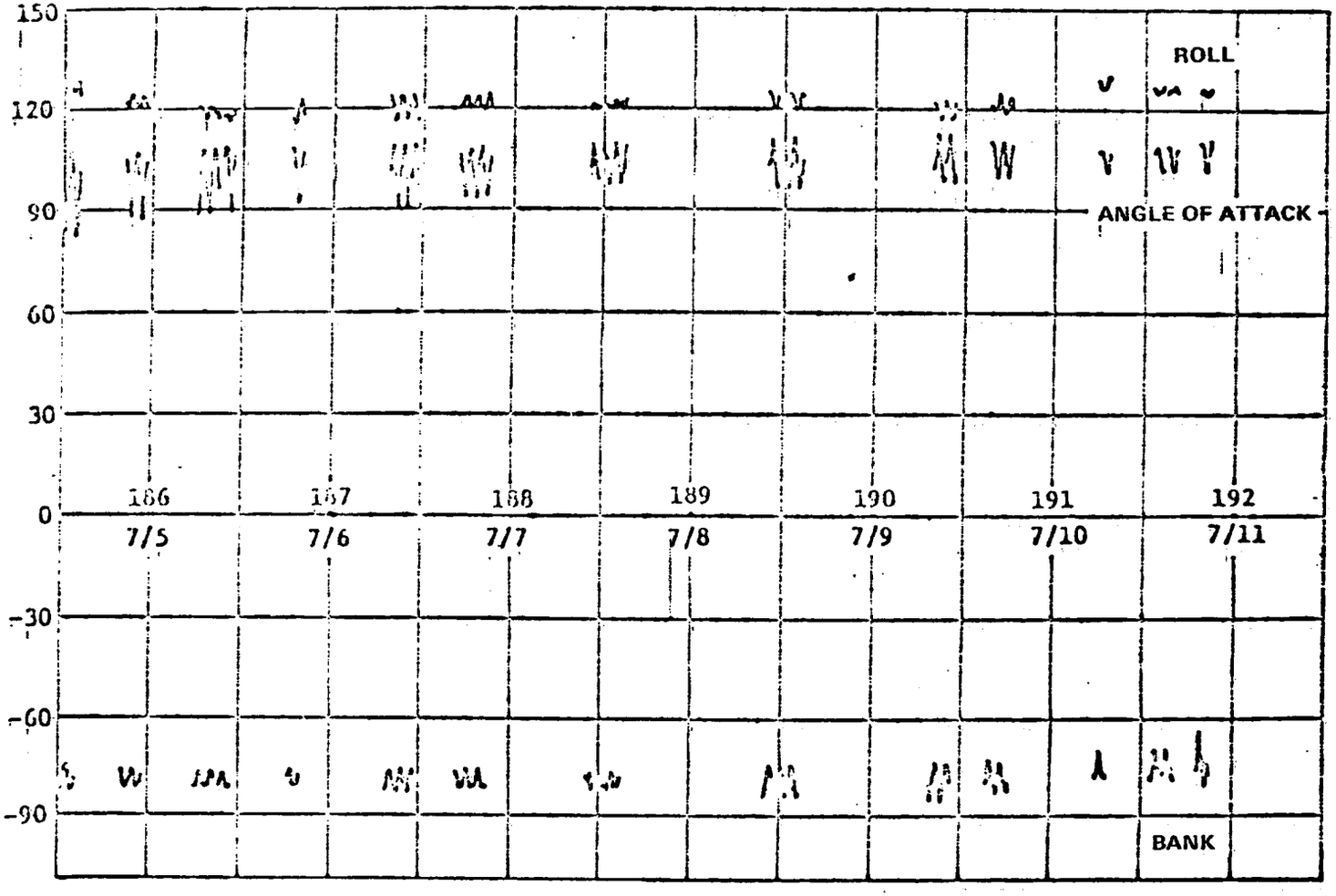

FIGURE 3-12

DOY 180.5. With the gradual removal of the ETLN3 the sensitivity to rate gyro drift was removed; however, the excellent control capability over the roll angle (and with it, the drag), also vanished. In fact, the actual roll angle could later not be influenced at all (the indicated roll angle also showed the effect of strapdown error about orbit north and this fact in conjunction with one fact that the actual roll angle was steady, allowed the use of the indicated roll angle for strapdown update about orbit north).

To illustrate the evaluation of the information on the ASAP tapes DOY 187:16:56:30 to DOY 187:20:56:30 are taken as an example. Table 3-6 shows the basic QBL/time information, the equivalent BAR angles are shown in Table 3-7 and graphed in Figure 3-13. The BAR angles were always evaluated for their avarage and a sinusoid of orbital frequency. The latter was fitted by a least-square fit, after the average had been subtracted. The results for our example are shown in Figures 3-14, 3-15 and 3-16. In the lower left quadrant of each figure there is a table of expected angle values (right column) as a function of the orbital angle (left column). Since the circle charts (Figure 3-17) show this orbital angle, the tables were used to check the actual BAR angles (live; from telemetry) against these reference angles.

The sinusoids in the angle-of-attack and roll angle were due to the relative wind direction oscillating about the vehicle velocity direction (since the atmosphere rotates with the earth). The sinusoid in the bank angle was due to the In Orbit Plane (IOP) strapdown error and the appropriate strapdown update is shown in the upper left hand corner of Figure 3-14, both with respect to orbital midnight and with respect to the actual time, the update is to be telemetered. For the latter a resolution of the error with respect to midnight had to be made.

Application of the various methods was severely hampered by lack of data and large delays between the ocurrence and the receipt of the data. If the strapdown error had drifted substantially there would have been no way to correct it in time. Fortunately, the rate gyro drift components in the orbital plane (if constant) integrate to exactly zero in one revolution and generally TEA control was not very sensitive to the drift components along the orbit normal. In-plane strapdown errors resulted from inaccurate navigation updates and from the sun motion of about one deg/day. For data on strapdown errors the on-board ASAP tape recorder had to be run for at least one full orbit (more consecutive orbits were desired for noise content reduction) during a quiet state i.e. the last slope update had

TABLE 3-6 QBL TIME INFORMATION

GBLCHECK
THE CURRENT QBL SET IS AS FOLLOWS:
THE COLUMNS ARE DISPLAYED AS ROWS FOR CONCISENESS

1	0.2275680	-0.1183[illegible]	-0.7917000	0.5544907	187:16:56:30.00
2	0.2345000	-0.1128001	-0.7694000	0.5846771	187:17: 1:30.00
3	0.2359000	-0.1268001	-0.7667000	0.5914403	187:17: 6:30.00
4	0.2343000	-0.1362000	-0.7548000	0.5973525	187:17:11:33.00
5	0.2324000	-0.1456[illegible]	-0.7453000	0.6080839	187:17:16:30.00
6	0.2336000	-0.1523[illegible]	-0.7314000	0.6223261	187:17:21:33.00
7	0.2374000	-0.1583[illegible]	-0.7211000	0.6326750	187:17:26:33.00
8	0.2422000	-0.1536000	-0.7133000	0.6334914	187:17:31:33.00
9	0.2435000	-0.1586[illegible]	-0.7136000	0.6374393	187:17:36:33.00
10	0.2378000	-0.1625000	-0.7361000	0.6125371	187:17:41:33.00
11	0.2252000	-0.1599000	-0.7545000	0.5953543	187:17:46:30.00
12	0.2184000	-0.1556000	-0.7725000	0.5753000	187:17:51:33.00
13	0.2193000	-0.1493000	-0.7792000	0.5710634	187:17:56:33.00
14	0.2115000	-0.1363000	-0.7958000	0.5660963	187:18: 1:33.00
15	0.2152000	-0.1263000	-0.7936000	0.5591059	187:18: 6:30.00
16	0.2213000	-0.1219000	-0.7971000	0.5484509	187:18:11:30.00
17	0.2256000	-0.1183000	-0.7991000	0.5445631	187:18:16:30.00
18	0.2269000	-0.1125000	-0.7947000	0.5516063	187:18:21:30.00
19	0.2351000	-0.1050003	-0.7780000	0.5730785	187:18:26:33.00
20	0.2341000	-0.1103000	-0.7689000	0.5846571	187:18:31:30.00
21	0.2351000	-0.1223000	-0.7599000	0.5935678	187:18:36:30.00
22	0.2310000	-0.1355000	-0.7587000	0.6036200	187:18:41:30.00
23	0.2297000	-0.1469000	-0.7437000	0.6103040	187:18:46:30.00
24	0.2322000	-0.1501000	-0.7328000	0.6217373	187:18:51:30.00
25	0.2373000	-0.1548000	-0.7187000	0.6349771	187:18:56:30.00
26	0.2422000	-0.1533000	-0.7106000	0.6423497	187:19: 1:30.00
27	0.2469000	-0.1529000	-0.7110000	0.6404225	187:19: 6:30.00
28	0.2377000	-0.1504000	-0.7370000	0.6116039	187:19:11:30.00
29	0.2253000	-0.1612000	-0.7612000	0.5863694	187:19:16:30.00
30	0.2169000	-0.1601000	-0.7748000	0.5718456	187:19:21:30.00
31	0.2080000	-0.1526000	-0.7760000	0.5744832	187:19:26:30.00
32	0.2093000	-0.1434000	-0.7820000	0.5689512	187:19:31:30.00
33	0.2150000	-0.1276000	-0.7897000	0.5602305	187:19:36:30.00
34	0.2230000	-0.1203000	-0.7953000	0.5519292	187:19:41:30.00
35	0.2212000	-0.1202000	-0.8015000	0.5424207	187:19:46:30.00
36	0.2252000	-0.1144000	-0.7960000	0.5489147	187:19:51:30.00
37	0.2333000	-0.1033000	-0.7832000	0.5602330	187:19:56:30.00
38	0.2302000	-0.1046000	-0.7686000	0.5876401	187:20: 1:30.00
39	0.2288000	-0.1183000	-0.7581000	0.5994210	187:20: 6:30.00
40	0.2388000	-0.1316000	-0.7581000	0.6059137	187:20:11:30.00
41	0.2311000	-0.1418000	-0.7420000	0.6131244	187:20:16:30.00
42	0.2320000	-0.1494000	-0.7294000	0.6259643	187:20:21:30.00
43	0.2301000	-0.1531000	-0.7282000	0.6333803	187:20:26:30.00
44	0.2451000	-0.1552000	-0.7145000	0.6366543	187:20:31:30.00
45	0.2409000	-0.1612000	-0.7224000	0.6247819	187:20:36:30.00
46	0.2359000	-0.1667000	-0.7376000	0.6103348	187:20:41:30.00
47	0.2244000	-0.1603000	-0.7591000	0.5896743	187:20:46:30.00
48	0.2138000	-0.1567000	-0.7731000	0.5766698	187:20:51:30.00
49	0.2064000	-0.1478000	-0.7828000	0.5683434	187:20:56:30.00

TABLE 3-7 BAR ANGLES FOR QBL18716

BARANGS			
1	76.19	106.35	120.81
2	76.50	101.91	120.21
3	77.66	100.90	121.15
4	78.81	100.17	121.65
5	80.14	98.77	121.97
6	81.19	96.68	122.34
7	81.40	94.98	122.54
8	81.41	93.71	122.90
9	81.62	93.94	123.44
10	81.23	97.85	123.67
11	81.25	100.93	122.69
12	80.67	104.04	122.25
13	80.59	105.00	121.11
14	79.36	105.64	120.34
15	78.03	106.38	120.13
16	76.72	107.48	120.67
17	75.92	107.76	120.92
18	75.71	106.76	120.41
19	75.38	103.45	119.99
20	76.34	101.93	119.98
21	77.54	100.65	120.75
22	79.22	99.43	121.24
23	80.55	98.59	121.80
24	81.10	96.84	122.05
25	81.66	94.65	122.65
26	81.51	93.29	122.83
27	81.05	93.31	123.22
28	80.88	97.98	123.36
29	80.94	102.17	122.98
30	80.90	104.59	122.45
31	81.21	104.68	121.02
32	79.97	105.37	120.37
33	78.18	106.25	120.17
34	76.87	107.09	120.33
35	76.34	108.28	120.71
36	75.86	107.21	120.48
37	75.45	104.37	119.58
38	76.36	101.73	119.14
39	78.04	100.22	119.69
40	79.16	99.20	120.74
41	80.17	98.13	121.47
42	81.24	96.24	121.91
43	81.40	94.83	122.60
44	81.20	93.97	123.31
45	80.86	95.49	124.30
46	81.60	98.26	123.87
47	81.09	101.76	122.76
48	81.19	104.13	121.73
49	80.68	105.59	120.59

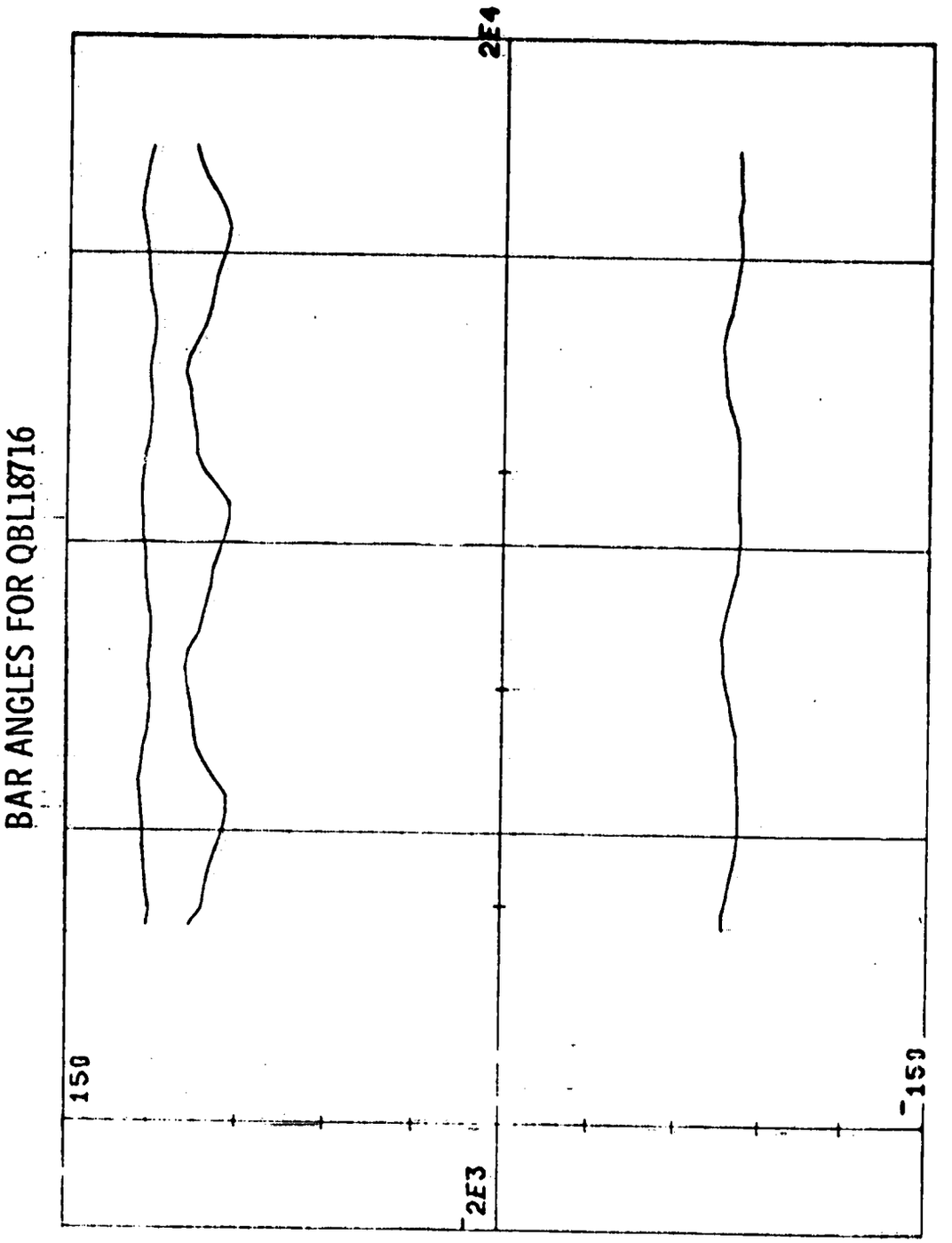

FIGURE 3-13

```
DETHL WRT MIDNIGHT 0.99947   0   -2.7012

SUGGESTED DETHL 2.8723   0   -0.21296

THE AVERAGE BANK ANGLE IS -79.186
        THE AMPLITUDE IS 2.8802
            THE PHASE IS 159.69
```

DESIRED UPDATE	188: 5:27: 0.00
MIDNIGHT TIME	187:17:21: 0.00
1 REV DELTA TIME	1:28:44.00
FIRST OBL TIME	187:16:56:30.00
LAST OBL TIME	187:20:56:30.00

0	-80.2
30	-81.4
60	-82.0
90	-81.9
120	-81.0
150	-79.7
180	-78.2
210	-77.0
240	-76.3
270	-76.5
300	-77.3
330	-78.7
360	-80.2

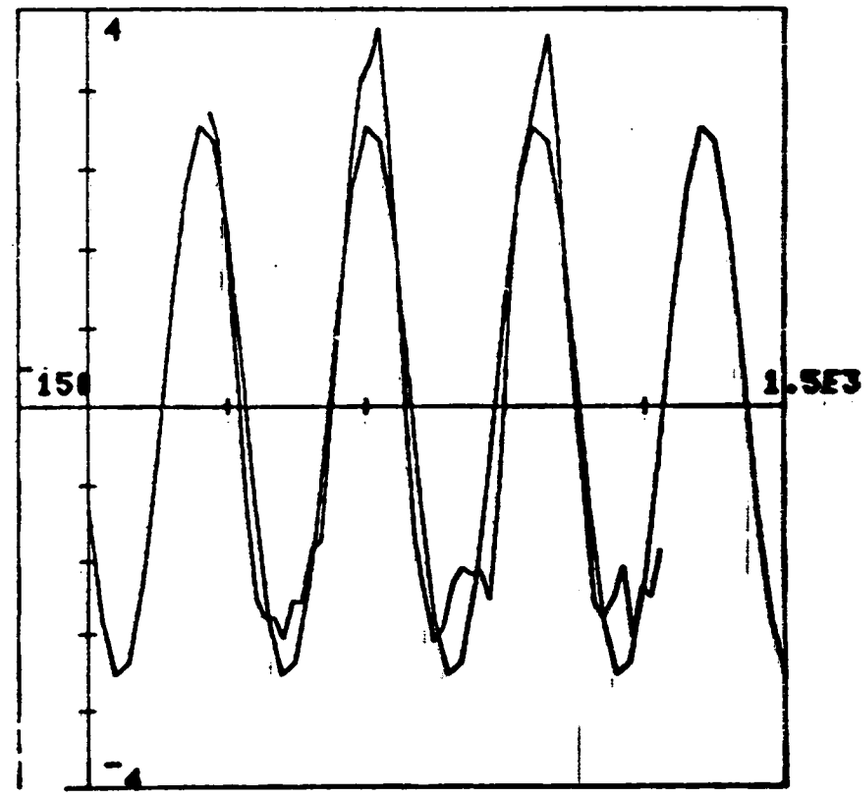

FIGURE 3-14

```
THE AVERAGE ANGLE OF ATTACK IS 101.51
                THE AMPLITUDE IS 6.41
                    THE PHASE IS 120.01

DESIRED UPDATE          188: 5:27: 0.00
MIDNIGHT TIME           187:17:21: 0.00
1 REV DELTA TIME              1:28:44.00
FIRST QBL TIME          187:16:56:30.00
LAST QBL TIME           187:20:56:30.00

     0       96.0
    30       95.1
    60       96.0
    90       98.3
   120      101.5
   150      104.7
   180      107.1
   210      107.9
   240      107.1
   270      104.7
   300      101.5
   330       98.3
   360       96.0
```

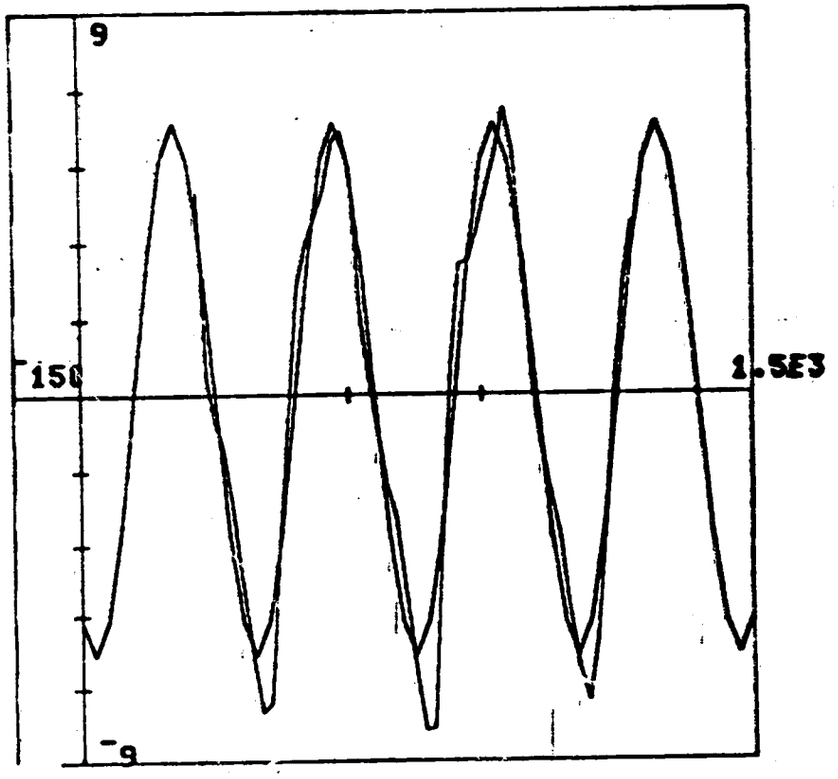

FIGURE 3-15

THE AVERAGE ROLL ANGLE IS 121.47
THE AMPLITUDE IS 1.6477
THE PHASE IS 335.18

DESIRED UPDATE	188: 5:27: 0.00
MIDNIGHT TIME	187:17:21: 0.00
1 REV DELTA TIME	1:28:44.00
FIRST QBL TIME	187:16:56:30.00
LAST QBL TIME	187:20:56:30.00

0	122.2
30	122.8
60	123.1
90	123.0
120	122.4
150	121.6
180	120.8
210	120.1
240	119.8
270	120.0
300	120.5
330	121.3
360	122.2

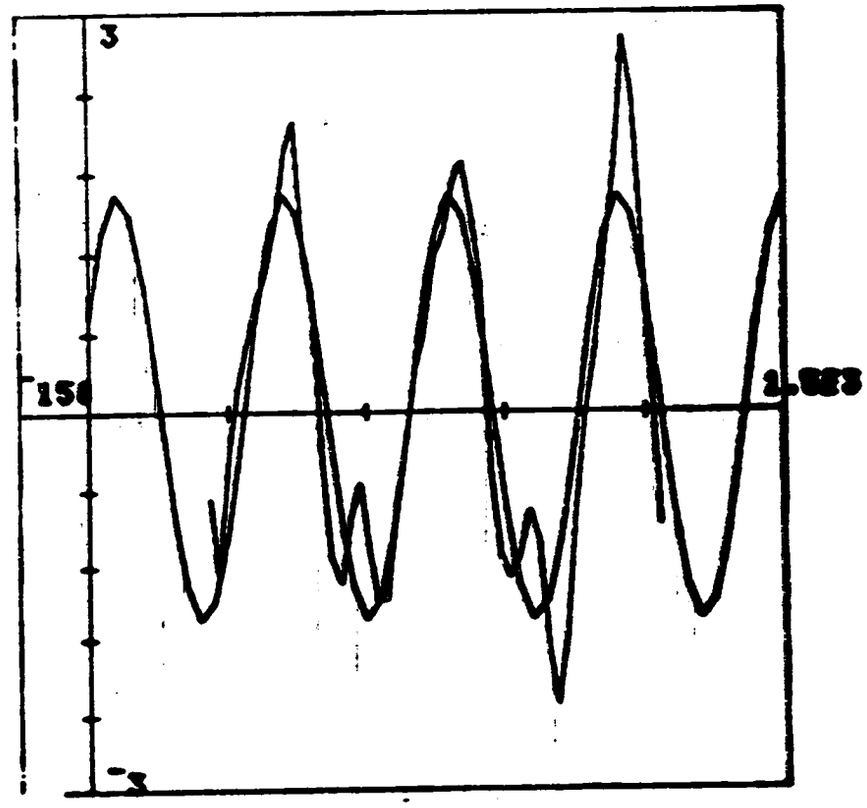

FIGURE 3-16

STATION ACQUISITION PERIODS FOR SKYLAB

TIME OF NORAD ELEMENT SET 12:09:17 GMT
7- 5-79

DATE	7- 7-79 (FIRST AOS)
ORBIT NUMBER	2
DAY NUMBER	188
BETA ANGLE	-25.4709 DEG

1 REV DELTA TIME	01:28:43.48	
ORBITAL MIDNIGHT	05:15:45.59	GMT
ORBITAL SUNRISE	05:33:52.81	
NIGHT TO DAY TERM	05:37:54.85	
ORBITAL NOON	06:00:06.50	
DAY TO NIGHT TERM	06:22:18.33	
ORBITAL SUNSET	06:26:20.79	
SI DUMP MIDNIGHT	06:41:33.61	
SUN SENSOR UPDATE	05:57:11.27	

STA	AOS	LOS	MAX ELV
ACN	05:27:28	05:35:00	73.6
TSR	05:35:01	TSC 06:19:22	

FDDU SAMPLE TIMES

1 - 05:37:54
2 - 06:00:06
3 - 06:22:18
4 - 05:15:45

NOTE - ER SAMPLE VALID ONLY BETWEEN SAMPLE POINTS 1 & 2.

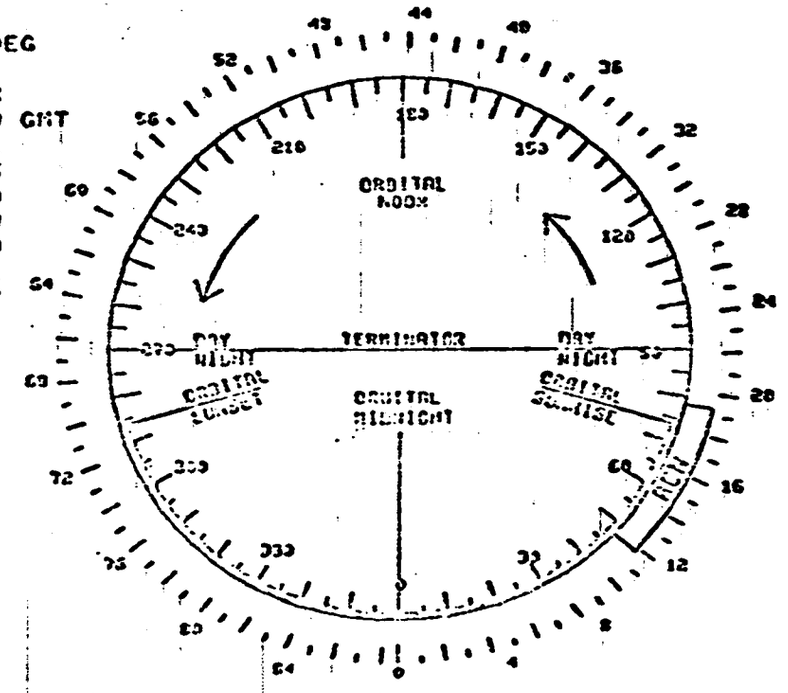

PROVIDED BY MSFC
SYS ANAL & INTEG LAB
MISSION ANAL DIV, EL-23

FIGURE 3-17

ORIGINAL PAGE IS
OF POOR QUALITY

to be done two orbits before and no other strapdown correction was permitted. Once the ASAP tape was dumped over a ground station, it took at least another half hour of data processing and parameter extraction to obtain results. The results were 18 sets of QAL's per orbit, which then had to be fed into the Sigma 5 computer to be evaluated with the appropriate programs. The actual updating of the prameters had to wait until the next ground station. The bottom line was, that the delay in the actual on board happening and the corrective action amounted to at least two orbits, sometimes more.

The ground support operations were aided by the "circle charts" (Figure 3-17) and telemetry formats (FORMAT 8 for TEA parameters is shown in Figure 3-18). The data on FORMAT 8 changed every second provided the Skylab was over a ground station, the circle charts were applicable for one orbit.

The circle chart has midnight at the 6 o'clock position; the outer numbers are minutes from midnight, the inner ones are orbital degrees from midnight. Orbital night time is indicated by the heavy part of the circle. The boxes on the outside of the circle indicate the ground station coverage; the ground stations were Ascencion (ACS), Bermuda (BDA), Goldstone (GDS), Madrid (MAD), and Santiago (AGQ).

FORMAT 8 showed the present and the past Δe, the present attitude refernce change $\Delta\Phi$ and any impending strapdown update $\Delta\Theta$. Also shown were the filtered total system momentum (in units of H), the CMG momentum (in % of 3H) and the inner and outer gimbal angles (to the nearest degree) plus their gimbal rates.

Of further interest are the quaternions QAL (QBL), QVA, and QVI. The first allowed evaluation of the current BAR angles, the second showed how well the vehicle was following the attitude reference, and the third indicated the attitude with respect to the solar inertial system (useful for determining the closest approach of the sun line to the center of the ACQ SS which then was used for strapdown update information).

The history of the TEA control parameters as well as the solar elevation angle with respect to the orbital plane are shown in Figure 2-7, and 2-22 through 2-25. The biasing history of the rate gyros is shown in Figure 2-23 Only one rate gyro was still operating in the Y axis (Y3), two each were averaged for the other two axes (X1 and X3; Z1 and Z2). As mentioned before (cf. middle of 3rd paragraph of this section) the initially introduced beneficial bias had to be taken out and replaced with a bias of the opposite sign. The fact that in two axes two rate

```
07-JUL-79 05:31:40   AM/ATM BLOCKS      158/   1708  AM/ATM/ATMDC */ /    ACN
                     TEA CONTROL PARAMETERS          RSDP GMT 188: 5:31:39.33
                        X          Y          Z          TMID-387:23:27:54.75
DELTA E          0.034180   0.054687  -0.025879         DMID      1:28:48.50
DELTA EP         0.023437   0.101562   0.031250         TGNT-387:23:12: 5.00
                                                          DELTA T  TEA  -289
DELTA PH         0.024170  -0.046753  -0.051025
DELTA TH        -0.004761   0.042969  -0.025879                BUS 11 29
                                                        TEMP      12 29  -COMMAND-
ETSF            -1.156250   0.023437  -0.234375          1   17  21 29  CUR 07777
                                                          5   18  22 29  MD1   237
CMG MOM             -27         12        -10           9   28  31 29  MD2     1
                                                         13   28  32 29  MD3    14
          -----CMG 2---  -----CMG 3---                  17   17  41 29  MD4  2001
IGA IGR     5   0.6357     4  -0.3828                   21   25  42  0  CNTR 0005
OGA OGR    52  -0.7793    48  -0.3486      PRESS  1  153  51 29  SADA 0025
WH SPD     8960                                     2  181  52 29  SADL 01C7
          DMIB     0  MIB  3296  JET 123456  TEMP  1   17  61 29  INTRUPT
                      FO   304                     2   27  62 29  -ERRORS--
                                                                  DATA ERR
OBL   0.2416382  -0.1369629  -0.7496948   0.5096094               MODE ERR
OVA   0.0126342  -0.0229492  -0.0256957  -0.9988989               UND CMD
OVI   0.6567366  -0.6428816  -0.0582274   0.3894033               DC REJ
```

FIGURE 3-18

gyro outputs were averaged allowed us to work effectively with half LSBs by biasing only one of the averaged gyros with a full LSB. A trimming of the rate gyros to within about 0.25 deg/orbit drift was therefore possible.

The large number of changes in ETLN1 (Figure 2-26) reflect the considerable effort given to controlling the roll angle to acceptable values. ETLN2 did not influence the TEA since it was parallel to the orbital velocity, but it affected the CMG gimbal angles and was therefore changed once (in two steps, to minimize the transients) to improve the actual gimbal angle traces.

Simulation predicted that TEA control in T121P was possible down to about 140 km (75 NM) and in T275 down to 130 km (70 NM). At these altitudes the gravity gradient and precessional torques were no longer large enough to achieve zero external torques in all axes simultaneously. Fortunately, Skylab was about to reenter on the most desirable orbit, one with the least population density beneath it. This orbit, however, did go over the United States, the southern part of Canada and Australia, but most of it was over water. Therefore, only a slight adjustment of the nominal impact point (which was in the Atlantic Ocean) was indicated and there was no need to maneuver to the low-drag T275 attitude (this attitude was on an unstable equilibrium point in all axes, and the equilibria were much more precarious than the ones in T121P). The slight impact point adjustment could be achieved by going to a random tumble (with somewhat less average drag than T121P) at an altitude of 150 km (81 NM). This was done by commanding a delayed maneuver from the T121P attitude to the solar inertial attitude. The latter, due to the high aerodynamic torques, could not be held, and a random tumbling resulted. On the average this random tumbling had the desired drag, which then lengthened the lifetime sufficiently to place the nominal impact at the desired location.

3.1.4.0 EOVV Control (1 CMG)

3.1.4.1 Introduction

In March 1978 while developing concepts for controlling Skylab to a low drag attitude, much concern was expressed for the long term survival of CMG #2. Previous experience suggested this CMG might be close to failure and thus there was much interest in the possibilities of EOVV control with CMG #3 alone. At first this idea was dismissed as impossible while the prospects that both CMG's would operate for an additional 18 months was not encouraging. Thus EOVV seemed destined to die before it was born because success depended upon CMG hardware operational probabilities that were low. The existence of a single CMG backup to EOVV began to be a very important consideration. As a result, a closer, more imaginative look at the problem was undertaken. A technique was discovered to point the X-principal axis (Xp) along the velocity vector. This attitude would experience nearly minimum drag as in 2 CMG EOVV. For convenience in this discussion we shall identify 2 CMG EOVV as EOVV2 and 1 CMG EOVV as EOVV1. A drawback was that, since a single CMG can only control 2 degrees of freedom, the vehicle would be uncontrolled about 1 axis. Since it was Xp we desired to point, this meant the vehicle would roll about Xp at an uncontrolled rate. All electrical power used onboard must eventually come from the solar arrays. It was necessary to be assured somehow of sufficient illumination on the arrays to power the average load. Simulations of EOVV1 indicated that power would be insufficient when the sun elevation angle out of the plane was less than 20-50 degrees. The range was due to the uncertainty of exactly how much power was required as well as uncertainty in the components of the power system which would remain functional. The momentum management scheme employed for EOVV2 had been developed with EOVV1 in mind and thus would also work for that case. The capability to control the total vehicle system momentum gave some control over the average spin rate about Xp. With this control a roll rate phasing scheme was developed which synchronized vehicle rate about Xp with the orbit so that it would rotate an integral number of times per orbit. Thus EOVV1 offered some backup capability for EOVV control and increased the overall probability for EOVV success. As a result, even though it turned out that it was never needed, it enhanced EOVV prospects and contributed to the eventual decision to proceed with Skylab reactivation. Also, since future vehicles may face similar problems, EOVV1 control techniques may well be useable in the future, giving additional redundancy without additional cost in hardware.

3.1.4.2 Control and Maneuvering

The attitude control and maneuvering logic of the Skylab vehicle as developed for the manned and unmanned original phases of the Skylab program were adequate for EOVV2 except that a new momentum management logic had to be developed. This was not the case for EOVV1. It was necessary to develop a new control law, a new CMG steering law and a new momentum management scheme for the vehicle. All of these things were accomplished quickly. The momentum management scheme developed here was also useable in EOVV2 and was adopted for both cases, although it had to be extended somewhat for EOVV1 because of the additional attitudes that had to be included. After it was realized there was inadequate power available most of the time for Xp along the velocity vector, more favorable orientations such as Xp POP (Xp along the orbit normal) were examined. This attitude could be used from time to time to replenish the spacecraft batteries. Such attitudes would increase the overall drag, however, and would have to be minimized for the longest orbital lifetime. This implied a scenario of repeated maneuvers between different attitudes or pointing directions of the Xp axis. We later found that if the Xp axis were pointed about 15 degrees below, i.e. south of the orbit plane and momentum managed to maintain the average roll rate about Xp to 1 roll per orbit, sufficient power appeared to be available. This would considerably reduce the workload on the ground controllers as the vehicle could be maintained in this position indefinitely. All of these considerations increased the complexity of EOVV1 over EOVV2. Now flight software requirements had to be developed for: 1. A new vehicle control law; 2.A new CMG steering law; 3. A maneuver scheme; 4. A momentum management scheme which would work at any allowed EOVV1 attitude; 5. A roll rate phasing scheme; 6. A strapdown offset estimation scheme which was independent of the sun sensor. All of these things were done and eventually implemented in flight computer code. These developments and the details of the software requirements will not be presented here (see Ref 18).

3.1.4.3 Momentum Management

In EOVV control, only the direction of the Xp axis was to be precisely controlled. This meant that any momentum management that was to be done had only the direction of Xp to work with. At this time it appeared only gravity gradient (GG) torques were well enough understood and large enough to do the job. We worked on the assumption that the vehicle inertia tensor was cylindrically symmetric with Xp as the symmetry axis. This was not strictly true but was approximately correct. This

assumption implies that the gravity gradient torque is independent of the vehicle rotation angle about Xp depending only its direction. It is a characteristic of GG torque that the component along the local vertical direction must vanish. Cylindrical symmetry forces the component along Xp to vanish also. Thus, the GG torque must lie along a mutually perpendicular direction. If Ur is the outward pointing local vertical direction unit vector, Uxp is the unit vector along Xp, Ia and It are axial and transverse moments of inertia, Wo is the orbit angular velocity, then the GG torque used for momentum management is

$$\underline{T}mm = 3\ Wo^2\ (It - Ia)\ (\underline{U}xp \cdot \underline{U}r)\ \underline{U}xp \times \underline{U}r$$

We can see from this equation that $\underline{T}mm = \emptyset$ when $\underline{U}xp$ and $\underline{U}r$ are orthogonal as they are nominally. The nominal direction of $\underline{U}xp$ was controlled to an angle $\emptyset$, a positive rotation about $\underline{U}r$ such that $\underline{U}xp$ was along the velocity vector when $\emptyset = \emptyset$. Small deviations from this were commanded to dump momentum that accumulated in the system.

The momentum storage "space" of CMG #3 was approximately a hemispherical surface centered about the negative vehicle X axis. The control law exchanged momentum between the vehicle and the CMG along the 2 axes normal to Xp with no concern for the parallel component other than it should remain negative. Thus as the CMG was moved about in controlling the direction of Xp, vehicle rate along Xp varied. The momentum scheme worked to maintain the total system momentum near null and this kept CMG #3 close to $-\underline{U}xp$ and hence the rate about Xp tended to remain constant at a value determined by adjusting the commanded momentum bias (ETN) along the orbit normal. The momentum management scheme maintains the average momentum at the desired bias value. The value of this bias determines the average roll rate. The roll rate was also a function of the angle of the Xp axis out of the orbit plane. It increases as Xp goes above the plane and decreases below. This fact was key in the roll rate phasing scheme.

Derivations will be found in a detailed report on EOVV. Essentially as in EOVV2 a specified periodic nodding motion about an axis parallel to $\underline{U}r \times \underline{U}xp$ was imposed on the vehicle with small variations of this as required to dump momentum. The so-called nodding angle was adjustable but was generally kept less than .15 radians. These small variations would have little effect on the average drag on the vehicle which depended mainly on $\emptyset$.

3.1.4.4 Strapdown Maintenance

A problem of much concern for EOVV1 was the maintenance of an accurate attitude reference or strapdown as it was also called. In EOVV2 the inclination angle of the solar arrays were controlled such that the sun sensor would nominally sweep across the center of the sun once per orbit allowing a 2-axis update of the strapdown. By this method alone, no corrections of strapdown offsets about the vector to the sun were made. This error was corrected by onboard software that related inplane bias torques to strapdown errors about the sunline. This was done through a rather low gain and caused trouble as mentioned elsewhere. For EOVV1 strapdown maintenance, we could not count on sun sensor data and thus decided to rely entirely on momentum data. The strapdown error could be extracted from that. This method was not as accurate as sun sensor data but would keep the errors within tolerable bounds. Our simulations showed that this technique would work satisfactorily.

3.1.4.5 Effects of Rate Gyro Drift

Rate gyro drift is defined as the rate difference between true body rates and those sensed by the gyros. For our purposes these can be thought of as 2 types: 1. Bias or constant drift; and 2. Scale factor error or drift proportional to the true rate along the sensing axis. Previous experience in SI indicated the bias values were extremely small. Therefore, only scale factor errors could generate significant drift. Gyro specifications required a scale factor error of less than 1 percent and thus drift rates from this source were limited to less than 3.6 degress per orbit. This is a substantial drift, however, which would produce intolerable errors in a very few orbits if uncorrected. The primary corrections means available was by gyro bias compensation which was already setup in the flight software. In EOVV2 the gyro drift generally caused the strapdown offset to grow along the orbit normal while remaining small in the plane because of the once-per-orbit rotation of the vehicle about the orbit normal. This causes the gyro drift which is constant in body axes to be resolved into inertial space as constant along the orbit normal and sinusoidal in the plane. This condition was modified somewhat by EOVV1 control. Since there was a rotation about Xp, constant drift rates in the body no longer resolved necessarily into constant rates along the normal and the drift was even more randomized meaning strapdown offset growth tended to be slower. The gyro bias compensation was less effective since it's effect was also randomized by the rotations described above. Thus ground supplied strapdown update biases available in EOVV1 software

were used. This was included primarily to correct for solar motion and orbit regression effects on the SI frame motion but would as well correct a gyro drift induced offset provided it was recognized in time. Simulations did not seem to show a severe problem here but it was a concern.

3.1.4.6 Roll Rate Phasing

As mentioned previously in the EOVV1 introduction, a roll rate control scheme was required to assure adequate electrical power availability. This was done by adjusting in a closed loop fashion the parameter ETN the commanded average bias momentum along the orbit normal. The actual system momentum was sinusoidal and nominally centered around ETN. The roll rate about Xp relative to local vertical coordinates was averaged over 1 orbit and mixed with the roll angle error. This result then was converted by a gain into a ΔETN to adjust the bias and correct the rate phasing so that the solar arrays would point to the sun or other desired direction at the appropriate place in the orbit. This technique was difficult to do in practise but was made to work fairly well eventually in that it would converge to the proper phasing from an arbitrary start. The fluctuations were sometimes rather large approaching 50 degrees or more but phasing seemed to hang in there. This seemed about the best that could be done in the face of all the other variables. That all these things worked at all seemed at times miraculous.

3.1.4.7 Conclusion

It is perhaps unfortunate that a chance to try out single CMG EOVV control never occured. All the bugs seemed to be ironed out of the basic scheme by simulation and many of the lessons learned from 2 CMG EOVV were incorporated such as finer scaling of the momentum computations and of the angles used for strapdown corrections. Procedures were developed for initialization in EOVV1 and some thought given to maintenance such as adjustments of roll rate phasing and strapdown updating but actual flight experience would have allowed us to demonstrate the techniques and smooth out the rough edges as was done in EOVV2.

The time and effort spent on EOVV1 should not be considered wasted. Much valuable experience was gained in developing and implementing the scheme into computer flight code. A backup mode was discovered that was previously thought to be impossible. Also, there are future vehicles such as the 25 kW

Power Module to which these developments could be applied. This scheme would provide additional control redundancy at little extra cost. A single CMG backup mode based on EOVV1 would be a natural step.

3.1.5 Rate Gyro Biasing

In EOVV and TEA the vehicle nominally rotated about orbital north. Any rate gyro drift along this axis resulted in a total strapdown drift. Any rate gyro drift in the orbital plane integrated to zero over one orbit. The Skylab software was only configured to accommodate rate gyro bias compensation, but not a scale factor compensation. As indicated by the near perfect operation in the SI mode, there was no need for a true bias compensation. However, a false bias compensation could be used to compensate for a scale factor error, but only for a given angular velocity component along the particular vehicle axis. The same scale factor error required then a different bias compensation if the vehicle was rotated and the rate along this particular axis changed. Being "the only game in town", this method was used.

The POP strapdown error, suitably averaged over several orbits, could be used to determine the total POP gyro drift. Due to the lack of any other information, this drift was prorated along the vehicle axes according to their POP direction cosines. The bias compensation had a resolution of about 0.5 deg/orbit. In the axes where the outputs of two rate gyros were averaged (all axes in EOVV; the X and Z axes in TEA) the effective resolution was 0.25 deg/orbit, since one LSB bias change in one gyro only had the effect of 0.5 LSB for the averaged output. The varying roll angle in EOVV as well as the change from EOVV A to EOVV B provided some insight as to which gyros should have what bias, aiding somewhat in predetermining what biases to use for the TEA control. Rate gyro integrals were used in the averaged axes to determine how to divide the biasing between the individual gyros (the biases were applied such that the integrals did not diverge from each other in the same axis).

3.2 THRUSTER ATTITUDE CONTROL SYSTEM

The use of the Thruster Attitude Control System (TACS) was a necessary element in gaining attitude control and supporting the various maneuvers required during the Skylab Reactivation Mission. Because TACS usage was constrained by the limited amount of propellant remaining from the manned mission, careful management of the onboard propellant resources was necessary to successfully support the reactivation mission. There were no hardware failures or detectable propellant leakage of the TACS throughout its orbital life.

3.2.1 System Description

The Thruster Attitude Control System (TACS) is one element of the Skylab Attitude and Pointing Control System (APCS) as presented in the simplified block diagram, Figure 3-19. The TACS is a cold gas blowdown system with six thruster nozzles located on the aft skirt of the Orbital Workship as shown in Figure 3-20. The propellant is gaseous nitrogen which is supplied from twenty-two 4.5 cubic foot titanium spherical pressure vessels and controlled at each thruster via a quad-redundant solenoid valve assembly. A schematic of the TACS hardware is presented in Figure 3-20.

Commands for TACS firings are provided via the Apollo Telescope Mount Digital Computer (ATMDC) and electrical power to open solenonoid control valves is provided from the Airlock Module power buses. TACS firings are conducted in either a Minimum Impulse Bit (MIB) or 100 percent duty cycle (Full-On) mode according to the magnitude of the attitude or rate errors. Firing times in the MIB mode can be varied from 50 milliseconds to 400 milliseconds in 10 millisecond increments. A Full-On firing is defined as a firing of one second command pulse width duration. Firings of longer duration are counted as individual one second Full-On firings equal to the number of seconds of the firing command.

A description of the complete Attitude and Pointing Control System together with a report on its Manned Mission performance (May 14, 1973, through February 9, 1974) can be found in Reference 4. Reference 5 provides a detailed description of the TACS.

ATTITUDE CONTROL SYSTEM

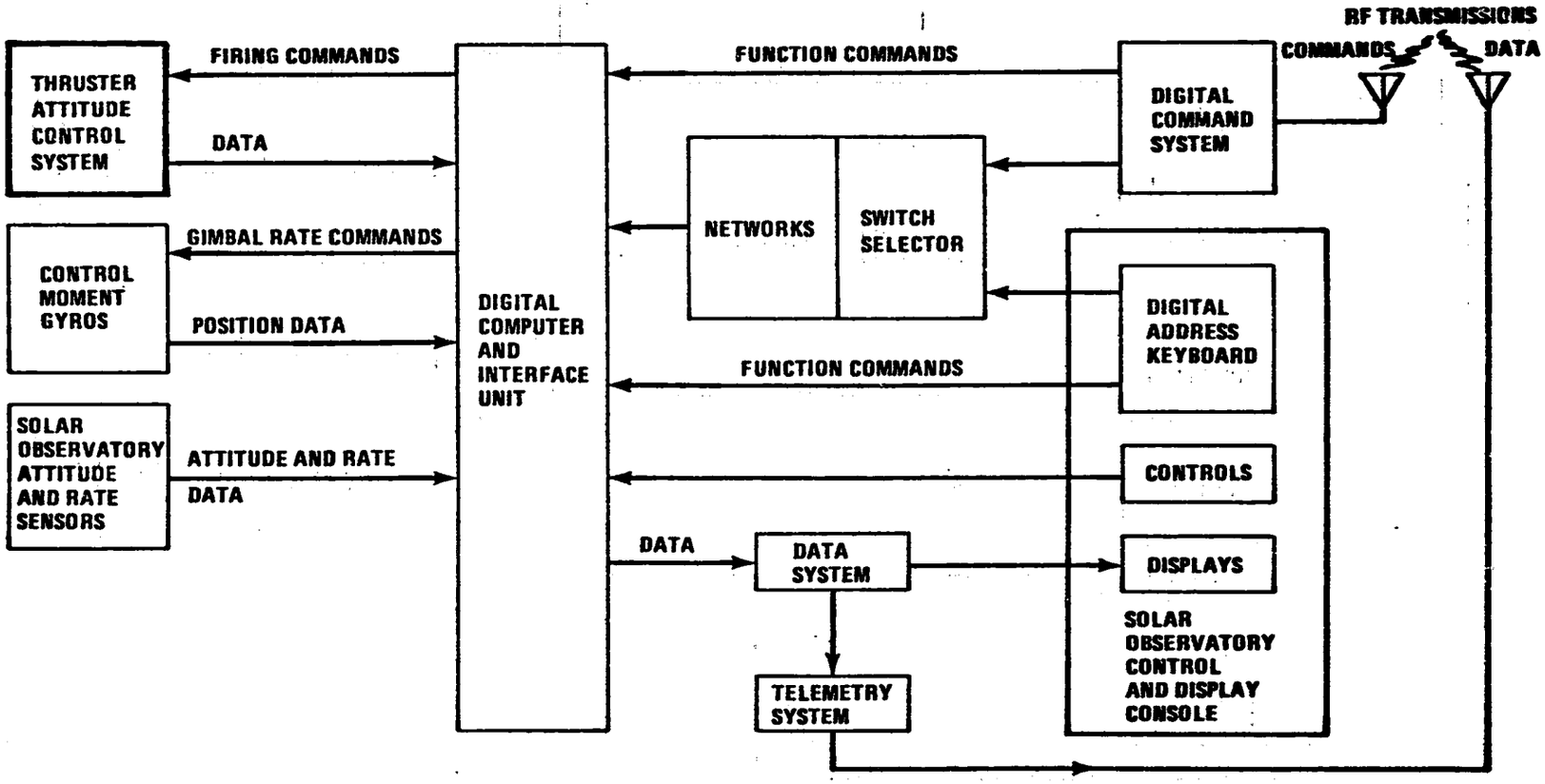

FIGURE 3-19

THRUSTER SYSTEM COMPONENT LOCATION

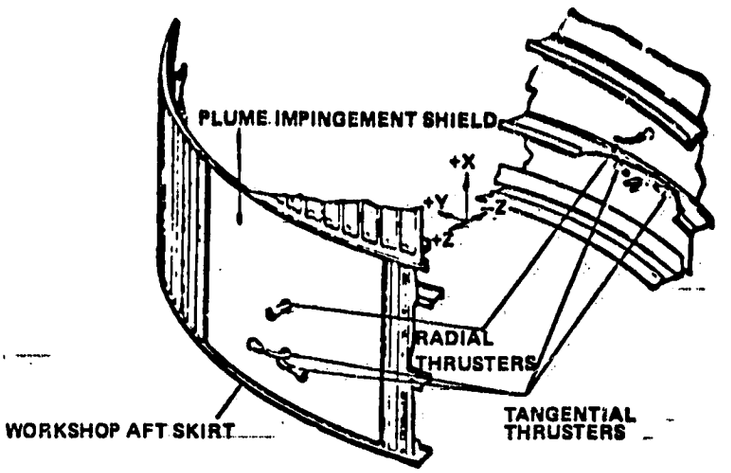

LEGEND

- THRUSTER
- SOLENOID VALVE
- FILTER
- FILL DISCONNECT
- (1) STORAGE SPHERE GN_2
- (P_t) PRESSURE TRANSDUCER
- (P_s) PRESSURE SWITCH
- TEMPERATURE TRANSDUCER

TACS HARDWARE SCHEMATIC

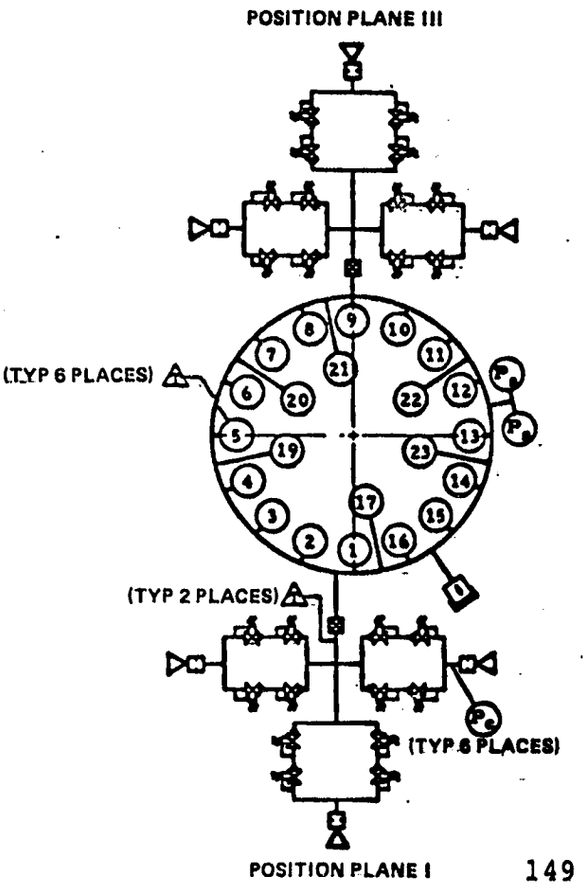

FIGURE 3-20

3.2.2 Reactivation Mission Performance Summary

When Skylab was successfully recontacted in March of 1978, telemetry data indicated that all TACS elements were in the same configuration as that following system deactivation in February 1974. The TACS propellant supply pressure was approximately 3.9 million N/m^2 (560 PSIA) with an average supply temperature of 268K (21° F). This relates to a propellant mass of approximately 138 KG (305 lbs) which is the same as that calculated at the end of mission in February 1974. This indicates that there was no measureable system leakage during the four year quiescent storage period which is consistant with the lack of detectable leakage during the nine month manned mission.

3.2.2.1 TACS Usage Summary

The TACS was required to support the Reactivation Mission attitude management during two periods. During the first period, (June and July of 1978) TACS was used to support the maneuvers required to place Skylab in the low drag End-On-Velocity Vector (EOVV) attitude and to provide backup attitude control required because of early mission system problems. During the second period (June and July 1979) TACS was used to support maneuvering to the Torque Equilibrium Attitude (TEA) and during the final reentry maneuvers. In order to assure conservation of TACS propellant, the TACS was disabled during much of the time between these two periods. Section 2 provides a detailed description of Skylab Attitude management during the Reactivation Mission including a definition of all attitudes and operating modes. A summary of TACS usage during the Reactivation Mission is presented in Table 3-8. The first Reactivation Mission usage of TACS occurred on June 9th, 1978 when the vehicle was placed under TACs control and the rotation rates which had accumulated during the quiescent storage period were stopped. TACS was then used to support the maneuvers to acquire a Solar Inertial (SI) attitude. After successful acquisition of SI a problem with switch selector #3 caused CMG #3 servo power to be turned off with a resulting loss of CMG control. This resulted in an increasing attitude error in the X axis such that TACS only control occurred three times during this period using approximately 1000 lb-sec impulse each time. On June 11th the vehicle was successfully maneuvered to the EOVV attitude. A total of 9569 lb-sec impulse was provided by the TACS during this period.

TABLE 3-8

TACS USAGE SUMMARY

DATE	EVENT	IMPULSE USED (LB-SEC)
9-11 JUNE 1978	STOP VEHICLE ROTATION RATES AND MANEUVER TO SOLAR INERTIAL (SI) ATTITUDE; MAINTAIN CONTROL WHEN CMG #3 SERVO POWER WAS INADVERTENTLY TURNED OFF.	9569
28 JUNE 1978	ASSIST CMG CONTROL AND MANEUVER FROM END ON VELOCITY VECTOR (EOVV) ATTITUDE TO SI BECAUSE OF MOMENTUM MANAGEMENT PROBLEMS IN EOVV.	292
6 JULY 1978	MANEUVER FROM SI TO EOVV.	475
19 JULY 1978	MANEUVER TO SOLAR INERTIAL FROM AN UNKNOWN ATTITUDE (ATTITUDE CONTROL WAS LOST ON JULY 9TH DUE TO ELECTRICAL POWER PROBLEMS) AND MAINTAIN CONTROL IN THE TACS ONLY MODE DUE TO CMG MOMENTUM PROBLEMS	3375
25 JULY 1978	MANEUVER FROM SI TO EOVV	279
20 JUNE 1979	MANEUVER FROM EOVV-B TO TORQUE EQUILIBRIUM ATTITUDE (TEA)	373
24 JUNE 1979	MAINTAIN CONTROL AND REACQUIRE TEA CONTROL WHICH WAS LOST DUE TO AN UPLINK OF THE TRANSPOSE OF A SLOPE MATRIX UPDATE.	1092
11 JULY 1979	SUPPORT TUMBLE MANEUVER DURING REENTRY	6825

On June 28, 1978, after 17 days in EOVV, large momentum errors and Z axis attitude errors were observed and the decision was made to enable TACS control to assist the CMG Control System. After one orbit, approximately 100 lb-sec of impulse had been used without significantly improving the CMG momentum state. The decision was made to return to Solar Inertial attitude with an additional 192 lb-sec of TACS impulse required to achieve steady solar inertial operations.

After the momentum management problem was understood and on-board software modified, the Skylab was returned to the EOVV attitude on July 6, 1978. This was accomplished by first maneuvering to an offset ZLV attitude and caging the CMG's while Skylab was performing in a rate only control mode under TACS control. This is a minimum TACS usage cage procedure. After the caging operation was completed Skylab was commanded into the EOVV control mode. The total amount of TACS impulse used for EOVV acquisition including the ZLV maneuver and the CMG cage was 475 lb-sec.

On July 9th, 1978, Skylab attitude control was lost when the ATM batteries automatically tripped off line due to low voltage. By July 18th the batteries were sufficiently charged to attempt to regain attitude control and CMG Spin-up was initiated. By this time Skylab was rolling approximately four revolutions per orbit as determined from telemetry data. On July 19th, the TACS was used to maneuver the vehicle to the solar inertial attitude where the solar panels were in the field of view of the sun. Due to momentum problems which accumulated after the SI acquisition maneuver, an automatic switch to TACS only control occurred when the X axis error reached 20 degrees. Approximately 3375 lb-sec of TACS impulse was used during the TACS only control mode period and to acquire the SI attitude. Approximately 2000 of the 3375 lb-sec impulse was used in the TACS only control mode. Because of the limited TACS propellant remaining, the flight program was modified to prevent any further automatic switch over to the TACS only control mode.

On July 25th, Skylab was maneuvered from the solar inertial attitude to the end-on-velocity vector attitude using approximately 279 lb-sec of TACS impulse. This maneuver was very similiar to the July 6th maneuver described above.

Between July 25th 1978 and June 20th 1979, there were two Skylab maneuvers, both of which were managed without the use of the TACS. The first, on November 4, 1978, was a maneuver of 180 degrees from the normal EOVV orientation (EOVV-A) with the MDA pointing toward the positive velocity vector to a new orientation (EOVV-B) with the orbital workshop leading. The purpose of this maneuver was to provide the most favorable thermal conditions to reduce the stress in CMG#2. The second

maneuver on January 25, 1979 was from the EOVV-B attitude to the solar inertial attitude for the purpose of reduced operational maintenance since extending Skylab's orbital life was no longer a mission objective.

The next TACS usage occurred on June 20th, 1979 after nearly eleven months of non-use. The onboard propellant mass of 113 lbs remained constant during this period reconfirming a leak tight system. On June 20th 1979 the Skylab was maneuvered from the solar inertial attitude to a Torque Equilibrium Attitude (TEA). The total maneuver to TEA Control, including an offset ZLV maneuver and CMG cage used approximately 373 lb-sec of TACS impulse.

On June 24th, 1979 TEA control was lost when the transpose of the desired matrix relating momentum errors to attitude errors about the torque equilibrium attitude was uplinked. The error was corrected and TEA reacquired. The entire process of losing and reacquiring TEA control use approximately 1092 lb-sec of TACS impulse. Although this usage was unplanned, sufficient propellant remained to support reentry maneuvers if required.

The last TACS usage occurred on July 11, 1979 approximately 9 hours prior to the Skylab reentry. The TACS firing limit was updated to its maximum value and Skylab was commanded to a solar inertial attitude. While maneuvering to SI, the aerodynamic torques increased significantly causing TACS firing in an attempt to maintain control. When the TACS propellant was expended, control authority was lost and the aerodynamic torques put the vehicle into a tumble. This tumble was initiated to obtain a predictable average drag during thr final hours of reentry to support computer reentry predictions programs.

3.2.2.2 TACS Performance Data

When Skylab was reactivated in March 1978 there was a total impulse of 22,280 lb-sec available for supporting the reactivation mission. Impulse usage during the reactivation mission is presented in Figure 3-21. Total impulse calculations were based on the propellant mass remaining following each TACS usage period as presented in Figure 3-22. Propellant mass calculations are dependent on the average gaseous nitrogen supply pressure from two supply manifold pressure measurements and the average supply temperature as determined from six nitrogen supply sphere temperature transducers which were distributed among the 22 supply spheres. Since the initial loading of the nitrogen supply was at a high pressure, approximately 3000 psia the supply pressure transducers were by necssity of a high pressure range of zero to 3500 psia. The-

potential instrument error resulting from using these high range pressure measurements to calculate mass at the relatively low supply pressure experienced during the reactivation mission could result in relativily high mass and impulse errors. Therefore, the results of analyses conducted using these pressure measurements were considered to be approximations.

The GN_2 supply pressures, temperatures and thrust available from TACS thrusters during the various usage periods is presented in Table 3.2-2. The thrust calculation is dependent upon the supply pressure with the assumption of a 7% drop from the supply pressure manifold to the thrusters during flow conditions. This pressure drop value had been determined by analysis and test and proved to be valid when used during the manned mission system analysis.

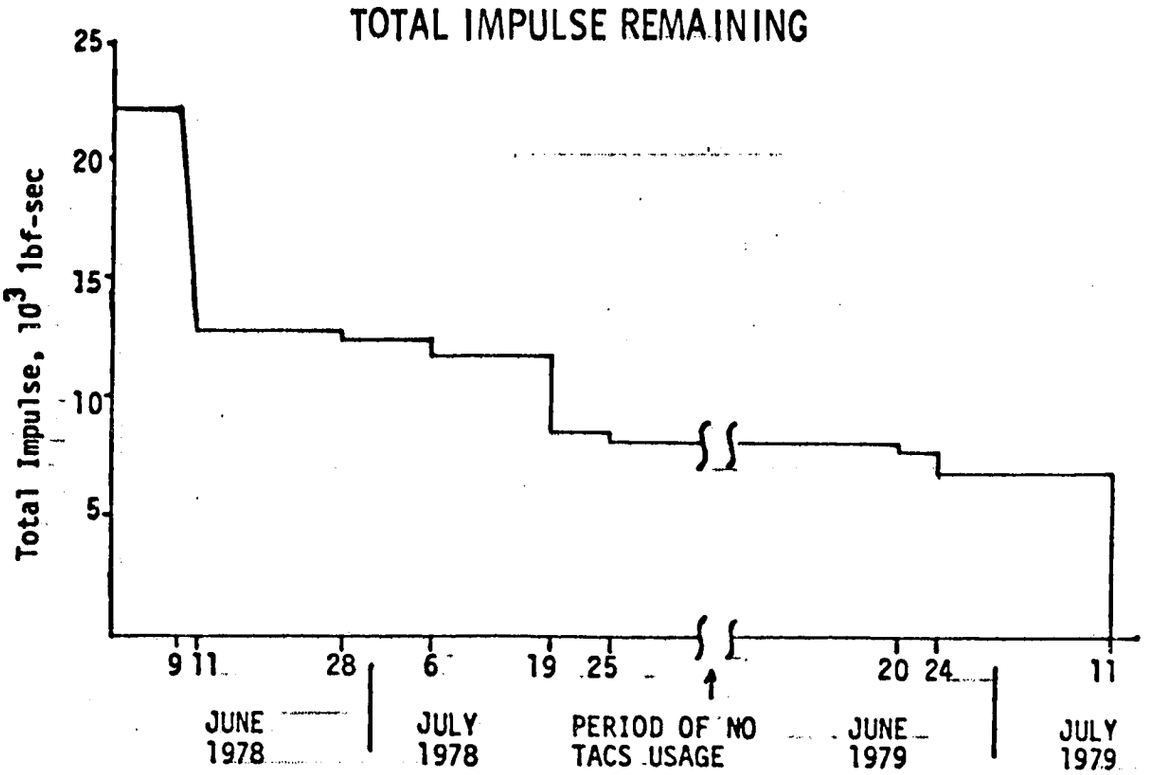

FIGURE 3-21

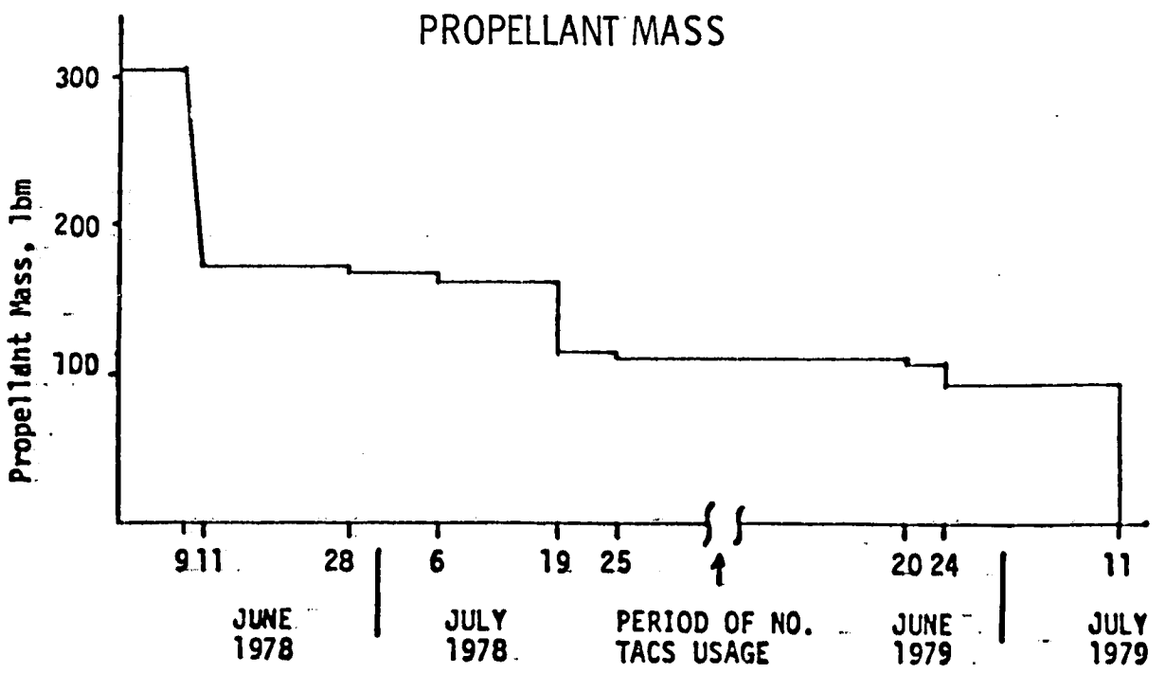

FIGURE 3-22

TABLE 3-9
TACS SUPPLY PRESSURE, SUPPLY TEMPERATURE AND THRUST

TACS USAGE PERIOD	SUPPLY PRESSURE (PSIA)	SUPPLY TEMPERATURE (°F)	THRUST (LBF)
	560	21	18.9
9-11 JUNE 1978	329	30	11.1
28 JUNE 1978	357	84	12.0
6 JULY 1978	313	38	10.5
19 JULY 1978	222	35	7.5
25 JULY 1978	211	25	7.1
20 JUNE 1979	211	41	7.1
24 JUNE 1979	182	47	6.1
11 JULY 1979	0	-	0

3.2.3 Conclusions and Lessons Learned

The cold gas propulsion system used to support Skylab attitude management has proven to be extremely reliable throughout the Skylab manned and reactivation missions. There were no hardware anomalies and no indications of propellant leakage throughout the more that 6 year orbital lifetime. The all brazed propellant supply system and the thruster valve design provided a leak tight system. Although the propellant supply was sufficient to support all manned and reactivation mission attitude control requirements, careful management of propellant resources were required due to higher demands on the system than had been anticipated prelaunch. While the TACS could have used additional gaseous propellant supplies, the Skylab environmental control system had an excess of gaseous oxygen (approximately 2200 lbs) and gaseous nitrogen (approximately 100 lbs) at the end of the reactivations mission. Should a future design use two similar systems, an interface between the two supplies with ground interface control may prove beneficial. However, potential decreased reliability impacts on both systems and the intermixing of oxygen and nitrogen supply systems, as would have been the case for Skylab, would require considerable analysis before such and interface design concept could be incorporated.

3.3 CONTROL MOMENT GYRO (CMG) SYSTEM

3.3.1 System Description

The Control Moment Gyro (CMG) consisted of a motor driven rotor which was gimbaled to provide two degrees of freedom within the limits of the electrical and mechanical stops. The instrument by utilizing its rotation momentum was capable of producing torques on a vehicle proportional to the angular rate of the gimbals. By controlling the CMG gimbal rates, attitude control of the vehicle was achieved. Figure 3-23 shows the assembled CMG.

Three vehicle mounted doubled gimballed CMGs were used as momentum exchange devices for maintaing vehicle attitude. The underlying principle of momentum exchange is the conservation of momentum. The total Skylab system momentum was made up of vehicle momentum plus CMG momentum and constrained such that the change in vehicle momentum was equal to zero. Any transient change in vehicle momentum due to external torques (i.e., gravity gradient or aerodynamic) was compensated for by an equal and opposite change in CMG momentum.

To compensate for an external torque, a restoring torque was generated by the CMG system. This was accomplished by rate commanding a change in direction of the three CMG spin vectors. The rate commands to the CMG gimbals were computed in the ATMDC as part of the CMG Control Law. The CMG system was capable of operating under conditions where one of the three CMGs had failed. A detailed description of the Skylab CMGs and their utilization in the APCS may be found in Reference 4.

3.3.2 Orbital Storage

No orbital storage effects were detected in any of the CMGs, CMG inverters or electronics. The performance of the two operating CMGs in the Skylab reactivation mission was identical to the original Skylab mission. The CMG runup curve of wheel speed vs. time was the same as for the original mission. This indicates that negligible change in bearing friction had occurred since the beginning of the original Skylab mission and little if any pressure had built up in the wheel cavity. The pressure evacuation valves were closed at the end of the first mission. All three CMG inverters and electronics operated throughout both missions without any failures or problems. CMG No. 3 performed flawlessly during both Skylab missions. The wheel speed indicator on CMG No. 3 was lost during the original mission, but this did not affect the CMG performance.

CONTROL MOMENT GYRO (CMG)

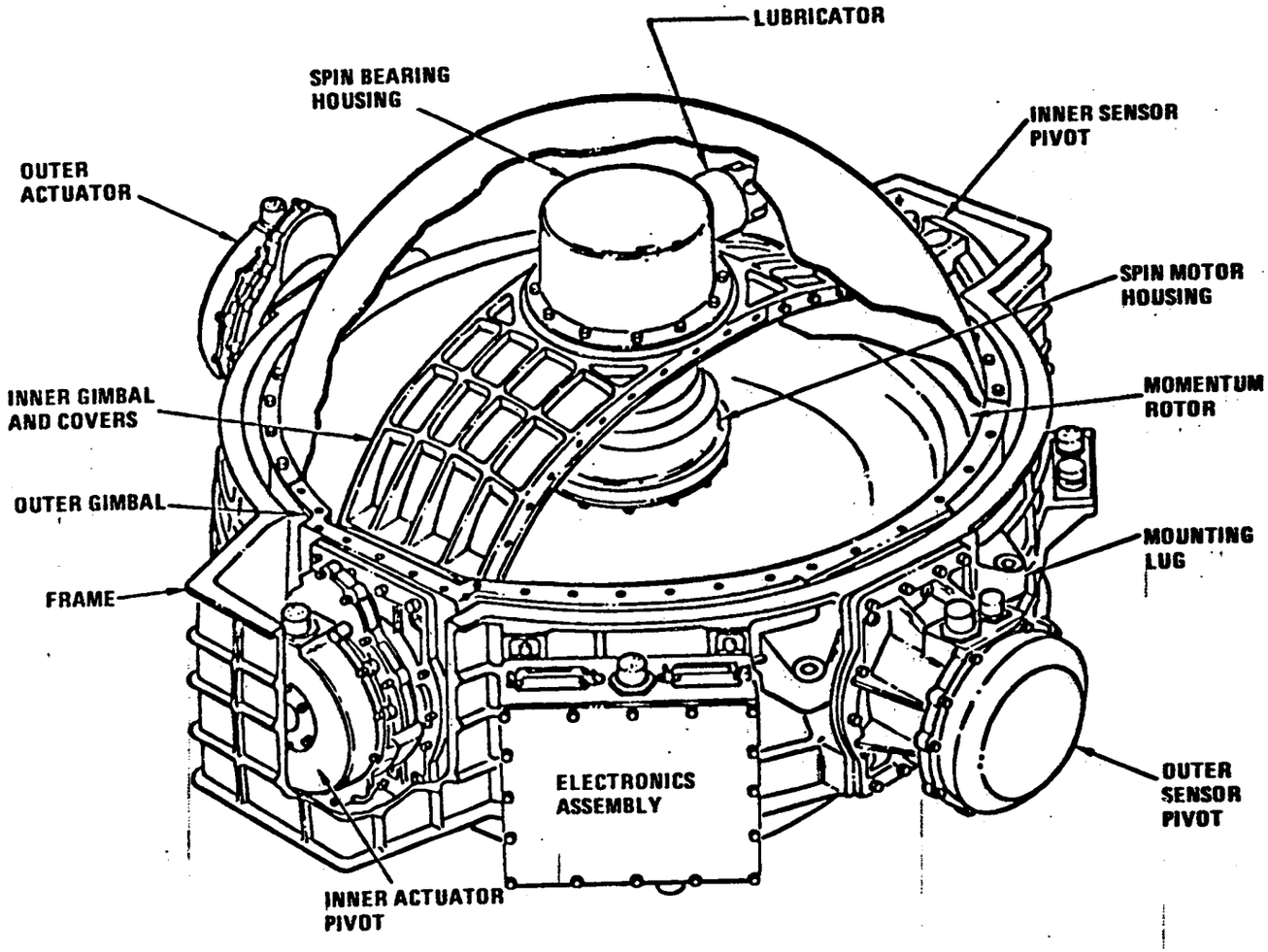

FIGURE 3-23

3.3.3 Reactivation Mission Operational Performance

The main concern with the CMG system performance during the reactivation mission centered around CMG #2. On DOY 327 of 1973, during the original Skylab mission, CMG #1 was powered off via DCS commands after an apparent catastrophic wheel bearing failure. An investigation was initiated to analyze the data from the 30 days prior to the DOY 327 to determine if there was a signature of the CMG parameters prior to failure. It was discovered through this analysis that there had been four "anomalies" or "distress points" before the failure. A distress point is characterized as the following:

1) One bearing temperature increases more rapidly than the other

2) An increase in phase current

3) A decrease in wheel speed

These would occur almost simultaneous over the same time period. The first distress point was noted about 20 days prior to the failure and the fourth distress point began approximately one hour before the first indications of a catastrophic failure. It was also discovered, during the CMG #1 failure characterization, that CMG #2 was also exhibiting the distress point signature. Between DOY 323 of 1973 and DOY 23 of 1974 a total of 39 distress points were observed (Reference 4). On DOY 23, a distress point signature started that lasted for a long period of time and would recover for only brief periods. This signature persisted essentially until CMG #2 was powered off at the end of the original Skylab mission. CMG #3 did not show any of the distress point characteristics.

Therefore, there was much concern about the health of CMG #2 for the Skylab Reactivation Mission. To help control the amount of torque applied to the CMG wheel bearings, the requirements for the initial EOVV software (FF81 buffers 1-8) provided for the capability to update the CMG gimbal rate limit (δ_L). This allowed the flight controllers to uplink a large δ_L when maximum control authority was essential and to reduce δ_L during relatively quiet periods to minimize stress on the CMG wheel bearings. During the original Skylab mission, δ_L had been 4 degree/second whereas during most of the EOVV operation, δ_L was either 1 or 1/2 degree/second. On some occasions, such as during the solar inertial operation over the first long period of no station coverage on June 9 and 10, 1978, following the regaining of CMG control on July 20, 1978 and during initial TEA control operations, δ_L was increased to 2 degree/second.

The CMG data was studied extensively throughout the mission. The CMG bearing temperatures, wheel currents and wheel speeds were analyzed to detect the presence of the CMG stress point signature. The CMGs performed nominally from the time of initial control acquisition on June 9, 1978 (DOY 160) until the #2 bearing temperature of CMG #2 dropped below 63 degrees F on September 22, 1978 (DOY 265). On this day, the first signature of a CMG #2 distress point during EOVV operation occurred. Three days later, on DOY 268, a second signature was observed followed by a third on DOY 271. These signatures are shown on Figure 3-24. During the Skylab reactivation mission, a total of 18 distress points occurred. These are listed on Table 3-10 with the date, beta angle, bearing temperature and mode of operation.

Evaluation of the CMG data indicated that the stress points were probably caused by retainer instability aggravated by marginal lubrication and was a function of bearing temperature. The bearing temperature of CMG #2 while in the EOVV mode is a function of the beta angle. A plot of the #2 bearing temperatures of CMG #2 versus beta angle for EOVV A is shown in Figure 3-25. As shown in the figure, the stress point occurred when the beta angle was less than -45 degrees causing the #2 bearing temperature to drop below 63 degrees F. At this time it was estimated that the minimum temperature required to avoid stress was approximately 65 degrees F.

In order to maintain the bearing temperature above 65 degrees F, a method was developed for flying the vehicle backward in the EOVV B mode for large negative sun angles and forward in the EOVV A mode for large positive sun angles (section 2). An additional advantage of these modes was that while it prevented the CMG from becoming too cold it also prevented the ATMDC from becoming too hot (See Section 3.6).

It was planned to change modes between EOVVA and EOVVB only when the absolute value of the beta angle would become greater than 40 degrees (-40 for EOVVA and +40 for EOVVB). This was considered sufficient to keep the bearing temperature above 65 degrees F, see Figure 3-26 for a plot of the #2 bearing temperature versus beta angle in EOVV B. However, on DOY 346, at a beta angle of 16 degrees and CMG bearing temperature of 78 degrees F, the fourth distress point occurred. This was the first distress point in EOVV B.

At this point the estimate of the stress point minimum temperature was revised upward to approximately 80-85 degrees. When three more distress points occurred on DOY 348, 349, and 358 (see Figure 3-27) it became evident that the vehicle would require an EOVVA/EOVVB transition for each pass through zero beta. By this time, however, the decision was made to abandon plans for a reboost/deorbit mission.

CMG NO. 2 BEARING TEMPERATURE, WHEEL CURRENT AND WHEEL SPEED SHOWING THE SIGNATURE OF DISTRESS POINT 1, 2, & 3

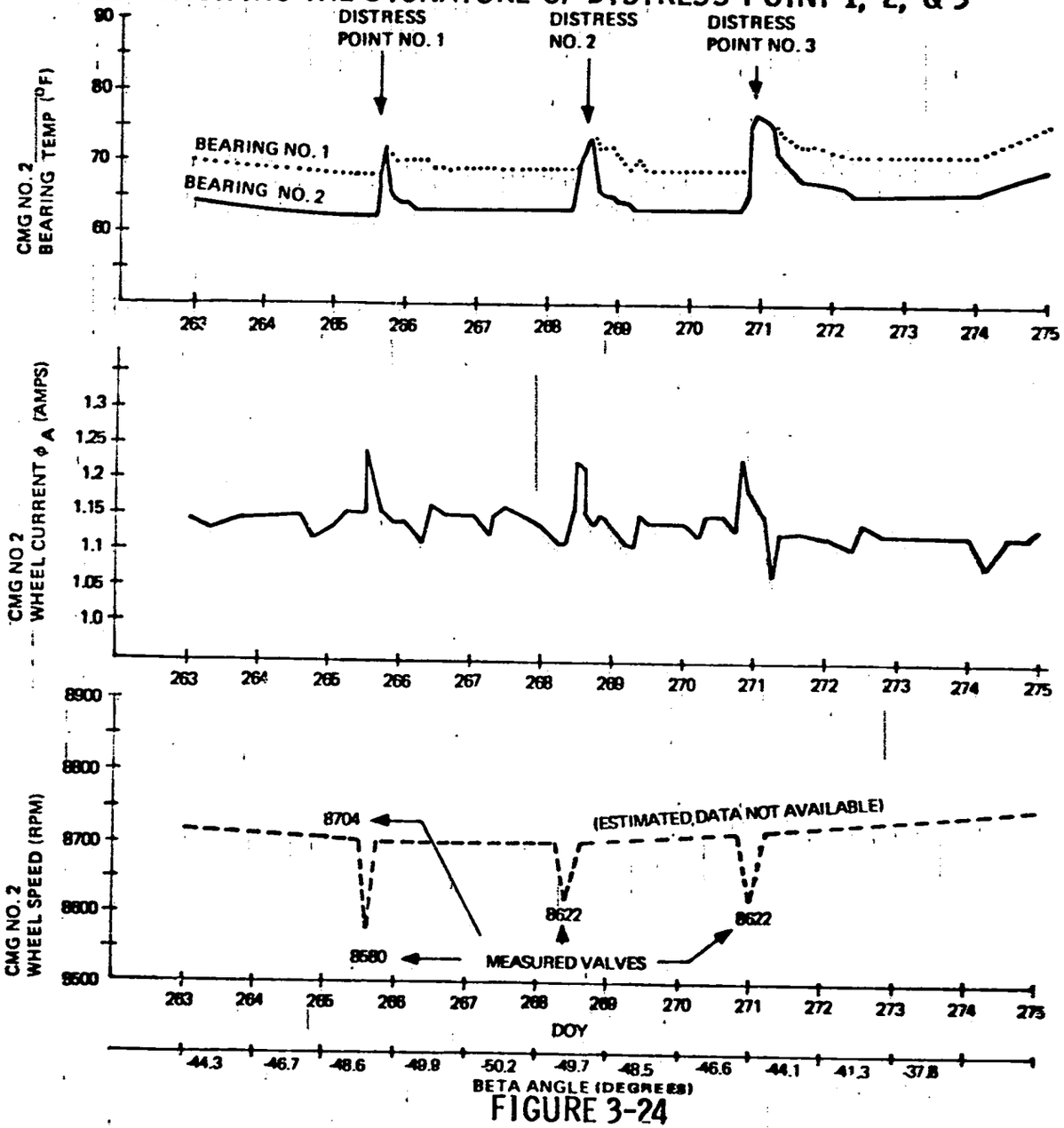

FIGURE 3-24

TABLE 3-10

CMG #2 DISTRESS POINTS DURING THE SKYLAB REACTIVATION MISSION

Distress Point	Date (DOY)	Beta Angle (Degrees)	Bearing Temperature (°F)	Mode	Comments
#1	265(1978)	-49°	62°	EOVV A	Minimum temperature to avoid stress believed to be 65°F.
#2	268	-50°	65°	EOVV A	
#3	270	-47°	63°	EOVV A	
#4	346	16°	78°	EOVV B	First distress point in EOVV B
#5	348	21°	77°	EOVV B	Estimate of distress point minimum temperature revised upward.
#6	349	24°	76°	EOVV B	
#7	358	19°	81°	EOVV B	Plans are made to rotate vehicle on each pass through zero beta.
#8	365	-5°	90°	EOVV B	CMG #2 is pointed toward the sun.
#9	365	-6°	92°	EOVV B	
#10	1(1979)	-11°	95°	EOVV B	It appears that distress points will be unavoidable for low beta angles.
#11	1	-13°	97°	EOVV B	
#12	2	-15°	102°	EOVV B	It is feared that the CMG lubrication is evaporating.
#13	2	-17°	104°	EOVV B	
SI #1	26	-35°	93°	Solar Inertial	First distress point in solar inertial.
SI #2	27	-30°	79°	Solar Inertial	
SI #3	27	-27°	76°	Solar Inertial	It is feared that the 5° offset is not enough, patch is started to allow larger offset.
SI #4	28	-25°	77°	Solar Inertial	
SI #5	29	-22°	80°	Solar Inertial	Last distress point, temperature stabilizes.

TEMPERATURE OF CMG NO. 2, BEARING NO. 2 VERSUS BETA ANGLE FOR EOVV A

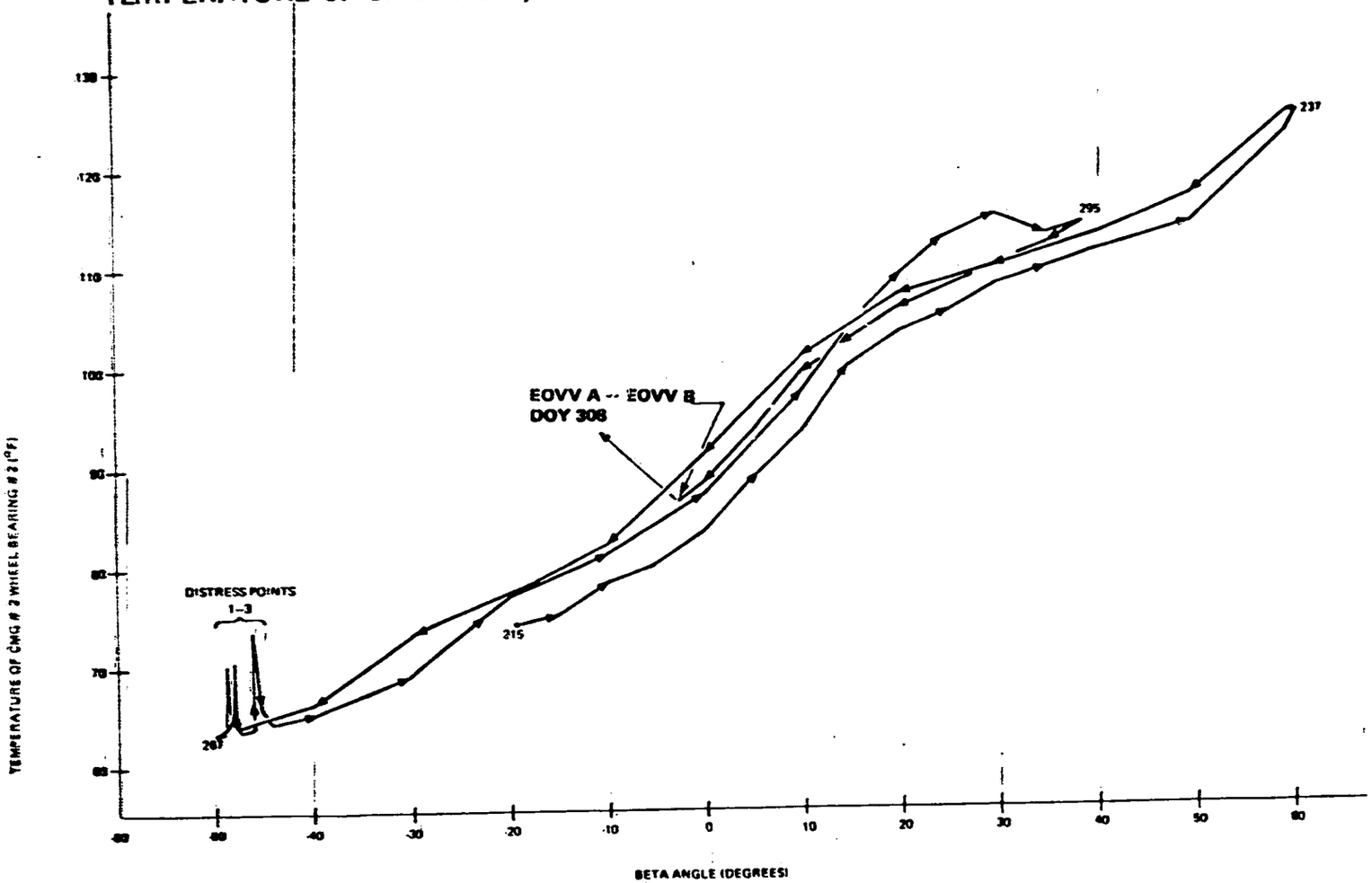

FIGURE 3-25

TEMPERATURE OF CMG NO. 2, BEARING NO. 2 VERSUS BETA ANGLE FOR EOVV B

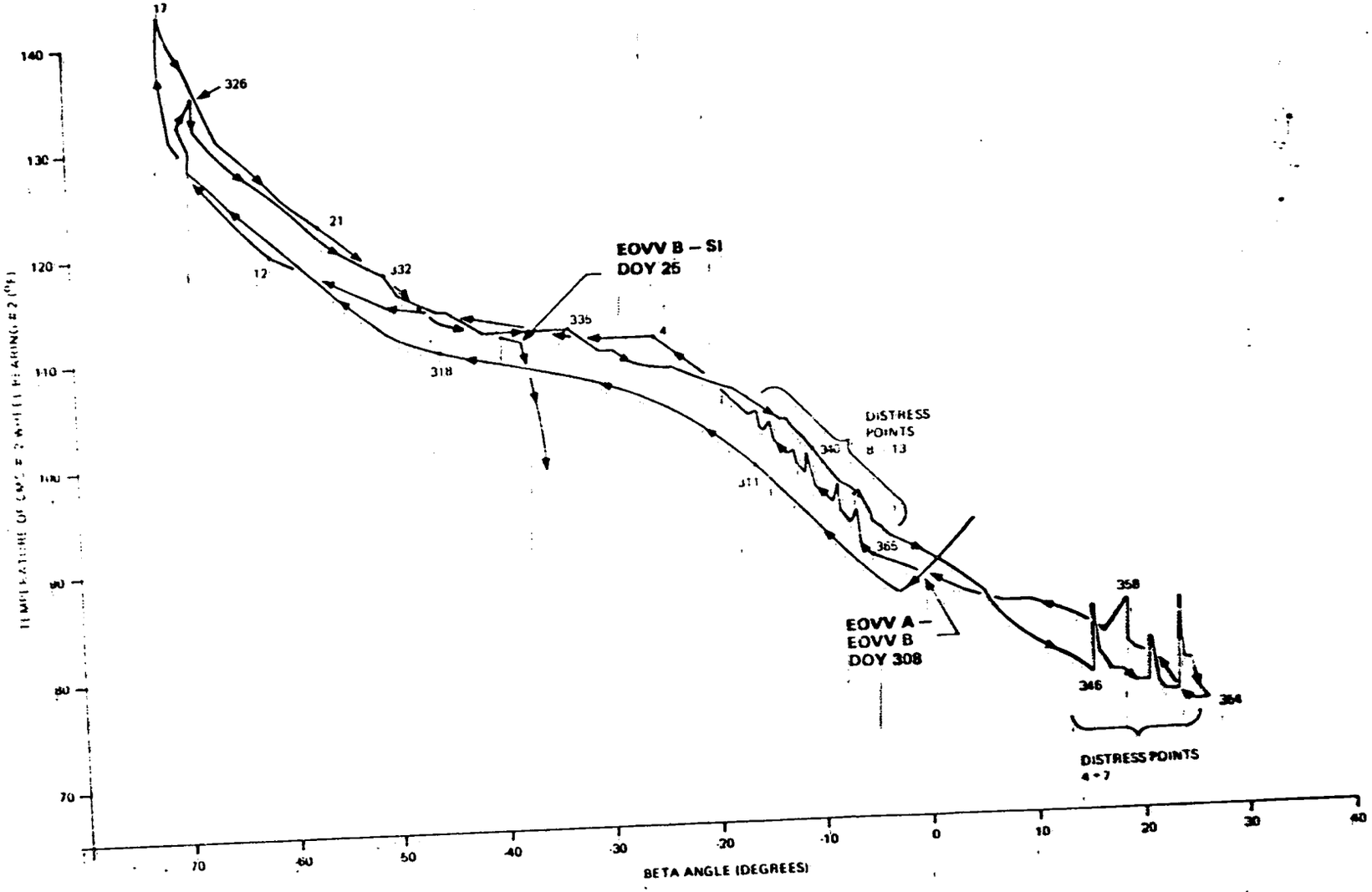

FIGURE 3-26

CMG NO. 2 BEARING TEMPERATURES, WHEEL CURRENT AND WHEEL SPEED SHOWING THE SIGNATURE OF DISTRESS POINTS 4, 5, 6 AND 7

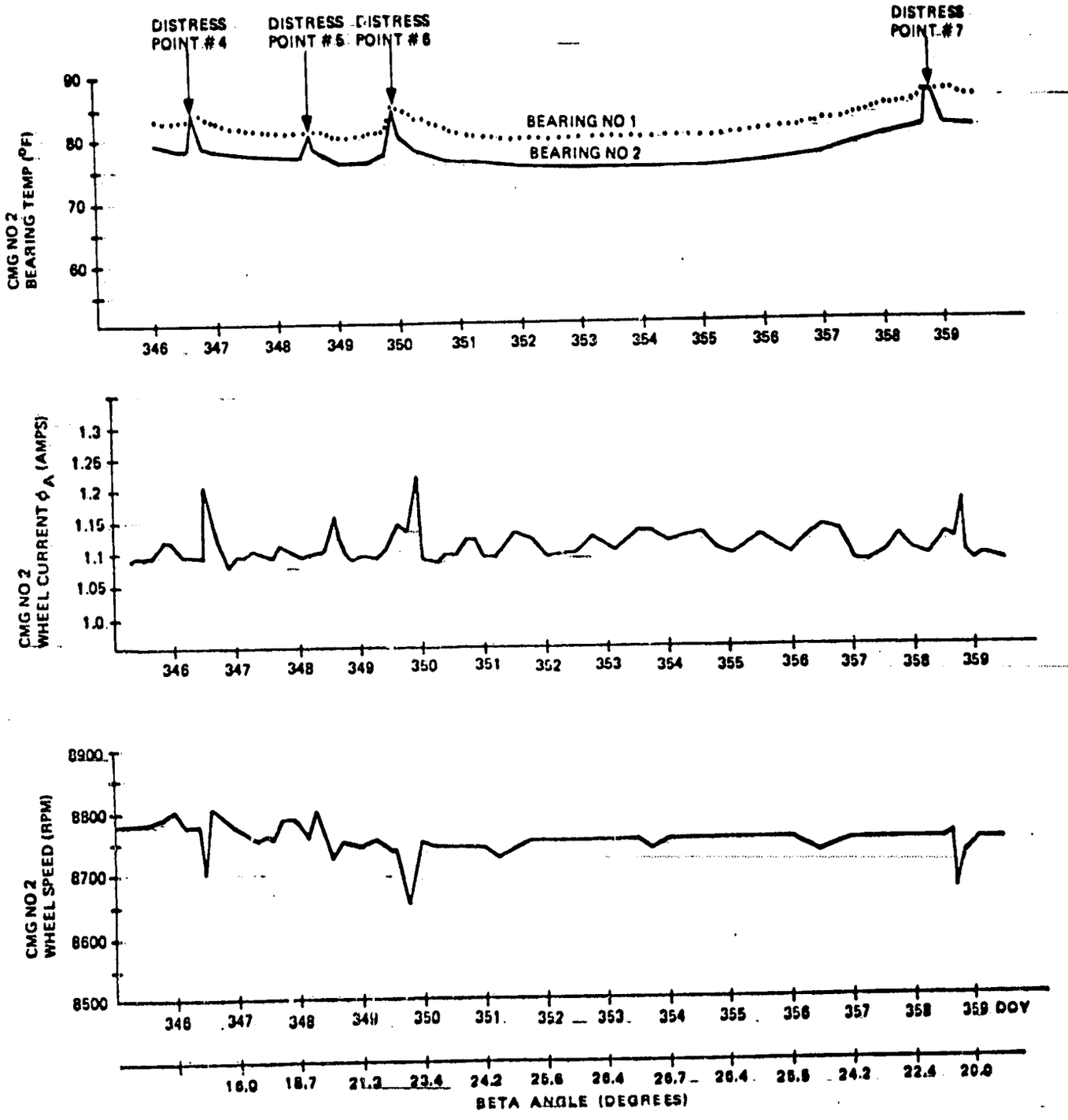

FIGURE 3-27

Between DOY 365 of 1978 and DOY 2 of 1979, six more distress points occurred. These took place when the beta angle was negative in the EOVV B mode which meant that the sun was shining directly on the CMG. It appeared that stress points would now be unavoidable for low beta angles even if the vehicle was rotated each beta pass. It was theorized that the CMG lubrication was evaporating and that distress points would occur at increasingly higher temperatures.

On January 25, 1979 the vehicle was maneuvered to the solar inertial attitude. Shortly afterwards, a 5 degree maneuver was commanded about the X axis to allow as much sunlight as possible to warm CMG #2. This was the maximum allowable rotation about the X axis that could be commanded in solar inertial operation.

Immediately upon acquiring the SI attitude, the bearing temperature began to fall (see Figure 3-28). On DOY 26, the first distress point in the solar inertial mode occurred. Four more distress points occurred during the next three days. It was feared that the 5 degree offset would not be sufficient to adequately warm the CMG. Therefore a program patch was generated to allow larger offsets during most of the daylight portion of the orbit and smaller offsets for ACQ SS strapdown updating and gravity gradient dump. The program patch was not implemented however because afte. the fifth distress point following SI acquisition, the temperature of the bearing stabilized at approximately 75 degrees F. From this point until the end of the mission, there were no further distress points.

3.3.4 Conclusions and Lessons Learned

After reevaluating the previous CMG distress points, it was decided that in addition to the marginal lubrication and low temperature, that the temperature gradient also contributed to the cause of the stress points. After the temperature became stable, the CMG behavior was normal. It was also concluded that orbital storage had no detrimental effects on the CMGs or their associated electronic systems.

CMG NO. 2 BEARING NO. 2 VERSUS BETA ANGLE FOR SOLAR INERTIAL MODE

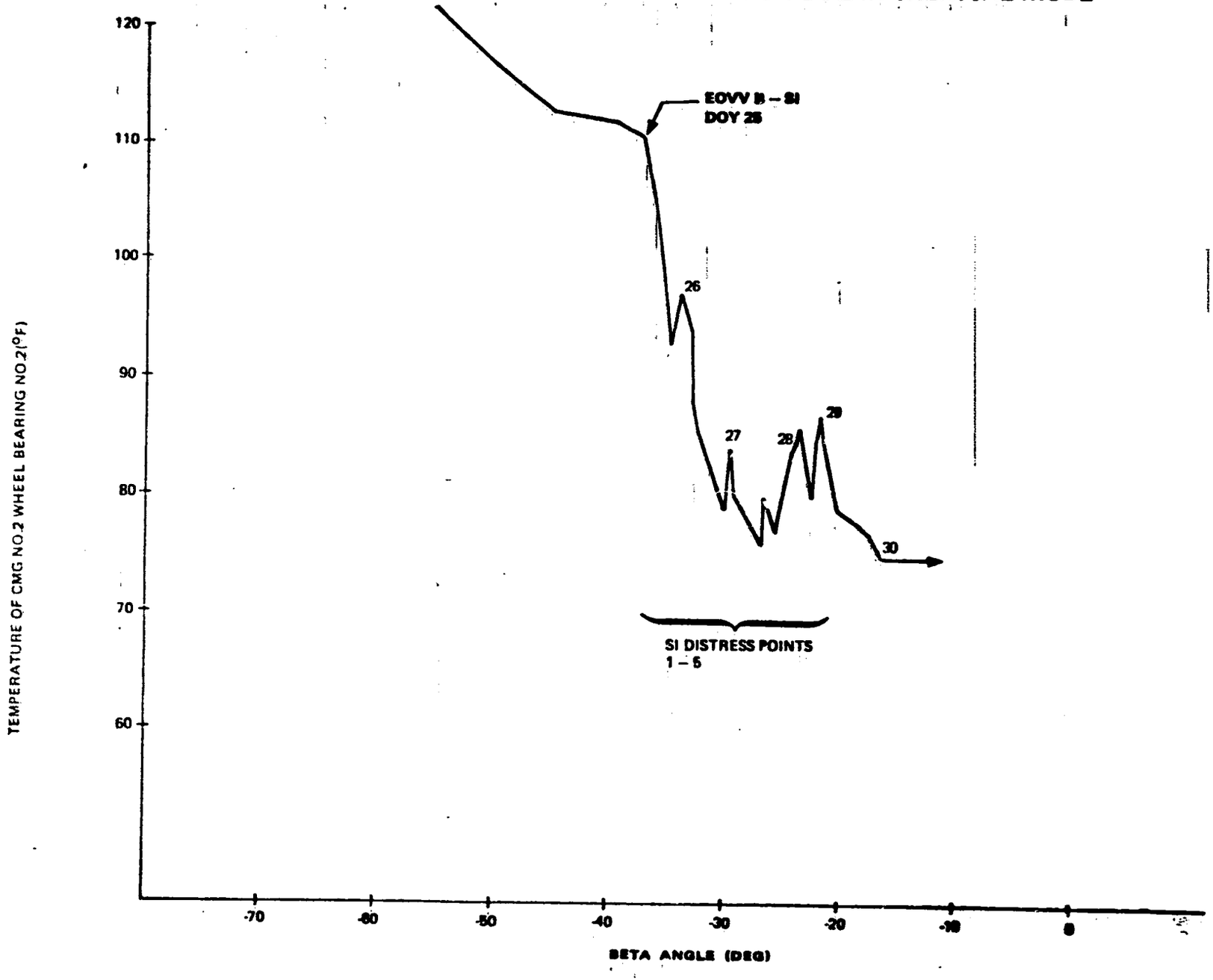

FIGURE 3-28

3.4 RATE GYROS

3.4.1 System Description

The ATM Rate Gyro Processor (RGP) consisted of a single Kearfott series 2519 rate integrating gyroscope and the electronics necessary to operate it in the rate mode, and was contained in a rectangular enclosure 30.28 X 21.74 X 14.60 centimeters. The RGP weighed 5.58 kilograms. Three rate gyros were utilized on each of the vehicles 3 control axes (X, Y and Z). During the original Skylab mission excessive drift in these gyros was of great concern (Reference 4). Because of this a special set of six gyros (the six pack) was developed and installed in Skylab during the third manned mission. At the end of the original Skylab mission the gyro configuration was as shown in Figure 3-29. Six pack # "5" gyros replaced # "1" designated gyros in the software while six pack # "6" gyros replaced the # "2" designated gyros in the software. X1 and Y1 rack rate gyros replaced the # "3" designated gyros in the software while the Z3 rack gyro retained its original designation.

3.4.2 Reactivation Mission Summary

On March 11, 1978, power was transferred to the Skylab APCS bus for approximately 5 minutes. This was the first time power had been applied to the rate gyros since the original Skylab mission shutdown on February 9, 1974. At this time, 5 of the 6 rate gyros in the "six-pack" came on and were operational. The Y2 rate gyro did not respond and was assumed to have been lost. Several weeks after the Skylab reactivation had been accomplished, the Y2 rate gyro inexplicably came to life and performed normally until April 23, 1979, when it again failed to operate.

The X2 rate gyro Failed to Operate several times during the reactivation mission, but it would later resume nominal operation. The X2 rate gyro anomaly was not a hard failure and suggested a failed intermittent power supply or electronic circuit, rather than a failed gyro.

On April 23, 1979, examination of the real-time telemetry data showed that the Y1 rate gyro was providing erratic outputs. Although the Y1 rate gyro was declared failed, because its signal characteristics had degraded, it was still operating and indicating rate measurements at reentry.

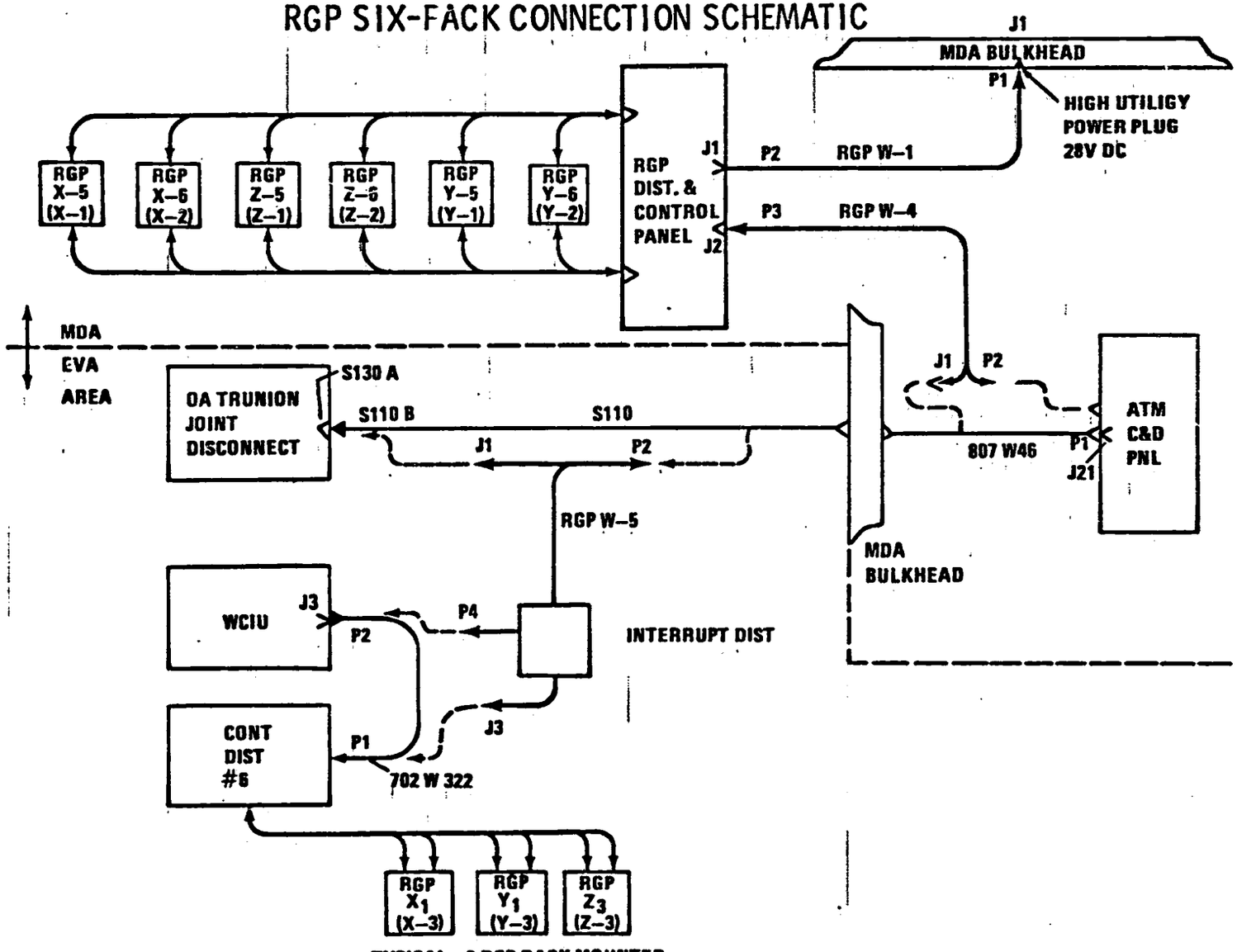
RGP SIX-PACK CONNECTION SCHEMATIC
J1
MDA BULKHEAD
P1
HIGH UTILIGY
POWER PLUG
28V DC
RGP
X–5
(X–1)
RGP
X–6
(X–2)
RGP
Z–5
(Z–1)
RGP
Z–6
(Z–2)
RGP
Y–5
(Y–1)
RGP
Y–6
(Y–2)
J1
P2
RGP W–1
RGP
DIST. &
CONTROL
PANEL
P3
RGP W–4
J2
MDA
EVA
AREA
S130 A
OA TRUNION
JOINT
DISCONNECT
S110 B
S110
J1
P2
J1
P2
807 W46
P1
J21
ATM
C&D
PNL
RGP W–5
MDA
BULKHEAD
WCIU
J3
P2
P4
INTERRUPT DIST
CONT
DIST
#6
P1
J3
702 W 322
RGP
X1
(X–3)
RGP
Y1
(Y–3)
RGP
Z3
(Z–3)
TYPICAL –9 RGP RACK MOUNTED

FIGURE 3-29

While in EOVV operations, on January 12, 1979, real-time telemetry showed that an error had been detected between the controlling Z-axis rate gyros Z1 and Z3. Telemetry indicated that the Z3 rate gyro output had failed to zero and flight controllers configured the Z axis to use rate gyros Z1 and Z2. The failed Z3 rate gyro was one of the three operating gyros mounted on the ATM rack. These rate gyros were exposed to a hard vacuum and an uncontrolled temperature environment and all but the Z3 rate gyro operated throughout the total Skylab mission.

3.4.3 Conclusions and Lessons Learned

There was no evidence that orbital storage had any adverse effects on the rate gyros. Even with all the rate gyro anomalies enumerated, redundancy still remained in the X and Z axes at reentry and the erratic Y1 rate gyro could have been used in the Y axis if it had become necessary.

3.5 ACQUISITION SUN SENSOR

3.5.1 System Description

The Acquisition Sun Sensor consisted of two major subassemblies, the Optical Assembly (OA) and the Electronics Assembly (EA). The Optical Assembly used a family of five photovoltaic cells arranged in a geometric configuration to generate voltage analogs of the sun's angular position about two orthogonal axes, linear to ±5 degrees, and a discrete signal any time the sun was within the field-of-view of the error detectors (9 ± 1 degrees circular). The Electronics Assembly used conventional electronics to shape and scale the signals from the Optical Assembly and then transmits the angular error signal and the sun presence signal to the APCS digital computers for subsequent processing and use in the Attitude and Pointing Control System. The Optical Assembly optical axis was aligned parallel to the Z-axis of the vehicle and measured angular errors about the X and Y-axes.

The Optical Assembly contained two pairs of fine-pointing detectors (one pair per axis) and a target detector. Each pair of detectors was connected so that the output currents were differenced and functioned as an energy balance null sensor. When the sensor was pointed directly at the sun both photocells received the same amount of energy and the electrical output was at a null. When not pointed directly at the sun, the optics (lenses and baffles) produced a difference in the solar energy reaching the two cells in the pair. The electrical output from the cells was proportional to the angle between the optical axis of the sensor and the sun line. The target cell detecting electronics triggered a discrete when the sun was within a ±2 degree cone of the solar vector.

The subsystem was completly redundant. There were two independent systems operating at all times.

3.5.2 Conclusions and Lessons Learned

There were no indications that orbital storage had any adverse effects on the sun sensors. The sun sensors performed throughout both Skylab missions without malfunction or failure. The sensors were in continuous operation from initial power-up to final power- down on the original Skylab mission and were on through all the reactivation mission.

The sun sensor was sensitive to reductions in solar light intensity, since it was designed to operate at one solar constant. Apparently, the sensor operated satisfactorily because there was no reduction in the scale factor on the analog angular rate error signal.

The sun sensors operated as designed and fulfilled all requirements with no anomalies.

3.6 ATM DIGITAL COMPUTER AND WORKSHOP COMPUTER INTERFACE UNIT

3.6.1 Introduction

The Skylab computer subsystem, which consists of two ATMDCs, WCIU, MLU and MLU tape recorder, performed without any failures during the primary Skylab mission. Both the primary and secondary computers were utilized during the primary mission and the operability of the onboard MLU and MLU tape recorder was successfully demonstrated at the termination of the mission. Therefore, at the conclusion of the primary Skylab mission, the entire complement of the Skylab computer subsystem was operational. A complete summary of the Skylab computer subsystem specifications and operational performance during the primary mission can be found in Reference 3.

This section briefly summarizes the performance of and concerns with the Skylab computer subsystem during the Skylab Reactivation mission.

3.6.2 Orbital Storage Effects

At the onset of the Skylab Reactivation mission, the operational status of the Skylab computer subsystem was not predictable because of the unknown environmental conditions experienced during the four years of orbital storage. The concerns with the effects of long term orbital storage were many; the major of which were as follows:

1) Thermal cycling

2) Degradation of the protective control surfaces

3) Decomposition of mylar tape in MLU tape recorder

Repeated thermal cycling occurred because of the random Skylab motion with respect to the sun and the occurance of earth shadowing (orbital day/night) each orbit for 16 orbits each day for the 4 years of orbital storage. Thermal cycling stresses component integrity and the major concern was the effect on internal and external connectors. The concern was that repeated thermal cycling could cause either poor electrical contact or no electrical contact between the pins and sockets in the connectors.

The thermal design of the ATMDC/WCIU was based on passive radiation of heat. An important part of that design was the use of a reflective paint to limit the amount of heat input from other sources. Photographs returned at the conclusion of the primary mission showed a significant discoloration of exterior surfaces of the computer subsystem components which suggested a degradation in the reflective paint. The major concern with degradation of the reflexive paint was that the temperature of the ATMDC in an operational state would exceed design specifications because of excessive heat input from other sources.

Although no plans existed for using the MLU tape recorder, a concern was voiced that the integrity of the mylar tape in the MLU tape recorder may have been degraded because the long term exposure in a vaccuum may have depressurized the sealed recorder. Concerns ranged from unreliable data on the tape to disintegration of the tape with movement. The operational status of the MLU tape recorder was never determined because it was not required during the Skylab Reactivation mission. However, the MLU tape recorder is identical to the ATM TM ASAP recorder which was used throughout the Skylab Reactivation mission without any discernible degradation in performance.

3.6.3 Operational Performance

There were three concerns relative to the operational performance of the ATMDC/WCIU during the Skylab Reactivation Mission. The concerns were the operational temperature range of the ATMDC/WCIU, the repeated power cycling of the ATMDC/WCIU during certain phases of the mission and the ATMDC/WCIU operational lifetime.

3.6.3.1 Thermal Performance

The operating temperature of the ATMDC/WCIU was of concern on two occassions during the mission. The first occasion was the initial power up temperature environment during the March interrogation tests (see Section 2.2.1) and the second occasion was operating in the EOVV A attitude with large negative sun angles (β).

3.6.3.1.1 March Interrogation Tests

At the conclusion of the primary Skylab mission, the primary ATMDC/WCIU was left connected to the APCS power bus. The relay which disconnected the computer subsystem from the APCS power bus was also activated by power from the same APCS bus. Furthermore, the internal heaters for the computer subsystem were also powered by the APCS bus. Therefore it was impossible to thermally condition the ATMDC/WCIU prior to the initial power up and also impossible to disconnect the primary ATMDC/WCIU from the APCS bus without first applying power to the ATMDC/WCIU. This situation was of concern since the temperature specification limit for ATMDC/WCIU power up was -20 degrees C and temperature measurements in the vicinty of the ATMDC/WCIU were indicating measurements in that range. The concerns with attempting a power up at excessively cold temperatures were several. First, the computer might not operate at all due to oscillator failure at low temperatures. Secondly, some permanent damage might occur in the hardware which could render the primary ATMDC/WCIU permanently inoperable. Thirdly, since the ATMDC utilizes a destructive readout memory, the attendant flight software may be destroyed or corrupted beyond use without any immediate recovery capabilities guaranteed. At 20:36 GMT on March 11, 1978, power was transferred to the APCS bus and the receipt of the ATMDC TM data at the Bermuda ground station confirmed that the ATMDC was cycling. ATMDC TM data indicated that the ATMDC and WCIU internal temperatures as measured by thermistors were -15.9 degrees C and -26.2 degrees C respectively at initial power up. Subsequent analysis of the ATMDC TM data indicated that the ATMDC/WCIU and attendant flight software were operational. In fact, as far as the onboard software program was concerned, the 4 year and 30 day off time appeared as only a temporary power transient; the power-up restart capability in the flight program picked up from where the program stopped cycling 4 years and 30 days ago.

3.6.3.1.2 EOVV Attitude

The EOVV attitude presented a signigicantly different thermal environment for Skylab than that experienced in the SI attitude. In the SI attitude, the Z vehicle axis is always pointed toward the sun and Skylab is presented with a relatively constant thermal environment. However, in the EOVV attitude the thermal environment for Skylab is directly related to the elevation/declination of the sun relative to the orbit plane.

In the EOVV attitude the vehicle longitudinal axis is nearly aligned along the orbit velocity vector with the vehicle rolled

about the longitudinal axis such that the solar panels point toward the sun near orbit noon. In the EOVV A attitude, the operating temperature of the ATMDC increased as the sun angle became more negative. (See Figure 3-30).

The acceptance test specifications for the ATMDC/WCIU required the ATMDC/WCIU to be operational, including initial power on, within design specifications between the temperature range of -20 degrees C (-4 degrees F) and +55 degrees C (+131 degrees F). All flight units successfully passed the acceptance tests. Additionally a qualification test was performed on one ATMDC in which the internal temperature of the ATMDC was maintained for 1 hour at 67 degrees C (153 degrees F) and the ATMDC remained operational within specifications. During the primary Skylab mission, the computer subsystem remained within the acceptance test thermal limits except for one brief occassion on DOY 14 in 1974 on which a ZLV maneuver was performed during a large sun angle condition (See Reference 3). Since the EOVV attitude is basically a subset of the ZLV attitude the operating temperature of the ATMDC for large negative sun angles was of concern. The ATMDC temperature while in the EOVV A attitude, based upon flight data from DOY 209 to DOY 258 (1978), is shown versus sun angle in Figure 3-30. As shown in Figure 3-30, the ATMDC temperature approached 55 degrees C as the sun angle aproached -40 degrees. The sun angle would reach -70 degrees at a later date and the thermal performance of the ATMDC in that situation was unknown. Predictions made by MSFC indicated that the ATMDC temperature would approach 152 degrees F for those conditions. However, this situation was never encountered because the attitude of Skylab was changed to the EOVV B attitude (180 degree rotation about local vertical from EOVV A attitude) when a large negative sun angle occurred. Skylab was placed in the EOVV B attitude because CMG 2 bearings experienced their lowest temperatures for large negative sun angles; a condition which was equated to enhancing the possibility of CMG #2 spin bearing failure.

ATMDC TEMPERATURE VERSUS β ANGLE FOR EOVV A

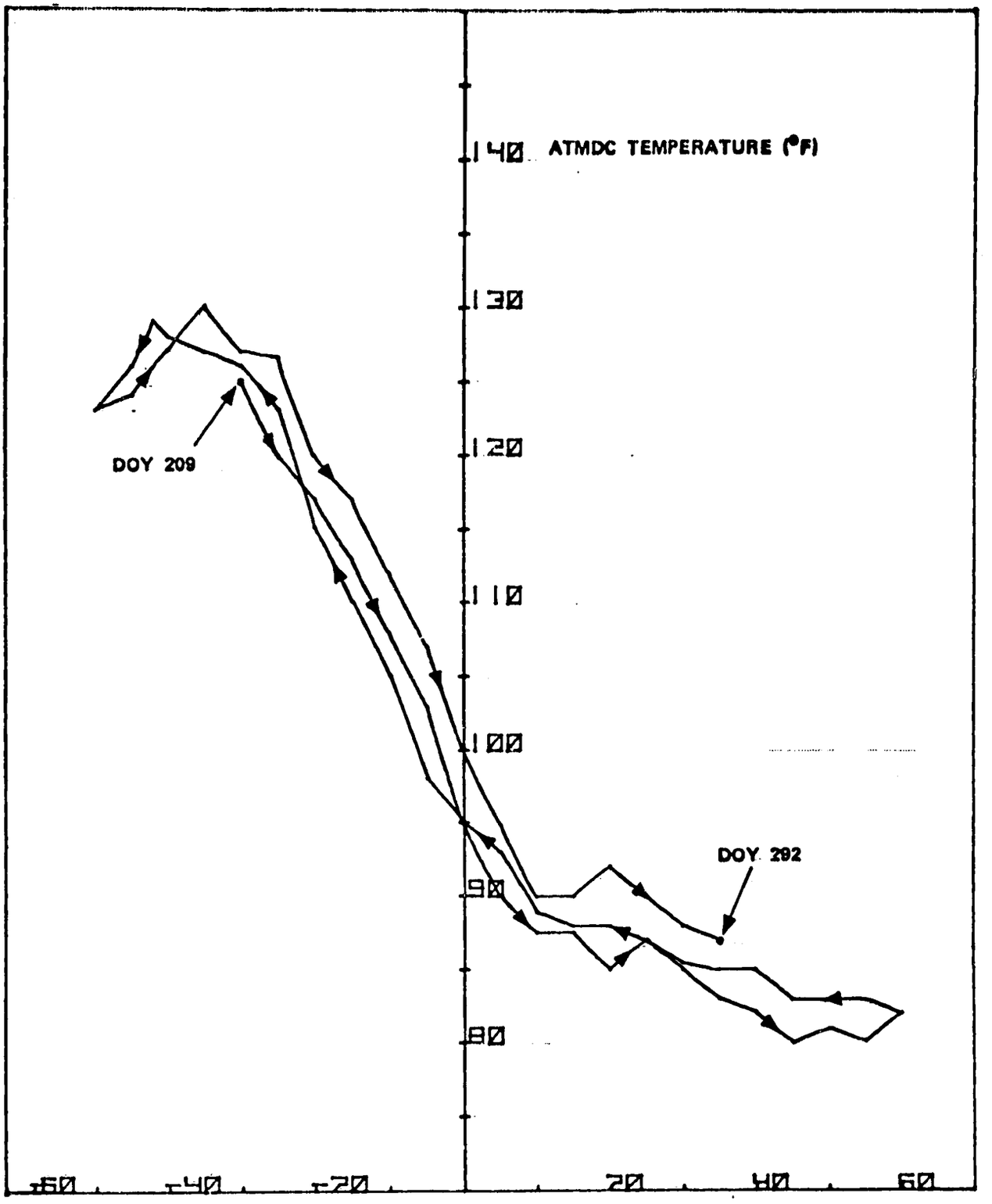

FIGURE 3-30

3.6.3.2 Repeated Power Cycling

As discussed in Section 3.6.3.1.1, the primary ATMDC/WCIU was connected to the APCS power bus and each time the APCS bus was energized, the ATMDC would power on. The onboard configuration remained in that state until the primary ATMDC/WCIU was disconnected from the APCS bus on June 7, 1978 because of a deficiency in electrical energy during CMG spin up. During the time period from the March interrogation tests until June 7, 1978, the primary ATMDC/WCIU was repeatedly cycled on and off due to interrogations of the APCS rate gyros, implementation of flight software patches into the ATMDC and unintentional operations. The primary ATMDC/WCIU was not removed from the APCS bus because an uncertainty in the operability of the onboard switch selectors generated a reluctance to change any operational onboard configuration unless absolutely necessary. Furthermore, since the specific switch selector command had never been issued during the primary mission, there was an additional uncertainty in its operability. However, when the energy shortage in the electrical power system occurred, the primary ATMDC was removed from the APCS bus and subsequently was successfully reconnected to the APCS bus.

The exact number of power cycles applied to the primary ATMDC/WCIU is unknown but estimates range from thirty to hundreds. The reason for the uncertainty is because on several occassions, the APCS bus was unintentionally left energized when the Skylab attitude was uncontrolled. This situation occurred as a result of the spurious switch selector command phenomenon which was not well understood at the time.

Although difficult to quantify, it was felt that repeated power cycling of the ATMDC/WCIU could adversely affect the lifetime capability of the hardware.

3.6.3.3 Operational Lifetime

The operational lifetime of the ATMDC/WCIU was of significant importance during the design phase of the APCS. The computer was considered to be one of the least reliable components in the APCS. Considerable effort was devoted to screening parts, rigorous testing and designing a redundant computer subsystem which could satisfy the planned 236 day mission lifetime. Originally the stated design reliability goal for the composite Skylab computer subsystem was a reliability of 0.70 for a 236 day mission. (See Reference 3). An ATMDC Failure Effects Analysis dated 1 July 1970, estimated a 236 day mission reliability figure of 0.869. The original ATMDC/WCIU design had

C-3

an estimated failure rate of 98.8 failures per million hours. The 16K memory contributed 73.3 of the 98.8 failures per million hours. The addition of the 8K flight program capability and the memory reload capabilities (MLU) increased the overall ATMDC/WCIU system reliability to Ø.971 for a 236 day mission. The Skylab computer subsystem operational lifetime far exceeded its design goals.

The total operational time for the primary and secondary ATMDCs and WCIU common TMR section is shown in Table 3-11. As observed in Table 3-11, the total accummulated hours on the computer subsystem is equivalent to 762.3 days of operation; and the computers were still operational when Skylab was destroyed upon reentering the earth's atmosphere.

TABLE 3-11 SUMMARY OF SKYLAB COMPUTER SUBSYSTEM OPERATIONAL HOURS

Component	Hours At Launch	Inflight Hours Primary Mission	Inflight Hours Reactivation Mission	Total Accumulated Hours (Days)
Primary ATMDC	1620	626	9432	11678 (486.6)
Secondary ATMDC	1147	5902	----	7049 (293.7)
WCIU Common	2335*	6528	9432	18295 (762.3)

*The primary and secondary ATMDCs were operated 432 hours without the WCIU common.

3.7 ATMDC FLIGHT SOFTWARE

3.7.1 Introduction

Software modifications developed to support all phases of the Skylab reactivation mission included extensive modifications to the ATMDC flight software as well as corresponding changes to off-line support software used for verification and performance analysis. The software development activity during the reactivation mission was concentrated around three major areas: two CMG EOVV operations, single CMG EOVV operation and TEA control. Each of these software development activities resulted in new ATMDC flight software which utilized the available APCS hardware to provide momentum management and vehicle control. The initial purpose was to maintain a minimum drag or End-On-Velocity-Vector (EOVV) attitude to prolong Skylab lifetime. Later, when plans for the reboost/deboost mission were dropped, the purpose was to enable vehicle control to be maintained as Skylab attitude decayed toward reentry.

A fourth area of activity, which applied to each of the major development areas, provided flight software modifications to improve Skylab system operation in the reactivation mission environment. The environmental considerations included unmanned operation, limited ground coverage, and limited APCS resources (i.e., TACS).

A description of the tools used for development of flight software; the methods and procedures used to define, analyze, program and verify software modifications into the ATMDC and a chronology and description of the modifications follows.

3.7.2 Development Tools

Prior to and during the original Skylab mission, there were several simulators which had been used for the Skylab performance analysis, flight software development, crew training and mission support. Upon completion of the Skylab mission these simulators were stored away or disassembled with no thought or plans for them ever becoming active again. When Skylab reactivation became apparent, an effort was initiated to bring the necessary simulators out of storage and update them to the configuration required to support EOVV flight program development.

Prior to and during the original Skylab mission, there were several simulators which had been used for the Skylab performance analysis, flight software development, crew training and mission support. Upon completion of the Skylab mission these simulators were stored away or disassembled with no thought or plans for them ever becoming active again. When Skylab reactivation became apparent, an effort was initiated to bring the necessary simulators out of storage and update them to the configuration required to support EOVV flight program development.

Prior to the beginning of the Skylab reactivation effort, all Skylab simulators were inactive. A study was made to decide what simulator requirements were needed for EOVV software development and which simulators could be reactivated in the time available to best meet these requirements. Simulator requirements were developed by experience gained from previous space related software development programs. These programs have shown that several different types of simulators are required to provide complete simulation support of software development.

A fast running simulator is needed to perform long term performance analysis where simulations of ten or more orbits are common. A simulator which has a model of flight software that is easily modified is needed for front-end studies on design schemes where many approaches are proposed or where the scheme is in a preliminary design phase and several changes are anticipated. Another simulator is needed with the capability for a large amount of control, data gathering and visibility of the flight program to perform detailed instruction-by-instruction testing. A real time simulator is needed for making performance studies using the actual flight software. Each of these simulators have unique characteristics which make them best suited for their particular task and, when used collectively, provide the total testing requirements of the ATMDC software.

The simulators used for software development in the reactivation mission were:

1) IBM System/360 Model 75 System Analysis Attitude Simulator - Version II (AS-II)

2) IBM System/360 Model 75 Interpretive ATMDC Workshop System Simulator (Interpretive Simulator)

In addition to the IBM simulators, the control system and momentum management scheme was developed on a NASA SIGMA 5 computer.

The AS-II simulator met both requirements for fast speed and easy modification.

The interpretive simulator met the requirement for the next type of simulator needed, i.e., extensive control, data collection and visibility. The interpretive simulator was an all-digital simulation which executed on an IBM System 360/Model 75 computer. The interpretive simulator had been saved intact on computer tapes and an IBM System/360 Model 75 computer was in operation at the Data Systems Lab at MSFC and was made available for EOVV software development.

Although the interpretive simulator existed on tape and an IBM System 360/Model 75 was available, there still remained considerable effort to reactivate the simulator. When the interpretive simulator had been used at the IBM Facility, all inputs for simulator control were made through computer terminals. At the Data Systems Lab, however, terminal did not exist and the simulator had to be modified to use computer cards. Also the interpretive simulator had been designed to read the ATMDC flight program from a specially formatted load tape.

An exhaustive search through the IBM facility computer tape files, records retention and all other possible locations failed to produce a single ATMDC flight program load tape. Some HSL flight programs were discovered in the old MSFC HSL facility where they had been stored for over four years. By modifying the interpretive simulator and developing a special program to reformat these tapes, a load tape was generated which could be used by the interpretive simulator. However, this load tape was missing many of the features that were part of the normal load tape and this caused many capabilities of the interpretive simulator to be precluded.

Another difficulty was that the IBM personnel who had developed and programmed the interpretive simulator had since transferred from the IBM Huntsvile Facility. These personnel had to be located and brought to Huntsville to perform the required modifications to make the interpretive simulator operational again.

The next type of simulator required was one which operated real time or near real time with an actual flight program. The candidate simulators were part hardware and this hardware had long since been disassembled with no plans for subsequent reactivation. The hardware had not been stored in any

systematic manner and therefore few of the pieces could be located. Some of the parts were even being used on current NASA projects. It was concluded that a real time simulator could be activated only by expending a large amount of resources and time that was not available. With the cost/time standpoint weighted against the risk involved, it was decided that a real-time simulator was not absolutely necessary.

Therefore, it was planned to eliminate the requirement for a real time simulator and to limit the amount of performance analysis with the actual flight program to nominal environments. Performance analysis in off-nominal situations could be performed on the AS-II and the NASA SIGMA 5. Although this left a "gap" in the testing of the software, it was decided to risk this exposure in order to develop the EOVV software in the time available.

3.7.2.1 IBM System/360 Model 75 System Analysis (AS-II) Simulator

The AS-II Simulator was used to validate the performance of proposed control system changes for Skylab developed on the NASA SIGMA 5 computer by performing digital simulations to obtain dynamical descriptions of the orbiting Skylab. This simulator performed a variety of analysis and/or mission support task. The most important ones were:

1) Determine parametric specifications of control system parameters needed to meet system accuracy requirements and satisfy energy constraints.

2) Determine the effect, over many orbits, of disturbance torques upon control system energy expenditure and attitude accuracy while maintaining desired vehicle attitude characteristics.

3) Recreate observed anomalies to gain in depth understanding of anomaly and insure proper onboard operations.

4) Evaluate and optimize recommended procedures for acquisition of different control modes and attitudes. Generate predicted performance data to use as a basis for real-time mission support.

The primary advantage of the AS-II Simulator was its capability to operate within the range of 10 to 100 times faster than real

time (depending upon output format options). Within the area of mission analysis, the AS-II Simulator was used effectively for determining critical design error limits and performance characteristics when the Skylab configuration underwent severe changes.

In addition to being able to operate at high speed, the AS-II was also relatively easy to modify. The AS-II model of the flight program is written in FORTRAN language which is much easier to code than the ATMDC language. This allowed the software requirements to be implemented into the AS-II and extensively tested with a long lead-time over ATMDC programming.

3.7.2.2 IBM System/360 Model 75 Interpretive ATMDC Skylab Simulator

The IBM System/360 Model 75 Interpretive ATMDC Skylab Simulator is an all digital model of the Skylab and the ATMDC flight program. The Skylab system hardware and vehicle dynamics are modeled by FORTRAN mathematical equations and logic statements. The flight program is modeled by converting ATMDC program instructions to the equivalent System 360/75 machine language instructions. The ATMDC hardware models generally remain fixed from run to run while the ATMDC flight program is input from a load tape. A detailed description of the interpretive simulator is given by Reference 17. This simulator was the only simulator available during EOVV and TEA software development which operated with the actual ATMDC flight program. A block diagram of the interpretive simulator is shown in Figure 3-31.

The interpretive simulator has an extensive input/output capability for controlling and analyzing simulations (see Reference 17). These capabilities give the software analyst a comprehensive tool for performing flight program verification. A summary of these capabilities are given below:

Repeatability - The simulator is designed to give repeatable results for runs with identical setups or with changes which do not alter timing. For this reason, if a problem is encountered which requires more data for anlysis, the run may be repeated with additional output requests. ATMDC program traces, ATMDC memory and accumulator snaps, and vehicle data output requests may all be added without affecting timing, and hence, repeatability.

Availability of Data -- Selected time intervals and the ATMDC memory areas may be traced, if necessary, to isolate a problem or to verify program flow through a selected region. The data output indicates the time since power up, instruction location,

SYSTEM 360/75 SIMULATOR

BLOCK DIAGRAM OF THE IBM SYSTEM 360/MODEL 75 INTERPRETIVE ATMDC SKYLAB SIMULATOR

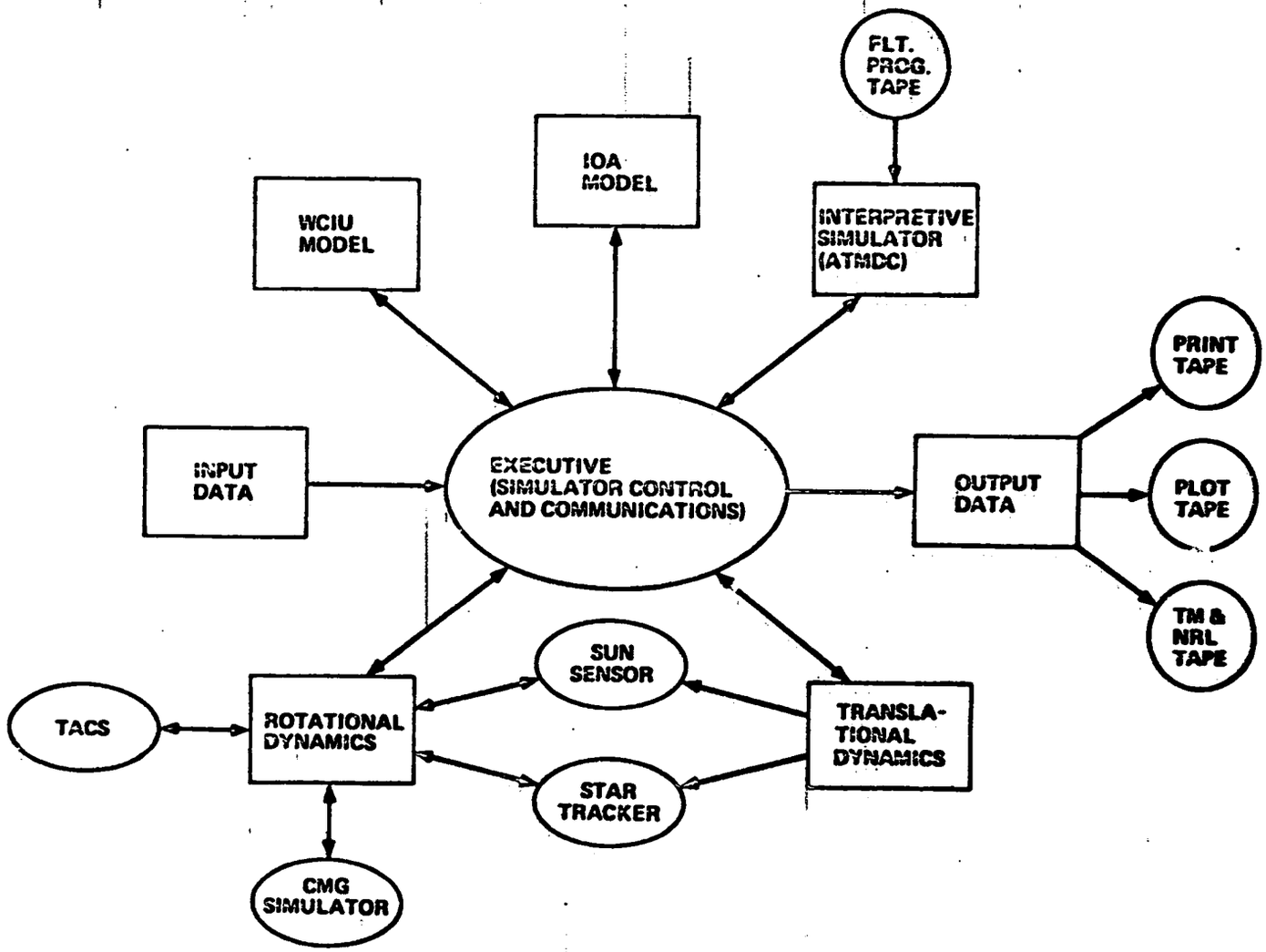

FIGURE 3-31

instruction executed, data location, and data used. The trace modes available are full trace (every instruction executed), block trace (selected memory regions), and time trace (selected time intervals).

A variation of the trace is the accumulator snap, which prints the trace information plus the scaled accumulator at selected locations.

Vehicle Perturbations - The capability to dock/undock the CSM or power up/down the CMG's is incorporated into the 6D vehicle simulation in order to evaluate the Flight Program and its interaction with the vehicle under common off-nominal conditions. Normal sequencing discretes and interrupts from the vehicle to the ATMDC may be selectively inhibited and forced to test various program backup modes.

Attitude Reference Perturbations - Rate gyro, sun sensor, star tracker and CMG direction cosine inputs may be modified in any of several ways to force program processing of unusual sensor data. Sensor readings may be simulated with scale factor errors, biases, and constant readings, which may be selectively modified for each computation cycle. Individual perturbations may be applied to each input address even though some addresses may be redundant reads of the same sensor input.

ATMDC Perturbations - Each data input register in the ATMDC may be loaded with data, and any bits may be set or reset, at selected time points. This capability is used to analyze program reaction to unusual input conditions, such as unexpected interrupts and discretes.

Extensive Output - Every variable used in program computations is available for printout after simulation. This permits examination of numerous parameters without resorting to traces or snaps and facilitates trouble-shooting problem areas. In addition, normal output from the ATMDC and 6D is synchronized so that all data printed in a print block is valid at one time point. Therefore, any problems which require analysis of both ATMDC and 6D data are more easily solved than if synchronous data were not available. Changes in state of each discrete register and BCD display are printed as they occur.

Error Checks - A number of checks on potential system errors are performed on every run. Potential program errors and system hardware violations are printed as they occur noting time, program locations and type of error. The errors checked include addressing of non-existent inputs, insufficient data conversion time, improper setting of discrete output registers, program overflows, and illegal instructions. This output is printed on every run in conspicuous fashion facilitating a rapid scan by the analyst.

The disadvantage of the interpretive simulator was its run ratio of between 15 and 20 to 1. This means that a simulation of 1 hour of flight time required 15 to 20 hours of CPU time. This was not a problem prior to and during the Skylab mission because the types of test cases which require long periods of time (such as performance validation runs) were made on one of the real time simulators. Since these simulators no longer existed, performance testing with the actual flight program had to be performed on the interpretive simulator. Because of the poor run ratio only a limited amount of performance testing could be accomplished in the time available.

3.7.3 Software Definition

All modifications to the ATMDC flight software developed during the Skylab reactivation mission were documented by IBM as Software Change Requests (SWCR's). These SWCR's are summarized later in Section 3. The procedures used to generate these SWCR's were basically the same as those used during the original Skylab mission to develop and control the configuration of ATMDC software.

The basic requirements for a SWCR originated either from MSFC or within IBM. Any requirements which effected momentum management or control operations were analyzed by NASA using the SIGMA 5 computer and by IBM, using the AS-II simulator. If necessary, the basic requirements were modified to meet the desired operating goals based on these performance simulations. In addition, each new requirement was analyzed to insure compatibility with existing flight software capabilities and mission support activities. The results of the performance and compatibility analyses were combined with the original requirements. The combined requirements were then documented as SWCR's to define the specification to which flight software modifications were programmed and verified.

3.7.3.1 Flight Software Baseline

The initial software configuration of the primary and secondary ATMDC's was determined by reviewing mission summary data provided at the end of the original Skylab missions (see Reference 3). The primary ATMDC contained the FF50 version of the 16K flight program. This was the result of a RF uplink, via the MLU, which was successfully executed just prior to termination of the original Skylab activities on 9 February 1974. The secondary ATMDC contained the FF80 version of the 16K flight program plus SWCR 3091. This was the result of several memory loads during the course of the original Skylab mission.

The flight software configuration defined as the baseline for the reactivation mission modifications was chosen to be the FF80 plus SWCR 3091 version of the 16K flight program. The primary reason for this decision was that this version was already resident in the secondary computer. By updating the primary computer to the same level as the secondary, both computers would contain the baseline software. This would simplify updating the secondary computer in case of switchover. A memory map of the FF80 plus SWCR 3091 program is shown in Figure 3-32.

The first flight software changes for the reactivation mission were defined relative to this FF80 plus SWCR 3091 baseline. The baseline for each subsequent change (i.e., SWCR) was defined relative to the software configuration existing, or planned to exist, at the time of its implementation (i.e., baseline plus all previously implemented memory loads).

FF80 PLUS SWCR 3091 MEMORY MAP

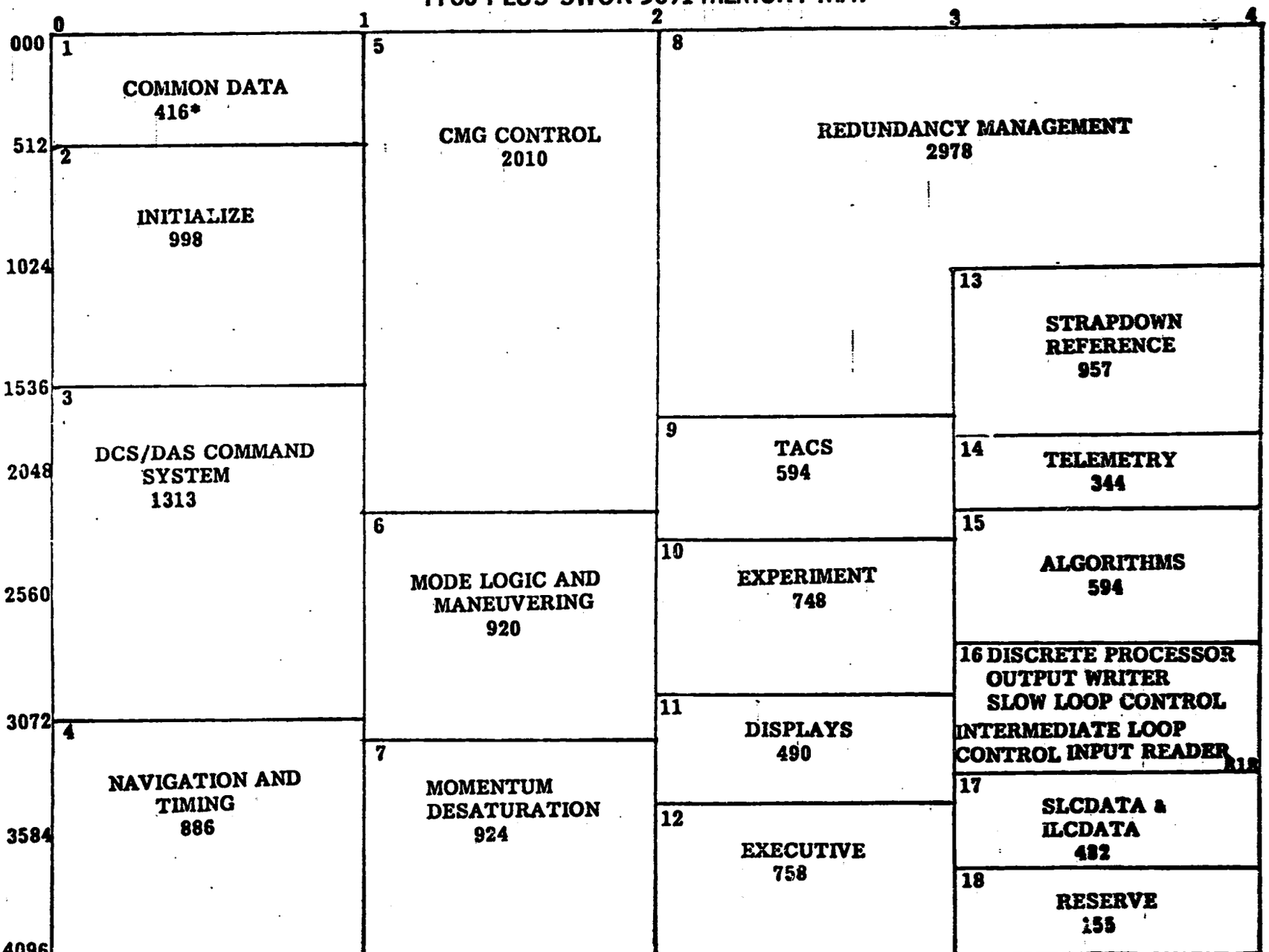

*MODULE SIZE

FIGURE 3-32

3.7.3.2 Requirements and Specifications

Most of the reactivation mission requirements dealing with the new control and momentum management laws for two and one CMG EOVV operation and for TEA control originated from MSFC. These requirements were generally given to IBM in rough equation and logic form.

From these requirements it was necessary to develop the detailed specifications necessary to design, code and verify changes which could be integrated with existing flight software. Areas, in addition to the basic requirements, which had to be specified for each change included:

1) ground command requirements and formats to provide manual control and/or trim capabilities

2) telemetry requirements for performance evaluation

3) initialization requirements

5) timing and sequencing requirements

6) implementation requirements to insure compatibility with existing software

The final requirements specification for each proposed change to the flight software was documented as a SWCR relative to a definition baseline consisting of the ATMDC Program Definition Document (PDD), Revision 22; plus the memory loads implemented, and documented by SWCR's, during the original Skylab mission; plus any previously defined changes for the reactivation mission. In addition to the requirements specification, several SWCR's also contained Program Notes to identify any operational constraints or peculiarities which would exist when the corresponding change was implemented into the flight software.

3.7.3.2 Requirements Analysis

All proposed requirements which effected Skylab control and momentum management operation were analyzed using the AS-II simulator. This simulator was the only analysis tool available which was capable of long flight-time performance simulations with models of the Skylab environment and vehicle dynamics and the ATMDC flight software equations and logic.

The equations and logic for each new control and momentum management requirement' were incorporated into the AS-II simulator. Simulations were made and analyzed to determine that the design goals could be achieved over the expected operating conditions (i.e., sun angle); to identify any operational limitations or constraints associated with the requirement; and to insure that existing performance capabilities were not degraded by inclusion of the new requirements.

Extensive analysis was also performed for every critical Skylab maneuver or operation. Each was simulated to determine the sequencing required to maximize usage of CMG control and momentum management operational capabilities and to minimize usage of TACS fuel. Conditions which were examined for the critical Skylab operations included: rate gyro drift and scale factor errors; attitude reference errors (primarily about the sun line); availability of ground stations; breakes in the planned maneuver sequences; and the range of sun angle (β). The simulations were not only required to design the required maneuver and operational sequencies but were also used to compare with and evaluate the actual system performance during the sequence execution.

Detailed simulations were performed for each of the following:

SI Attitude Acquisition - The operation of acquiring SI attitude with a spinnning vehicle (1.7% about the X-principle axis) and an unknown attitude reference was simulated to estimate the TACS fuel requirements, the attitude overshoot, and the time and procedures required to settle the X-principle axis in the orbit plane. These were performed in the TACS only mode since CMG control was not enabled at this time. Simulation estimates closely follow the actual operation.

SI To EOVV-A Maneuver - The planned maneuver sequence to acquire the EOVV-A attitude (EOVV with MDA forward) from SI was simulated to predict system performance (i.e., TACS usage, settling time, etc.) during and following the maneuver. The simulation and actual flight data were in agreement when the maneuvers were performed.

EOVV-A To EOVV-B Maneuver - The maneuvers from EOVV-A attitude to EOVV-B attitude (EOVV with MDA trailing) were simulated to determine a maneuver sequence which would not require TACS and to predict performance during and following the maneuver. The simulation and actual flight data were in agreement when the maneuvers were performed.

EOVV-B To EOVV-A Maneuver - Although these maneuvers were not executed, they were simulated to determine a maneuver sequence which would not require TACS and which would establish EOVV parameters within their nominal ranges for EOVV-A operation.

EOVV-B To SI Maneuver - This maneuver was simulated to determine the sequence for maneuvering from EOVV-B to SI which would require no TACS usage and which would place the Skylab control system within the capabilities of nominal SI operation. The actual flight data from this maneuver agreed with simulation data.

Continuous SI Offset - SI operation with a continuous 5 degree offset about the X-axis was simulated, over the range of expected sun angles, to insure that the SI momentum management performance would not be adversely affected. A proposed change which would extend the SI offset capability to 10.3 degrees or more (35 degrees maximum) was also simulated. Simulations showed no adverse effects which was in agreement with actual flight data for a 5 degree X-axis offset.

SC-EOVV Operation - The proposed EOVV operations with momentum management and CMG control laws for a single CMG (SC-EOVV) were simulated. Simulations of the SC-EOVV acquisition sequence, the SC-EOVV out-of-plane maneuvering capability, and the SC-EOVV roll rate phasing logic for Skylab power maintenance were analyzed. After modifications were made to the roll rate phasing logic, the overall SC-EOVV operating goals were determined to be achievable.

SI Dump Performance - The SI momentum management operation was simulated over the range of expected sun angle, solar activity, and altitude to determine the expected SI dump performance as Skylab's altitude decayed toward reentry. Results of these simulations defined the ground maintenance activities required to support SI control operation as well as identified the altitude and sun angle limits where SI dump capability would be lost.

TEA Control - TEA control operations over the expected altitude and atmospheric ranges were simulated. This included modifying the AS-II simulator to model atmospheric effects and generating TEA control parameters as a function of altitude, density, and momentum bias. Simulations for: initial TEA acquisition (T121G and T121P); continuous TEA operation (T121G, T121P, and T275) under nominal, navigation error, attitude error, and rate gyro error conditions; and maneuvers between equilibrium attitudes (i.e., T121P and T275) were performed. Results of these simulations provided expected TACS usage data for maneuvers and TEA control maintainability data which were in agreement with actual flight data as well as similar MSFC simulations.

3.7.4 VERIFICATION

Software verification is the process by which the accuracy and adequacy of the flight program is demostrated by ensuring that the on-board software meets all mission requirements and is not the limiting factor in the success of the mission. The verification of the Skylab reactivation flight software was performed by subjecting the software to an exhaustive series of tests using the AS-II and interpretive simulators.

3.7.4.1 Verifications Techniques

The technique used to verify the reactivation flight software were developed on previous verification effort of real-time space related software such as the Saturn Program and the Skylab mission. The success of these programs has demostrated that these methods, when properly applied, will result in verified, error-free software. The software is verified by applying the techniques one at a time in the following order:

1) Baseline Program Validation
2) Coding Analysis
3) Logic Analysis
4) Equation Implementation Tests
5) Performance Validation
6) Mission Procedure Validation

3.7.4.1.1 Baseline Program Validation

Prior to deactivation of the Skylab vehicle, the primary computer was loaded with as FF5Ø level flight program by MLU and RF uplink and the secondary computer had an FF8Ø program plus software modifications for SWCR 3Ø91. When Skylab was reactivated, the primary computer was still in control and the FF5Ø program was resident and unaltered after four years.

The plans were to first update the primary computer from the FF5Ø level to the same level as the secondary computer. This was to be done by the first three memory load buffers. The subsequent buffers (which were numbered starting with FF81

Buffer 1) would then update the program to the EOVV (or FF81) level. By using this method, if a primary computer failure forced switchover, the secondary computer could be updated to the FF81 level by resending all buffers except the first three. The baseline software was therefore defined as the software in the secondary computer, i.e., FF80 plus S3091.

Since the FF50 and FF80 plus S3091 programs had already been completely verified during the Skylab mission, no reverification was considered necessary. However, a method had to be developed to verify that the FF50 program could be correctly updated to the FF80 plus S3091 level.

A problem developed when no tapes of the FF50 program could be located. Some flight program tapes had been found in the old MSFC HSL facility but these were FF60, FF70 and FF80 plus S3091 flight programs. To determine the difference between FF50 and FF60, the computer program listings were compared and all miscompares were documented.

To ensure that all differences between FF50 and FF60 had been found, the miscompares were summed in the same way that the flight program computes sum checks. The results were then checked against the differences of FF50 and FF60 sum checks and a favorable comparison gave a high degree of confidence that all miscompares had been found. The differences between FF60 and FF80 plus S3091 were detected by a special tape compare computer program.

The total differences between FF50 and FF80 plus S3091 were then formatted into DCS commands for three memory load buffers with each buffer cantaining new sum check constants. The uplinking of these buffers were simulated on the interpretive simulator and after uplinking each buffer, the program was executed through at least two sum check cycles. Successful execution of the sum check tests verified that the memory loads were correctly implemented. The sum checks from the last memory load were compared against the sum checks in the FF80 plus S3091 flight program. By ensuring that these sum checks were identical and by performing a desk check of all memory load DCS commands, the baseline for the EOVV flight program was validated.

3.7.4.1.2 Coding Analysis

This phase of the verification effort was to examine the actual coding of the flight program to determine compliance with programming ground rules and to verify compliance with the Software Change Request. Experience has shown that this phase

is by far the most efficient; i.e., many more program problems are uncovered per manhour expended than in any other phase. The following paragraphs outline the procedure which was followed to effect a systematic approach to this effort.

The initial step required for a complete analysis of the programming techniques was the construction of flow diagrams of every module. These flow charts were drawn from the program coding and were very near to the instruction level. Information relative to scaling and flight program organization were included. The diagrams were then used in conjunction with the program listing to accomplish the coding analysis phase of verification.

The following items were investigated for every module, subroutine, logic statement, equation and parameter changed in the flight program.

1) Consistency in parameter scaling between modules

2) Consistency in parameter scaling with maximum expected values

3) Interrupt protection when required

4) Correct logic statements considering specification

5) Correct equation implementation

6) Correct use of "scratch pad" memory

7) Potential problem areas with trigonometric functions

8) Interaction of parameters and program control words which might be changed in different modules

9) Interference with use of parameters and control words in different modules

10) Correct use of the shift instructions

11) Correct protection against taking square root of a negative number

12) Correct use of divide operations

3.7.4.1.3 Logic Analysis

This phase of the verification is designed to ensure that the flight program is operationally consistent with the requirements of the SWCR. It involves investigating the specifications in the SWCR on a sectionalized (modular) basis and designing short time duration simulation runs to check the corresponding logic path in the flight program. All logic paths were excercised and interactions with other parts of the program code were checked. Consequently, this phase of verification required extensive use of the System 360/75 Interpretive Simulator.

3.7.4.1.4 Equation Implementation Tests

As logic paths are cycled, calculations of all parameters were checked by comparing against hand calculations or against the results of independent programs on the HP 9820A calculator created specifically as verification tools. The inputs to the equations were varied from run to run to cover the expected possible range. This method was invaluable for finding accuracy problems, scaling problems and equation implementation errors.

3.7.4.1.5 Performance Validation

The capability to accomplish performance validation with the actual flight program was extremely limited due to the lack of a real time simulator. The available resources can best be utilized by making one simulation run of approximately 1 1/2 orbits with the interpretive simulator while the flight program is operating in a nominal mode. Details of the performance of this run were compared to an AS-II simulation run with the same initial conditions. This nominal performance case was run when all of the logic and equation analysis had been completed, because minor software errors could invalidate the entire run which required 27 hours of CPU time and a minimum of 50 manhours analysis time. The intent of this run was to check the implementation of the control scheme in the flight program. Many more runs of considerably longer duration are required to properly verify all aspects of this implementation, but the resources were not available. Therefore, all off-nominal performance validation was performed with the AS-II Simulator.

3.7.4.1.6 Mission Procedure Validation

The baseline program (FF8Ø plus S3Ø91) was a completely verified program and, because of time and simulator constraints, the parts of this program that were unchanged were not reverified. The verification effort was directed mainly toward flight program changes and to interactions between the changed and unchanged parts of the program. However, some of these interactions were not obvious, and to check as many interactions as possible, the mission procedures were validated.

Mission procedures validation consists of simulating procedures on the interpretive simulator prior to implementing them in the mission. These simulators were analyzed to ensure that the procedure was executed correctly and that no unusual interactions or timing situations occurred. Examples of the procedures that were validated were: initial maneuver to EOVV, maneuvers from EOVV A to EOVV B, return to solar inertial and maneuvers to TEA control attitudes. In addition to mission procedures, several contingency procedures were simulated such as APCS mode changes, redundancy management reconfigurations, entry into single CMG control, etc.

3.7.4.2 Configuration Control

Configuration control is the process of ensuring that the delivered software is identical to the software that successfully passed all verification tests. Prior to the Skylab mission the large number of programmers, analysts and verifiers which were involved in software development made configuration control a major concern. A rigid set of guidelines were formulated which required documentation for all program releases, program trouble reports and software modifications. A Software Review Board consisting of representatives from the different areas of software development managed the software configuration control. All change to the program were tracked from conception until final verification. Every precaution was made to ensure that the delivered program was completely tested and verified.

The requirement for configuration control with the reactivation software was significantly reduced. The personnel involved in reactivation software development was a very small group working in the same area and sometimes numbering only four people. Configuration control was maintained during reactivation software development as described in the following paragraphs.

The first step in configuration control was the establishment of a baseline for each buffer development. The FF80 plus SWCR 3091 was the baseline software for the initial EOVV software development. When the initial software modifications (FF81 buffers 1-8) were uplinked between June 1 and June 5, 1978, this software then became the baseline for FF81 Buffer 9 development. Thereafter, as each buffer was implemented, that software became the new baseline for programming the next buffer. The same method applied for the development of the single CMG control law which was labeled the FF90 flight program. The software which contained all FF81 buffers through Buffer 14 was the baseline for the initial single CMG control program. FF90 Buffer 1 through Buffer 16 contained the initial single CMG control requirements (SWCR 4014) and became the baseline for FF90 Buffer 17 (SWCR 4017).

For each set of baseline software a corresponding set of sum checks were computed. An incorrect set of sum checks would cause computer switchover. By using the SNAP capability of the interpretive simulator, the sum checks were included in the simulation printout and if switchover did not occur, the flight program configuration was thereby known.

Software development of the new buffer load would be initiated by the release of a software change request (SWCR). Modification to the baseline flight program would then be programmed so that the requirements specified by the SWCR would be loaded into the ATMDC computer. These modifications, along with their sum checks were then implemented into the interpretive simulator by the HEX card capability for verification testing.

The modifications were then subjected to a series of tests. Any errors that were found were documented as program trouble reports (PTR's). The software was then reprogrammed to correct the error, new HEX cards were formatted and a new set of sum checks were computed. By snapping the sum checks in the interpretive simulator, the software that was being tested was always known. All program corrections were retested until the software passed all verification tests.

When verification was complete, the program modification were formatted into DCS commands. The DCS commands were formatted on program cards for shipment to JSC in Houston, Texas. Before these cards were released, they were reformatted by a special DCS convert program into DCS commands for the interpretive simulator. The memory load uplink of the buffer was then simulated on the interpretive simulator. By performing a desk analysis on the DCS commands and verifying that the simulator did not switchover after memory load implement, the configuration of the DCS memory load commands was assured.

A continuous simulation was maintained in which the memory load buffers were loaded as they were verified. A restart point was made at the implementation of each buffer and was the starting point for the next buffer load. In this way, the configuration of the flight software was maintained. Each restart point was saved so that if a buffer that had been verified and delivered, but for some reason not loaded, the previous restart point could be used for another buffer development.

3.7.4.3 Exposures

Only two simulators were available for flight software development during the reactivation mission; the AS-II and interpretive simulators. In order to develop the best software in the time available, certain risks had to be taken. These risks, or exposures, are listed below:

1) No performance validation was made with a real-time simulator

2) No verification was made with a hardware simulator

3) No off-nominal performance analysis was made with the actual flight program

4) Unchanged flight program modules were not reverified

5) Sensitivity of the new equations to variations in Navigation parameters, patch data commands and APCS component characteristics were not ascertained.

6) Interaction of new logic with non-related existing capabilities of the flight program was not verified except by nominal performance and mission procedure validation.

Although these risks would not have been taken for the original Skylab mission, they were considered acceptable for the reactivation mission software development.

3.7.5 Implementation

Modifications to the ATMDC flight software were implemented using the DCS memory load capability which was resident in the ATMDC flight software. This capability was used 14 times during the original Skylab mission (Reference 3) and for all memory modifications during the reactivation mission. An additional capability was made available late in the reactivation mission which allowed high rate updating of any amount of memory using the 72 Kbps RF uplink, via the MLU, to the ATMDC.

The DCS command and memory load buffer descriptions were delivered to NASA for each flight software modification. The format of these was similar to the formats used during the original Skylab mission and was jointly agreed upon by IBM, MSFC, and JSC prior to the reactivation mission. The DCS command description contained the octal and hexidecimal command format, command type (i.e., load begin, address, data, etc.), hexidecimal addresses and data words to be loaded, and a load sequence number for each command. The memory load buffer description contained the memory load buffer addresses and corresponding data words in hexidecimal format with special notation buffer words used by the memory load routine itself (i.e., pointers).

The procedure for real-time modification of the flight software involved ground verification of the memory load buffer. The memory load DCS commands were transmitted, in sequence, to the operating ATMDC where they were stored, by flight software, in a special area of the computer memory reserved for the memory load information. This memory load buffer was telemetered, upon command, back to the ground support centers prior to implementation. The telemetry data was manually verified at MSFC and JSC and if correct, the memory load implement DCS commands were issued to the ATMDC. If the buffer telemetry was incorrect, the memory load buffer was reinitialized, the uplink commands were checked and corrected if necessary, and the memory load procedure performed again.

3.7.6 Chronology/Description of Flight Software Modifications

Flight software changes were developed prior to and during the Skylab reactivation mission. The purpose of these modifications was to extend the capabilities of the existing flight and ground systems to control Skylab during its remaining lifetime with the expected hardware configuration and environmental conditions. Table 3-12 contains a list of the software modifications developed in support of the reactivation mission. Table 3-13 shows the modification timeline for the memory load buffers implemented into the ATMDC flight software. A brief description of each memory load buffer is contained in the following paragraphs. Numbered buffers (1-23) were modifications to the ATMDC software baseline and were all documented with SWCR's. Buffers with numbers preceded by a "P" or "T" were not documented with SWCR's. The "P" buffer set was a preliminary software modification to establish a comman software baseline in both ATMDCs by bringing the FF50 level software residing in the Primary ATMDC up to the equivalent FF80 level plus SWCR-S3091 which was known to reside in the Secondary ATMDC. These "P" buffers were a combination of the changes made and documented during the original Skylab mission (Reference 3). The "T" buffers were temporary patches which were either implemented or overriden soon afterward or prepared to reset other buffers in case of any difficulties with their operation.

Buffer P1, P2, P3: The purpose of this change to the ATMDC flight software was to bring the FF50 level software residing in the Primary ATMDC up to the same level as the software residing in the Secondary ATMDC (FF80 plus SWCR-S3091). This established a common software baseline to which all Skylab reactivation mission software changes were made. Implemented into the Primary ATMDC on 5/31/78.

Buffer 1 through 8: The purpose of the changes to the ATMDC flight software was to provide conputations and logic for attitude maneuvering, momentum management, and strapdown reference updating over extended periods of operation in the End-On-Velocity-Vector control mode. This new mode of operation provided the capability to maintain a minimum drag orientation for extension of Skylab lifetime.

Buffers 1 through 8 contained the baseline EOVV computations and logic and were defined by SWCR-S4000. Buffers 1-5 were implemented into the Primary ATMDC 6/1/78. Buffers 6 and 7 were implemented into the Primary ATMDC 6/2/78. Buffer 8 was implemented into the Primary ATMDC 6/5/78.

Buffers T2 and T1: The purpose of the T2 buffer was to temporarily change the TACS control gains in the Z axis

TABLE 3-12 SOFTWARE MODIFICATIONS FOR SKYLAB REACTIVATION

Modification	Title	Number of Buffers	Final Disposition
P	Upgrade ATMDC Software from FF50 Level to FF80 Level + S3091	3	Implement Buffer P1-P3 in Primary ATMDC 5/31/78
S4000	2 CMG EOVV operation including revision to EOVV Strapdown Update Test Constant	9	Implement Buffer 1-8 In Primary ATMDC 6/1 to 6/5/78 Implement To Buffer 9 In Primary ATMDC 6/11/78
T0	Change "Z" Axis TACS Only Control Gains	1	Delivered to NASA 6/1/78
T1	Restore "Z" Axis TACS Only Control Gains (Reset T0, T2)	1	Implement Buffer T1 in Primary ATMDC 6/9/78
T2	Change "Z" Axis TACS Only Control Gains (FF80 + Buffers 1-8)	1	Implement Buffer T2 in Primary ATMDC 6/9/78
S4001	EOVV Sun Presence Flag Definition and ATMDC Telemetry Changes	1	Implement Buffer 10 in Primary ATMDC 6/26/78
T3	Change "Z" Axis TACS Only Control Gains (same as T2 but for FF80 + Buffers 1-10)	1	Delivered to NASA 7/10/78
T4	Restore "Z" Axis TACS Only Control Gains (same as T1 but for FF80 + Buffers 1-10)	1	Delivered to NASA 7/10/78
S4002	Prevent TACS Only Selection	1	Implement Buffer 10A in Primary ATMDC 7/24/78
S4003	μ_z Update for EOVV	1	Implement Buffer 11 in Primary ATMDC 8/12/78
S4004	Change in η_y Calculation	1	Implement Buffer 11 in Primary ATMDC 8/12/78
T11	Reset of S4003 and S4004 (Buffer 11)	1	Delivered to NASA 8/5/78

TABLE 3-12.

SOFTWARE MODIFICATIONS FOR SKYLAB REACTIVATION (CONTINUED)

Modification	Title	Number of Buffers	Final Disposition
S4005	η_{yc} Change After Strapdown Update	1	Implement Buffer 13 in Primary ATMDC 9/11/78
S4006	Automatic e_{TN} Update	1	Implement Buffer 12 in Primary ATMDC 9/8/78
S4007	EOVV Backup Strapdown Update Logic	1	Implement Buffer 13 in Primary ATMDC 9/11/78
T13	Reset of S4005 and S4007 (Buffer 13)	1	Delivered to NASA 8/24/78
S4008	Enable/Inhibit Standby Mode Following Switchover	1	Implement Buffer 12 in Primary ATMDC 9/8/78
S4009	Change V_{ref} Test Constants	1	Implement Buffer 12 in Primary ATMDC 9/8/78
S4010	Automatic CMG Failure Detection	-	Canceled 8/1/78
S4011	TACS Firing Limit	1	Implement Buffer 12 in Primary ATMDC 9/8/78
S4012	TACS Desaturation for EOVV	-	Canceled 8/1/78
S4013	New TACS Only Control Gains	-	Implement Buffer 17 in Primary ATMDC 1/30/79
S4014	Single CMG Control Law (SC-EOVV)	16	Delivered RF Tape Containing SC-EOVV to NASA 1/15/79
S4015	Gimbal Rate Limiting Accuracy Improvement	1 1	Implement Buffer 14 in Primary ATMDC 9/20/78
S4016	Definition of Backward EOVV Operation	1	Implement Buffer 15 in Primary ATMDC 1173/78

TABLE 3-12 SOFTWARE MODIFICATIONS FOR SKYLAB REACTIVATION (CONTINUED)

Modification	Title	Number of Buffers	Final Disposition
S4017	SC-EOVV Roll Rate Phasing Changes	3	Delivered RF Tape Containing S4017 to NASA 1/15/79
S4018	New Requirements to Support SC-EOVV Activation	-	Canceled 11/10/78
S4019	Correction to Orbital Z-Axis Momentum Prediction	1	Implement Buffer 16 in Primary ATMDC 12/3/78
S4020	Experiment Pointing Mode Enable DCS Commands	1	Implement Buffer 17 in Primary ATMDC 1/30/79
S4021	Solar Inertial Roll Operation	1	Verified 2/9/79
S4022	TEA Control	5	Implement Buffer 18-22 in Primary ATMDC 5/19/79 and 5/20/79
T14	Nominal Q_{BL} for T121P Operation	1	Implement Buffer T14 in Primary ATMDC 6/21/79 & 6/22/79
S4023	Q_{BL} Normalization	1	Implement Buffer 23 in Primary ATMDC 6/22/79

TABLE 3-13. MEMORY LOAD BUFFER IMPLEMENTATION TIMELINE

Date	Buffer	Description
5/31/78	P1, P2, P3	Upgrade ATMDC Software from FF50 Level to FF80 Level Plus SWCR-S3091 (See Reference 2)
6/1/78	1-5	First Five Buffers for 2 CMG EOVV Operation (SWCR-S4000)
6/2/78	6-7	Next Two Buffers for 2 CMG EOVV Operation (SWCR-S4000)
6/5/78	8	Last Buffer for 2 CMG EOVV Operation (SWCR-S4000)
6/9/78	T2	Change "Z" Axis TACS Only Control Gains
6/9/78	T1	Restore "Z" Axis TACS Only Control Gains
6/11/78	9	Revision to EOVV Strapdown Update Test Constant (SWCR-S4000)
6/26/78	10	EOVV Sun Presence Flag Definition and ATMDC Telemetry Changes (SWCR 4001)
7/24/78	10A	Prevent TACS Only Selection (SWCR S4002)
8/12/78	11	μ_z Update for EOVV and Change in η_y Calculation (SWCR-S4003 and S4004)
9/8/78	12	Automatic e_{TN} Update, Enable/Inhibit Standby Mode Following Switchover, Change V_{ref} Test Constants, and Provide TACS Firing Limit (SWCR-S4006, S4008, S4009, and S4011)
9/11/78	13	η_{yc} Change After Strapdown Update and EOVV Backup Strapdown Update Logic (SWCR-S4005 and S4007)
9/20/78	14	Gimbal Rate Limiting Accuracy Improvement (SWCR-S4015)

TABLE 3-13 MEMORY LOAD BUFFER IMPLEMENTATION TIMELINE (CONTINUED)

Date	Buffer	Description
11/3/78	15	Definition of Backward EOVV Operation (SWCR-S4016)
12/3/78	16	Correction to Orbital Z-Axis Momentum Prediction (SWCR-S4019)
1/30/79	17	New TACS Only Control Gains and Experiment Pointing Mode Enable DCS Command (SWCR-S4013 and S4020)
5/19/79 5/20/79	18-22	TEA Control (SWCR-S4022)
6/21/79 6/22/79	T14	Nominal Q_{BL} for T121P Operation
6/22/79	23	Q_{BL} Normalization (SWCR-S4023)

following the initial reacquisition of the Solar Inertial attitude. These gains provided rate damping to +0.025 deg/sec in the Z axis while allowing gravident-gradient torques to position the X-principle to its normal SI orientation near the orbit plane. A +7Ø degree attitude deadband was also provided to prevent large attitude oscillations during the settling interval. The purpose of the T1 buffer was to restore the Z axis TACS gains back to their nominal values after the x-principle axis had settled near the orbit plane.

Buffer T2 was implemented in the Primary ATMDC 6/9/78 immediately after acquiring the SI attitude about the vehicle X and Y axes. Buffer T1 was implemented in the Primary ATMDC 6/9/78 approximately two orbits following Buffer T2.

Buffer 9: The purpose of Buffer 9 was to lower the EOVV strapdown update test constant. This was required because lower then nominal ACQ SS outputs, outside of its linear operating range, were causing EOVV strapdown updates to occur early (during the non-linear range). This situation was detected soon after entering EOVV operations. SWCR-S4ØØ defines the updated test constant values. Buffer 9 was implemented into the Primary ATMDC 6/11/79.

Buffer 1Ø: The purpose of Buffer 1Ø was to use the Sun Presence Redundancy Management output as the EOVV sun presence indication instead of the logical OR of the sun presence discrete inputs. This prevented the possibility of erroneous strapdown updates due to sun presence failures during EOVV operation. In addition, Buffer 1Ø provided five more EOVV parameters on ATMDC telemetry to aid ground controllers in evaluating and maintaining EOVV operation. SWCR-S4ØØ1 defines buffer 1Ø requirements. Buffer 1Ø was implemented into the Primary ATMDC 6/26/78.

Buffer 1ØA: The purpose of Buffer 1ØA was to prevent automatic selection of TACS only control, and the resulting TACS fuel loss, for all conditions. Buffer 1ØA also desensitized the modified outer gimbal drive logic to prevent unnecessary gimbal drives during EOVV operation. Automatic TACS only selection, which occurred twice prior to Buffer 1ØA, required a large amount of TACS fuel (1ØØØ lbf-sec) which was critical to future operations. SWCR-S4ØØ2 defines Buffer 1ØA requirements. Buffer 1ØA was implemented into the Primary ATMDC 7/24/78.

Buffer 11: The purpose of Buffer 11 was to eliminate X, Y axis cross-coupling into the EOVV Z-axis strapdown updates and to eliminate EOVV Y-axis offset errors during offset limiting conditions. SWCR-S4ØØ3 and S4ØØ4 define Buffer 11 requirements. Buffer 11 was implemented into the Primary ATMDC 8/12/78.

Buffer 12: The purpose of Buffer 12 was fourfold:

1) automatically adjust the EOVV nominal momentum to provide a more timely response to current operating conditions than was available with existing tracking station coverage

2) provide DCS command capabilty to enable/inhibit Standby Mode selection in the event of a computer switchover to minimize TACS usage following a switchover.

3) desensitize CMGIA reference voltage test constants to minimize the change of an unwarrented CMG failure.

4) provide an automatic TACS firing limit, updatable via DCS, to conserve limited TACS fuel resources.

Buffer 13: The purpose of Buffer 13 was to compensate the EOVV Y-axis offset command for EOVV strapdown updates and to update the backup strapdown reference when isolating rate gyro failures. SWCR-S4005 and S4007 define Buffer 13 requirements. Buffer 13 was implemented into the Primary ATMDC 9/11/78.

Buffer 14: The purpose of Buffer 14 was to increase the accuracy of the CMG gimbal rate limiting computations. The computational accuracy at low rate limit values (1 deg/sec was selected to minimize CMG wear) actually allowed larger gimbal rates (2 deg/sec) prior to limiting. SWCR-S4015 defines the Buffer 14 requirements. Buffer 14 was implemented into the Primary ATMDC 9/20/78.

Buffer 15: The purpose of Buffer 15 was to provide the capability for EOVV operation either with the MDA toward the positive velocity vector (EOVV A operation) or with the MDA toward the negative velocity vector (EOVV B operation). The EOVV A and B attitudes were selected, via DCS command, based on the sun angle (β) being positive and negative, respectively. This prolonged CMG 2 lifetime by increasing its operating temperature with solar heating. Buffer 15 also provided increased capabilities for delayed ZLV and SI maneuvering to maneuver between EOVV A and B attitudes independent of tracking station coverage. SWCR-S4016 defines the Buffer 15 requirments. Buffer 15 was implemented into the Primary ATMDC 11/2/78.

Buffer 16: The purpose of Buffer 16 was to modify the orbital Z-axis momentum prediction during EOVV operation to include all four momentum samples during EOVV B operation. Different timing in EOVV B operation caused some sample data to be ignored. SWCR-S4019 defines the Buffer 16 requirements. Buffer 16 was implemented into the Primary ATMDC 12/3/78.

Buffer 17: The purpose of Buffer 17 was to change the TACS only control gains to be compatible with the lower TACS impulse that was available during the reactivation mission. Buffer 17 also provided the capability to activate, via DCS command, Experiment Pointing Electronic Assembly (EPEA) functions during any mode of operation. SWCR-S4013 and S4020 define the Buffer 17 requirements. Buffer 17 was implemented into the Primary ATMDC 1/30/79. The EPEA activation capabilities were never used in order that any chance of jeopardizing future reboost/deorbit plans could be avoided.

Buffers 18 through 22: The purpose of Buffers 18 through 22 was to provide the capability to control Skylab as its altitude decayed toward reentry in a Torque Equilibrium Attitude (TEA). Vehicle control in the SI and EOVV operating modes became impossible below the 140-145 n.m. altitude range and Skylab reentry pans required that vehicle control be maintained down to the 80-70 n.m. range. SWCR-S4022 defines the buffer 18 through 22 requirements. Buffers 18 through 22 were implemented into the Primary ATMDC on 5/19/79 and 5/20/79.

Buffer T14: The purpose of Buffer T14 was to reinitialize the desired attitude reference for TEA control. This was necessary to reinitialize the reference quaternion to compensate for computation drift in TEA control operation. Buffer T14 was implemented into the Primary ATMDC three times from 6/21/79 to 6/22/79 while a permanent software modification was being prepared.

Buffer 23: The purpose of Buffer 23 was to maintain normalization of the TEA reference quaternion thus eliminating the effects of computational drift associated with reference updates during TEA control operation. SWCR-S4023 defines the Buffer 23 requirements. Buffer 23 was implemented into the Primary ATMDC 6/22/79.

One additional memory load buffer was implemented into the Primary ATMDC during the reactivation mission. This buffer was developed prior to and used during the original Skylab mission to reenable the use of external interrupts declared to be occurring excessively by onboard software tests by resetting an interrupt inhibit mask. SWCR-S3013 from the original Skylab mission defined the requirements for this buffer. The interrupt mask reset buffer was used several times during the reactivation

to reenable use of the 24 pps interrupt which failed when the ATM transmitters were cycled to conserve electrical power.

Several other memory load buffers, most notably the 16 buffers associated with the Single CMG Control law, were developed during the reactivation mission (See Table 3-12) but were not implemented into either ATMDC.

4.0 THERMAL ENVIRONMENTAL CONTROL SYSTEM

4.1 INTRODUCTION

Two of the Skylab Thermal/Environmental Control Subsystems were used during the reactivation period. The Airlock Module cooling loops were used to provide cooling for the Airlock Module battery and electronics modules. The O2/N2 gas supply system was used to maintain the Skylab internal pressures above .1 psia to provide a passive environment for the rate gyros. The following paragraphs provide brief functional descriptions of these systems, summaries of the status of the systems at the end of the active Skylab Missions, and summaries of performance and operation during the reactivation period. More detailed system descriptions and active Skylab Mission performance information are available in Reference 16. Brief discussions of the Skylab thermal environments, status of the OWS sun shields and Skylab temperatures during the final orbits are also provided.

4.2 AIRLOCK MODULE COOLING LOOP

4.2.1 System Functional Description

The Airlock Module (AM) cooling system (Figure 4-1) performed several functions during the active Skylab missions. It removed latent sensible heat from the internal atmosphere, provided cooling for the crew during EVA activities, cooled EREP and TM equipment, and provided cooling to a variety of other equipment including the Airlock Module battery modules and electronics modules which contained transmitters and other communications components. Two separate (primary and secondary) coolant loops were provided for redundancy.

Temperature regulation within each cooling loop was provided automatically by three temperature control valves. The key control points were the 47 F control valve at the inlet to the atmosphere temperature control heater exchangers and the 40 F valve at the inlet to the battery/electronics modules. The system was designed to allow the atmosphere heat exchanger inlet valve to take precedence and let the battery module valve control whenever total system load permitted.

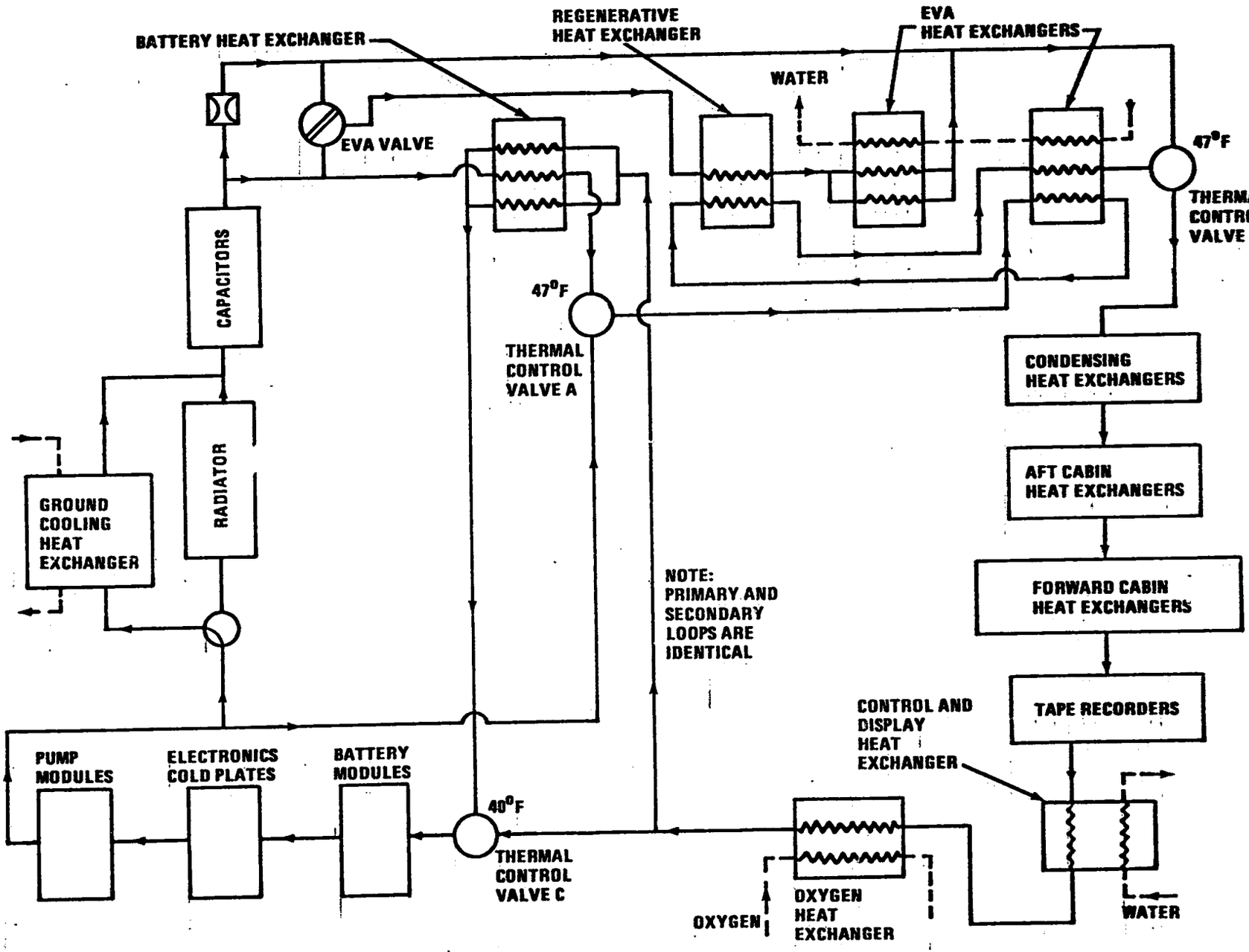

FIGURE 4–1. AIRLOCK MODULE COOLING SYSTEM

Each loop had two pump packages containing three coolant pump/motor units. Three inverters were provided for each loop to convert spacecraft supplied DC power to the AC power required by the pump motors. During normal orbit operations, one pump/inverter combination was operated in each loop. However, during conditions of low system load (e.g. storage between missions), one pump in a single loop was operated.

Heat was transported from the various sources within the system by Coolanol 15 to a radiator mounted on the Multiple Docking Adapter (MDA) and AM Structural Transition Section (STS) where it was rejected to space. Transient heat rejection was supplemented by two thermal capacitors (charged with tridecane wax) plumbed in series with the radiator. The total heat rejection surface area of the radiator was 432 ft.

4.2.2 Status After Skylab Missions

Although some problems occurred, the Airlock Module Cooling loops generally performed well during the active missions. Pump flowrates were always higher than specification requirements and overall cooling capabilities exceeded preflight predictions for nominal conditions. At the end of the last mission, all components within the coolant loops were operational except for inverter one in the secondary loop which had failed during the first manned mission. The major problems associated with the system during the active missions were coolant loop leakage and sticking of control valves. The status of the system at the end of the missions relative to these problems are summarized in the following paragraphs.

4.2.2.1 Sticking of Thermal Control Valves

During the first Extra Vehicular Activity (EVA) on the first manned mission, the 47 degree F control valves at the inlet to the atmosphere temperature control heater exchangers stuck in a fixed position in both the primary and secondary loops. It was determined that the sticking was caused by contamination which originated in heat exchangers which were only used during EVA operations. Procedures were developed and implemented which resolved the problems and returned the valves to normal operation. However, whether or not the valves would function properly was a concern when the cooling loops were reactivated in April 1978.

4.2.2.2 Coolant Loop Leakage

Both the primary and secondary coolant loops leaked during the Skylab Missions. The leakage in the primary loop depleted the reserve coolant in the reservoirs during the Skylab Missions. The leakage in the primary loop depleted the reserve coolant in the reservoirs during the second manned mission. A reservicing kit was designed and fabricated and carried to Skylab by the crew for the third manned mission. The loop was successfully serviced and normal operation of the loop was restored. However, fluid continued to leak from the loop. While the secondary loop did not require reservicing, by the end of the last mission the reservoirs were almost empty. Without coolant fluid in the reservoirs, the required pump inlet pressure could not be maintained. This would result in reduced flowrates, pump cavitation and, possibly, pump failure. Since it was expected that leakage would have continued over the four year period between the last manned mission and the reactivation period, this constituted a major concern at the time of reactivation.

4.2.3 Reactivation to Splashdown

During the initial communications with Skylab in March 1979, telemetry data was received which indicated that adequate Coolanol 15 was probably present in both the primary and secondary coolant loops to permit operation of the loops. A direct comparison with loop pressures at the end of the Skylab Missions was difficult at this point since overall loop temperatures were significantly higher due to the vehicle attitude. However, the loop pressures indicated that some fluid was still in the reservoirs of both systems. This was not expected based on leakage rates seen during the active missions. The initial communications also verified that temperature and pressure instrumentation in the cooling loops was still operational. Most of the sensors which were functioning at the end of the last Skylab Mission were sitll providing realistic data.

Both the primary and secondary loops were activated during the reactivation period on April 24 and 25, 1979, to determine their operational status and capability to provide cooling for the battery and electronics modules. The checkout consisted of operating one coolant pump/inverter combination in each loop and monitoring appropriate data.

The temperature control valves in both loops modulated properly and provided outlet temperatures within their design control band. Pump differential pressures were nominal. The following brief data summary illustrates the operational status of the coolant loops.

After two orbits of operation of the primary loop, the following data was obtained:

1) The temperature at the outlet of the control valve upstream of the cabin heat exchangers was 47°F (design range, 47±3°F).

2) The temperature at the outlet of the control valve upstream of the battery electronics module was 41°F (design range 40°+2° or -4°F).

3) The pump differential pressure was 57 psia which was a nominal value for design flowrates.

4) The pump inlet pressure was 21 psia with the pump operating as compared to 24 psia at the end of the missions.

The following data was obtained during an eight minute operation of the secondary loop:

1) The temperature at the outlet of the control valve upstream of the cabin heat exchangers modulated from an initial temperature of 53°F to 48°F (see Figure 4-2).

2) The temperature at the outlet of the control valve upstream of the battery electronics module modulated from an initial temperature of 56°F to 41°F (Figure 4-3).

3) The pump differential pressure increased to 75 psia when the pump was turned on and decreased to approximately 57 psia during the operational period (Figure 4-4). This was representative of nominal startup operations.

4) The coolant flowrate into the warm inlet port of the 47°F control valve upstream of the cabin heat exchangers increased to approximately 240 pounds per hour during the operational period. As can be seen from Figure 4-5, there was a delay of approximately 50 seconds prior to initiation of flow into this port. This was representative of nominally expected operation since the valve and coolant fluid in the lines connected to the cold inlet port were above the control point of the valve which would result in the valve being fully open to this port. The delay was

required to bring cold fluid from the radiator to the valve. The flowrate was representative of values observed during the active missions for similar conditions.

5) The pump inlet pressure was approximately 18.7 psia with the pump operating as compared to approximately 19 psia at the end of the Skylab Missions. The coolant reservoir fluid low level indication was on, as it had been at the end of the Skylab Missions.

It was thus established that both coolant loops were operational and that key components within the loops still functioned properly. Except for some additional coolanol 15 loss due to leakage, the status of the loops appeared not to have degraded since the end of the Skylab missions. The major uncertainty relative to the continued capability to support planned operations was associated with coolant leakage. The coolant leakage rate over the four year period between final Skylab deactivation on February 9, 1974, and reactivation on April 24, 1978, was significantly lower than observed during the Skylab Missions. The average leakage rate for the primary loop prior to reservicing during the active mission was approximately .09 pounds/day and the average leakage rate after reservicing was approximately .012 pounds/day. Over the four year storage period the leakage rate was approximately .0017 pounds/day.

Since the coolant loop was operated during the Skylab Missions (with resulting higher overall system pressure levels) and was off during the long storage period, a strong possibility existed that loop operation was a major factor in the difference in leakage rates. While average system temperatures could also have contributed to the difference, the vehicle attitudes to be employed after reactivation would reasonably approximate the Active Mission environment and if storage attitudes had been favorable, this factor would not be present. If the primary loop leakage rate returned to the rate observed prior to reservicing, more than 25 days of continuous operation would completely deplete the fluid in the reservoirs. Therefore, a decision was made to turn one of the coolant loops on only when required to maintain battery and electronics equipment below allowable temperature limits. In order to minimize the required loop operational time use of elements of the Airlock Module Power Conditioning Group (PGG's) was carefully controlled by monitoring equipment temperatures and bringing elements on and off-line to the maximum extent possible to allow cooling without use of the coolant loop.

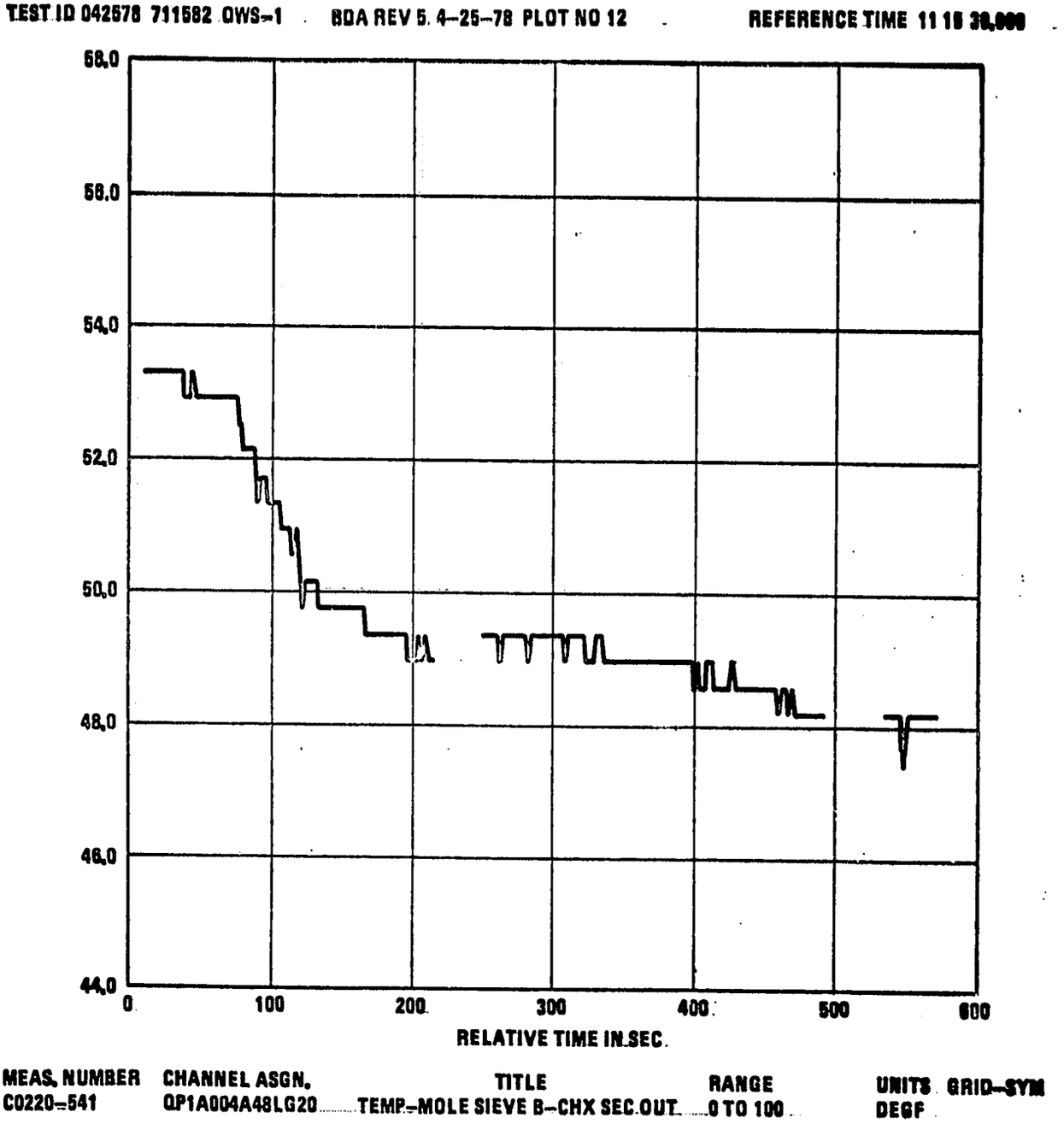

FIGURE 4-2. TEMPERATURE, °F, OUTLET OF 47°F CONTROL VALVE UPSTREAM OF CABIN HEAT EXCHANGERS

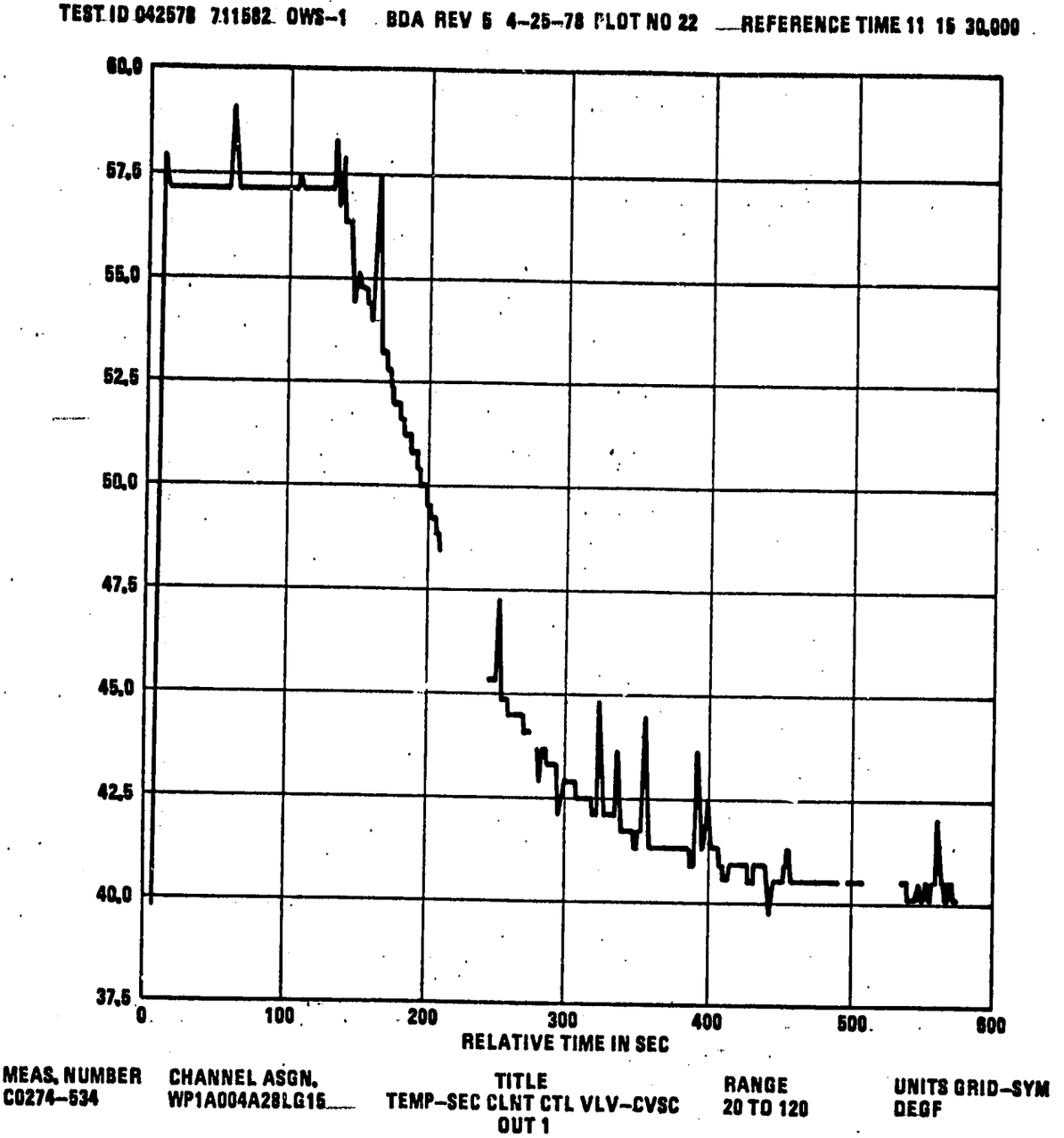

FIGURE 4-3. TEMPERATURE, °F, OUTLET OF 40°F CONTROL VALVE UPSTREAM OF BATTERY/ELECTRONICS MODULES

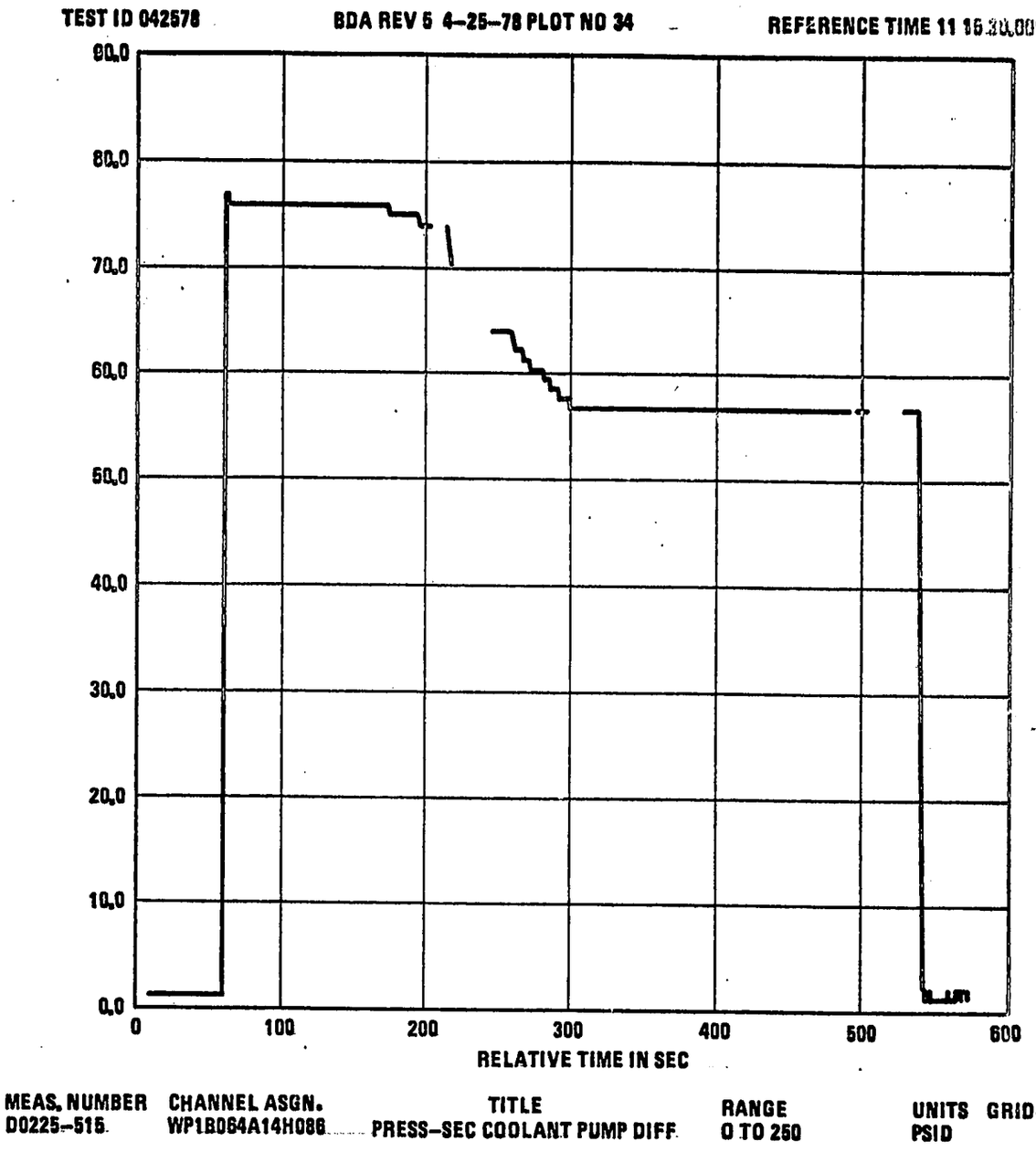

FIGURE 4-4. SECONDARY COOLANT LOOP DIFFERENTIAL PRESSURE DURING INITIAL ACTIVATION

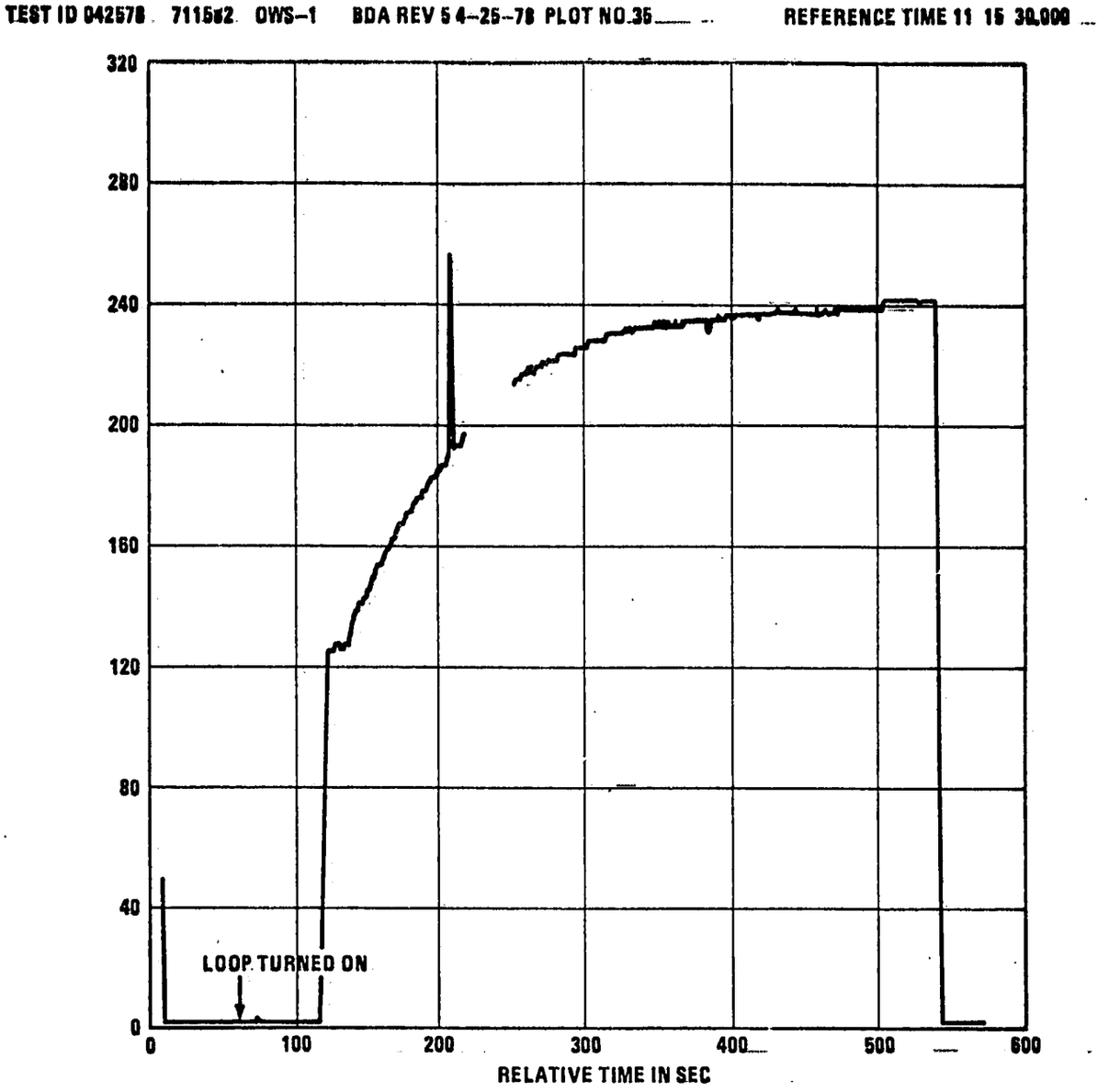

FIGURE 4-5 FLOWRATE (POUNDS PER HOUR) INTO WARM PORT OF 47°F CONTROL VALVE DURING INITIAL ACTIVATION OF THE SECONDARY LOOP

Even with restricted operation, it was quite likely that the reservoirs in the primary loop would be depleted long before the end of Skylab activities and the coolant loops would be required to operate at inlet pressures far below the design value. Data generated during the Skylab Missions indicated that the coolant pump would operate with inlet pressures as low as 1.0 psia. However, the pump was cavitating at pressures below 3 psia and no data was available to give an indication of expected life in this regime. Therefore, a series of ground tests were conducted at MSFC to provide additional performance data at low inlet pressures and to establish performance characteristics. A coolant pump was operated at an inlet pressure of .75 psia for total of 515 hours with the pump being turned on and off 351 times (once every 90 minutes). At this inlet pressure level, the flowrate was 224 pounds/hour. The pump was then operated at an inlet pressure level of .35 psia for a total of 100 hours with the pump being turned on and off 68 times. At .35 psia, the flowrate was 50 pounds/hour. It was also established that at .28 psia, no flow occurred and the pump was operated for 3 hours at this level. After these tests, the pump package was completely disassembled and inspected for signs of damage or unusual wear and none was detected. These tests indicated that the coolant pumps could be expected to provide sufficient flow for cooling the battery and electronics module as long as the pump inlet pressure remained above .35 psia.

The residual coolant fluid in the secondary loop reservoirs was depleted soon after reactivation. (The exact date is unknown due to system anomalies during May which made the secondary pump inlet pressure sensor data unavailable.) On July 22, 1979, during a routine operation of the primary loop, the pump inlet pressure decreased to 8.0 psia, indicating that leakage had depleted the fluid in the reservoirs. After depletion of fluid in the reservoirs (and resulting loss of positive pressure control), the pump inlet pressures varied, depending on average fluid loop temperatures. The minimum value observed in the primary loop was 1.9 psia. When operated at this pressure the flowrate was approximately 160 pounds/hour (nominal flowrate for either loop is approximately 260 pounds/hour). The nominal minimum indicated pressure for the secondary loop was .3 psia but values of 0.0 were occasionally seen during pump operation. At inlet pressures of 0.3 psia, the flowrate was observed to vary between 30 pounds/hour and 100 pounds/hour. Some uncertainty exists on the actual pressure levels present in the loop due to pressure gauge inaccuracies. The range of the gauge was 0-100 psia.

Although the flowrates sometimes were lower than design values, the coolant loops were always capable of providing the cooling required. This can be attributed largely to the very low total heat rejection requirements for reactivaion activities as

compared to the design capability of the system which included significant heat rejection requirements from equipment not functioning during the reactivation period. The secondary coolant loop was frequently operated in the cavitation regime, but no evidence of damage was detected. Both coolant loops were still operational at the end of Skylab's life. The secondary loop was on and data indicated that it was operating properly over the last ground station (ACN) during reentry.

4.3 GAS SUPPLY SYSTEM

4.3.1 System Functional Description

The Airlock Module gas supply system (Figure 4-6) provided oxygen and nitrogen to maintain the Skylab internal pressure at design levels, oxygen for use by the crew during EVA, and nitrogen for experiment use and for maintaining required pressures on selected systems. Gaseous oxygen was stored in six cylindrical metal lined fiberglass tanks located on the fixed Airlock Shroud. A total of 6113 pounds were initially loaded into the tanks. Gaseous nitrogen was stored in six spherical titanium tanks located on AM trusses. A total of 1620 pounds were initially loaded into the tanks.

The pressure within the oxygen and nitrogen tanks was initially approximately 3000 psia. The oxygen passed through a 120 psig regulator assembly to solenoid valves which were used to supply oxygen for internal pressurization to quick disconnects for EVA use and to a 5 psia cabin pressure regulator for automatic control of internal pressure. The nitrogen passed through a 150 psig regulator assembly to solenoid valves which were used for internal pressurization to the cabin pressure regulator, to the Molecular Sieve pneumatics, to a 35 psig regulator for pressure control of the OWS water tanks and to a 5 psia regulator which maintained pressure on the EVA and ATM C&D/EREP cooling system reservoirs. A supply line was also provided directly from the nitrogen storage tanks for experiment use. Both the nitrogen and oxygen systems also contained latching solenoid valves downstream of the storage tanks. All six oxygen storage tanks were connected into a common tubing and gas from all tanks was utilized for all system functions. Four of the nitrogen tanks were connected by common tubing which supplied all system functions. The two remaining tanks were normally reserved for experiment use but could be connected to the main supply system by opening a valve. This function could only be performed by the crew.

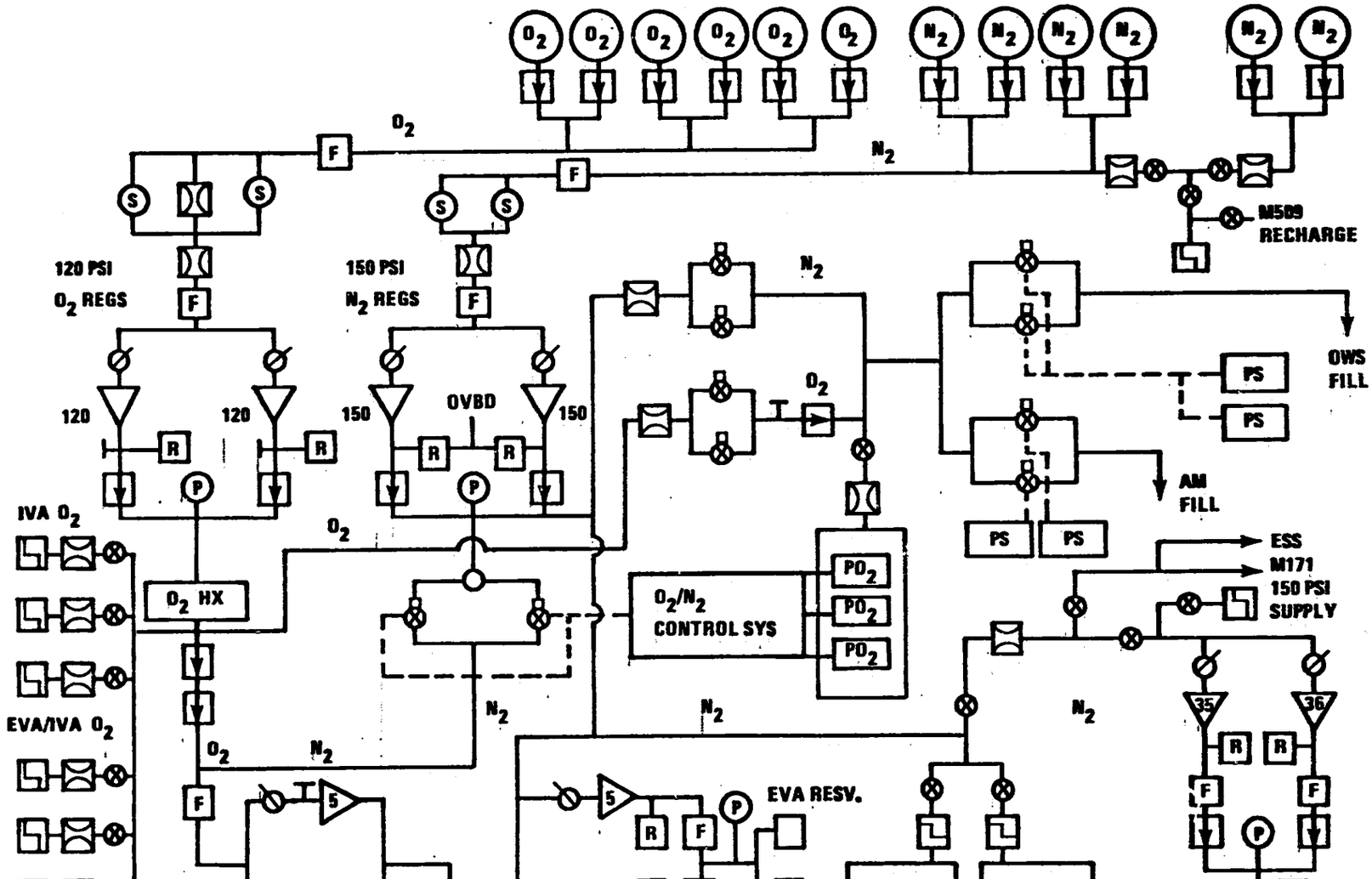

FIGURE 4–6 GAS SUPPLY SYSTEM

4.3.2 Status After Skylab Missions

The gas supply system performed as expected during the Skylab Missions and no major anomalies were observed. Since sufficient nitrogen was available without the two nitrogen tanks reserved for experiment use, they were never connected to the main supply system. Therefore, the residual nitrogen in these tanks was not available for Skylab pressurization during the reactivation period. At the end of the Skylab Missions, approximately 2442 pounds of nitrogen remained in the four tanks connected to the nitrogen supply system. Another 331 pounds remained in the two isolated nitrogen tanks.

4.3.3 Reactivation to Splashdown Period

Data obtained during the initial communication with Skylab in March 1979, indicated that relatively little oxygen or nitrogen had been lost from the tanks. A status is provided in Table 4-1. These data, when compared with data from February 9, 1974, indicate that less than 60 pounds of oxygen and less than 85 pounds of nitrogen had leaked from the system.

On May 16 and 17 the Skylab pressurization system was activated and the habitable volume was pressurized with nitrogen to approximately 0.6 psia. The nitrogen 150 psig regulator provided outlet pressures within its design specifications. Fill and supply solenoid valves also operated correctly.

The pressure was monitored over a three week period following the initial pressurization to establish overall Skylab leakage rates. Data from internal pressure gauges located in the MDA, Airlock and Orbital Workshop were used. The range of calculated leakage rates varied between 1.03 pounds/day and 1.47 pounds/day at an average indicated internal pressures which ranged between 0.43 and 0.55 psia. When extrapolated to the nominal operating pressure of 5 psia, the overall leakage was approximately equal to the specification value of 14 pounds/day. Similar evaluations during the storage periods between manned Skylab Missions had established leakage rates of approximately 2.7 pounds/day at 5 psia. Thus, overall leakage had increased by a factor of approximately five, but was still quite low. This indicated that the various seals employed in the Skylab design had not seriously degraded and that no meteroroids had penetrated the habitable volume structure.

Since the quantity of nitrogen available in the four tanks connected to the pressurization system would have been inadequate to maintain the desired internal pressure over the

expected length of the reactivation period, a decision was made to use the oxygen system along with nitrogen and to maintain the O2/N2 mixture within the habitable volume near the design value of approximately 70 percent oxygen and 30 percent nitrogen. On July 20, 1978, use of oxygen was initiated. The 120 psig regulator provided outlet pressures within its design specifications and O fill and supply valves also functioned properly. Data obtained from the two active oxygen partial pressure sensors in the Airlock Module indicated that the sensors (and associated electronics) were still functioning. The oxygen partial pressure indicated by the sensors was quite close to the expected value. This was unexpected since the sensors were limited life items. Spares had been provided on-board for possible replacement during the active Missions. Use of the pressurization system on a periodic basis continued throughout the reactivation period. No anomalies were detected.

TANK NO.	P_{O_2} (PSI)	T_{O_2} (^{0}F)	m_{O_2} (lb)
1	1240	45^0	417.4
2	1285	45^0	432.5
3	1280	43^0–49^0	430.0
4	1280	57^0	420.8
5	1040	51^0	345.9
6	1040	57^0–65^0	339.3
		TOTAL	2385.9

TANK NO.	P_{N_2} (PSI)	T_{N_2} (^{0}F)	m_{N_2} (lb)
1	1710	60^0	165.3
2	1700	56^0	165.9
3	620	60^0	60.1
4	738	59^0	70.8
5	665	53^0	65.3
6	720	56^0	70.3
		TOTAL	598.9

TABLE 4–1 STATUS OF O_2/N_2 TANKS IN MARCH 1978

4.4 SKYLAB THERMAL ENVIRONMENT

4.4.1 Skylab Thermal Control Status After Skylab Missions

Thermal control for the ATM, AM, MDA and OWS was achieved with a wide variety of passive control techniques, heaters and coolant loops. The design techniques and performance summaries for the active missions are contained in References 7, 8, and 9. Except for the anomalies associated with the Airlock Coolant Loop discussed in section 4.2, there were no identified concerns based on performance observed during the active missions which might have impacted the success of the Skylab reactivation. One area of interest, however, was the status of the sun shields which had been installed on the side of the OWS meteroid shield during launch. Data obtained during reactivation indicated that the shields were still intact and effective (see section 4.4.3).

4.4.2 Environment During Storage

Thermal analyses were conducted in 1974 (Reference 10) to establish the expected range of Skylab temperatures for the gravity gradient attitude which the vehicle was expected to maintain. While this attitude was not maintained over the four year storage period, the predictions did represent the temperature extremes which might have occurred. Some representative extremes are provided in Figure 4-7. A review of available data prior to the reactivation period indicated that most Skylab equipment would probably not have experienced temperatures which would have resulted in damage. One area of concern, however, was the ATM batteries. Minimum predicted temperatures for these batteries for the worst possible attitude indicated potential temperatures of -130°F which is near the freezing point of the electrolyte. Had the electrolyte frozen, it was expected that the batteries would not recharge. However, the batteries were successfully recharged during the reactivation period, indicating that freezing did not occur.

Another concern was that the predicted minimum temperatures in the MDA/AM area could have frozen the water in the EVA or ATM/C&D coolant loops which interfaced via heat exchangers with the Airlock Module coolant loops with resulting potential rupture of heat exchangers and leakage of coolant. Performance of the Airlock Module coolant loops after reactivation indicated that this did not occur.

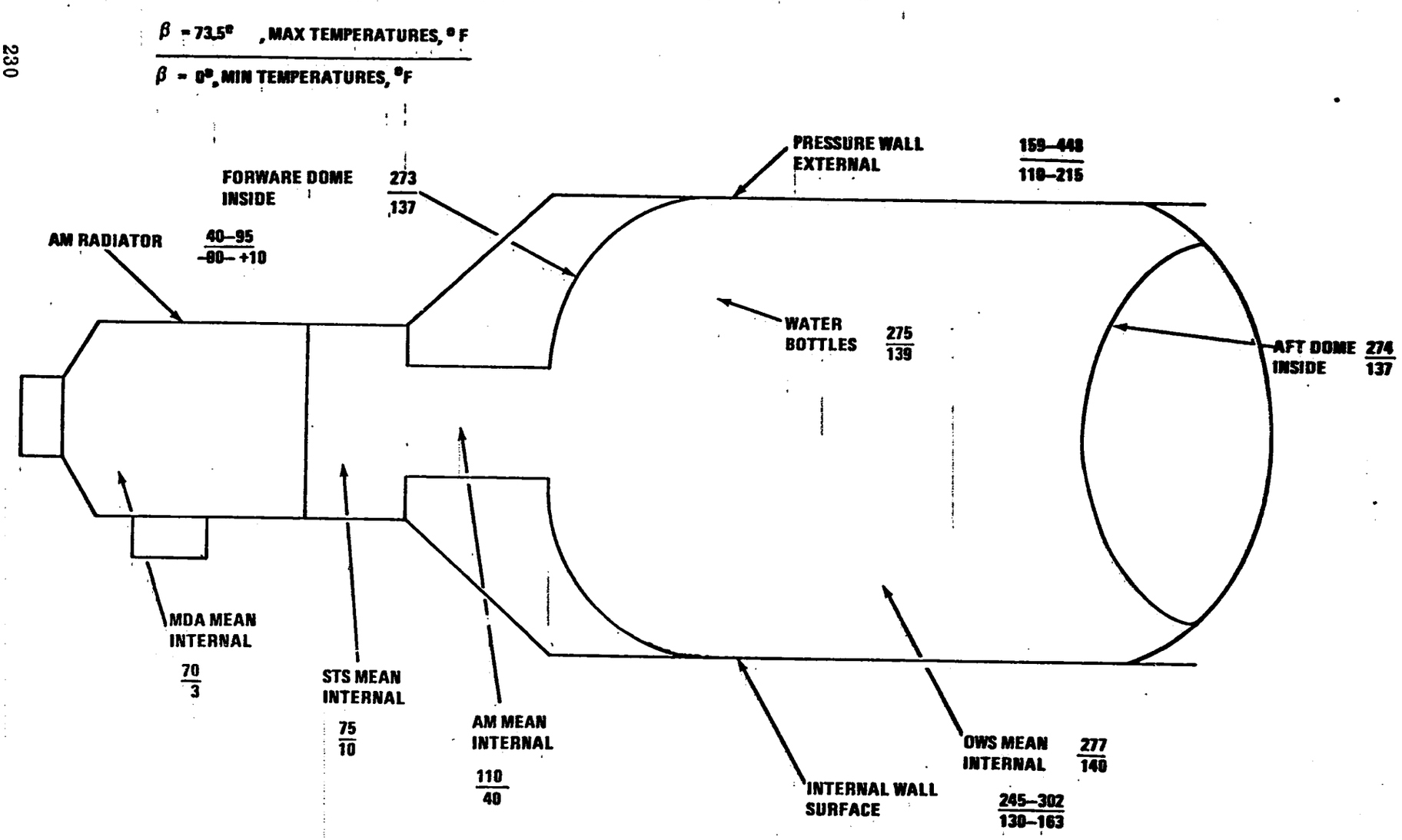

FIGURE 4–7 POTENTIAL TEMPERATURE RANGES DURING STORAGE FOR GRAVITY GRADIENT ATTITUDE

4.4.3 Reactivation to Splashdown

Data obtained during the initial activation phase prior to achieving attitude control indicated relatively moderate temperatures throughout Skylab. A brief summary of representative temperatures is provided below.

MDA

Internal Temperatures 50 to 55 F

External Temperatures
- Under radiator 50 to 55 F
- Black Surface 100 to 110 F

AM

Internal Temperatures 50 to 60 F.

ATM

Overall Temperature Range 5 to 40 F.

Fixed Airlock Shroud

Overall Temperature Range 55 to 75 F

OWS

Internal Average Temperature ≥ 120 F.

External Cylindrical Wall Temperatures 100 to 190 F.

Radiator Temperature - 90 to -100 F.

After attitude control was achieved, the vehicle was placed first in the solar inertial (SI) attitude (which had been the predominant attitude during the active missions) and later into the End on Velocity Vector (EOVV) attitude. When these attitudes were obtained, which resulted in returning the OWS sun shields to their correct orientation, the OWS internal temperatures began to decrease. At the time of vehicle reorientation, the OWS average internal temperature was greater than 120 F (sensor limit). Over the next few days, the cool down of the OWS interior was consistent with the cool down seen after the initial shield (parasol) was deployed at the beginning of the first manned mission (Figure 4-8). These data indicated that the sun shields were still intact and effective in limiting the OWS internal temperatures. OWS internal temperatures

remained at expected levels throughout the reactivation period when the sun shields were correctly orientated.

Representative external structural temperature measurements on the OWS, FAS, MDA and OWS radiator were monitored during the final Skylab orbits and during the initial reentry phase to provide data on aerodynamic heating of the vehicle. Data from five hours through the last available data at ACN are shown in Table 4-2. No discernable increases in temperature were observed prior to the reentry orbit. Temperatures were observed to increase significantly on some surfaces over the 15 minutes between BDA and ACN. The maximum temperature seen at 57 nautical miles over the final ground station was 275 F at one point on the Fixed Airlock Shroud. As can be seen from the data, however, most temperatures were still quite low.

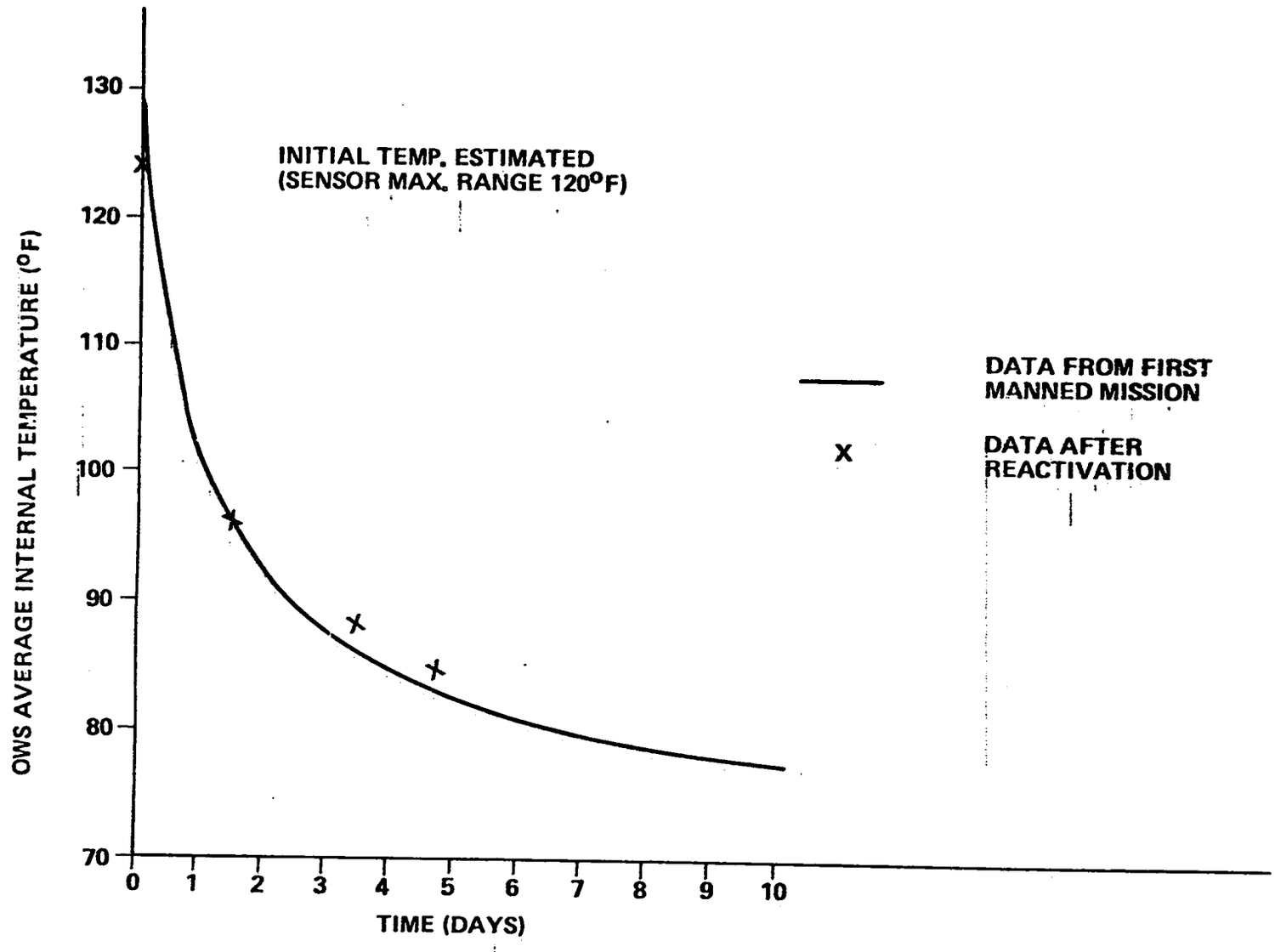

FIGURE 4–8 COMPARISON OF OWS AVERAGE INTERNAL TEMPERATURE DECREASE AFTER DEPLOYING PARASOL ON FIRST MANNED MISSION WITH DECREASE AFTER ATTAINING ATTITUDE CONTROL DURING REACTIVATION

TABLE 4–2. SKYLAB EXTERNAL TEMPERATURES DURING INITIAL REENTRY PHASE

TIME, GMT, JULY 11	ALTITUDE NAUTICAL MI.	TEMP (°F) (1) FIXED AIRLOCK SHROUD θ = 10	θ = 100	θ = 190	θ = 280	TEMP. (°F) OWS EXTERNAL θ = 90	θ = 180	TEMP (°F) OWS RADIATOR	TEMP. (°F) MDA, EXTERNAL FWD DOME
11:22	76	(2)	40	(2)	85	148	80	22	75
12:52		65	60	100	105	157	87	18	75
14:03		62	50	80	100	152	83	15	115
15:47	63	200	50	165	185	165	112	FULL SCALE (100)	110
16:02	57	(2)	70	240	275	169	130	" " "	135

(1) θ = DEGREES FROM +Z AXIS

(2) NO DATA

5.0 ELECTRICAL POWER SYSTEM

5.1 INTRODUCTION

The Skylab power system consisted of two power sources, the ATM Charger Battery Regulator Modules (CBRM's), and the AM Power Conditioning Groups (PCG's) and a distribution system. Figure 5-1 depicts the relationship of the key elements in the system. Reference 11 gives a complete description of the system. The fact that it was able to survive four years of orbital storage and still maintain most of its operational capability was truly remarkable. In the sections that follow the Skylab power system will be taken through its orbital storage period, system activation, system operation, equipment failures and finally through a section dealing with lessons learned.

5.2 Orbital Storage

The most important element of the orbital storage environment affecting the power system was the temperature extremes experienced by the batteries, solar arrays and electronics. Thermal analysis of the gravity gradient attitude, which the vehicle was left in at the end of the manned mission, indicated the concern would be the cold temperatures. The ATM batteries could be expected to go to -90 C and the AM batteries to -43 C. The power electronics, chargers and regulators, were in close proximity to the batteries and experienced the same temperatures. The analysis did not specify temperature extremes for the Solar Arrays. Data from the gravity gradient attitude at the end of the manned mission indicated the Solar Arrays would range down to and below -60 C. At the beginning of the manned mission, when off-nominal attitudes were used to limit internal Skylab temperatures, Solar Array temperatures went below -85 C. These two data points represent the type of environment probably seen by the Solar Arrays for most of the storage period and indicate their probable range of cold temperatures.

The ATM batteries each had a small parasitic load which completely discharged them within a few months after the start of the orbital storage period in February of 1974. Four of the AM batteries were left powering their respective Amp Hour Integrators and completely discharged in a matter of weeks. The other four AM batteries were at 70 to 85% state-of-charge (SOC) and left open circuited. These batteries still showed over 30 VDC when first checked again from Bermuda in March 1978 after four years of storage.

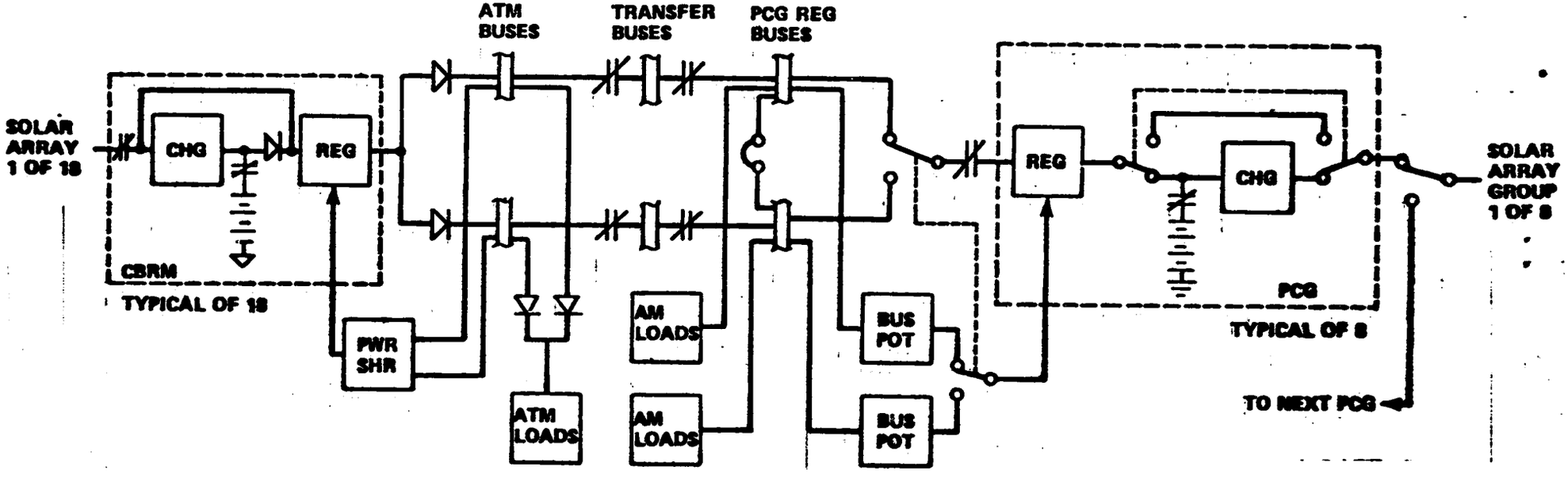

FIGURE 5-1
SKYLAB POWER SYSTEMS

The generally colder environment presented two specific concerns for the power system: degradation of the solder interconnects on the Solar Arrays and electrolyte freezing in the batteries. Pre-mission testing of the Solar Array designs had indicated a significant increase in the degradation of the Solar Cell interconnects when temperatures were cycled this low. There was a concern that the interconnect system had deteriorated sufficiently to drastically reduce the available Solar Array power. The ATM batteries were expected to go well below the freezing point of their electrolyte and the resultant effect on the cells was difficult to predict. Although the power electronics were not qualified to these colder temperatures there was not a specific mechanism that made them more susceptible than any typical piece of electronic hardware. Subsequent experience did not indicate any appreciable system degradation from any of these effects. Measurement of the actual environment was not possible because when the vehicle was first reactivated in March of 1978 it was no longer in a stable attitude. Instead, it was tumbling, which resulted in a much more favorable temperature environment for the vehicle.

5.3 Power System Reactivation

5.3.1 AM Battery Reactivation

The recommended procedure for returning a Ni-Cad battery to full capability after an extended storage period involves several complete charge/discharge cycles at a very low rate. The purpose of this is to aid in the even redistribution of electrolyte on the active surfaces so that hot spots will not result when the battery is used at normal charge/discharge rates. Such full cycles were not possible with the electronics associated with the AM batteries but it was possible to accomplish a low rate shallow cycling that would leave the battery at a low SOC. This was attempted on two of the AM batteries in early March 1978 at Bermuda when it was determined that the intermittent Solar Array power available on the tumbling vehicle would not allow any useful activity unless supplemented by battery power. Batteries 3 and 7 were configured for this shallow cycling for two days and then put on full charge. Because of problems in the telemetry down link at that time no battery data was available to verify the configuration. It was only after the down link was reestablished that it was determined that the Power Conditioning Group (PCG) charger on battery 3 had not responded to the commanded configuration. Battery 7, however, was fully charged and demonstrated an ability to support high discharge loads.

Preparation for the increased vehicle activity anticipated when a better support system was ready at JSC involved putting three more batteries, 2, 4, and 5, into the shallow cycling configuration. These batteries were left in that mode until the vehicle reactivation was continued from JSC in late April 1978. At the beginning of the reactivation activity at JSC it was found that PCG 2's charger had apparently experienced problems similar to those of PCG 3 as battery 2 was no longer shallow cycling. The problem in PCG chargers 2 and 3 was later identified and appeared to result from a spurious command that had disabled the chargers. When the chargers were enabled again it was possible to charge their batteries. It was decided to charge all the AM batteries to provide maximum operational flexibility in supporting the planned vehicle reactivation. However, the preliminary shallow cycling was not implemented because at that time the problems with chargers 2 and 3 had not been identified and they had experienced failures while in the shallow cycle configuration. Table 5-1 summarizes the preparation done on each battery before bringing it up at full charge rates. Subsequent mission performance did not show any noticeable differences in characteristics among the batteries, regardless of how they had been reactivated.

TABLE 5-1

BAT	PREPARATION
4 & 5	Shallow Cycle for about 6 weeks
7	Shallow Cycle for two days
3	May have shallow cycled for up to two days, then 6 weeks open CKT stand
2	Shallow cycle at least one day, possibly up to 6 weeks
1, 6 & 8	No preparation

5.3.2 ATM Battery Reactivation

Reactivation of the ATM batteries was originally thought to be impossible since the CBRM electronics had an automatic battery cut-off feature that would disconnect the battery if its voltage was below 26.4 VDC. As the CBRM batteries had been completely discharged by parasitic loads, this automatic disconnect would prevent charging of the batteries. However, testing performed on the ground showed that a small burst of charge would get into the battery every time a "CHARGER ON" command was issued. If this command was given repeatedly the battery voltage would slowly build up until it was high enough such that the battery would stay on. The battery would then be charged at the full rate as the CBRM chargers did not have a selectable charge rate.

This procedure was initiated on the vehicle in late April 1978. "CHARGER ON" commands were issued to a particular CBRM as rapidly as the vehicle command system could process them; about 4 to 5 times per second. It became evident that this procedure was less effective if the battery was warm, above 10 C. Fortunately, the combination of vehicle attitude and changes in the orbit beta angle (sun angle) reduced the thermal environment of the warmer batteries and allowed them to be activated. Typically, over a thousand commands were required to bring up one battery. By the end of May 1978, all but 4 of the 18 CBRM batteries had been reactivated.

The four batteries in CBRM's 3, 4, 15 and 16 were never reactivated. CBRM 3 had lost its regulator during the manned missions and its regulator was still failed. The charger in CBRM 4 would not respond to the "CHARGER ON" commands so its battery could not be brought up. CBRM 15 initially appeared to be fully operational but its Solar Array contactor stuck open again, as it had in the manned mission, and it could not be used after that. Charger 16 initially responded very poorly to the commanding but modifications to the commanding sequence did eventually bring the battery voltage up above 26.4 volts. However, as the full charge rate then brought the battery voltage up, the battery again tripped off. Apparently the battery voltage high trip circuit had failed such that it would trip the battery off at normal charging voltages. In these 4 CBRMs only the regulators in 4 and 16 could be used. These regulators could be turned on to help supply some of the load in power critical situations.

The battery in CBRM 6 did not require this procedure as this CBRM apparently had turned on sometime during the storage period due to a failure in its "SYSTEM ON" command circuitry. This prevented any of the normal CBRM cut-off functions from operating. The battery had cycled at a normal rate but at a very low SOC as this single CBRM could not support the parasitic loads on the ATM buses. When other CBRMS were brought on to share the load, this battery then charged up and began to operate normally except for evidence of one or two shorted cells.

5.4 Power System Operation

5.4.1 System Characteristics

The Skylab power system's two power sources, the ATM CBRM's and the AM PCG's, and a distribution system are shown in Figure 5-1. The power distribution system allowed the two sources to be tied together and thus any vehicle load could receive power from either source. Management of this system was directed at effecting the proportion of the total load that was supplied by each source.

Determination of the desirable load distribution was influenced not only by the maximum energy available from each source but by the operational constraints associated with each source. The PCG's were very flexible: the PCG Regulators could be switched between two busses, each Solar Array Group (SAG) could be switched between two PCG's and PCG Regulators could be left on line without the battery connected and would deliver power when the SAG's were illuminated. The major constraint was that the PCG's were designed to operate with a coolant loop for heat rejection. The chargers and regulators functioned fairly well on passive cooling because they would operate properly even though they were well above 100 °F. The batteries, however, could not take these temperatures very long without significant capacity degradation. Therefore, utilizing more of the energy available from the PCG's required activating the coolant loop more frequently. As there was concern for the lifetime of the coolant loops it was desirable to minimize their usage.

The CBRM's were passively cooled and more of the maximum energy available could be used with minimal temperature concerns. The capability to tailor a particular CBRM to any situation was limited to turning its regulator on or off.

The CBRM contained several automatic cutoff functions designed to protect the electronics and battery which could turn off parts or all of the CBRM under certain conditions. It was one of these cutoff functions that hampered utilization of the regulator unless the battery was on. The regulator could be turned on and operated whenever its Solar Array was illuminated, but when the Solar intensity on the arrays went to zero, because of vehicle attitude or earth shadowing, the regulator would trip off unless the battery was on also. This meant that a CBRM regulator, without its battery, would supply power only during the sunlight period when it was turned on. Then it would have to be turned on again during the next sunlight if it was needed again. Another automatic function that effected power management criteria was the battery voltage low cutoff. As was

mentioned earlier, this function was why thousands of commands were required to activate the batteries. The main problem, operationally, was that if a battery did trip off, it would not come back on automatically whenever there was power to charge it back up. This, combined with the other automatic functions, had the effect that whenever a battery would trip off, the entire CBRM would be disabled until corrected by ground commands. This behavior made the CBRM system less tolerant to errors in estimates of its capability. If one CBRM tripped off this significantly increased the load on those remaining as the system had now lost the entire output from that particular Solar Array. The increased load could then push another CBRM to cutoff and so on until all CBRM's were tripped off. The ability to detect and interrupt this process was primarily dependent on the ground station coverage. In contrast, if a PCG were loaded beyond its capability the battery would be discharged down to about 30 volts but below that the regulator could not draw power from the battery. As nothing was disconnected or "cutoff" the PCG would again supply power and charge its battery whenever solar power returned Although a PCG in this situation could not provide a continuous source of power, the entire output from its Solar Array was still utilized. This response mechanism did allow more battery stress as the low voltage discharge could cause cell voltage reversal but it also minimized the propagation of an overload on one PCG to other PCG's.

These different characteristics of each system dictated the fundamental premise of the system management guidelines. The CBRM's should supply only slightly less than their maximum capability to minimize the thermal problems on the PCG's but still allow for contingencies in the CBRM system. This allowance for contingencies was primarly a function of available ground station coverage. If contact with the vehicle was possible at least once an orbit, the CBRM's could be loaded very close to their maximum capability. When the gap in coverage was 3 hours or more the CBRM load was reduced to allow for at least one or sometimes more CBRM or PCG failures.

5.4.2 System Management Options

The methods available for implementing a desired load distribution involved changing the characteristics of either source or the impedance tying the two sources together. During the manned missions the load distribution was adjusted by changing the output voltage of the PCG regulators with on-board manual potentiometers (Figure 5-1). There was one of these on each of the two main PCG busses. Their setting determined the output voltage of any PCG regulator that was connected to that bus. Adjustment of the potentiometers was not possible during

this mission. However, the difference in the settings they were left at made it possible to change the output voltage of the PCG regulators by switching them from one bus to the other.

The output characteristics of the CBRM's could be changed only with the "POWER SHARING" circuit. This was a circuit that was designed to affect power sharing between the CBRM's by having them match their output currents. Another effect of this circuit was to reduce the impedance of the CBRM outputs to about 40% of its value when the circuit was turned off. As the CBRM's would share power reasonably well, even with the circuit turned off, it was used as a power management tool.

The CBRM's and PCG's could be tied together through two power transfer busses. The impedance of this tie depended on whether one or both transfer busses were used. The impact of opening one of the transfer busses depended on how much power was being transferred at that time.

Another tool used for system management involved a reduction in, rather than a redistribution, of the total system load. In most areas of the system only those loads that were required or could not be removed were on. However, the ATM TM subsystem was normally left on continuously even though it was only required while the vehicle was over a ground station, typically 5 to 15 minutes per 90 minutes orbit. There were two reasons it was usually left on: a concern for the lifetime of critical TM subsystems if they were frequently cycled on and off; also, there was sometimes an adverse effect on the ATM digital computer when a backup reference signal, provided by the TM system, was cycled on and off. Thus, the ATM TM system was not cycled on and off over ground stations unless other power management techniques could not maintain the system balance. The AM TM subsystem was normally cycled because it could not be left on unless a coolant loop was left on also.

5.4.3 System Modes of Operation

The primary factor affecting the maximum available power was the vehicle attitude. From the power system viewpoint, the vehicle attitude presented four different profiles: tumbling, Solar Inertial (SI), End on Velocity Vector (EOVV) and Torque Equilibrium Attitude (TEA). Figure 5-2 depicts the Solar Array power profiles that were typical for each attitude.

The solar power was minimal whenever the vehicle was tumbling but this was balanced by the fact that the vehicle guidance system did not have to be powered up which reduced the vehicle loads substantially. The typical power system configuration in

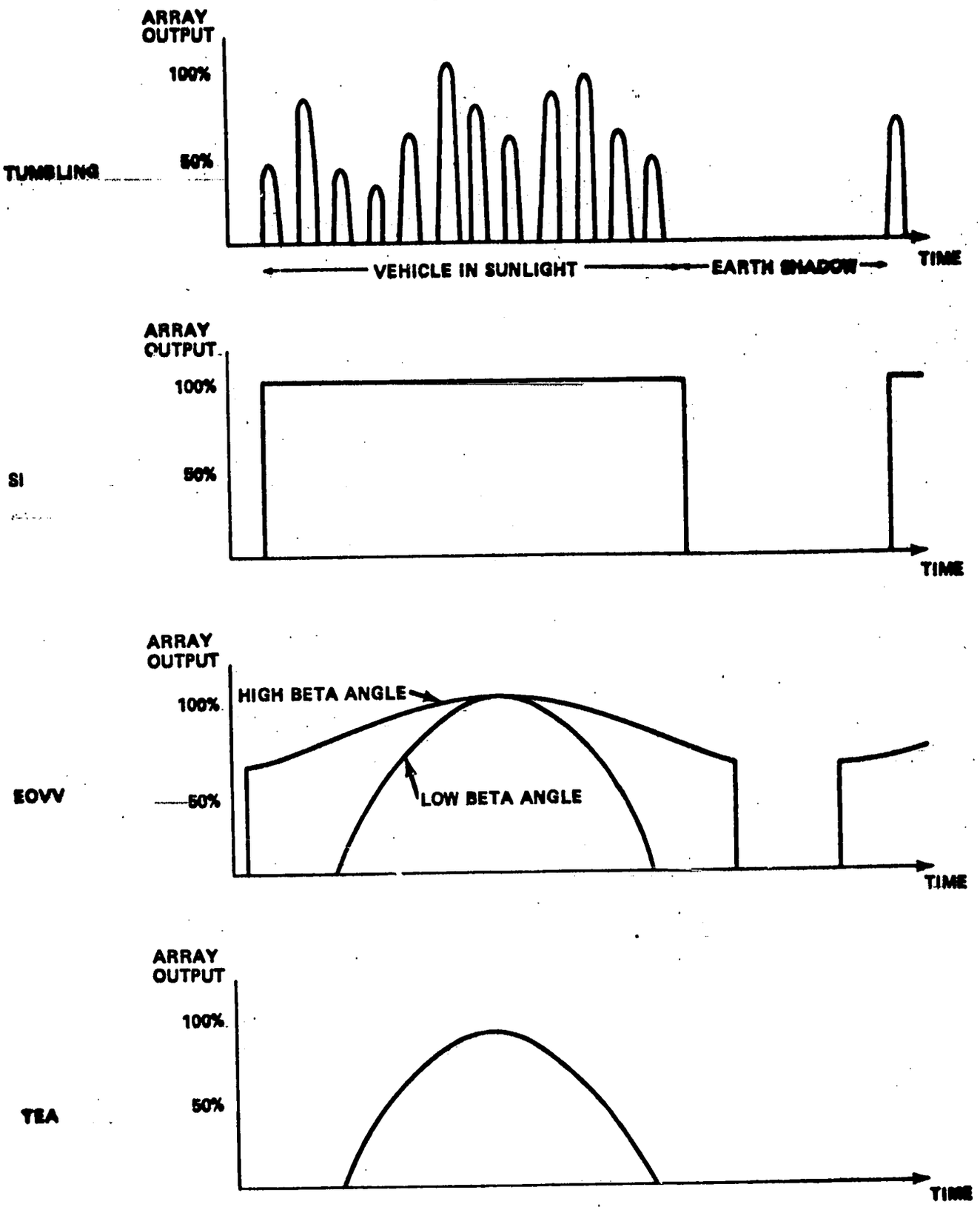

FIGURE 5-2
SOLAR ARRAY POWER PROFILES

this mode was the "CBRM POWER SHARE" circuit on, both transfer ties closed and several of the PCG batteries on line with their regulators tied to the higher voltage bus. SAGs normally associated with a battery that was not currently in use were either connected to another PCG to help recharge its battery or were connected to the bus through their regulator so they would deliver power whenever illuminated. This latter SAG configuration, by itself, did not require coolant loop usage but it did not make the most effective use of the SAG power. The regulator would use only 15 to 20% of the peak SAG power and the rest went unused because there was not a battery configured to store the available excess power. Although several PCG batteries were usually in use, the load on each was low enough that activation of the coolant loop was required for about only one orbit per day. Tumbling was encountered during the early reactivation period before the first stabilization of the vehicle. Later, because of a power drop out resulting from some errors in power system management concurrent with sparse ground station coverage, a similar tumbling occurred for about 10 days before the vehicle was stabilized again.

Solar inertial was the nominal attitude during the manned mission and was used during this later activity as a backup attitude whenever there were problems with the EOVV configuration. Because of the abundant Solar Array power in this attitude none of th PCG batteries were usually needed. The PCG regulators were all connected to the higher voltage bus, both bus ties were closed and the CBRM power share circuit was off. This maximized the power supplied by the PCG's during solar array illumination which meant that most of the ATM solar array power could be used to recharge the ATM batteries. During the dark portion of the orbit the ATM batteries carried the entire load. The only time that PCG batteries were used in SI was later on in the mission when the reduced number of CBRM's left operating caused concern as to whether the lower capacity batteries could carry their share of the load for even one discharge cycle. Only one or two PCG batteries were usually used in these circumstances and this allowed the other batteries to cool down passively before they were needed again. When a PCG had its battery turned on, its regulator would be switched to the bus with the lower voltage setting. The difference in the voltage settings between the busses was enough that, when in sunlight, the regulators on the high bus would pick up almost all the load. In the dark the regulators on the low bus would relieve the CBRM's of some of the load.

The power system configuration used for EOVV went through several iterations when that attitude was initially encountered but then settled into a well defined pattern with the basic arrangement similar to that used in SI. The CBRM power share circuit was off, both transfer ties closed and all PCG regulators were on the high voltage bus unless their battery was on. The number of batteries that were on the low voltage bus depended on the beta angle: between $\pm 20°$ beta there were two AM batteries on, if the magnitude of beta was between $20°$ and $40°$ only one was needed, and for a beta outside $\pm 40°$ no AM batteries were on. This system was very effective and it was found that usage of the AM batteries could be scheduled such that use of the coolant loop was very infrequent. The only additional management was when the beta angle was near zero: then it was decided to cycle the ATM TM off during long gaps in the ground station coverage to provide more safety margin.

The most intensive power management was required in the latter part of the mission when it became necessary for the vehicle to be placed in the TEA attitude. The character of the solar power profile changed as different phases of this attitude control were implemented but it was always somewhat below that of an EOVV profile at beta zero. Use of a key management tool, ATM TM cycling, was hampered by the requirement for certain amounts of recorded data to evaluate the attitude control system. This meant that although the TM transmitters could be cycled the rest of the TM subsystem had to frequently be left on for several consecutive orbits. The power configuration used for TEA involved sustained usage of all available AM batteries. This meant frequent use of the coolant loops. However, the duration of this mode was only a matter of weeks and as both coolant loops were still providing adequate performance at the beginning of TEA this was not considered a serious problem. It was decided to configure such that the PCG's would carry close to their maximum capability. This was desirable because with usage of the coolant loops the PCG system was more tolerant to an overload condition: weakness in a particular PCG did not readily propagate to other PCG's. The appropriate system balance was found with the CBRM power share circuit on, both bus ties closed and all PCG's on the high voltage bus. Extracting the maximum available power from the PCG's involved continuous manipulation of their individual configurations. This was required because although all were connected to the same bus potentiometer setting the power sharing between the individual regulators was not very precise. Thus, when one of the PCG's that was carrying more than its share lost too much on the battery SOC, it was necessary to either give it another SAG temporarily, by taking one away fom another PCG that could afford to lose it for a while, or to turn off its regulator to allow the battery to recharge. When this type of manipulation could not keep th PCG batteries charged the total load on the

PCG's would be reduced by temporarily opening one of the transfer ties and/or reducing ATM TM recorder usage as much as possible.

5.5 EQUIPMENT FAILURES

5.5.1 PCG's

The battery chargers were the only problem area for the PCG's. The difficulties with chargers 2 and 3 were apparently from extraneous commands and when normal charger operation was restored they did not show any other anomalies. PCG 1's charger failed in June of 1978. The failure mechanism was never identified nor did it ever clear itself. Shortly thereafter, in early July 1978, PCG 5's charger exhibited the same symptoms as PCG 1. With the occurrence of this second charger failure there was considerable concern that something inherent in our method of using the chargers was causing the failures. As a result the power system was reconfigured so as not to use any of te PCG chargers or batteries until their use could be evaluated further. The new configuration placed a little too much load on the CBRM's and before it was corrected the vehicle experienced a power drop-out and a resultant loss of attitude control. During the following activity to reestablish attitude control when PCG 5's charger was exercised it functioned normally. For the remainder of the mission all the PCG electronics, except charger 1, functioned normally. Further analysis of the chargers did not indicate any specific failure mechanisms nor any way to reduce the high temperature stresses on the chargers when their use was required.

5.5.2 CBRM's

The ATM power system experienced failures in the electronics and the solar arrays. Problems in the Solar Array area were evident when the vehicle was first reactivated from Bermuda. The configuration of the CBRM electronics is such that with any insulation breakdown to structure in the CBRM or upstream from it, the resultant current flow passes through the shunt that was used for measuring the CBRM output current. Examination of the initial data from Bermuda showed output current from three CBRMs- 2, 9 and 10 that were turned off. The profile of this current was in exact proportion to the illumination on the solar arrays which indicated that the faults were probably out on the arrays. The currents on 2 and 9 were small in magnitude and never prevented normal utilization of those CBRMs. The problem

was more pronounced on CBRM 10 but initially the box was usable. Later the fault progressed to where that CBRM could not provide any output.

Small currents were measured in CBRM 11's output also when the reactivation was picked up again from JSC in April 1978. In June 1978, the fault current increased to almost full solar array output and CBRM 11 was no longer usable. CBRM 18 began to experience solar array problems in late June 1978. By July it also was showing fault currents equal to the total solar array capability. However, in August the major problem cleared itself and although small fault currents later reappeared, they did not prevent utilization of the CBRM. In late July CBRM 12 suddenly began to show high fault current also. In this instance it persisted and CBRM 12 was not usable for the remainder of the mission.

There were a variety of electronics failures starting with the 4 CBRM's whose batteries were not reactivated. Those electronics problems were explained earlier. CBRM 6, which was found ON at initial reactivation, operated normally until early September 1978 when it appeared to suffer a short on its regulator output. Its problem could not be identified further or corrected. CBRM 5 still had the shorted charger that had failed during the manned missions and was being utilized similar to CBRM 4 and 16. Its battery could still be kept charged, using the shorted charger, and used in certain power critical situations. However, in early December 1978, its regulator began to show erratic operation and could not be utilized after that. The specific problem with the regulator was never identified.

The only Solar Array that had shown intermittent faults to structure during the manned missions was associated with CBRM 17. However, throughout the reactivation period it never gave any indications of recurrence. The first problem with this CBRM was in March 1979, when it appeared the battery discharge diode had opened. This diode also protected the charger power electronics from reverse biasing. After repeated checks to see if the problem was still there, the charger power electronics finally shorted. This provided a path from the battery to the regulator input so the battery could supply load during the night portion of the orbit. The CBRM's characteristics were now identical to those of CBRM 5 before its regulator failed: the battery could be charged through the shorted charger with charging terminated by the battery voltage high cutoff. When the charging was normally terminated by this cutoff, it made full use of the CBRM very cumbersome. However, when the TEA attitude was implemented the power balance was so critical that CBRM 17 rarely reached battery cut-off limits, either high or low. Thus, it made an equal contribution along with the working CBRMs. The most notable difference was a much higher battery

temperature, indicating that the battery was usually being overcharged.

5.6 LESSONS LEARNED

5.6.1 Automatic Cut-Offs in CBRMs

The experience gained in the manned portion of the mission had already shown that management of the CBRMs, with their many automatic cutoff functions, was more cumbersome than anticipated. The usual response to this problem is to regret not having put overrides in the system. However, this would have presented another design option: does one override disable all automatic functions in a box or is it necessary to provide individual overrides for each function. The latter solution can easily involve a large demand on a vehicle command system while it is not always useful to have to inhibit many protective functions when only one is the problem.

The problem can be better evaluated by categorizing the possible automatic functions by the nature of the stress they are designed to alleviate. Table 5-2 lists the anomaly categories applicable to the CBRM circumstances and the specific responses.

In the first category, stresses from internal failures, the high battery voltage circuit was a factor in problems with CBRMs 5, 16 and 17. In two of these cases, 5 and 17, an override capability would not have been used as severe battery damage would have resulted if the shorted charger were left to overcharge the battery. If the power balance allowed enough overcharge to trip off the battery, then the contribution of that CBRM was not essential and it could be left off. The cut-off protected the battery for later use when a critical power balance allowed that CBRM to stay on line without any override capability. CBRM 16's battery appeared to have been disabled by a failure in the cutoff circuit itself and in this instance an override would have been the only way to overcome the problem.

TABLE 5-2

CBRM Anomaly Categories

	Malfunction Type	CBRM Responses
1)	Stress on CBRM from internal source	High Battery Voltage or Discharge Current shuts off Battery
2)	Stress on system from CBRM	Internal Bias Supply out of tolerance, shuts off Regulator
		High Regulator Output Voltage, shuts off Regulator
3)	Stress on CBRM from System	Low Battery Voltage or High Battery Temperature shuts off Battery

The culprit in the second category was a transient out-of-tolerance condition in the CBRM Bias Supplies. This would occur whenever the CBRM experienced a sunrise or sunset on its solar array and the battery was not on. Thus, to use any of the CBRM regulators, without their batteries, they had to be turned back on during each sunlight portion of the orbit. An inhibit for this cutoff would have solved the problem. A better solution would have been for the detection circuit to have had sufficient delays built in to prevent it from reacting to transient startup conditions.

The most troublesome cutoff affecting system management was the low battery voltage detection circuit. Whenever this response was implemented it was because the system configuration had placed too much load on the CBRMs. Because of mismatch in regulator output or solar array input capability, a few CBRMs would reach this cutoff well before the others. When the first ones disconnected themselves this accelerated the decline of those still on line. An override capability could have prevented this domino effect but it would have allowed stress conditions on those batteries that had low voltage but were still supplying rated load. A better solution would have been a proportional response. When the battery voltage approached a critical level it would cause the regulator to reduce its output, thereby reducing the load on the battery and slowing or stopping the drop in battery voltage. In an overload situation all the batteries would still eventually reach cutoff levels but the system could endure that condition much longer before a complete power drop out occurred.

High battery temperature cutoffs were never a factor in system management but a similar proportional response feature would have been desirable here also. Comparison of the circuitry used to implement the cutoffs with what would have been required for typical proportional response applications indicates a very small increase in complexity compared to the benefits realized.

Experience with the CBRMs showed only one instance where an override capability would have been the best method for handling automatic response problems; the high battery voltage cutoff in CBRM 16. In the numerous other problem situations the best answer was either a better design to tolerate normal transients or a proportional response to preceed or replace the discrete cutoff. Although these conclusions come from experience with one system they are applicable in any circumstance where power is derived from multiple parallel sources. For example, the PCG's had, in effect, a proportional response to low battery voltage in that the regulators could not deliver power to the bus unless their source voltage was slightly higher than the bus voltage. Thus, a PCG regulator could not discharge its battery below about 30 VDC even though the battery was still connected

in the circuit. Although ideally the battery voltage should have been held at a slightly higher level this still provided some battery protection while the PCG was kept on line to store and deliver power whenever solar array power became available again. This feature of staying on line and delivering whatever was available minimized the domino effect inherent in using cutoffs to respond to system overloads.

5.6.2 NiCad Battery Stress Tolerance

Batteries in both systems were exposed to normal discharge rates while at a low SOC. The specific consequence that causes concern in this situation is voltage reversal of the weaker cells. Because there was no instrumentation on the individual cells in flight this reversal can only be assumed based on ground test results. What was revealing was the battery's tolerance of this as long as it was not a sustained or frequent occurrence. In the CBRM's the low voltage cutoff prevented this from happening to any except CBRM #6 which had a failed ON command circuit. As a result this battery experienced repeated low voltage, high rate discharges with the result being at least two cells failed short. Each of the PCG batteries were discharged at normal rates down to 30 VDC, about 1 VDC per cell, at least once. Only PCG 5 experienced this more frequently, apparently due to problems in its Amp Hour Integrators which sometimes prevented full recharge of the battery. This battery showed no detrimental effects until the latter part of the mission when it appeared that it too had at least one shorted cell. This experience should not be overlooked when evaluating battery protection schemes in future systems.

5.6.3 Solar Array Degradation

Considerable analysis and testing has been devoted to Solar Array degradation phenomena. The greatest concern in Solar Arrays is generally in the area of cell to cell interconnects and solder integrity, both of which suffer when subjected to long-term thermal cycling. The ATM Solar Array had test modules which had been subjected to approximately one year of ground thermal cycling (nonvacuum). When this experience was extrapolated to predict the solar array capability that would be available for the reactivation of Skylab, approximately 4 years after completion of the mission for which it was designed, even the most optimistic predictions were not encouraging. Effects on solar array materials under the unknown environment (particularly thermal) to which they had been subjected was at best a guess. When the vehicle was finally reactivated, it was

a pleasant surprise to learn that approximately 90% of the original array capability was still there. The lesson to be learned from apparent breakdowns of some of the insulation substrates is of dubious value since the substrate materials design life as well as their design thermal limits were greatly exceeded. The value is lessened further by the fact that a significant part of their lifetime was spent in an unknown environment.

The survival of the interconnect system does invite speculation as there is considerable ground test data verifying the detrimental effects of temperature cycling on soldered interconnects. The most plausible explanation seems to be that although the interconnects became very fragile the absence of gravity or a corrosive environment allowed them to still maintain electrical continuity. While it is difficult to quantify the benefits of a zero-G vacuum environment in this instance, the fact that the Solar Array performance greatly exceeded expectations should not be forgotten in future planning.

6.0 INSTRUMENTATION AND COMMUNICATION

6.1 INTRODUCTION

The Skylab Instrumentation and Communication (I&C) Systems provided for the transfer of information between the SWS and the Manned Spaceflight Network (MSFN) during the Skylab's manned and reactivation missions.

Information transferred during the manned mission phases included instrumentation system data, messages for the Digital Command System (DCS), voice communications, caution and warning alerts, range information between the CSM and SWS, and transmission of television data to the MSFN.

Reactivation operations utilized the instrumentation system for both real time and recorded data, and the DCS for SWS control. These systems operated with the same high level of effectiveness upon reactivation as at the close of the manned mission.

6.2 SYSTEM DEFINITION

An overview of the Skylab I&C systems is shown in Figure 6-1. The I&C systems interfaced with the CSM, the Saturn Instrument Unit, Skylab Experiments, the Spaceflight Tracking and Data Network (STDN), and other Skylab systems.

Two independent data acquisition and transmitting systems processed the engineering and experiment data for the AM/MDA/OWS and ATM modules. This data from 2060 separate measurements was transmitted in real time when over a STDN ground site. Equipment was provided to record data for playback when contact with a selected STDN station was reestablished. The RF systems incorporated redundant 10 watt transmitters on both the ATM and AM to assure availability of transmitters during the life of the program. A 2 watt transmitter incorporated in the AM data system, and redundant in frequency to one of the 10 watt units, was used during boost and selected flight periods.

Two seperate Digital Command Systems provided control of AM/MDA/OWS and ATM module functions from the ground. The ground commands controlled many functions, including updates to the ATM digital computer. See reference 12 for detailed systems description.

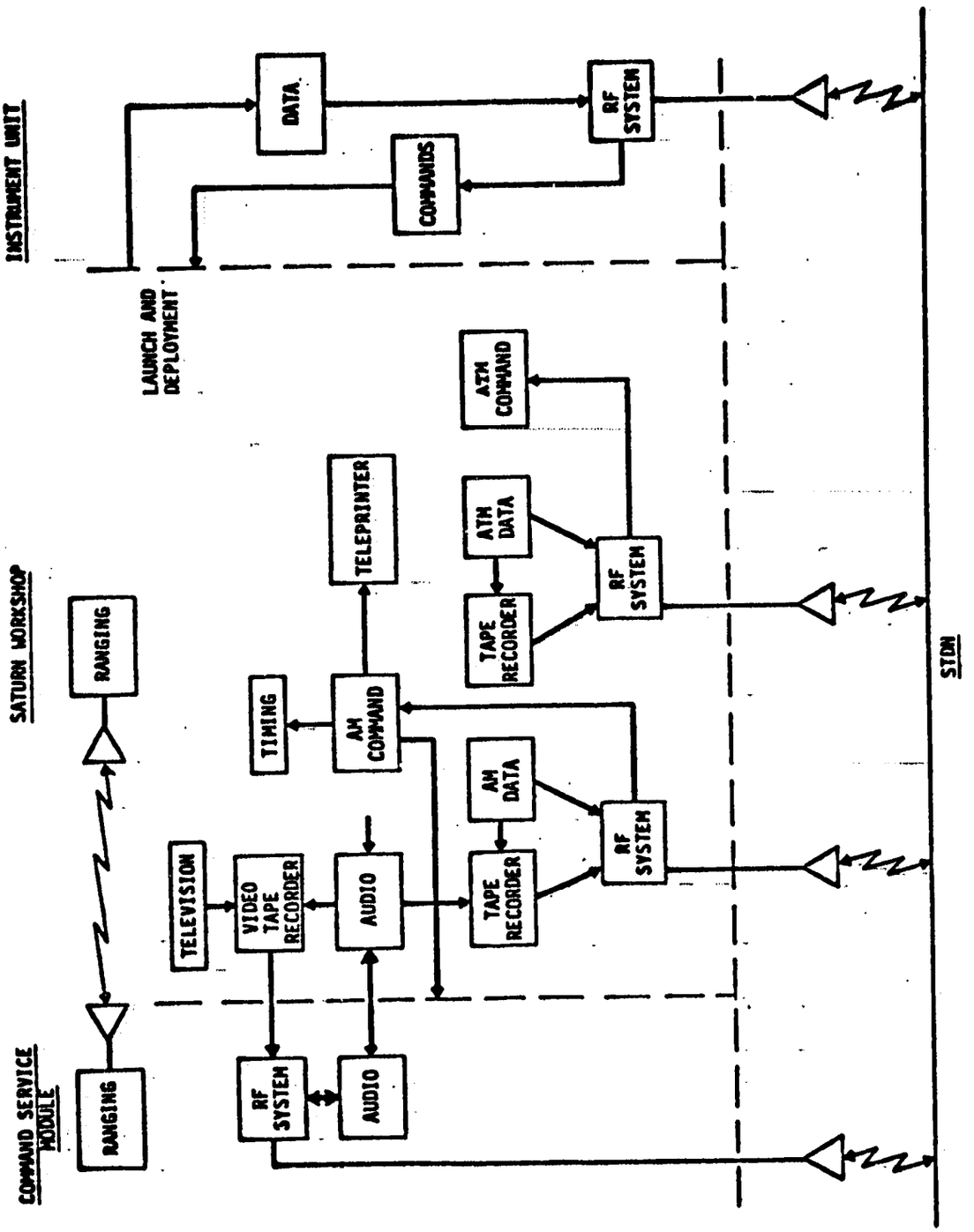

FIGURE 6-1 SKYLAB INSTRUMENTATION AND COMMUNICATION SYSTEM

6.3 MANNED MISSION PERFORMANCE

During the initial phase of the Skylab program, due to various attitude maneuvers required when the OWS meteoroid shield was lost during boost to orbit, I&C equipment was exposed to off-nominal temperatures, both excessive heat and cold, which caused many temperature sensors to read off-scale and systems to approach the upper operating limit temperatures. When thermal stability was reestablished, the I&C system operated for the duration of the 272 day program without evidence of deterioration due to temperature extremes exposure. The majority of the I&C systems operated continuously for 6506 hours. The anomalies that did occur did not really affect the return of data. For details on I&C system performance and anomalies, see reference 12.

ATM Data Acquisition - The ATM data acquisition system performed its functions as required. Although system redundancy was available, it was not needed due to the efficient operation of the primary ATM data acquisition system. The secondary system was not turned on except for end-of-mission testing. The original procedure to use a single ATM magnetic tape recorder as a primary unit and a second identical unit as a backup was changed when the thermal problems at time of launch necessitated establishing a use schedule to prevent the tape recorders from exceeding their thermal operating limits. With the exception of these recorders, the redundant ATM data acquisition system was not activated during the Skylab mission. A 40 hour post-Skylab test that energized the redundant system was initiated and satisfactorily completed. This post flight test verified proper operation of both ATM acquisition systems.

ATM Command System - The ATM Command System performed its functions as required, throughout the entire Skylab mission even though the system was used much more than intended during the first portion of the Skylab mission. No anomalies or discrepancies were attributed to the ATM command System. Approximately 59,650 commands were executed during the mission.

AM Data Acquisition - The AM Data Acquisition System performed its functions as required during the Skylab manned mission with some of the hardware units operating continuously for the entire mission. During the first manned period an AM transmitter developed a low signal output and a work around was initiated that required real time data transmission normally handled by this unit to be switched to the 2 watt transmitter.

During the second manned mission period the low-level multiplexer B output became intermittent. However, alternate backup data provided adequate system performance information for the duration of the Skylab mission.

During the third manned mission, a noisy second-tier switch in low-level multiplexer P caused eight measurements, common to the switch, to be excessively noisy. Mission objectives were not jeopardized, however, since alternate measurements provided these data. A signal line short is thought to have caused AM low level multiplexers to experience erratic data approximately midway through the mission (DOY 357). The loss of data from these units was a compromise to the AM Data System but did not impose any restriction on the mission.

AM Command System - The AM command system functioned efficiently through the whole Skylab mission.

End of Mission Status - After the 272 days (6506) hours of operating time for the Skylab I&C systems, a third crew deactivated and secured the vehicle for indefinite storage. After undocking, certain test were performed to ascertain the operational status of equipment that either had not been used during the mission or had failed during the mission.

The ATM Data Acquisition and Command Systems remained configured essentially as launched until the post mission test. The backup equipment was energized and operated properly during these checks. The configuration of the AM data System at the end of mission was altered by the change-out of tape recorders, the failure of OWS low level multiplexer B, the failure of the first 8 channels on all AM low level multiplexers, the failure of an AM 10 watt transmitter and the loss of 134 measurements. A majority of the measurement losses were due to low-level multiplexer problems (78 measurements lost), loss of the OWS Solar Array Wing 2 (15 measurements lost). The planned consumable replacement items were used as scheduled. The configuration of the Data System at the end of the mission would have adequately supported continued activity.

The AM command System at the end of the mission was altered only by the replacement of the teleprinter with the onboard spare. The planned consumable replacement items were used as scheduled. The VHF ranging system functioned properly during the rendezvous of the three CSM's, and was powered down for storage.

6.4 REACTIVATION PERFORMANCE SUMMARY

The Skylab Instrumentation and Communication (I&C) System satisfactorily supported all Skylab reactivation activities. Initial support was provided during an eight day period of limited systems reactivation and status determination during early March 1978. More than fourteen months of support was provided from 24 April 1978 through 11 July 1979 for Skylab

systems reactivation and attitude management. A summary of the significant I&C Systems events during these periods is presented in table 6-1.

Table 6-1

I&C SYSTEM SIGINIFICANT EVENTS - REACTIVATION MISSION

Date	Event
6 March 1978	Initial AM commands and receipt of AM telemetry data. Loss of AM telemetry modulation due to DC-DC converter failure.
10 March 1978	Activated AM backup telemetry. Played back AM Tape Recorder 1(10 minutes from End of Mission data received and processed; could not decom 2 minutes of reactivation recorded data).
11 March 1978	Initial Activation of ATM command and telemetry systems.
13 March 1978	All systems commanded off.
24 April 1978	Reactivated AM telemetry
25 April 1978	Reactivated ATM telemetry
27 April 1978	Long periods of continuous commanding to charge ATM batteries (e.g. 7762 commands sent at 64 ms intervals to charge ATM battery no. 7).
1 May 1978	AM-B and ATM-2 Transmitters inadvertantly left on for one orbit with transmitter temps increasing from approximately 60 degrees F. to 150 F.
2 May 1978	Operated on AM 2 watt transmitter with reduced data quality. Dumped AM tape recorder 2 with one revolution of recorded data.

Date	Event
11 May 1978	Conducted the first of a series of tests on switch selectors 1 and 3.
19 May 1978	Unable to lock on to AM sub-frame #2 data.
22 May 1978	AM sub-frame #2 data reacquired
2 June 1978	Spurious Switch selector #1 command caused added electrical loads and loss of ATM electrical power.
6 June 1978	Lost plus 24 VDC on AM DC-DC converter #2.
9 June 1978	Spurious Switch selector #1 command turned off CMG amp #3 causing excessive TACS usage.
22 June 1978	CMG #2 wheel speed transducer failed.
21 July 1978	DC-DC converter #2 recovered. Connecting PCG 8 Battery to its charger caused shorting of the AM DC-DC converter #1.
31 July 1978	Unable to turn off the ATM experiment bus with the true command, however, the compliment command worked.
18-24 August 1978	ATM tape recorder dumps successfully played in from all remote sites.
17 November 1978	ATM 2 transmitter power output dropped from 14 watts to 5 watts.
5 January 1978 and 21 April 1979	Spurious command by Switch selector #1 caused a secondary power share on command.

Date	Event
Feb 9 to Reentry	The ATM recorders were run frequently to gather data for guidance and navigation updates and to evaluate the electrical power system.
11 July 1979	AM and ATM transmitters and instrumentation systems were operating and producing valid data during the final ground station pass over Ascension approximatly 45 minutes prior to Reentry at an altitude of approximately 59 n.m.

Early in 1978, after the decision was made to attempt a reactivation of Skylab through ground control, the Bermuda ground station of the Space Tracking and Data Network (STDN) was chosen as the gound command base. Bermuda was chosen due to the existance of Skylab compatible command and telemetry receiving hardware. The necessary software was prepared for command and limited on-site real time data processing. A team of NASA engineers were sent to Bermuda to verify ground hardware and software compatibility and to conduct the initial Skylab reactivation operations.

On March 6, 1978, ground command control of Skylab was successfully obtained from the Bermuda ground stations. The AM telemetry systems were activated and valid data were received at the ground station for approximately two minutes when telemetry reception was lost. After approximately three minutes the telemetry carrier signal was reaquired but without modulation. The loss of telemetry after two minutes of reception was due to a power loss cause by the loss of sunlight on the solar arrays. It was determined that Skylab was spinning about the X-axis at a rate slightly greater than 1 degree per second causing the solar arrays to experience cyclic periods of sunlight and darkness. The loss of telemetry modulation was due to a failure of a DC-DC converter.

On March 10, 1978 the AM backup telemetry system was activated using a different DC-DC converter and telemetry data was again successfully acquired. The AM tape recorder was placed in the record mode for two minutes and then played back. Ten minutes of data still on the recorder from the end of the manned mission

was recieved and processed but the two minutes of data just recorded could not be decommutated by the Bermuda ground station.

Electrical power was successfully transferred from the AM to the ATM on March 11, 1978 and the ATM telemetry system was successfully activated. During the initial contact period from March 6 through March 13, 1978 the airlock module telemetry data was acquired during seven passes over Bermuda and ATM data was acquired during two passes. A limited amount of this data was processed in real time at Bermuda to verify system operation. All of the data was recorded on magnetic data tapes and processed at a later date for engineering evaluation. It was verified that all AM and ATM telemetry measurements were operative and downlinking valid data. All telemetry multiplexers were operating including the AM low level B multiplexer which was intermittent during the manned mission and nonoperative at the end of that mission.

With the exception of the three AM batteries which were left to trickle charge, Skylab systems were deactivated on March 13, 1978 and the NASA operations team returned home to prepare for the next phase of Skylab reactivations. During late March and early April 1978, a Skylab control room at JSC was configured with the necessary hardware and software to allow for real time monitoring of Skylab data to support the flight control team. Ground commands would continue to be uplinked directly from the STDN ground station following verbal direction from the JSC flight control team. During April and May 1978, an operations support center was established at MSFC with capability to monitor in real time the same data processed at JSC for the flight control team.

The STDN ground station at Madrid, Spain was configured to support Skylab operations and joined the Bermuda ground station beginning on April 24, 1978. The Goldstone tracking station was activated on June 2, 1978, Ascension on August 10, 1978 and Santiago on October 15, 1978 to complete the STDN gound station compliment on 5 sites. The five site configuration allowed for telemetry coverage of Skylab on each orbital pass in support of ground operations.

AM telemetry was successfully reactivated on April 24, 1978 and ATM telemetry on April 25, 1978. Following this the I&C systems successfully supported all Skylab reactivation activities for more that fourteen and one-half months until Skylab reentry occurred on July 11, 1979.

Charging of the AM and ATM batteries was one of the initial tasks to be conducted. Due to the design characteristic of the ATM batteries, which would automatically disconnect the charging

system when low battery voltage was sensed, a special charging procedure was required. This procedure required that multiple charge commands be uplinked to allow for incremental battery charging until the low voltage cutoff threshold was exceeded. To accomplish this, a ground procedure was established which would result in a battery charge uplink command every 300 milliseconds. This resulted in heavy cycling of the command system including the ATM #1 Switch Selector. For example, 7762 commands were required for charging ATM battery #7 which was one of fourteen ATM batteries charged. This excessive cycling may have contributed to the switch selector anomolies which occurred at various times throughout the reactivation mission.

On May 1, 1978, as a result of miscalculating ground station acquisition and loss of signal (AOS/LOS) times, Skylab was allowed to pass out of ground station range prior to commanding the AM-B and ATM-2 transmitters off. As a result, the transmitters were left on with the AM transmitter increasing in temperature to approximately 153 degrees F by the next station pass. The nominal temperature of this transmitter was approximately 60 degrees F. The primary coolant loop was commanded on for two revolutions to bring the transmitter back to a nominal temperature operating range. There was no apparent effect on transmitter performance as a result of the high temperature. A similar occurrence happened on May 6, 1978, when the Madrid ground station had command problems and could not turn off the AM-A transmitter. The transmitter temperature rose to 110 degrees F and was cooled to normal temperature by commanding the primary coolant loop on for one revolution. Again, there was no degradation of data transmission quality.

To conserve electrical power during a low Beta angle period on May 2, 1978, the AM 2-Watt transmitter was used with a resulting reduced data quality. On May 3rd control was switched back to the AM-B 10 watt transmitters to regain the better data quality.

Due to a significant number of command problems during the reactivation mission period a series of tests on switch selectors #1 and #3 were initiated on May 11, 1978. After testing it was concluded that Bit 3 on switch selector #1 and Bit 5 on switch selector #3 were intermittent during operation. During mid September 1978 Bit 3 on switch selector #1 failed to the "0" position. Compliment commands were used to work around this failure. The reason for the switch selector anomolies is unknown but it is believed that the multiple command cycles required to charge the ATM batteries were instrumental in the failure. Some of the more significant problems associated with switch selector #1 failures included the commanding of APCS Bus 1 & 2 on and depleting electrical power on June 2, 1978, commanding the CMG servo amp #3 off causing attitude control

problems on June 9, 1978, and causing a power share on command to be executed on January 5 and April 21, 1979.

On May 19, 1978, it became impossible to lock on the AM sub-frame 2 data. This problem caused the loss of 116 measurements which were used for Skylab experiment data and did not effect the operational data. The problem cleared itself three days later on May 22, 1978.

The DC-DC converter #2 24 VDC system was lost on June 6, 1978 but recovered on July 21, 1978. The reason for this intermittent failure was unknown. It was learned that the AM DC-DC converter #1 would power to a short circuit wherever the AM battery #8 was connected to its charger. This problem was circumvented by commanding one of the two systems off whenever the other was being used.

On June 22, 1978, the CMG #2 wheel speed measurement was lost. After this date every time the wheel bearing temperatures on CMG #2 exceeded approximately 123 degrees F the wheel speed measurement indicator read zero. When the bearing temperatures decreased below approximately 123 degrees F the measurement indicator would read the proper wheel speed. The wheel speed measurement was backed up by a Phase A, B, and C wheel currents measurements thus minimizing any mission impact when the bearing temperatures exceeded 123 degrees F. The ATM-2 transmitter power dropped from 14 to 5 watts on November 17, 1978. The transmitter appeared to operate normally, except that the output power was only 5 watts. The #2 transmitter was used for the remainder of the mission with no further problems.

The ATM tape recorders were both used extensively during the last six months of the reactivation mission for the purpose of gathering electrical power and control system data. During the last few days prior to reentry, the recorders were run almost continuously to gather data for guidance, navigation, and control system updates. Early in the reactivation mission a problem occurred in decommutating the AM-1 tape recorder when first attempted on March 10, 1978.

The AM tape recorder #2 was used periodically to collect battery discharge test data and other system data with no apparent problems. Both ATM and AM tape recorder performance proved to be very satisfactory during the reactivation mission.

Overall telemetry system performance was good throughout the reactivation misión. Acceptable data was recieved through the final ground station pass over Ascension on July 11, 1979, just 45 minutes prior to Skylab reentry. At this time the space vehicle had descended to an altitude of approximately 59 nautical miles and had been commanded into a tumble mode.

A summary of the Instrumentation and Communications System Failures with their effect on the Skylab Reactivation Mission is presented in table 6-2. A detailed analysis of both the ATM and AM measurement systems performance during the reactivation mission was conducted and is reported in the following section. The individual end-of-mission instrument performance proved to be excellent with a total failure of 4 measurements out of 692 measurements evaluated for an overall measurement system performance of 99.4%.

6.5 MEASUREMENT SYSTEM PERFORMANCE ANALYSIS

During the Skylab Reactivation Mission a selected set of system performance measurements were processed in real time and presented to flight control personnel in digital display format to support real time operations. All down linked Skylab data was recorded at the STDN ground stations on magnetic tape for post pass processing when required. A selected number of these tapes were shipped to the MDAC-HB data reduction facility for processing and presentation in an analog engineering data format to be used for more extensive system performance analysis. It was this data, which included 495 AM/MDA/OWS analog measurements and 383 ATM analog measurements, which was used to conduct the measurement system performance analysis.

Overall instrumentation system performance was summarized in Section 6-1. While large blocks of data were sometimes lost due to instrumentation system problems such as intermittant operation of transmitters, power supplies, and multiplexers the end instruments proved to be extremely reliable with an overall performance of 99.4%. The worksheets used to evaluate measurement system performance are included as an appendix to this report and include individual measurement values at four selected time periods. These measurement values may prove beneficial as performance reference data for all Skylab systems.

The Skylab Measurement System performance analysis is divided into two parts: (1) the manned mission, which is briefly summarized herein, and is detailed in reference 12; and (2) the Reactivation Mission, commencing on March 6, 1978, for the AM/MDA/OWS and on March 11, 1978 for the ATM, and continuing through last data transmittals, prior to reentry, over Ascension Island on July 11, 1979.

It should be noted that although the Skylab data system was used throughout the reactivation period, measurement performance was analyzed on a selective basis dependent on processed data availability. Data in the Appendix is from the following dates:

TABLE 6–2
I&C SYSTEM FAILURES SUMMARY

FAILURE	EFFECT ON REACTIVATION MISSION
INTERMITTANT LOSS OF AM DC–DC CONVERTERS 1 & 2	NONE. BACKUP CONVERTER WAS AVAILABLE. TO PROVIDE TELEMETRY SYSTEM POWER.
AM TAPE RECORDER 1	NONE. TAPE RECORDER 2 USED TO RECORD AND PLAYBACK ALL NECESSARY DATA.
ATM SWITCH SELECTORS 1 & 3	VARIOUS SPURIOUS COMMAND EFFECTED SYSTEMS OPERATION. TWO OF THE MORE SIGNIFICANT EFFECTS WERE THE ADDITION OF ELECTRICAL LOADS CAUSING COMPLETE LOSS OF POWER AND THE COMMANDING OFF OF CMG SERVO AMP NO. 3 CAUSING EXCESSIVE USE OF THRUSTER ATTITUDE CONTROL SYSTEM GAS.
INTERMITTANT LOSS OF AM SUB–FRAME NO. 2 DATA	NONE. DATA LOST WAS NOT REQUIRED FOR OPERATIONS SUPPORT
CMG # 2 WHEEL SPEED TRANSDUCER	NONE. CMG PHASE CURRENTS USED AS BACKUP.
SHORTING OF AM DC–DC CONVERTER 1 WHEN CONNECTING AM BATTERY NO. 8 TO ITS CHARGER	NONE. OPERATING PROCEDURES USED TO WORK AROUND FAILURE.
ATM 2 TRANSMITTER OUTPUT POWER DROPPED FROM 14 WATTS TO 5 WATTS	NONE. SWITCHED TO ATM 1 TRANSMITTER.

- o February 9, 1974 — End of the manned mission
- o March 6, 1978 — Reactivation of AM/MDA/OWS
- o March 11, 1978 — Reactivation of ATM
- o July 11, 1979 — BDA and ACN prior to reentry

Data from June 27, 1978, and May-28, 1979, was used to verify measurement status when there was a question concerning data reliability from the selected data dates.
Measurement "status" evaluation involved 4 possible conditions:

(1) Good (G): Measurement performance was valid throughout the manned and reactivation phases of Skylab's life.

(2) Questionable (Q): Those measurements that were part of systems that were not reactivated, or remained at the same zero or off scale values as recorded at the end of the manned mission, and therefore, could not be further evaluated.

NOTE: An assumption may be made that the measurements classified as "questionable" are in all probability good, in that actual measurement failures were an extremely small percentage of the total Skylab measurement system.

(3) Manned Mission Failure (MF): Those measurements considered manned mission failures, as reported in ref 12.

(4) Failure (F): Those measurements that failed during the quiescent storage or reactivation mission.

6.5.1 Manned Mission Performance

The Skylab data system was activated during Skylab 1 launch countdown and continued successful operations during all operational phases, a total of 6,506 hours. Of the 1,164 Skylab system measurement monitored by the data system, 134 were no longer providing usable information at the end of the manned mission representing a recovery rate of 88.5%. The great majority of these losses were due to instrumentation system problems (e.g., multiplexers) as opposed to individual measurement failure. The overall data system had no problems that caused any significant impacts to the Skylab missions. Detailed manned mission performance data may be found in reference 12.

6.5.2 Reactivation Mission Performance Summary

The Skylab Data System was activated on March 6, 1978, and supported reactivation mission operations until reentry on July 11, 1979. During the storage and reactivation phases of Skylab, the measurement system developed no significant additional problems. Data System measurement performance at reentry (July 1979) was essentially the same as at the end of the manned mission (February 1974) more than five years earlier. There was a total of four measurement failures indentified during the reactivation mission for an overall measurement recovery rate of 99.4%.

6.5.3 AM/MDA/OWS Measurement Analysis

Four-hundred ninety-five (495) measurements were evaluated with respect to operational reliability with the results noted in Table 6-3.

The measurement failures during the reactivation mission were:

C - 0302-512	TEMP TM XMTR BIO CASE
C - 0052-806	TEMP EXT CM DOCKING PORT TUNNEL
D - 7001-436	PRESS, RS, PR LOOP, PUMP DIFF

These failures did not adversely effect reactivation mission operations support.

The AM/MDA/OWS Reactivation Mission measurement performance rate was 99.2%. The performance rate is defined as the ratio of good measurements to good plus failed measurements. The questionable measurements probably would show the same high performance rate were they able to be evaluated.

6.5.4 ATM Measurement Analysis

Three-hundred eighty-three (383) measurements were evaluated with respect to operational reliability with results noted in Table 6-4.

TABLE 6–3 AM/MDA/OWS MEASUREMENT EVALUATION

		STATUS			
TYPE	NO.	GOOD	QUESTION–ABLE	MANNED MISSION FAILURE	REACTI–VATION FAILURE
TEMPERATURE	276	230	18	26	2
PRESSURE	64	57	6		1
VOLTAGE	94	74	5	15	
CURRENT	40	23	7	10	
MISC	21		2	19	
TOTALS	495	384	38	70	3

TABLE 6–4 ATM MEASUREMENT EVALUATION

		STATUS			
TYPE	NO.	GOOD	QUESTION–ABLE	MANNED MISSION FAILURE	REACTI–VATION FAILURE
TEMPERATURE	158	140	12	6	–
PRESSURE	11	4	7	–	–
VOLTAGE	99	80	19	–	–
CURRENT	73	55	18	–	–
MISC	42	25	15	1	1
TOTALS	383	304	71	7	1

The only ATM measurement failure identified was T-0002-702, CMG # 2 wheel speed, which was intermittent as a function of CMG #2 bearing temperatures. The CMG #3 wheel speed indication had failed during the manned mission. The wheel speed transducer was believed to be the most probable failure. This measurement was backed up by Phase A, B and C wheel currents and therefore, created no mission impact. Based on this one failure, the overall ATM reactivation mission measurement performance rate was 99.7%.

7.0 UNCONTROLLED VEHICLE MOTION

The progress of the Skylab from its initial stable state to a very dynamic condition just prior to the resumption of control was a very interesting technical problem to analyze. One approach to such an analysis is to compute all the pertinent external torques acting on the vehicle and numerically integrate the equations of motion to obtain time histories of the vehicle motion. While this has the advantage of providing accurate results with few if any approximations, it generally makes the physics of the problem difficult to understand and explain. A better approach and the one used in this analysis draws upon simplified theoretical work to explain the nature of the motion in certain regimes. The numerical approach is then used to substantiate these conclusions and to combine the various effects. Theory and numerical results can be checked against each other at every stage and this greatly enhances confidence in the results. The major advantage, however, is in the explanation and interpretation of results. This is especially important in a problem of this type where much of the observed data seemed to contradict some elementary dynamics concepts. For example, data showed the vehicle had left the gravity gradient equilibrium orientation where it had stayed for over three years. Instead the vehicle seemed to be oriented with the long axis perpendicular to the orbit plane (an unstable gravity gradient orientation). Also, the vehicle had developed a relatively rapid spin rate about the long axis and this gave every indication of accelerating. Since spin about this axis is generally unstable in the presence of energy dissipation (usually found in real systems) the development and persistence of this motion was puzzling.

Skylab's motion after it was parked in 1974, probably built up in stages, but the exact time of transition between stages may never be known because the observations were made infrequently. It is known, however, that for many months it remained in its original gravity gradient orientation. In 1977, data showed the vehicle out of the gravity gradient equilibrium position and rotating through large angles. While some singular event, such as meteoroid strike, a gas bottle leak, etc., could have been responsible, this seems unlikely since the status of the on-board systems did not support such an occurrence. Interestingly enough, there are other less dramatic explanations for what took place. A number of papers have been published dealing with the instability produced when a gravity gradient stabilized body is subjected to a torque which forces it slightly away from the true gravity gradient equilibrium position (i.e., axis of minimum inertia aligned with the perpendicular to the orbit plane). This is sometimes called the "Garber Instability" after the author of the original paper

(reference 19). It was shown by both Nurre (reference 20) and Sperling (reference 21) that in the original Skylab configuration (i.e., two OWS solar arrays) aerodynamic forces could produce the necessary perturbation, subjecting the vehicle to this instability. Both of the last two investigators were working with mass properties associated with the original Skylab configuration (i.e. two OWS solar arrays). An effort was therefore made to asses the effect of the absence of one solar panel on the aerodynamic torque disturbance and hence on the possible equilibria and stability of the Skylab. Nurre and Sperling used Fourier series to represent the aerodynamic forces and torques, taking advantage of symmetries, simplifications and various invariance conditions to achieve a reduction in the number of terms used. For our study such reductions were not always possible because the actual Skylab configuration did not exhibit these symmetries. Not withstanding these conditions, the study basically paralleled the work of Sperling. The analytical determination of the equilibria of the equations of motion proved to be somewhat intractable. An attempt to do a complete search for equilibria for a given altitude and density combination was too costly and prohibitive by computer time requirements. However, from our large simulation, equilibrium orientations were obtained. A linearized infinitesimal analysis was then used to study the stability of the equilibrium orientations. An examination of the coefficients of the sixth degree characteristic polynomial of our system revealed that the coefficient of the fifth power was identically equal to zero. Since this coefficient is the sum of the roots of the characteristic polynomial, not all roots can have negative real parts. These results agree with Sperling's conclusion about the stability of the Skylab. An indication of the Skylab instability as a function of altitude is shown in a comparison of the time constants: the approximate time constants are 2350 and 2130 orbits for altitudes of 235 and 150 n.m. orbits, respectively. It was also found that the roots were very sensitive to relatively small displacements from the equilibrium positions, thus tending to confirm the highly nonlinear nature or our problem.

With the weak instability indicated by these large time constants, a very small amount of energy dissipation (damping) could stabilized the vehicle. However, as the density increased (due to altitude decay or solar activity), the required damping to maintain stability would have to increase. On a vehicle like Skylab, energy dissipation is probably small in relative terms and could not be increased. An assessment to determine how much damping was available and the source of such damping was made when the first indications were received that the Skylab had left the gravity gradient attitude. Calculating backwards from the observed density, it appears that the system damping available should have been on the order of .01 percent of

critical. The sources of damping considered were: 1) external damping as a result of interaction with the Earth's atmosphere and magnetic field (these were assessed and found to be below the required value); and 2) internal damping which would result from structural vibrations and the relative motion of internal parts. Once a structure is excited, structural damping values on the order of 0.5 percent (reference 22) have been observed. In this case, however, the frequency of the gravity gradient motion is very low (only about 0.5 cycles per orbit). The lowest flexible body mode had a frequency approximately 1000 times greater (reference 22) and would, thus, be very difficult to excite. Internal motion of large quantities of material inside the vehicle was difficult to justify. Liquids were thought to still be restrained by bladders and most equipment was secured in some fashion. Above all the very low rates and acceleration levels being observed offered no plausible mechanism for exciting the material. It would then appear that the very small damping value backed out of the stability analysis is consistent with that required to have maintained the Skylab in a stabilized gravity gradient attitude prior to the Fall of 1977.

In view of these findings, it is our conclusion that (1) the system damping for the vehicle in gravity gradient attitude was very small (i.e. on the order of 0.01 percent of critical) and (2) the vehicle went out of its gravity gradient orientation when the increase in atmospheric density caused the instability to exceed the threshold established by the small system damping value.

Given this instability it was inevitable that large amplitude motion would build up. When this happened, another relatively small aerodynamic effect began to be felt. Because of the asymmetric OWS solar array configuration of this vehicle, the aerodynamic moments were unbalanced producing a tendency to spin about the longitudinal axis. That is, if the vehicle were rotated slowly about the X axis and the aerodynamic roll moment recorded, the integral over one complete revolution would not be zero. This effect is analogous to the aerodynamic effect which causes an anemometer to spin. Once started, rotation about this axis slowly accelerates. This effect was suspected after examination of the aerodynamic data (reference 23) and was confirmed when these data were input to a dynamic simulation. At this point the puzzle as to why the vehicle had left its gravity gradient attitude and begun to spin had been largely answered. For a better understanding of the motion of the vehicle's spin axis in the orbital coordinate frame, it was decided to consult some of the analytical work on spinning satellites published during the past 20 years.

Because the moments of inertia about the Y and Z principal axes are nearly the same (see Table 7-1), the problem closely resembles the classic body of revolution spinning about its axis of symmetry. The case of a symmetrical rigid body in a circular orbit has been considered by a number of authors and some of these results were very helpful in understanding both the observed vehicle motion and the computer simulation results. Pringle (reference 24) formulated the problem in terms of a dynamic potential function, U, which he derived from the Hamiltonian. With the potential function he was then able to determine equilibrium orientations where a static balance existed between gyroscopic and gravitational torques. The stability of these equilibria was then examined and closed contours of the potential function used to illustrate the types of vehicle motion possible as a function of spin rate and inertia ratio. For a symmetric vehicle with the Skylab inertia ratio, contours of the potential function are shown in Figures 7-1 and 7-2 for two spin rates over the range observed. These contours are plotted on the surface of a sphere with the viewer looking down the orbit normal. The filled circles represent stable equilibria and the contour lines can be interpreted as bounds on the motion of the spin axis. That is, if the spin axis is initially placed within a closed contour surrounding a stable point it will not cross that contour although its path will not necessarily parallel it. Note that for no spin, equilibrium is found with the axis of symmetry along the radius vector. As the spin rate increases, the equilibria move out of the single, stable orientation with the spin axis perpendicular to the plane. It was found that this description was consistent with the results obtained from integrating the equations of motion. Equilibrium orientations were found where predicted and the closed contours were not violated. To determine the effects of the mass assymetry, aerodynamic torques, and orbital regression, these were incorporated into the simulation individually and the resulting changes noted. By and large, these were found to be second order influences, but they were retained in the simulation for completeness. Actually, these effects have also been treated analytically in previous works, but not in a single analysis. Meirovitch (reference 25) extended Pringle's work to include the effect of simple aerodynamic torques. In the cases he treated, this produced a small shift in the equilibrium point and a distortion in the countour lines. It was possible to confirm this qualitatively in our simulation, but because of the more complex aerodynamics a quantitave check could not be made. Several investigations (Cochran (reference 26), Pringle (reference 27), and others) have examined the effect of orbital regression on long term vehicle motion. Briefly put, for spin rates below a critical value, the vehicle will precess and follow the orbital plane. If the rate is too fast, the body will try to remain inertially fixed and will not follow the movement of the orbital plane. In

TABLE 7–1
SKYLAB MASS PROPERTIES

PRINCIPAL MOMENTS OF INERTIA

I_{xp} = .759 X 10^6 Kgm^2 (.562 X 10^6 SLUG–FT^2)

I_{yp} = 3.896 X 10^6 Kgm^2 (2.873Z X 10^6 SLUG–FT^2)

I_{zp} = 3.823 X 10^6 Kgm^2 (2.8196 X 10^6 SLUG–FT^2)

DIRECTION COSINE MATRIX BODY TO PRINCIPAL AXES

$$[A]_{PB} = \begin{bmatrix} .9842 & -.0210 & .1760 \\ .0162 & .9781 & -.2073 \\ -.1765 & .2069 & .9623 \end{bmatrix}$$

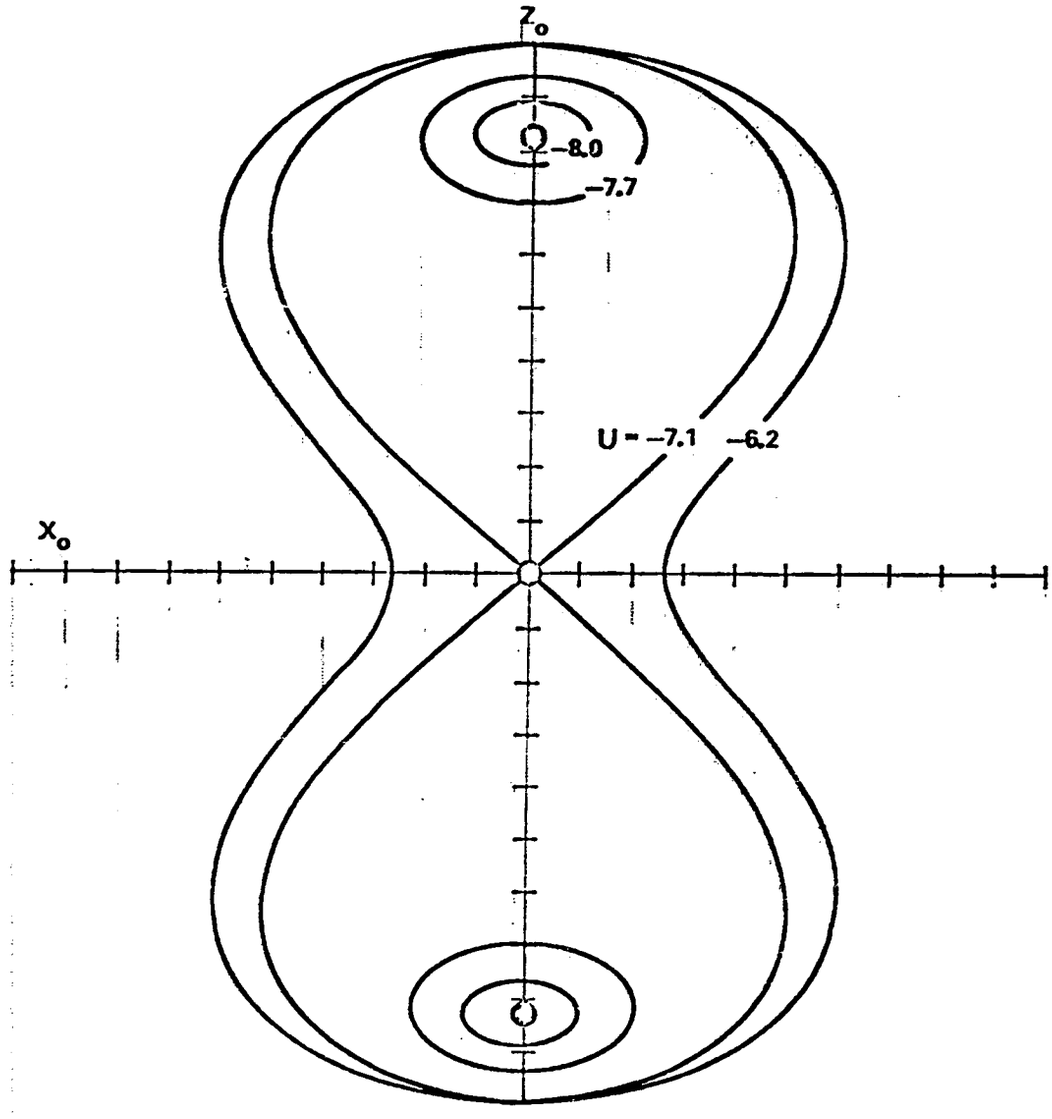

FIGURE 7-1 DYNAMIC POTENTIAL CONTOURS VIEWED IN THE ORBITAL FRAME
SPIN RATE = 0.5 °/SEC

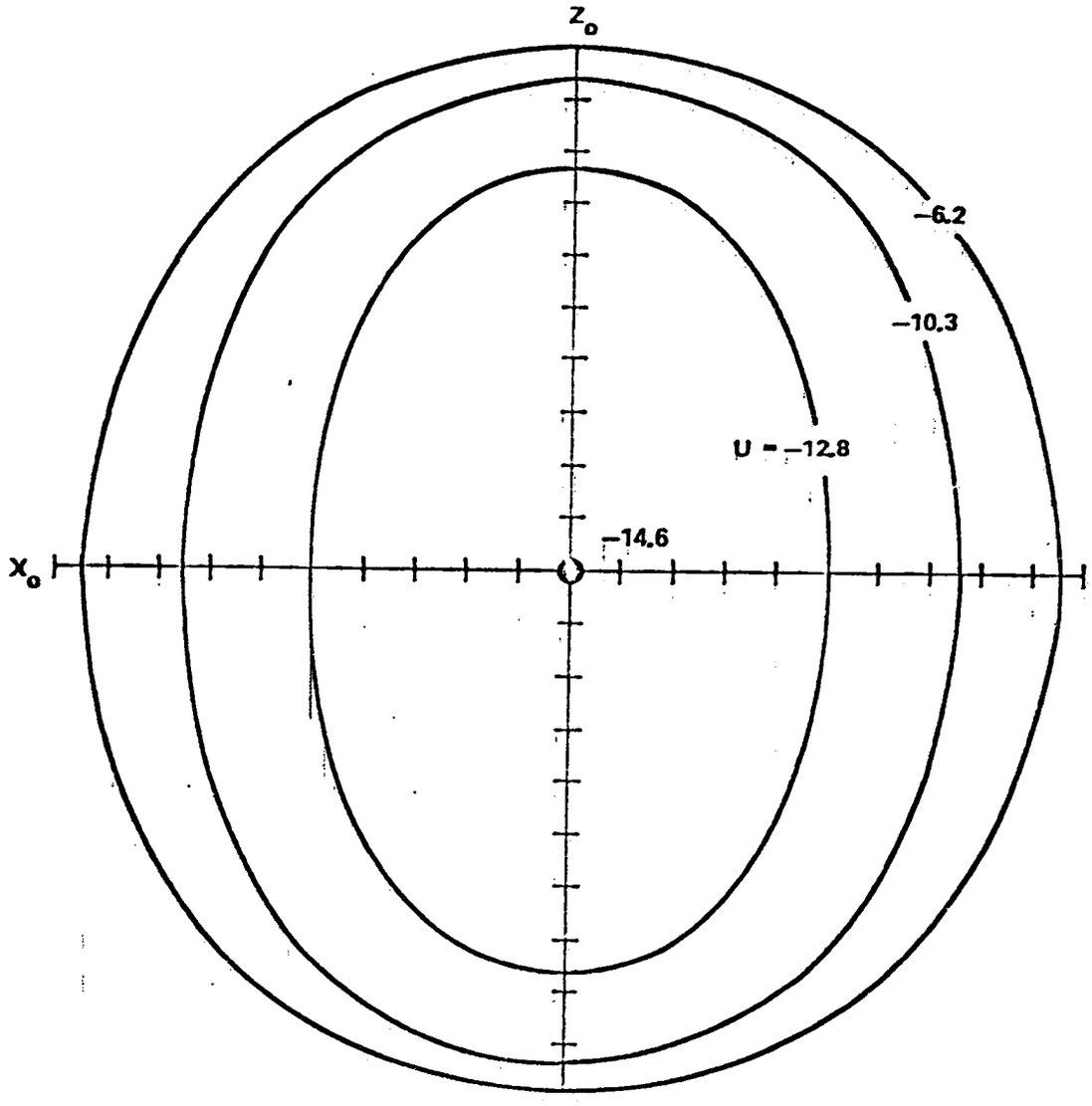

FIGURE 7-2 DYNAMIC POTENTIAL CONTOURS VIEWED IN THE ORBITAL FRAME
SPIN RATE = 1.1 °/SEC

In the case of Skylab, the rates were low and the motion did not follow the orbital plane. These analyses as well as work presented in references 28-31 helped establish confidence in the numerical solutions obtained from the simulation program and provided a guide in evaluating the contributions of the various effects. Without such a framework, this task would have been much more difficult.

7.1 SIMULATION DESCRIPTION

The uncontrolled motion of the Skylab vehicle in orbit was simulated using a 6-degree-of-freedom digital program on the Honeywell CP-V system. The equations of motion for a small rigid body in orbit about the earth have been published in numerous documents and will not be restated here. If the reader is interested he is referred to reference 21 for a typical example. The rigid body program utilizes an oblate rotating earth model and includes the effects of perturbing torques due to gravity gradient and aerodynamic forces. Quaternions were used to represent the attitude of the uncontrolled vehicle and a variable step-size, five pass Runge-Kutta integration scheme was used. Using this scheme, the Skylab motion could be simulated for approximately a month's time without appreciable integration round-off errors.

The Jacchia 1970-3 atmosphere model and the predicted solar and geomagnetic activities data use to determine density profiles were provided by Space Sciences Laboratory, MSFC. These predicted data were based on the smoothed 13 month mean values and were updated monthly. A detailed description of the model is given in reference 32.

The Skylab in-orbit aerodynamic data are given in Reference 23. Force and moment coefficients for each of the three body axis are given as a function of angle of attack and aerodynamic roll angle. The data cover all possible orientations of the Skylab and were used on the simulation in table look-up form.

In the following section results obtained from this simulation are presented and compared with data obtained from vehicle telemetry.

7.2 COMPARISON OF TELEMETERED DATA AND SIMULATION RESULTS

After contact was established with the vehicle in March, data were available from the on-board sensors and these were examined

for clues to the vehicle's behavior. The two major sources of data were the vehicle's rate gyro system and the solar array system; however, each of these had certain limitations. The rate gyros provided an accurate source of rate information, but were scaled so that only rates below 1 degree per second could be measured. Since the X axis rate was greater than this, only the sign was available for this axis. A fairly accurate measurement of the roll rate magnitude could be obtained by timing the light-dark cycle observed in the solar array output, but the axis of rotation could not be determined accurately. The strength of the output from the solar arrays gave some indication of the sun incidence angle on the solar arrays. Occasionally the sun would pass within the field of view of the acquisition sun sensor. These were the only sources of information concerning the orientation of the body in space. Both the data from the simulation and the spacecraft indicated that while the vehicle was undergoing considerable motion and the pattern was rather complex, the motion was not random.

An example of the motion observed can be obtained by initializing the simulation program using data from the on-board rate gyros and sun sensors. These data were taken in March 1978 about 24 hours prior to the activation of attitude control. Initially the Skylab was oriented with the X principal axis in the Y_o-Z_o plane, approximately 8 degrees off the orbit normal. The Z body axis was directed up, 2 degrees off the radius vector in the Y_o-Z_o plane. This resulted in a 15 degree angle between the solar panels and the sun line. The Skylab was spinning about the X principal axis at a rate of 1.73 degrees/sec (ω_1). The total angular rate about the Y and Z principal axes was 0.203 degrees/sec. Figure 7-3 shows the initial orientation of the vehicle, the angular momentum vector H and the angular rate vector ω in the orbital coordinate system.

Since the external torques are small and the vehicle is approximately symmetrical about the X_p axis, the motion over a short time period (15-30 minutes) can be compared to that of a torque-free spinning body of revolution (reference 33). If we consider the torque free motion, the angular momentum would remain constant in magnitude, and its direction fixed in space. For the angular rates of 1.73 degrees/sec and 0.203 degrees/sec, the angle between ω_1 and H would remain constant at 31 degrees. The angle between H and the orbit normal would be a constant 24 degrees. If viewed by a space fixed observer, both ω and ω_1 would precess about the angular momentum vector at a rate of 0.4 degrees/sec (15 minutes/cycle). Simulation results, which include both the effects of external torques and an asymmetric vehicle are shown in Figure 7-4 through 7-6 for approximatelyab 1/3 of an orbit (30 min). The OI coordinate system is inertially fixed and is initially aligned with the orbital coordinate frame O. A unit vector along the angular momentum is

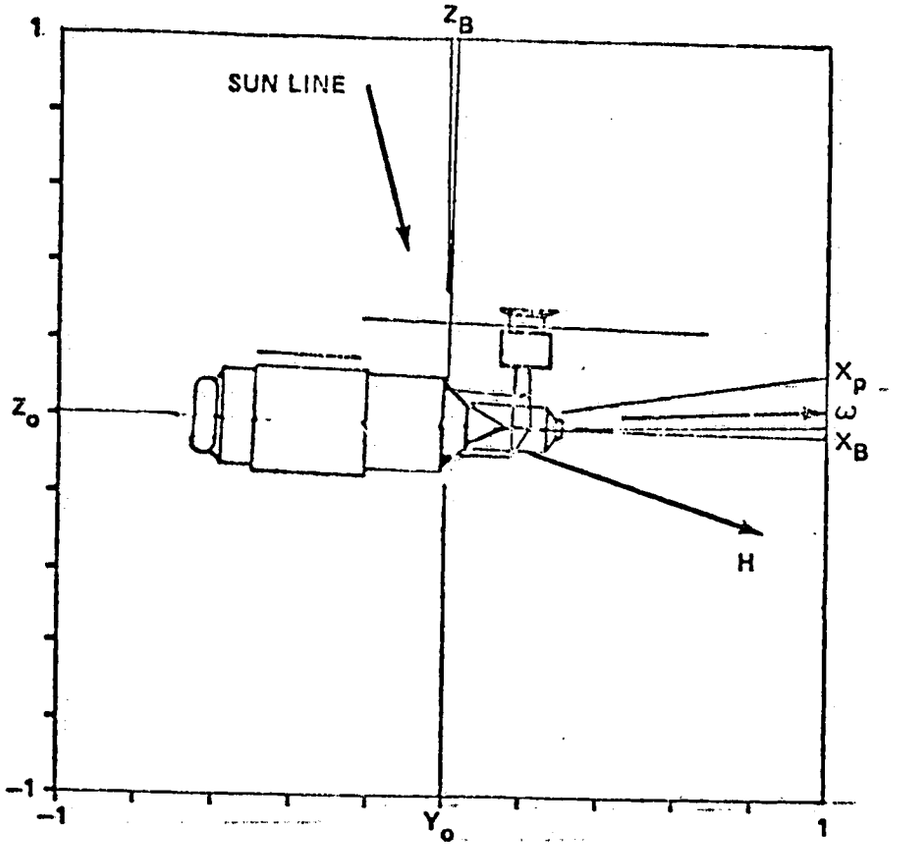

FIGURE 7-3 INITIAL VEHICLE ATTITUDE FOR SIMULATION RESULTS

represented by a solid line and the symbol O. The long-short dashed line with the symbol Δ represents a unit vector along ω and short dashed line with the symbol X represents a unit vector along the X_p (ω_s) axis. Figure 7-4 presents traces of these unit vectors in the orbital plane (X_{oi}-Z_{oi}) as viewed from the orbit normal. During this 30 min interval, the momentum vector remains nearly constant in this plane, while the ω and ω_s vectors complete a little more than two revolutions about H. Figures 7-5 and 7-6 show the same data in the X_{oi} -Y_{oi} plane and the Y_{oi} -Z_{oi} plane, respectively, and show that the motion of these vectors is confined to one side of the orbit plane. For the torque-free symmetrical body motion, the momentum vector would appear as a single point, while the ω and ω_s vectors would trace repeating circles about that point.

In late 1977, when observations indicated the Skylab was no longer in the stable gravity gradient attitude, it was first thought to be in a random tumble mode. At best, the ground observations could give the orientation of the longitudinal axis of the Skylab, and at times, the direction of the solar panels. Figure 7-7 is the motion of H, ω and X_p in the orbit plane as they would appear in the rotating orbital coordinate system O. While the motion appears more complex when viewed in this system, there still exist a definite pattern. Because of the offset of the principal spin axis from the longitudinal body axis (≈10°), determining the motion of the Skylab based on ground observations was more difficult. Figure 7-8 shows again the motion of X_p in the orbit plane as it would appear to a ground observer. In addition, the motion of the X body axis is represented by the solid line with the symbol □ . As the principal axis comes about the angular momentum vector at a rate of 0.4°/sec, the body axis is rotating about the principal axis at a rate of 1.73 /sec.

In view of the similarity between the numerical results and the torque-free solution, it seemed that the body rates measured by the on-board rate gyro system should also exhibit some consistency when viewed in the same way.

Table 7-2 presents measured rate data from the vehicle obtained in early March. As previously stated, the X rate gyro was saturated and the roll rate determined from the solar arrays was 1.20°/sec. This rate was assumed to be along the X_p axis. The angle between X and the angular velocity vector, θ, and the angle between X and the momentum vector, Φ, were computed using the equations of reference 33. In the same fashion, the precession and nutation rates $\dot{\psi}$ and $\dot{\nu}$ were determined from the given rate data.

If the torque-free approximation were strictly true and if the measurements were free from error, all four of these parameters

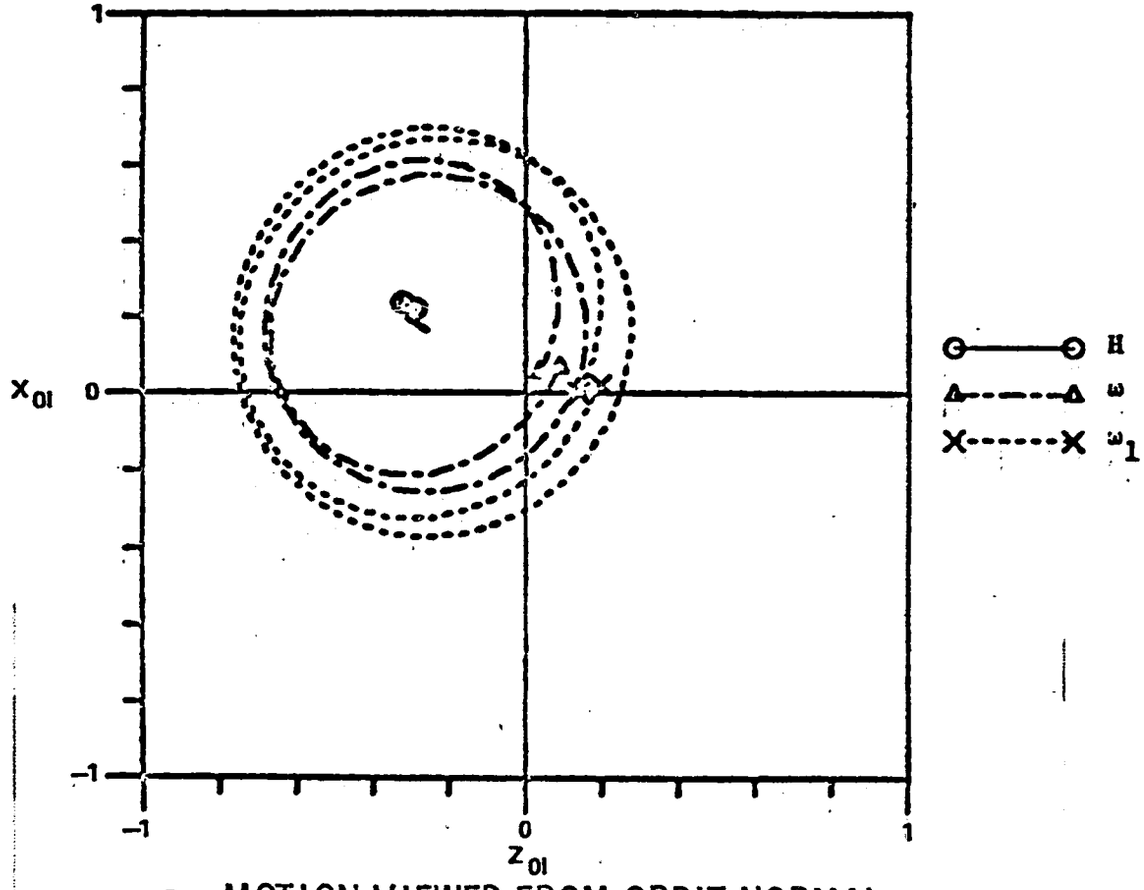

a. MOTION VIEWED FROM ORBIT NORMAL

FIGURE 7-4 MOTION OF THE MOMENTUM VECTOR, ANGULAR VELOCITY VECTOR, AND SPIN AXIS IN AN INERTIALLY FIXED SYSTEM INITIALLY ALIGNED WITH THE ORBITAL COORDINATE FRAME

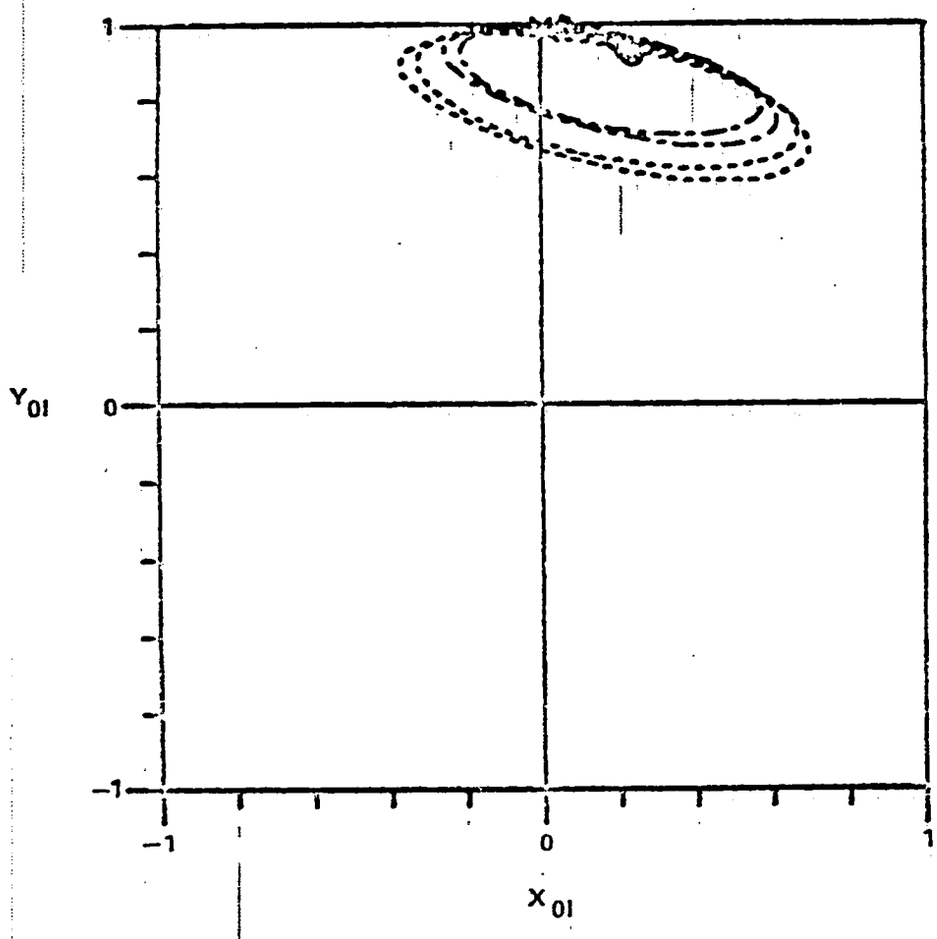

FIGURE 7-5 MOTION VIEWED ALONG INITIAL LOCAL VERTICAL

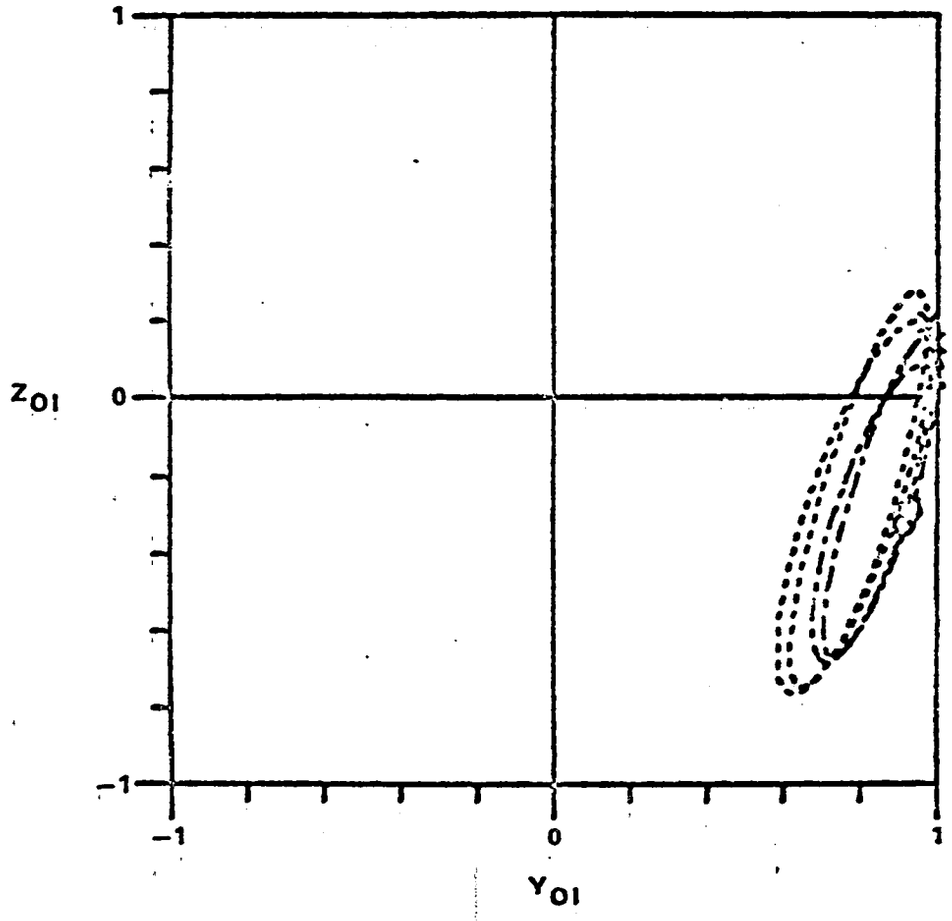

FIGURE 7-6 MOTION VIEWED ALONG INITIAL VELOCITY VECTOR

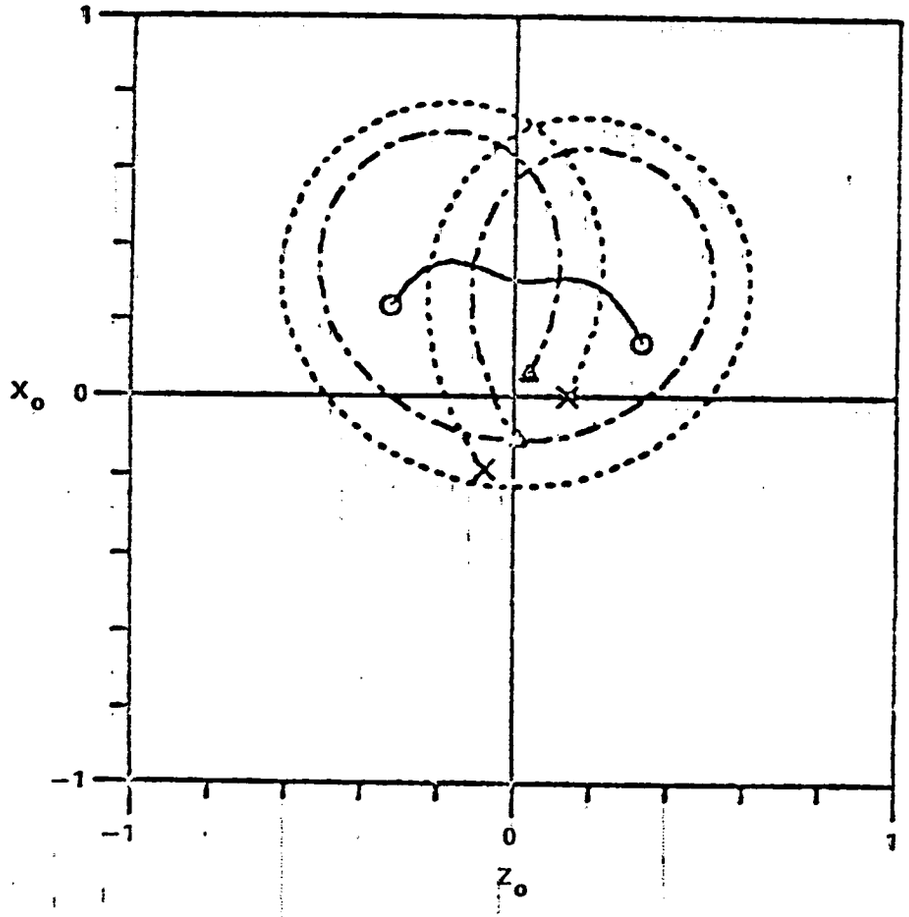

a. MOTION OF MOMENTUM VECTOR, ANGULAR VELOCITY VECTOR, AND SPIN AXIS PROJECTED ON ORBITAL PLANE.

FIGURE 7-7 MOTION IN A ROTATING ORBITAL COORDINATE FRAME

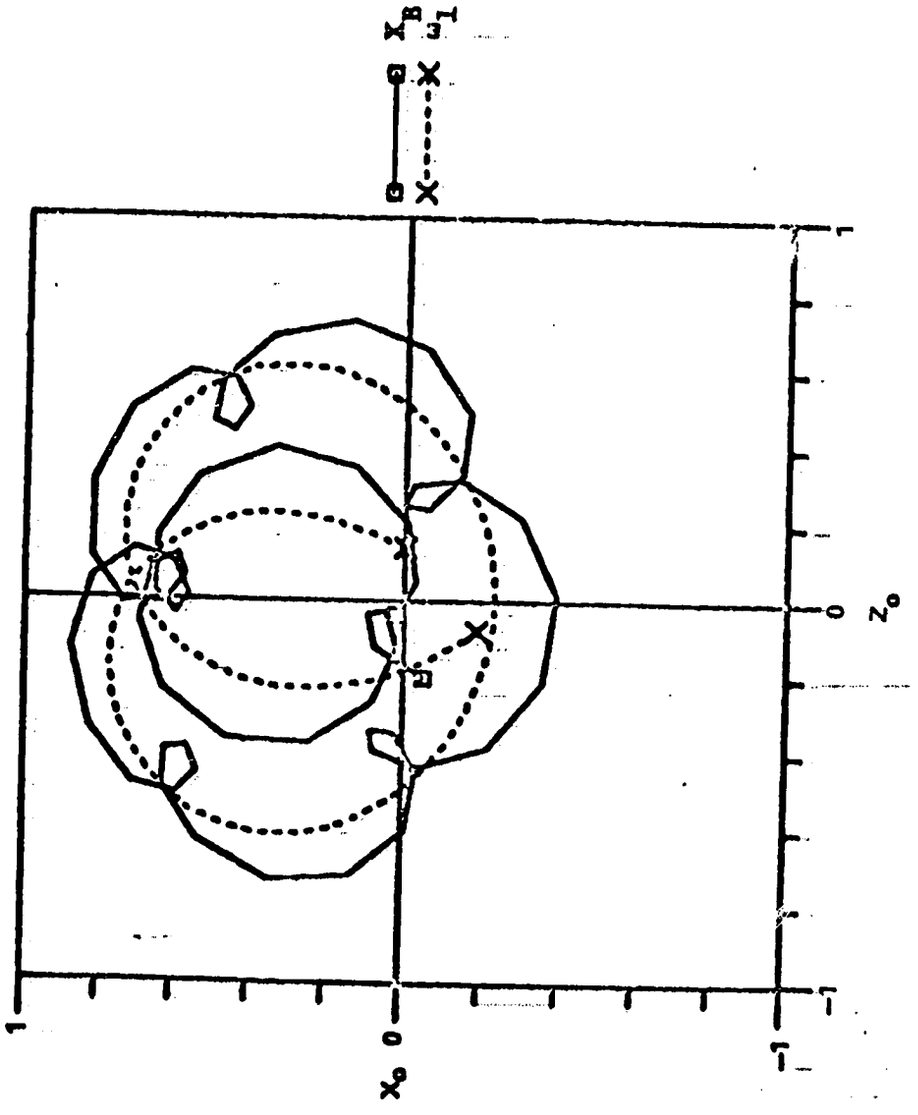

FIGURE 7-8 MOTION OF SPIN AXIS AND X VEHICLE AXIS PROJECTED ON ORBITAL PLANE.

TABLE 7-2
SKYLAB BODY RATES
MEASURED 3-11-78

TIME HR: MIN:SEC	RATE ABOUT X_p ~ °/SEC	RATE ABOUT Y_B ~ °/SEC	RATE ABOUT Z_B ~ °/SEC	Φ ~ °/SEC	θ ~ °/SEC	$\dot{\psi}$ ~ °/SEC	$\dot{\gamma}$ ~ °/SEC
20:38:50	1.20	+ .014	+ .165	12.2	2.3	.24	.96
39:00		+ .009	+ .166	12.3	2.3	.24	.96
39:20		− .002	+ .170	12.6	2.4	.24	.96
39:40		− .010	+ .178	12.3	2.3	.24	.96
40:00		− .015	+ .186	12.1	2.3	.24	.96
40:20		− .012	+ .198	10.3	1.9	.24	.96
40:40		− .012	+ .260	15.2	2.9	.24	.96

would have constant values. While this is not precisely correct, note the consistency that is introduced by viewing the data in this form as opposed to looking at the body rates themselves. Data taken on subsequent days also showed the same pattern and gave confidence that this approach was applicable. When the processed data from several days was examined some long term trends were indicated (Table 7-3). These data represent all the measurements obtained from the vehicle rate gyro system between initial contact (3-6-78) and control moment gyro activation (6-9-78). These data show that over this period the spin rate increased with time, as did the precession and nutation rates. During the same time, the angle between the X principal axis and the momentum vector grew from 12 to 30 giving a much wider cone.

While the torque-free approximation can be used for the short-term motion, the effect of the external torques must be considered for the long-term motion. These torques, though small, cause the momentum vector to precess about the orbit normal. For this case, the period of precession is approximately 14 hr.

Simulation results covering 21 hr are shown in Figure 7-9. The solid line shows the motion of the angular momentum vector in the inertial system as viewed from the orbit normal. For clarity, the X principal axis is represented by dots with its motion for a 30 min period at the beginning and ending of this time from indicated by the dashed circles. A pictorial representation of this motion as it would appear to an inertially fixed observer is shown in Figure 7-10.

While the cone angles and rates in late 1977 differ from the simulation results shown here, the basic motion of the Skylab was the same. Thus, it is easy to see that early ground observations, with sighting times of only a few minutes duration, might give the indication of a random tumble.

Shown in Figure 7-11 are the angular rates about the principal axes. These simulation results show that while the rates about the Y and Z axes oscillate between $\pm 0.2^{\circ}$/sec, their average value remains constant. The rate about the X axis has a small short term oscillation with the average value increasing at a constant rate due to the aerodynamic torque. Figure 7-12 presents another comparison of measured data and simulation results. Just prior to activation of the attitude control system, a systematic effort was made to deduce the vehicle's attitude. This was important because the vehicle had to be maneuvered to face the sun and, as there was no on-board attitude reference , some idea as to where the vehicle was expected to be pointed at a given time was needed. The vehicle's solar array system was perpendicular to the vehicle's

TABLE 7-3
TRENDS DERIVED FROM MEASURED RATES

DATE	ϕ ~ o	θ ~o	$\dot{\Psi}$ ~^{o}/SEC	$\dot{\gamma}$ ~^{o}/SEC	RATE ABOUT X_p ~^{o}/SEC
3-11-78	12.4	2.3	.24	.96	1.20
5-5-78	22.8	4.7	.34	1.28	1.60
5-7-78	23.9	5.0	.35	1.28	1.60
5-10-78	21.2	4.3	.34	1.28	1.60
5-30-78	28.1	5.9	.39	1.41	1.76
6-01-78	27.0	5.7	.39	1.41	1.76
6-06-78	36.0	8.1	.42	1.39	1.73
6-07-78	31.0	6.7	.40	1.39	1.73

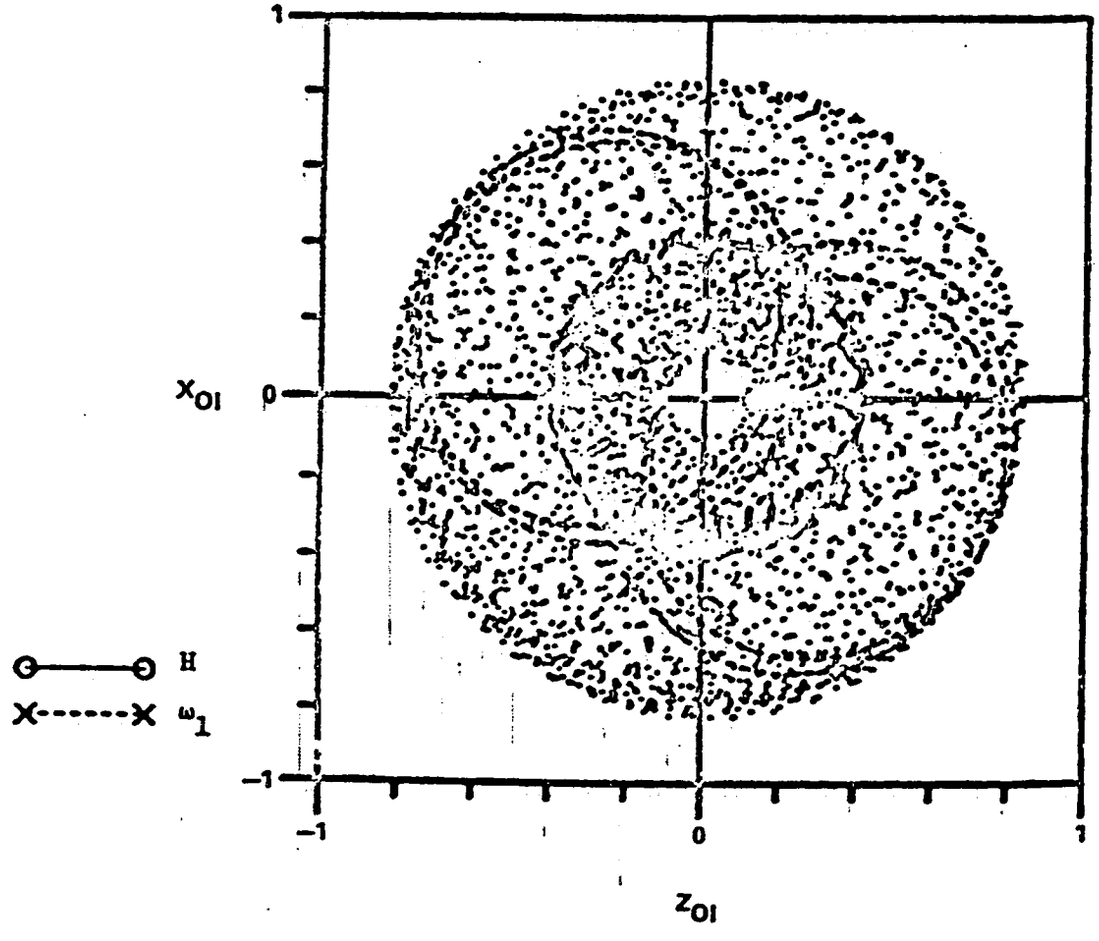

FIGURE 7-9 MOTION OF MOMENTUM VECTOR, ANGULAR VELOCITY VECTOR, AND SPIN AXIS FOR 24 HOUR PERIOD AS VIEWED IN AN INERTIALLY FIXED SYSTEM

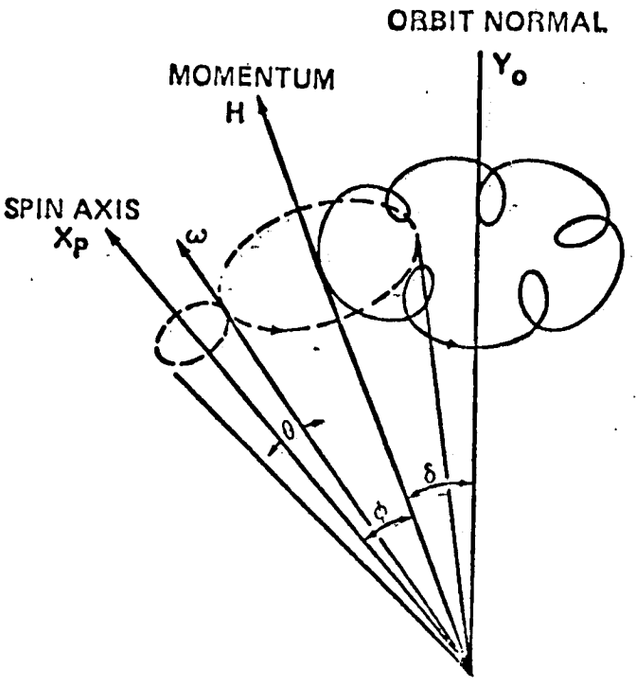

FIGURE 7-10 MOTION OF VEHICLE AXIS OF SYMMETRY, X_p, ANGULAR VELOCITY VECTOR, ω, AND MOMENTUM VECTOR, H, AS VIEWED INERTIALLY.

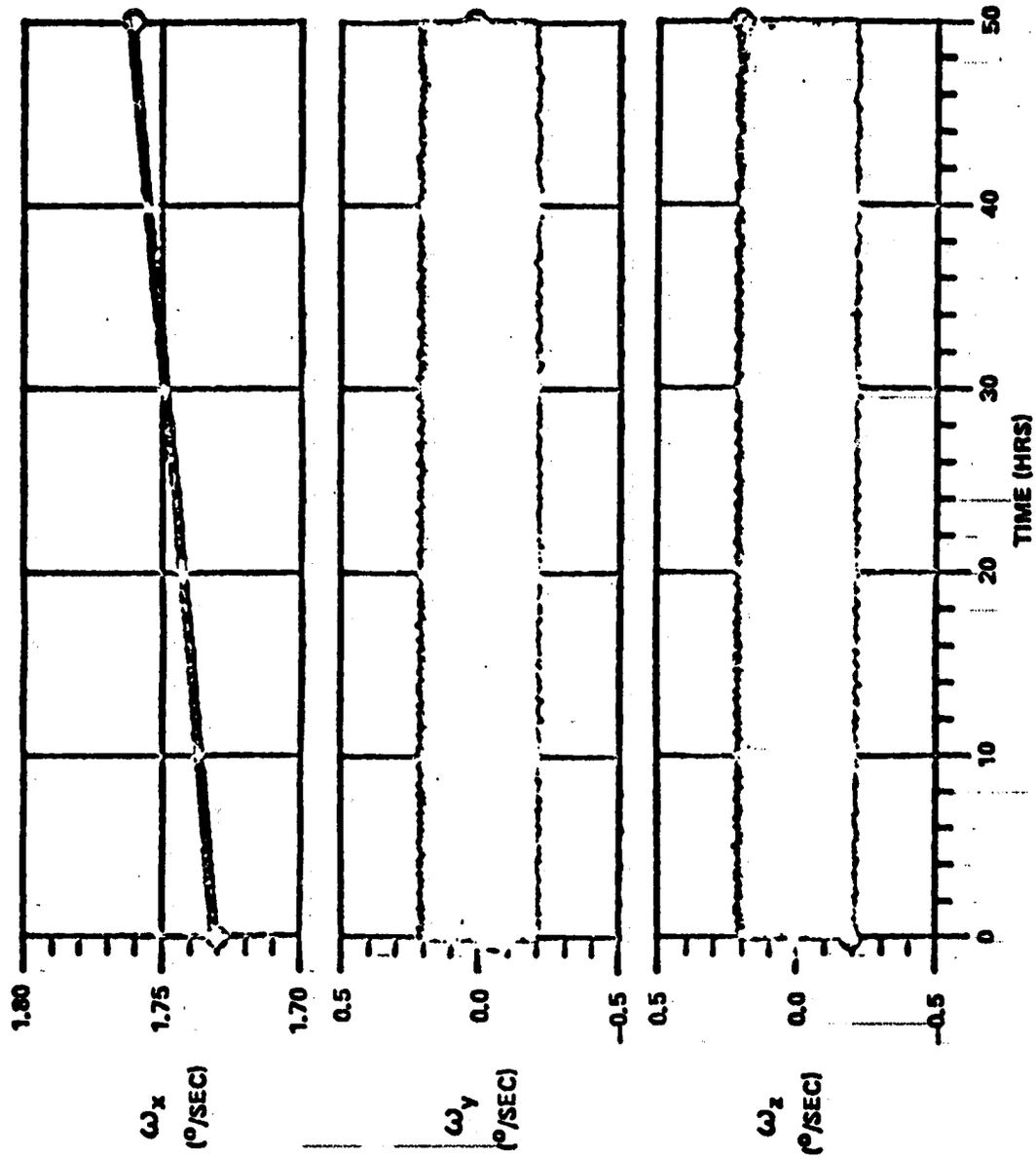

FIGURE 7-11 BODY RATES VS TIME

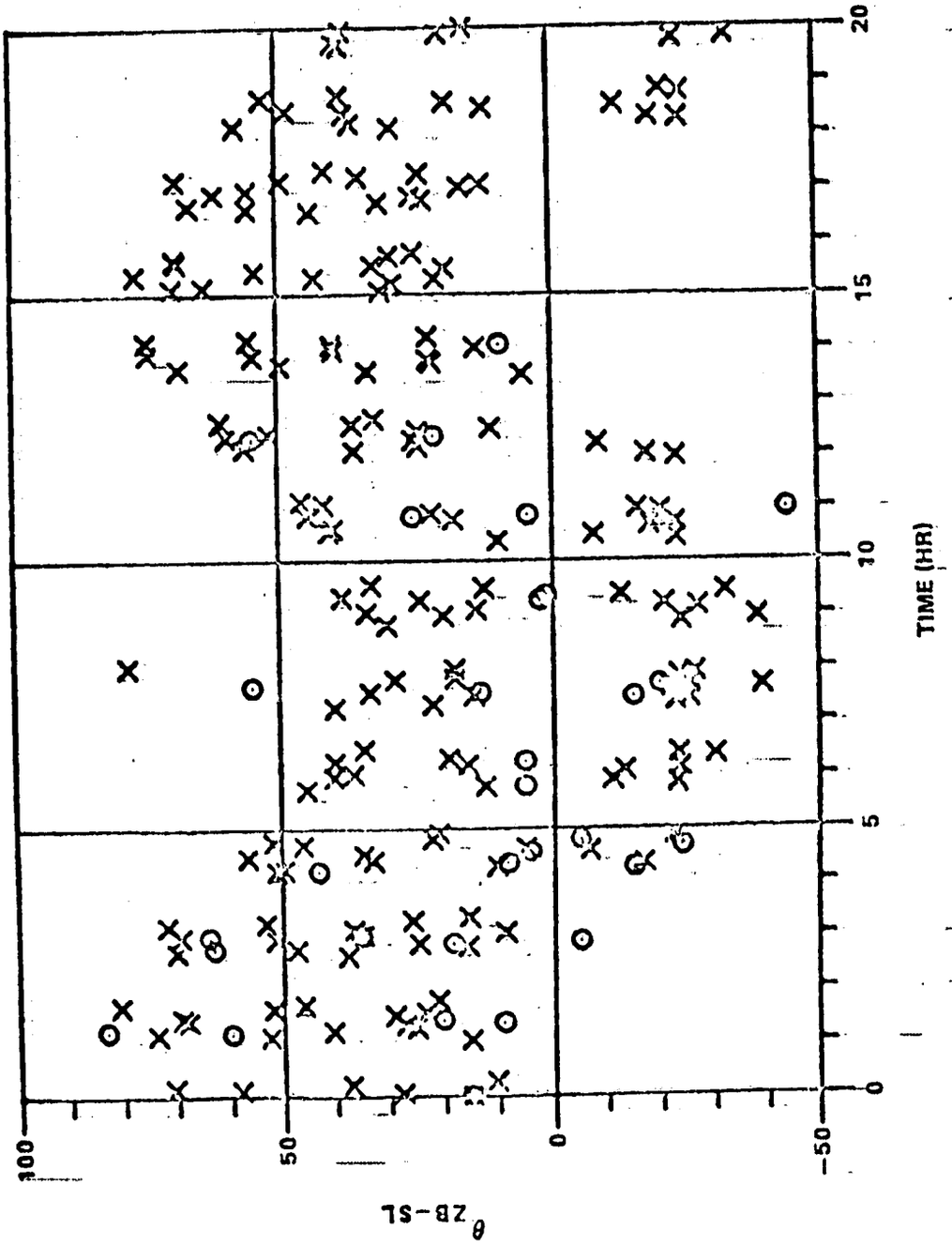

FIGURE 7-12 COMPARISON OF MEASURED VEHICLE ATTITUDE RELATIVE TO SOLAR VECTOR WITH SIMULATION RESULTS

Z_B axis. Since the vehicle was rotating at nearly 2°/sec about the X_B axis, the side of the arrays with the solar cells attached would go through a light-dark cycle every three minutes. From an examination of the maximum output level and knowledge of the array performance, one could estimate the minimum angle between the Z_B axis and the sunline ($\theta_{Z_B\text{-}SL}$). This would only give a magnitude, however, and other data had to be used to determine sign. Fortunately for most of this period, the acquisition sun sensor was available and, though the angles were usually beyond its linear range, its signature did indicate sign. The O points plotted in Figure 7-12 are the result of combining these data to give the minimum angle between Z_B and the sunline. Note, there are some data gaps. These were due to the necessity of having the vehicle simultaneously in the sun and over the ground station.

The X points in Figure 7-12 were obtained from the simulation and represent the vehicle's attitude to the solar vector in the manner indicated above. Since the flight data consist of discrete points covering quite a range, it would be incorrect to say that the simulation results duplicate the observed data in the usual sense. However, the simulation results and observed data do exhibit the same ranges and periodic characteristics leading one to conclude that the vehicle's motion was probably very close to that indicated by the simulation.

7.3 SUMMARY

The motion of Skylab prior to the resumption of active control provided an illustration of the effect of aerodynamic and gravity gradient torques on vehicle motion. Once the vehicle began to rotate, gyrodynamic effects began to play an important part and this became more pronounced as the spin rate increased. Though complex, this behavior can be predicted both numerically and analytically. In the course of this study, the complementary roles of both numerical integration and closed form analysis were demonstrated. In cases such as this, a combined approach will produce better results than either approach alone.

8.0 MISSION ANALYSIS

8.1 INTRODUCTION

This section discusses the mission analysis and trajectory aspects of Skylab from the end of the active manned phase, February 8, 1974, until impact on July 11, 1979, at 16:37:30 GMT.

8.2 BACKGROUND

At the end of the Skylab manned mission Skylab was expected to remain in orbit between 5 1/2 and 9 years. (Mid 1979 to 1983). This prediction was based on the 1974 prediction of solar cycle 21, a theoretical ballistic coefficient and assumption that Skylab would remain in a gravity-gradient attitude until impact. The theoretical ballistic coefficient ($BC = W/C_D A$), was calculated for the OWS solar panel trailing the direction of flight, where W is the weight in kg., C_D is the drag coefficient, and A is the area in M^2. The ballistic coefficient was calculated as 207 kg/m^2. Six months later the BC was determined to be 140 kg/m^2 based upon the comparison of Skylab's actual and predicted decay. This change reduced the expected Skylab reentry by approximately 2 1/2 years.

It was determined in the fall of 1977 that Skylab had left the original gravity gradient attitude and was experiencing an increased orbital decay rate. In addition, there was a greater solar activity increase than expected at the beginning of solar cycle 21. This increased activity increased the drag forces on the vehicle. Skylab was then predicted to reenter the earth's atmosphere in late 1978 or early 1979 unless something was done to reduce the drag forces acting upon it. It was necessary to make a decision to either accept an early uncontrolled reentry of Skylab or to attempt to actively control Skylab in a lower drag attitude thereby extending its orbital lifetime until a Shuttle mission could effect a boost or deorbit maneuver with Skylab. From the fall of 1977 on, it became increasingly important to accurately determine the remaining lifetime of Skylab in order to ascertain which of several options might be available to NASA in regard to the disposition of Skylab. As the mission progressed and the various attitude options were selected their effect on mission lifetime had to be continually monitored.

As is now apparent, the combination of the above-mentioned conditions and others to be discussed (changes in the ballistic

coefficient, changes in Skylab's attitude, changes in the predicted solar maximum date and magnitude) resulted in the earlier than orginally expected Skylab reentry. Predicting Skylab's lifetime was a very complex and non-deterministic analysis which continually required updating as new information became available.

8.3 SOLAR ACTIVITY

A predominant factor in predicting the lifetime of orbiting vehicles is the orbital atmospheric density level that the vehicle is expected to experience. The density is a function of solar activity and altitude. For reference Figure 8-1 summarizes the predicted peak solar (smoothed sunspot number, $\bar{R}_{13}$) activity level for solar cycle 21 made throughout the time period Skylab was in orbit from December 1972 through May 1979. It should be noted that it was the integrated effect upon the vehicle's lifetime of the actual orbital density and not a single peak value for the cycle that determined the lifetime of Skylab. The 50% (nominal) and the 90%/95% confidence bands are shown. Several other solar predictions made during the period by other organizations are shown for comparison purposes.

The 50% or nominal value of the predicted peak sunspot number at the time of Skylab's impact was greater than the upper level of the 90% confidence band for the predictions made at the end of the manned period in early 1974. Figure 8-1a is provided for reference on the predicted behavior of sun spots to $\bar{F}_{10.7}$ cm flux activity since the $F_{10.7}$ cm data is what is actually utilized in the atmospheric density model used to predict satellite lifetimes. The predicted date of the solar activity maximum along with the maximum sun spot magnitude and the corresponding $\bar{F}_{10.7}$ cm solar flux magnitude are shown as a function of the date of the solar activity prediction. The predictions are shown for the entire period Skylab was in orbit along with some preflight and post flight predictions. The predicted date of the solar maximum, also shown on Figure 8-1a, varies from early 1982 for the 1974 predictions to late 1979 at the time of Skylab's impact. The combination of higher peak and earlier date of the peak reduced the Skylab lifetime since both factors cause an increase in density.

Figures 8-2 through 8-5 show the actual solar activity during Skylab's orbital lifetime. The daily $\bar{F}_{10.7}$ cm solar flux, the 162 day average of solar flux ($\bar{F}_{10.7}$) and the daily geomagnetic index (Ap) variations are shown. During the time Skylab was in orbit the maximum 162 day solar flux average reached a maximum of 185.

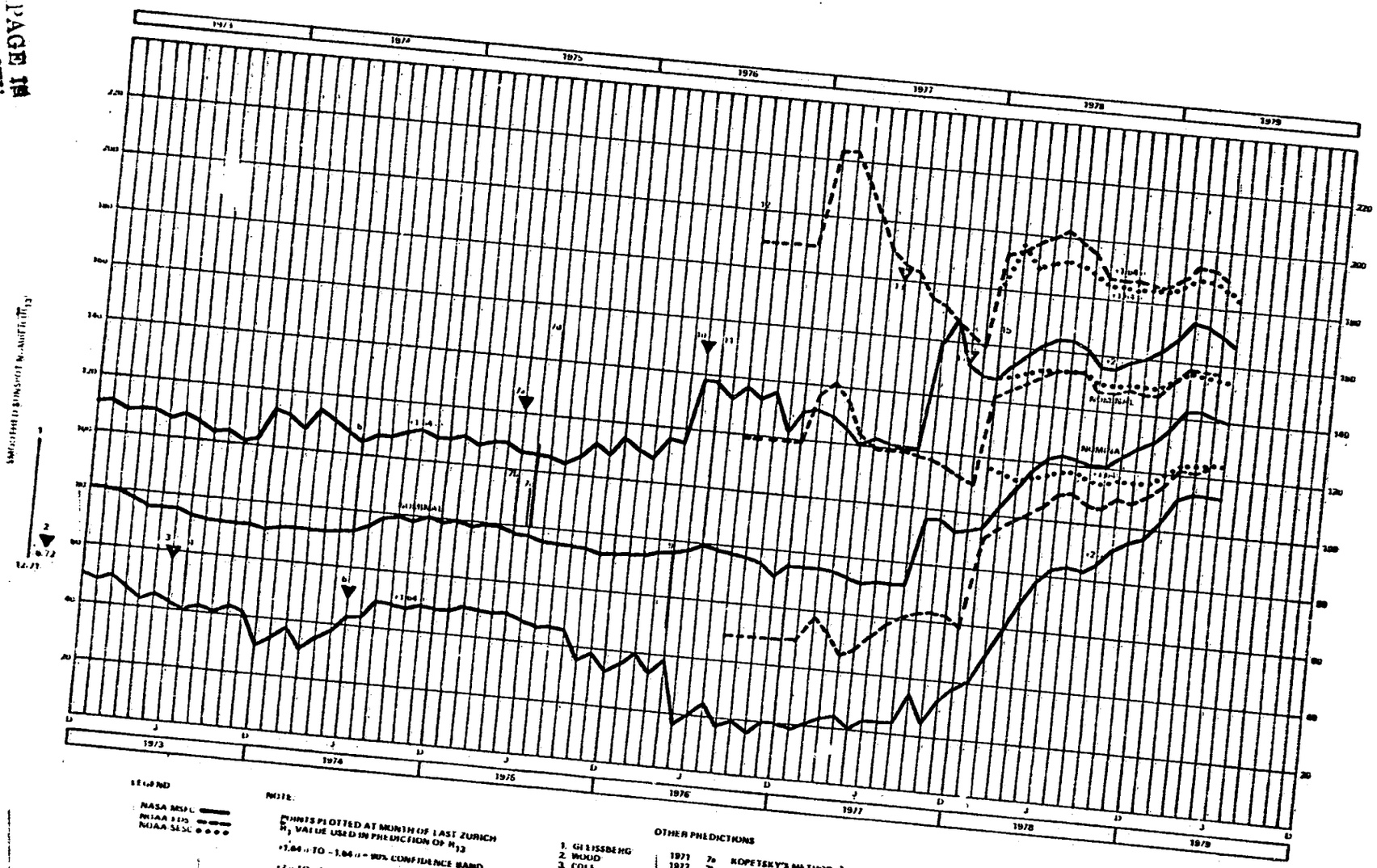

FIGURE 8–1 SOLAR CYCLE 21 PREDICTED PEAK SMOOTHED SUNSPOT NUMBER ($\overline{R}_{13}$)

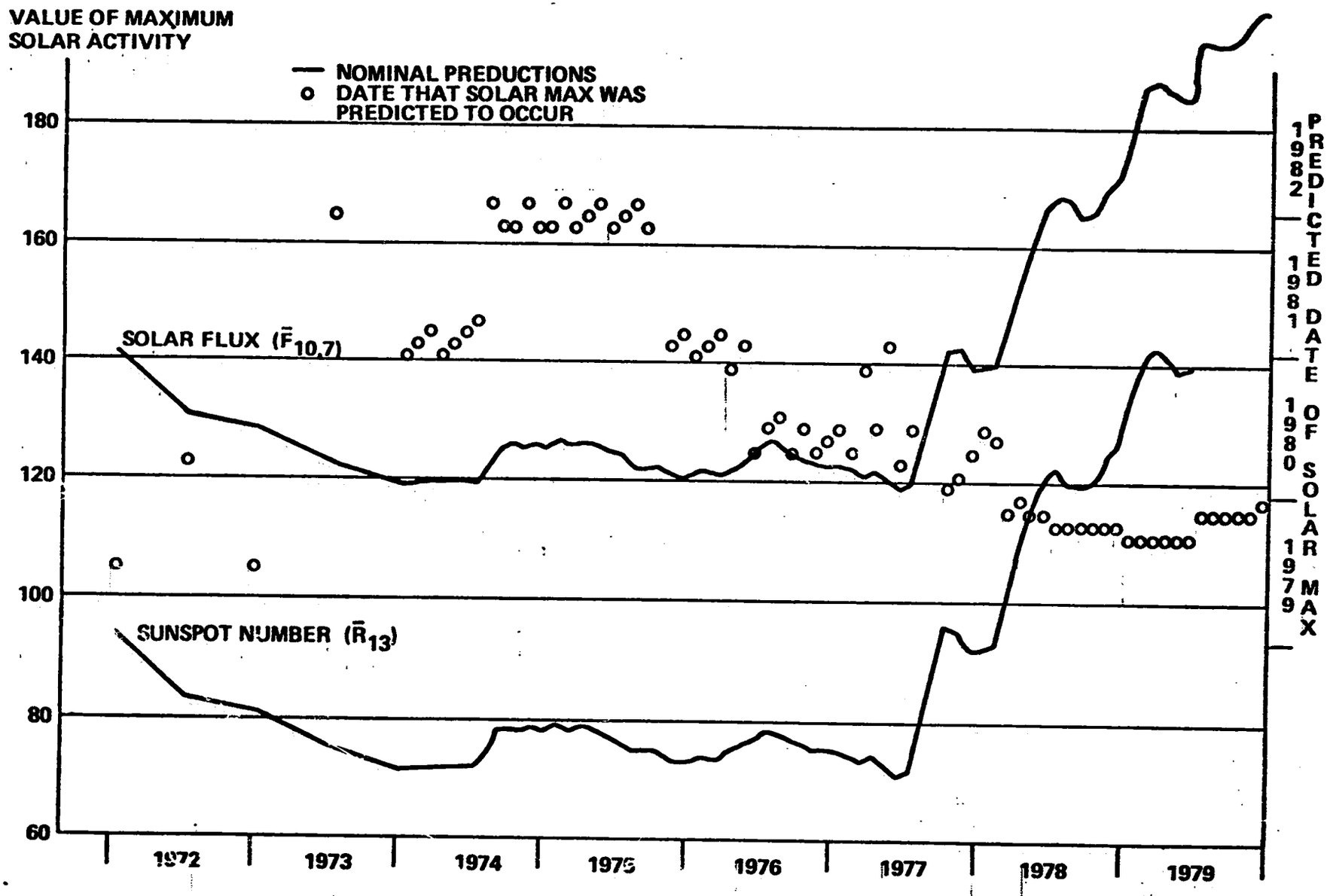

DATE OF SOLAR ACTIVITY PREDICTION (MSFC)

FIGURE 8-1A SOLAR MAX PREDICTIONS

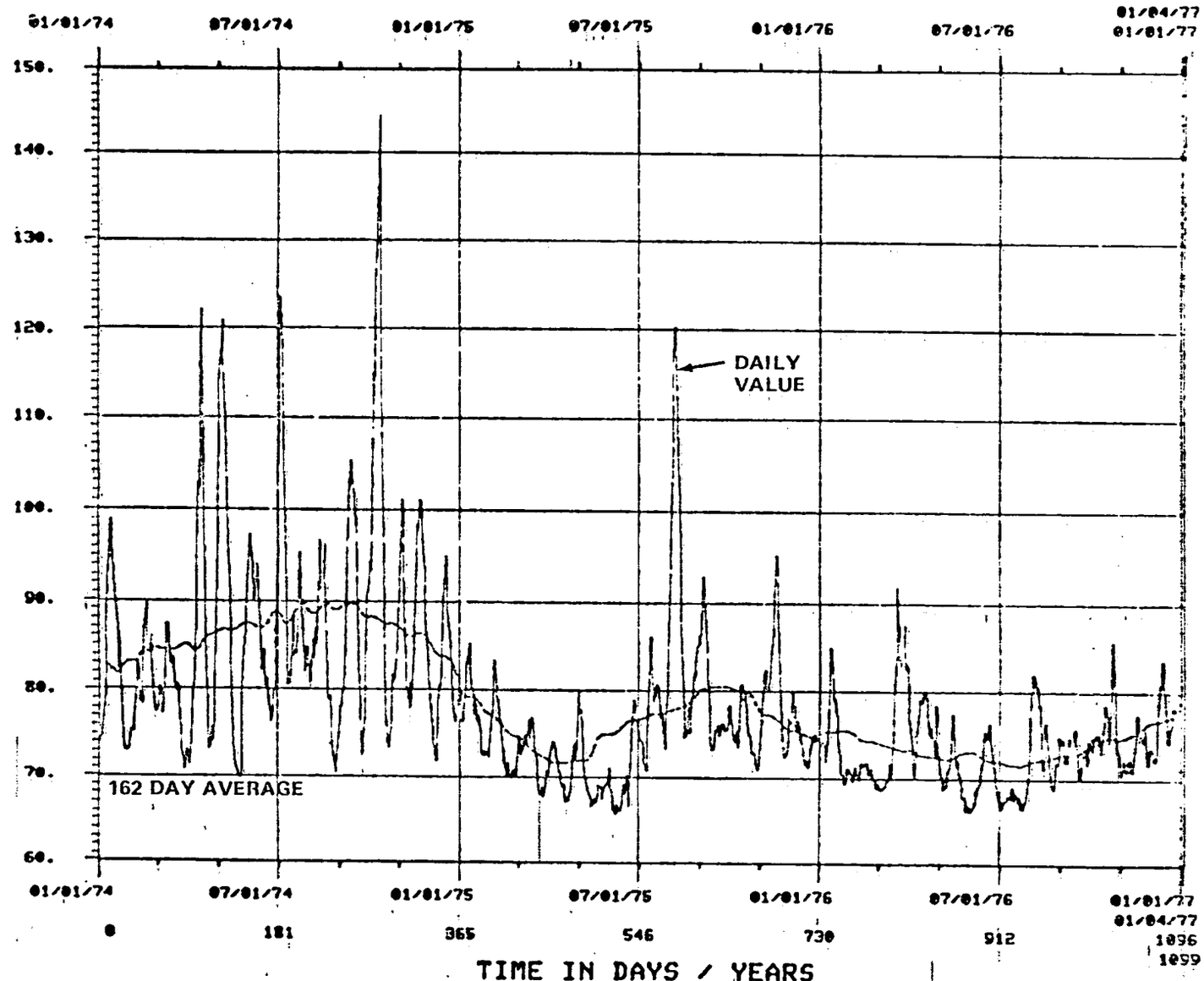

F10.7 & F10.7 AVERAGE DATA

MIPS>

FIGURE 8-2 ACTUAL DAILY AND AVERAGE F10. 7cm SOLAR FLUX

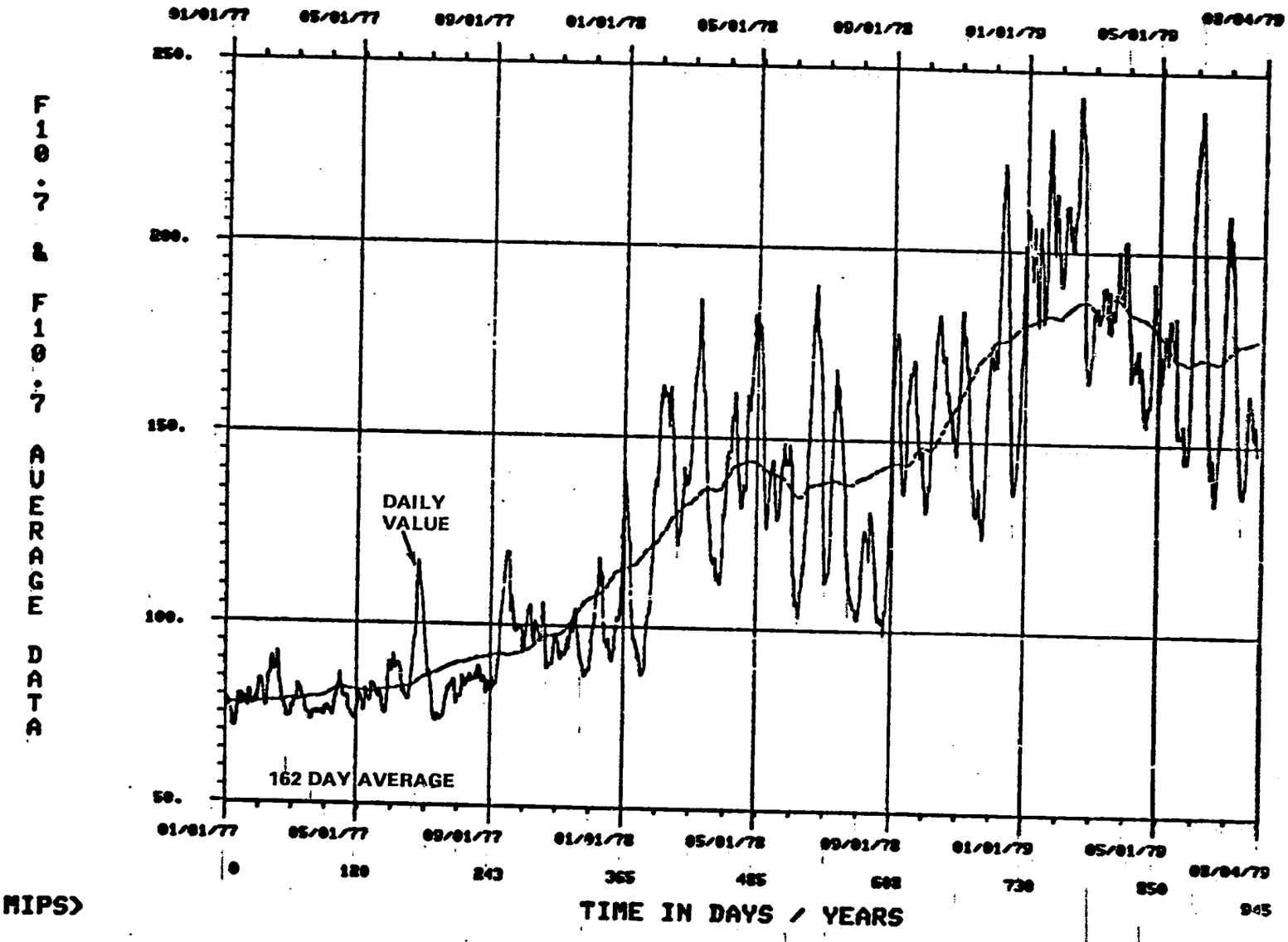

FIGURE 8-3 ACTUAL DAILY AND AVERAGE F10. 7cm SOLAR FLUX

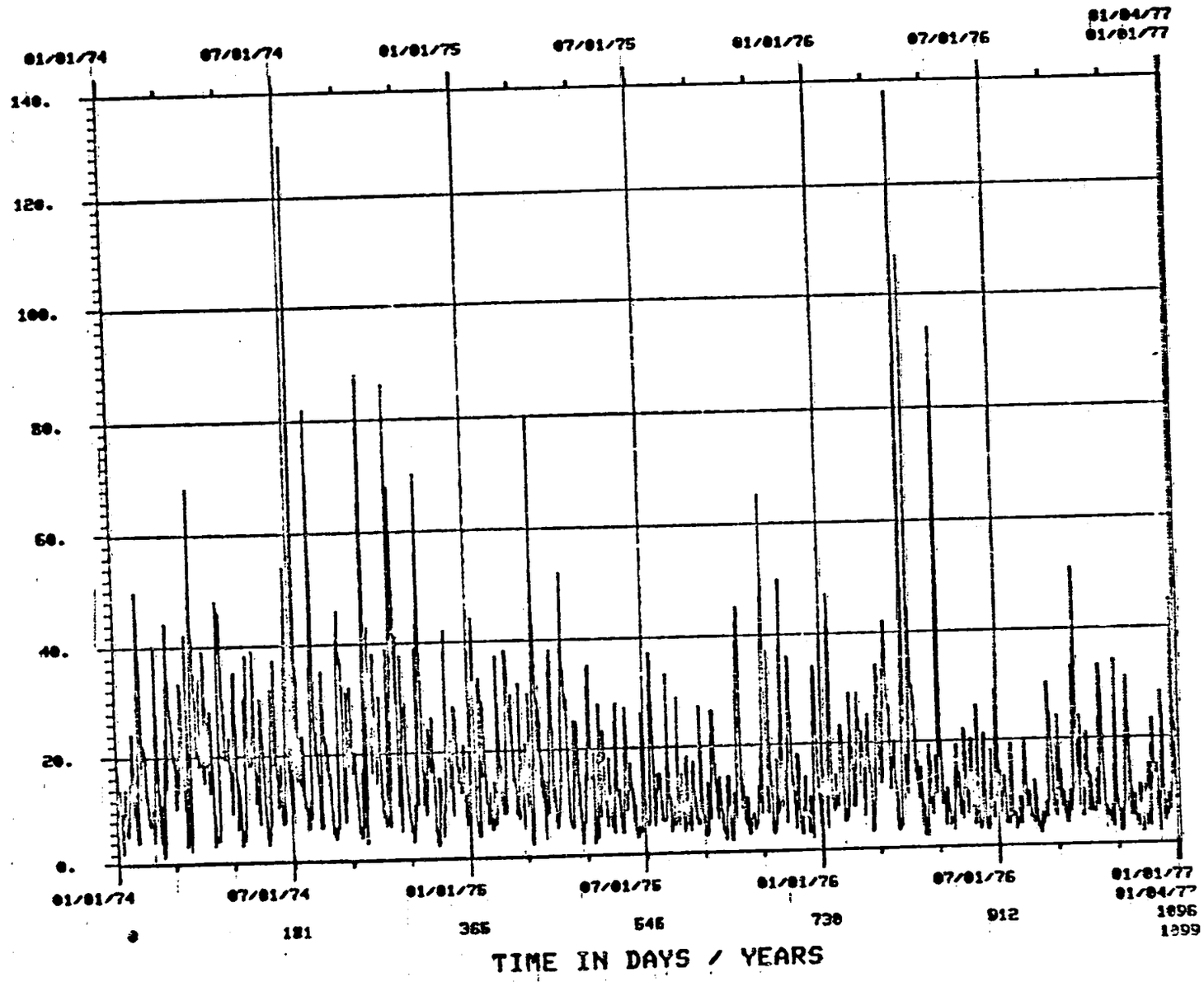

FIGURE 8-4 ACTUAL GEOMAGNETIC ACTIVITY

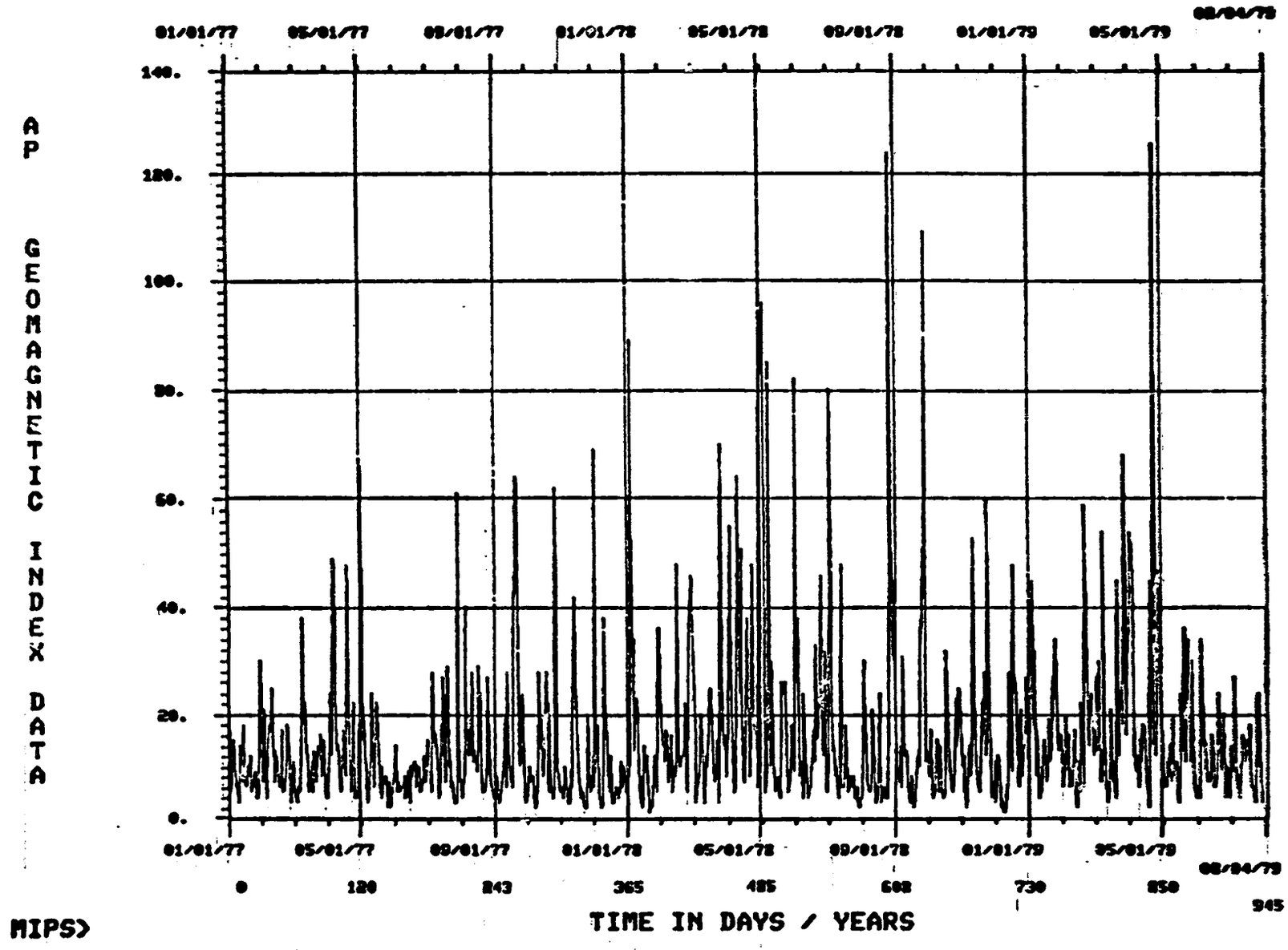

FIGURE 8-5 ACTUAL GEOMAGNETIC ACTIVITY

8.4 SKYLAB ORBITAL DECAY MAY 1974 TO JUNE 1978

Skylab began experiencing orbital decay as soon as it was placed in orbit in May 1973. During the manned portions of the Skylab mission several attitude adjustments were made to compensate for the orbital decay. Shortly before the last crew left Skylab (February 1974) the Apollo Command and Service Module boosted Skylab into an orbit slightly higher (238 nm) than the original 235 nm orbit. After the last crew left, Skylab was commanded to a gravity-gradient stabilized attitude. Figure 8-6 shows the decay of the Skylab orbital altitude from launch to impact. Mean orbital elements were received from NORAD (North American Air Defense) on a regular basis during the passive Skylab period. One of the parameters received was mean motion from which the mean semi-major axis could be calculated. With the actual semi-major axis for comparison and the actual solar activity data, the lifetime prediction program could be utilized to determine a ballistic coefficient that matched the actual decay. During the passive period the "best" decay comparison was found utilizing a ballistic coefficient of 130 kg/m^2. Figures 8-7 and 8-8 show the predicted (based on the ballistic coefficient of 130 kg/m^2) and the actual altitude decay and the decay rates during the passive Skylab period. The actual and predicted decay matched well until the middle of 1976 when the predicted decay began to slightly exceed the actual decay. By the end of 1977 the actual decay was exceeding the predicted decay. Over the entire passive period the actual and predicted altitudes differed no more than 1 km. Decay comparisons made for shorter periods (6 months to 1 year) resulted in different ballistic coefficients (From 120 to 144 kg/m^2). Figures 8-9 shows the Beta angle history during the passive Skylab period.

A number of Skylab lifetime predictions were made during the passive period which are depicted on Figure 8-10. The 50% or nominal and the 97.7% or +2 level predictions are shown. The ballistic coefficient used in making the predictions are shown. The ballistic coefficient used in making the prediction are denoted along with the predicted impact time. The preflight value of 122 kg/m^2 was based upon the two panel configuration, the best available weights, and the preflight theoretical aerodynamics, assuming that the vehicle would be controlled in the SI attitude to impact.

During the unmanned period between the first and second visit (approximately 5 weeks) a decay comparison was made to determine the ballistic coefficient. That is, the actual orbital decay was compared to the decay predicted with the lifetime prediction program. The resulting ballistic coefficient that gave the "best" decay comparison was 170 kg/m^2. After the manned Skylab mission was completed the vehicle was understood to be left in a

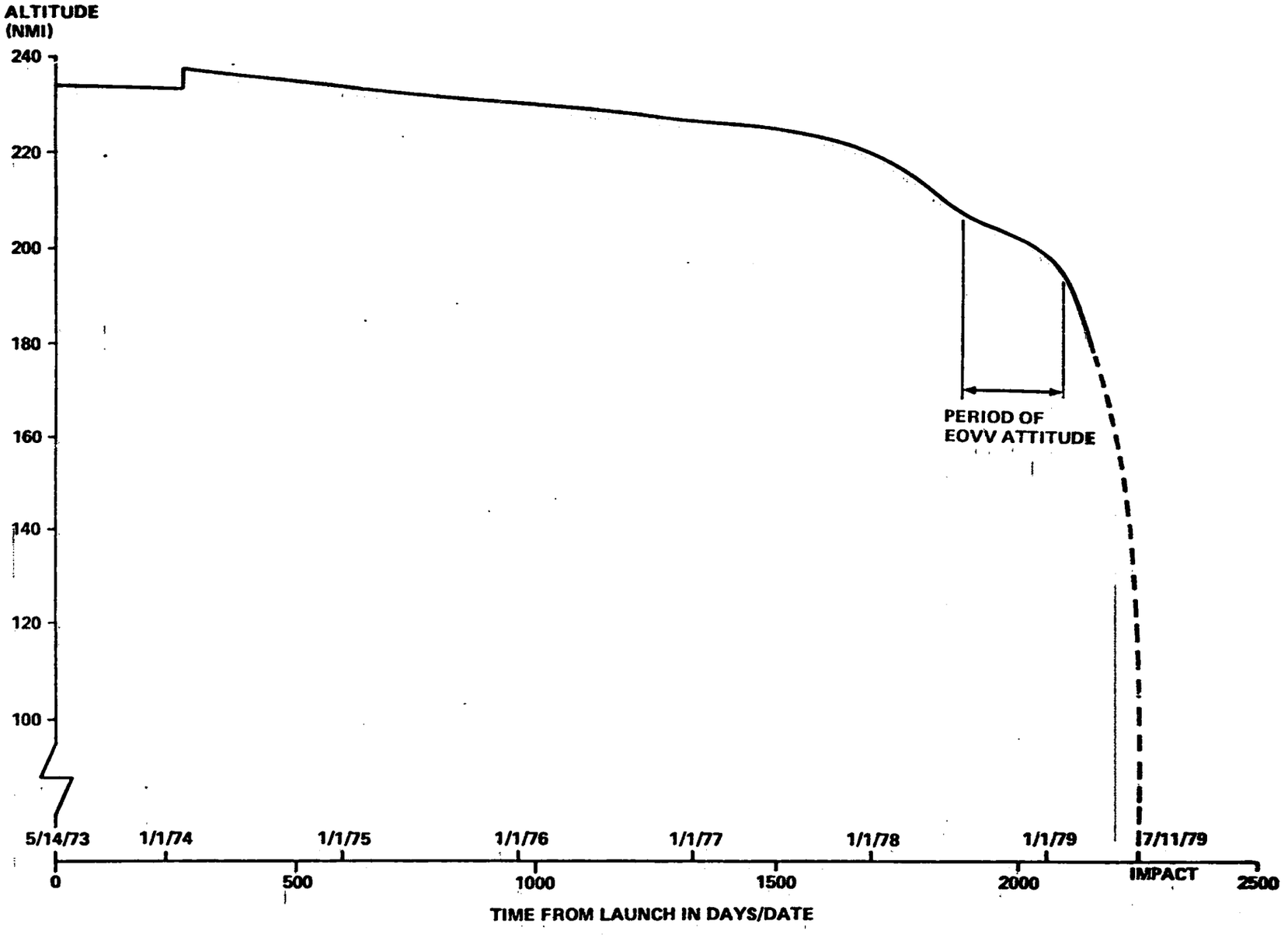

FIGURE 8-6 SKYLAB ORBITAL DECAY LAUNCH TO IMPACT

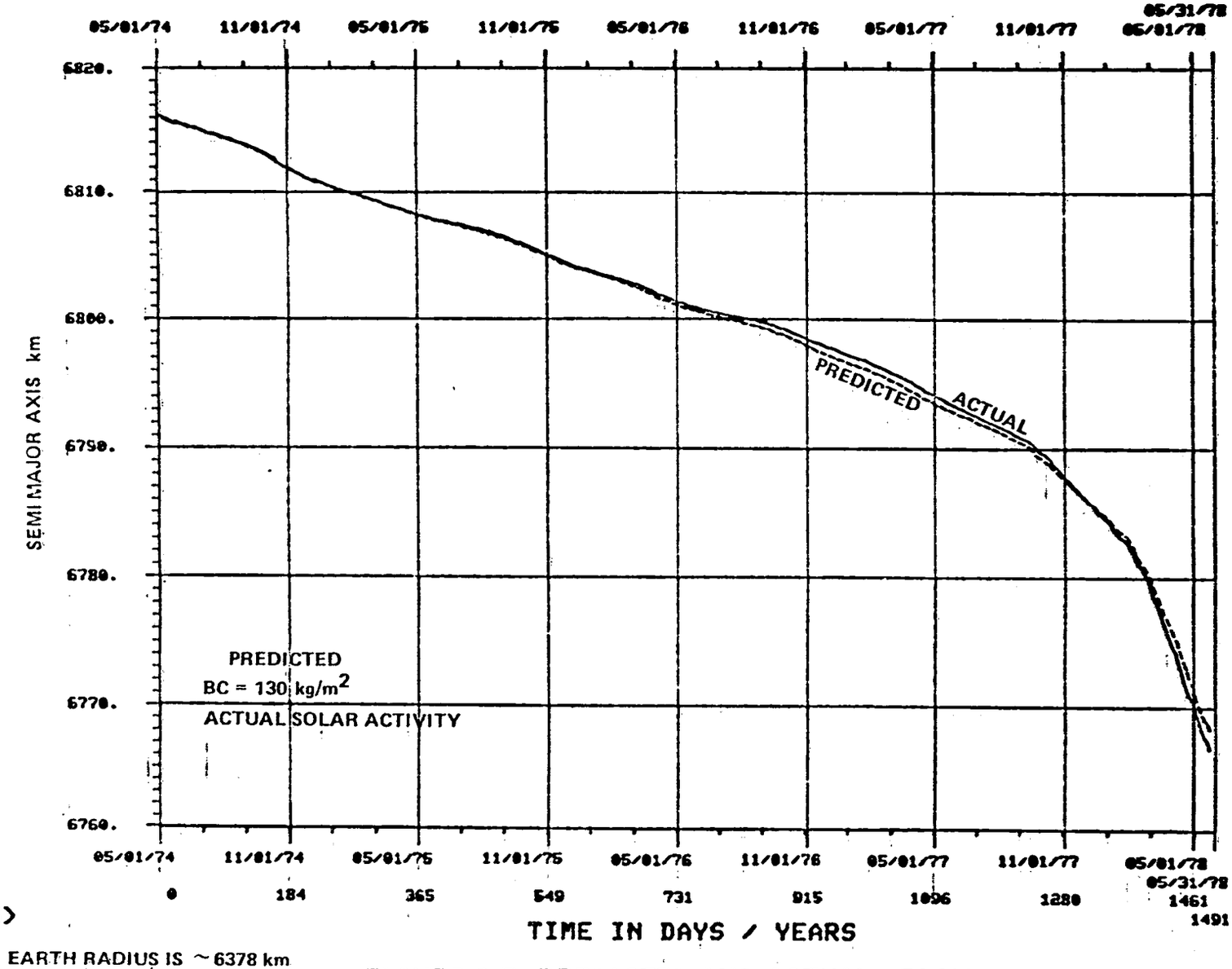

MIPS>

NOTE: EARTH RADIUS IS ~6378 km

FIGURE 8-7 PREDICTED AND ACTUAL DECAY

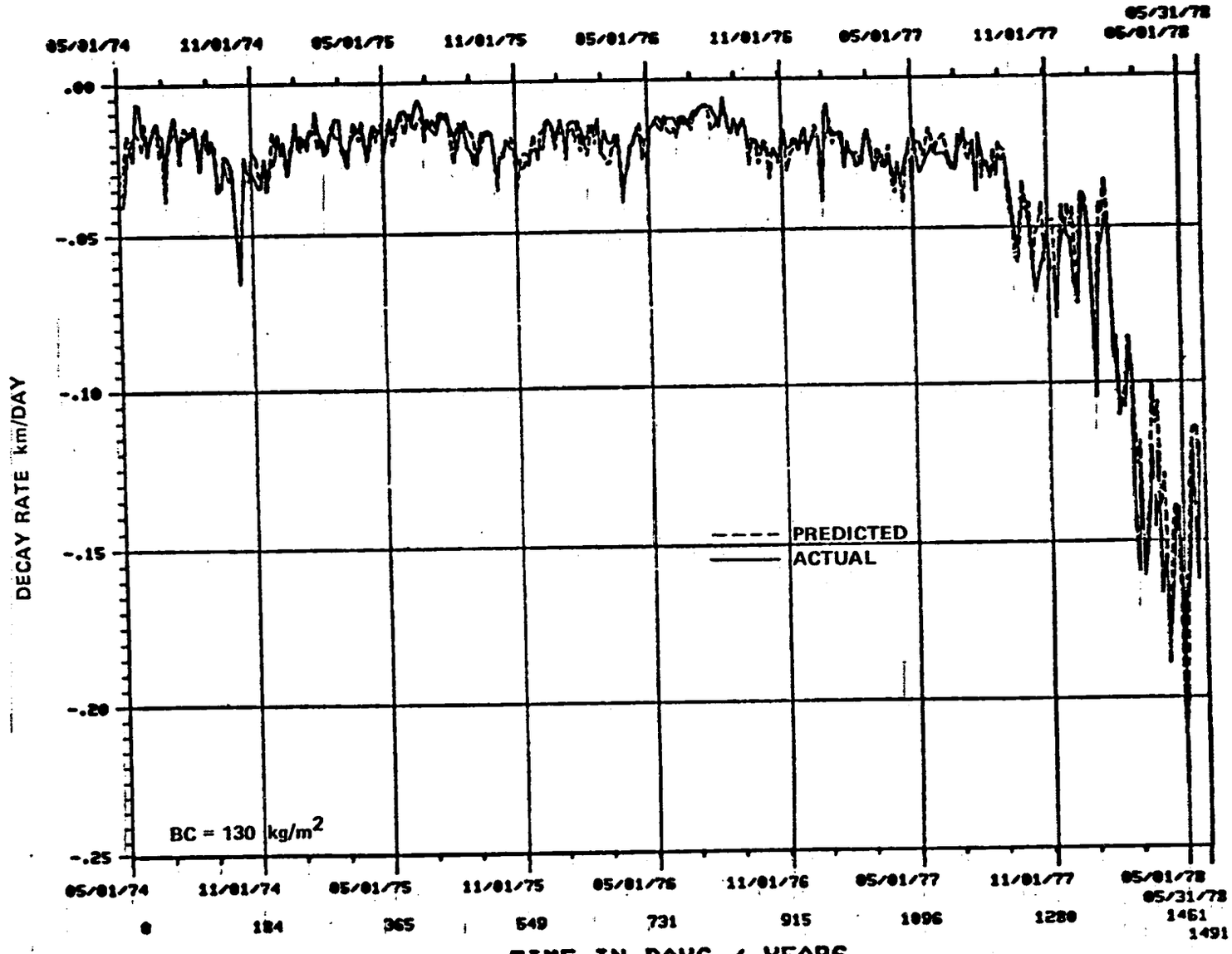

MIPS>

FIGURE 8-8 PREDICTED AND ACTUAL DECAY RATES

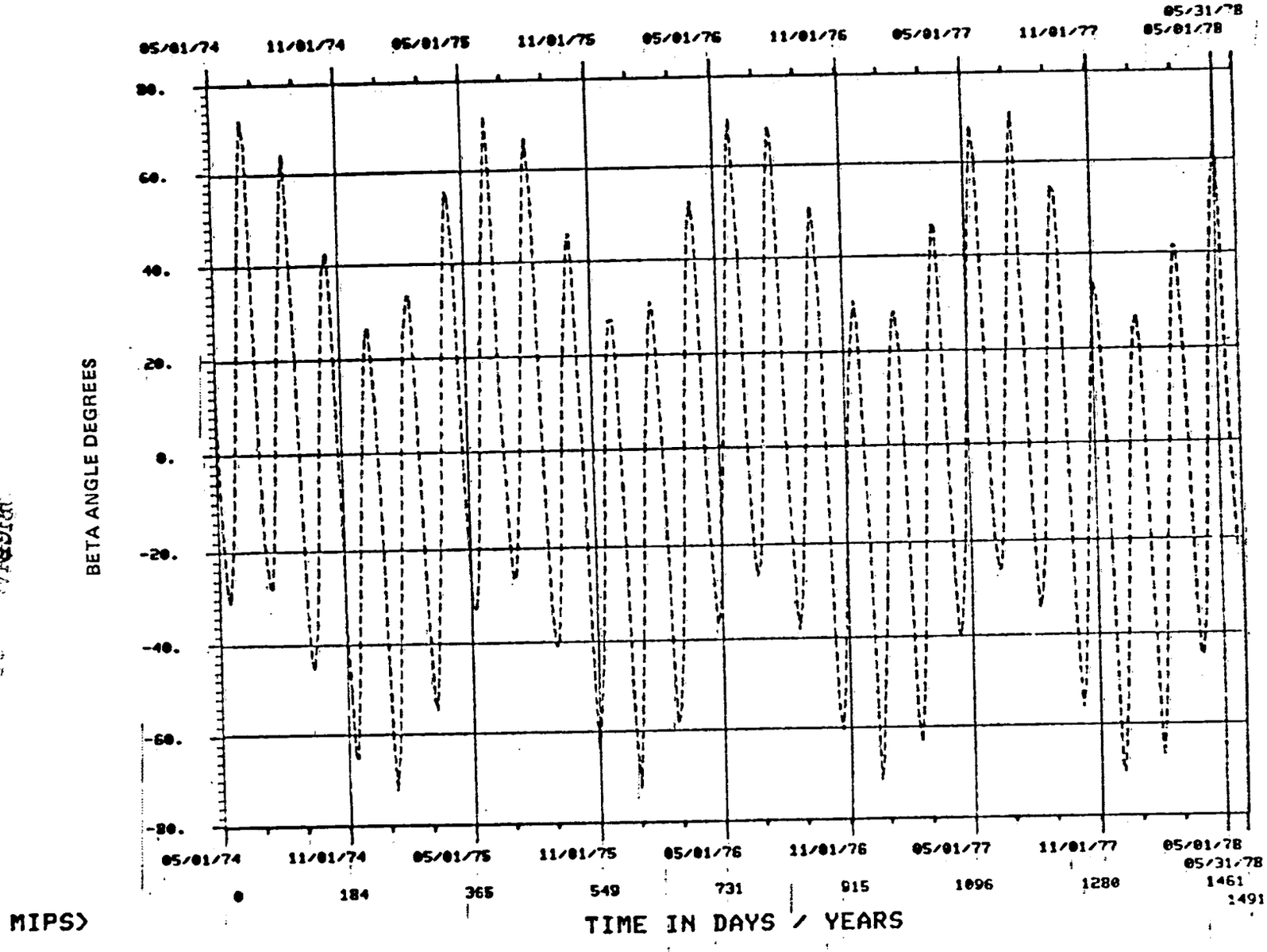

MIPS>

FIGURE 8-9 SKYLAB BETA ANGLE VS DATE

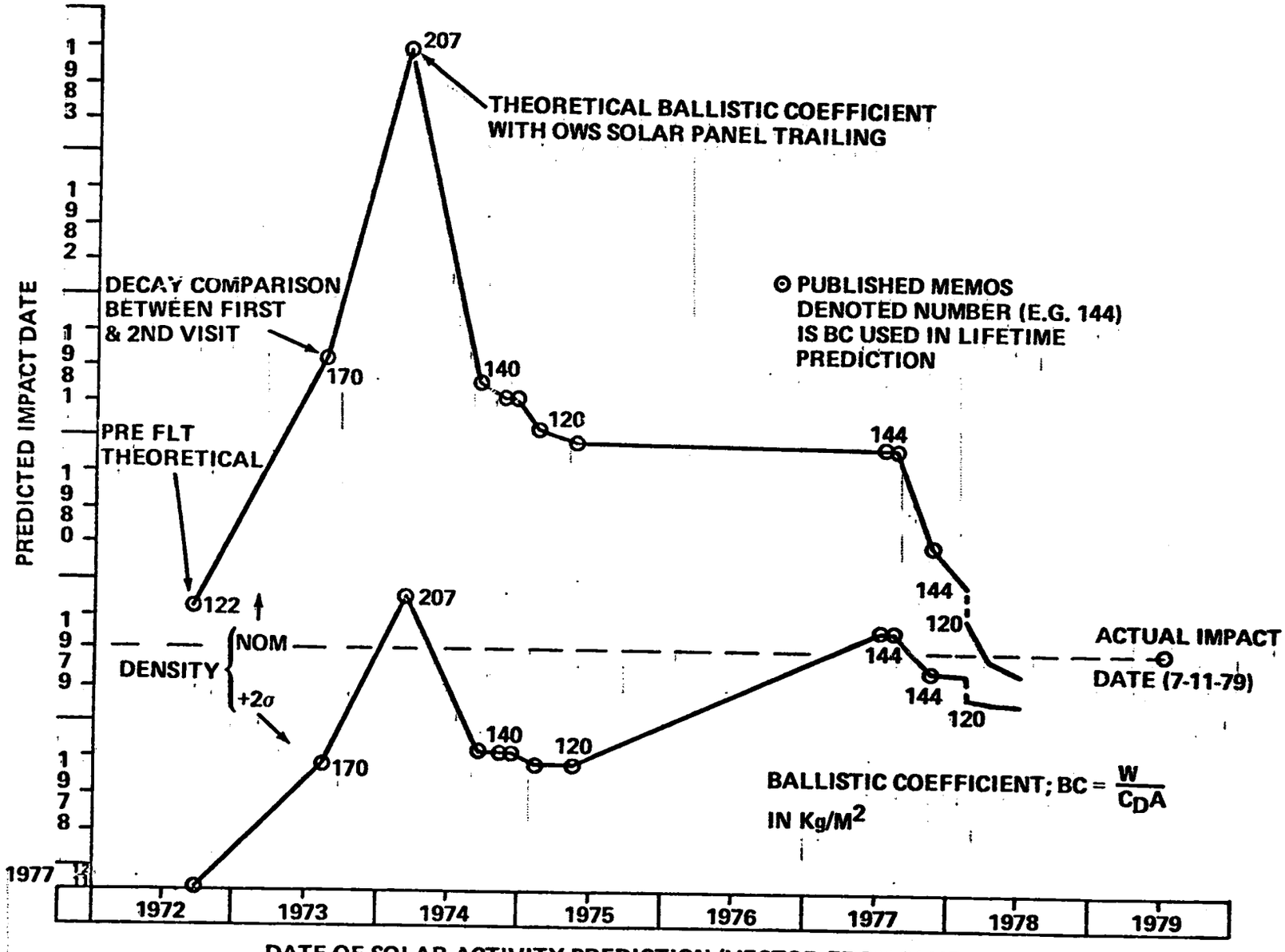

FIGURE 8-10 LIFETIME PREDICTIONS

gravity-gradient stabilized attitude (x-local vertical, docking port away from the earth, and a roll attitude such that the OWS solar panel was trailing in relation to the orbital motion). This was the basis for the 207 kg/m^2 used in making the end of mission lifetime prediction, rather than the smaller value (122/170) for the solar inertial attitude. However, in 1977 when renewed interest in Skylab's impact developed it was learned that Skylab was left in the above attitude with the exception that the ATM was trailing rather than the OWS solar panel. This made a significant difference in the area relative to the velocity vector. The resulting theoretical ballistic coefficient for this attitude was 96 kg/m^2. All other ballistic coefficients shown on Figure 8-10 are based upon decay comparisons of 6 months to one year in duration. Once enough time had passed that a decay comparison could be made, Skylab's ballistic coefficient was determined to be 140 kg/m^2 for the period just after the last manned mission. Thus the gravity-gradient stabilized attitude of Skylab was not with the ATM or OWS solar panel exactly trailing the direction of orbital motion. In fact, the ballistic coefficient was almost midway between the ballistic coefficients of these two attitudes. Other decay comparisons were made which resulted in approximately the same magnitude ballistic coefficient. However, toward the end of the Skylab's flight the impact predictions occurred earlier. This is because the actual solar activity began its dramatic increase during the latter part of 1977. This increase was subsequently reflected in the solar activity predictions and contributed to the earlier predicted impact dates.

8.5 SKYLAB ORBITAL DECAY JUNE 1978 THROUGH JANUARY 1979

Development of the EOVV control mode (see Section 2.1.1) resulted from the decision to extend Skylab's orbital life until a reboost or deorbit via an orbital retrieval system could be accomplished. Skylab was in the EOVV attitude from June 11, 1978 through January 25, 1979 except for a short time in June/July. The effect of the EOVV attitude on orbit decay is illustrated in Figure 8-6. A noticeable decrease in orbit decay rate (from 128 m/day to 51 m/day average) is evident when Skylab was first maneuvered into the EOVV attitude in June 1978. Likewise, an increase in the orbit decay rate (from 144 m/day to 385 m/day average) occurred when Skylab was maneuvered from the EOVV attitude to the Solar inertial attitude in January 1979. The time spent in the EOVV attitude extended Skylab's orbital lifetime approximately 3 1/2 months. If Skylab had remained in the EOVV attitude until impact, reentry would have probably occurred very early in 1980. While Skylab was in the EOVV attitude the ballistic coefficient varied as a function of the

beta angle. This was due to the solar panels being held toward the sun. Figure 8-11 shows the Beta angle over the EOVV attitude period. Figure 8-11a shows how the ballistic coefficient varied while in the EOVV attitude. The ballistic coeficient varied from 303 to 333 kg/m^2.

As in the passive phase of Skylab's orbital life, comparisons of the actual decay and predicted decay over the EOVV control period were made using the variable ballistic coefficient time history in Figure 8-11a and actual solar activity inputs to the orbital atmospheric density model. Figure 8-12 shows the actual and predicted altitude history. Figure 8-13 shows the actual and predicted decay rate. It is obvious that after about two months of very good comparison the predicted altitude does not decay rapidly enough. This behavior is attributed in part to rapid changes in the solar activity that are not totally accounted for in the orbital atmospheric density model utilized in the orbit lifetime prediction program. This phenomenon was verified in-house and in discussions with SAO (Smithsonian Astrophysical Observatory) whose model forms the basis for NASA SP-8021, as well as by observation and comparison with other satellites. The derived bias of the density model averaged approximately 6% over the EOVV period. Figures 8-14 and 8-15 show the actual and predicted decay comparison using the 6% atmospheric density bias. A much better comparison between the actual and predicted data was obtained. Numerous lifetime predictions were made during the EOVV period. Table 8-1 summarizes the lifetime predictions. The EOVV attitude was assumed to be held until impact in these predictions.

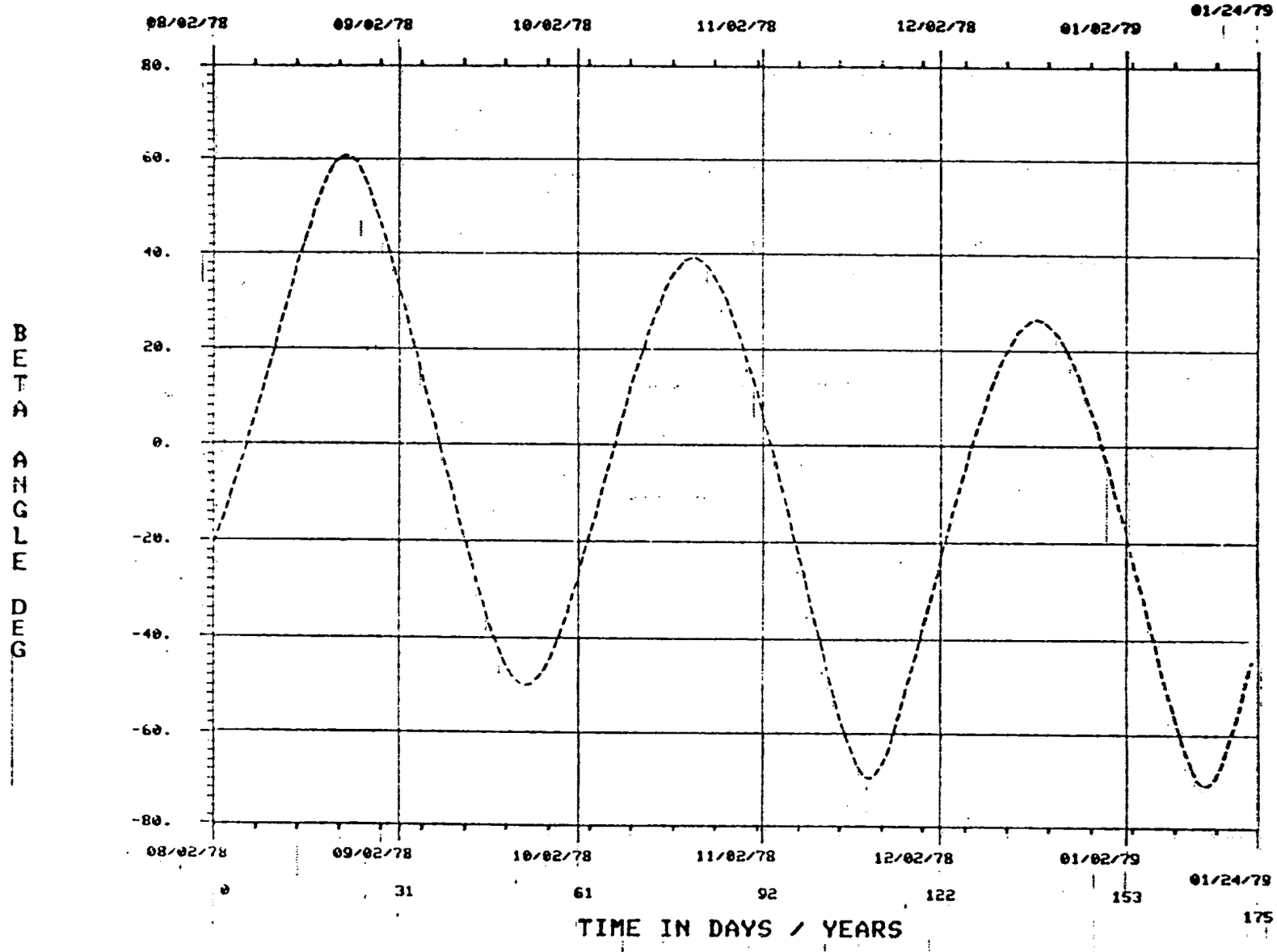

FIGURE 8-11 BETA ANGLE DURING EOVV PERIOD

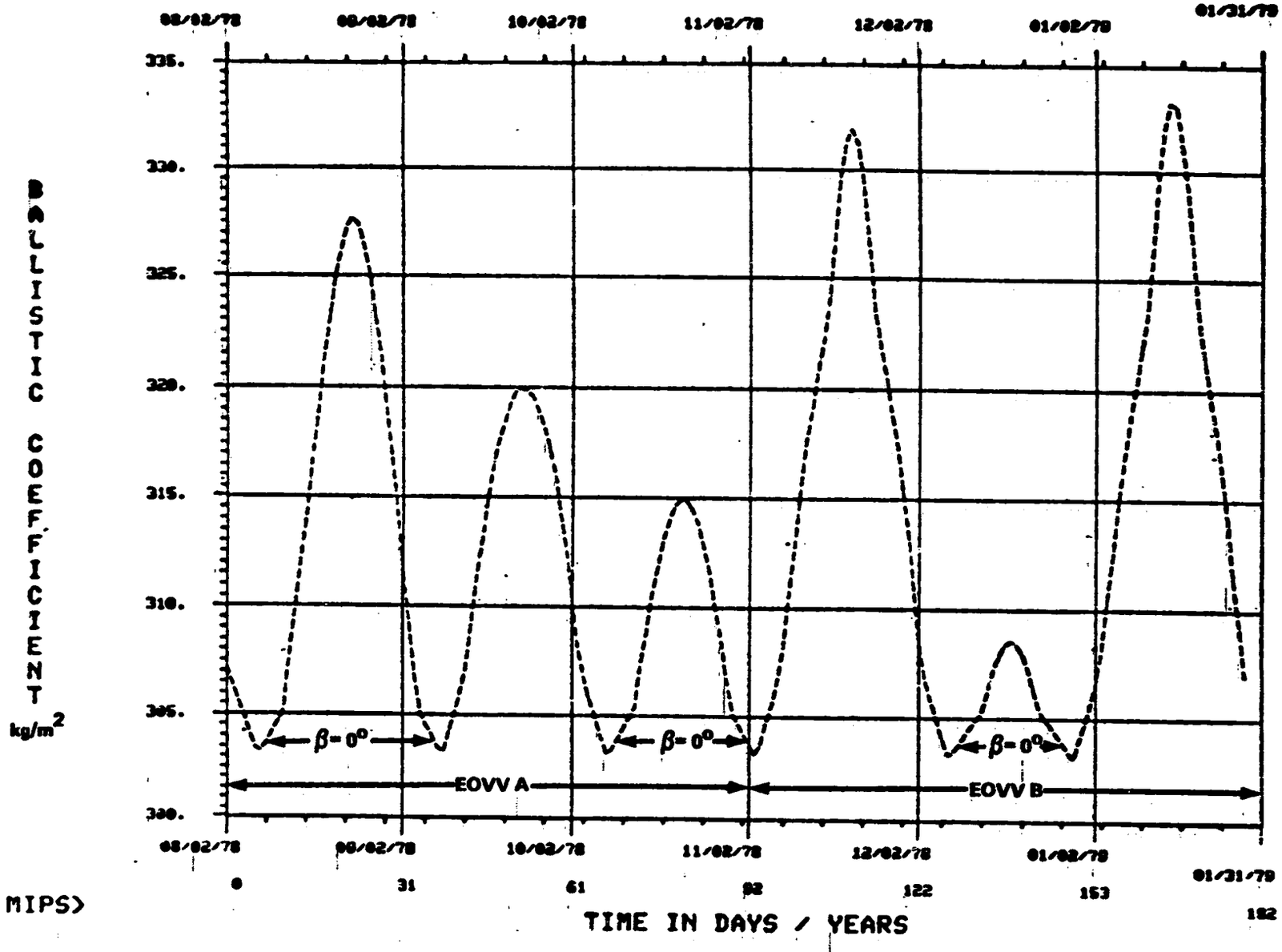

FIGURE 8-11A SKYLAB BALLISTIC COEFFICIENT VS DATE

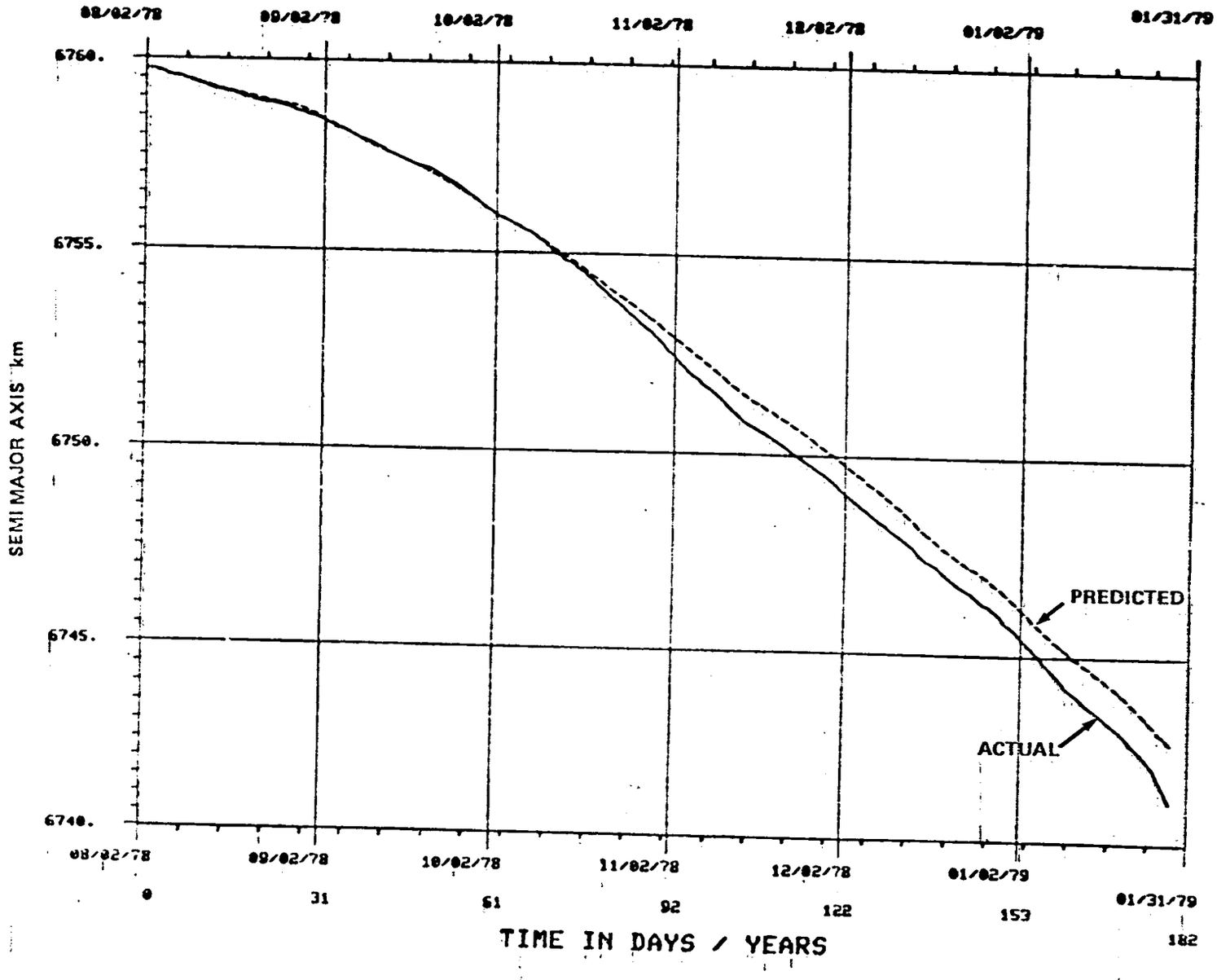

MIPS>

NOTE: EARTH RADIUS IS ~6378 km

FIGURE 8-12 PREDICTED AND ACTUAL DECAY

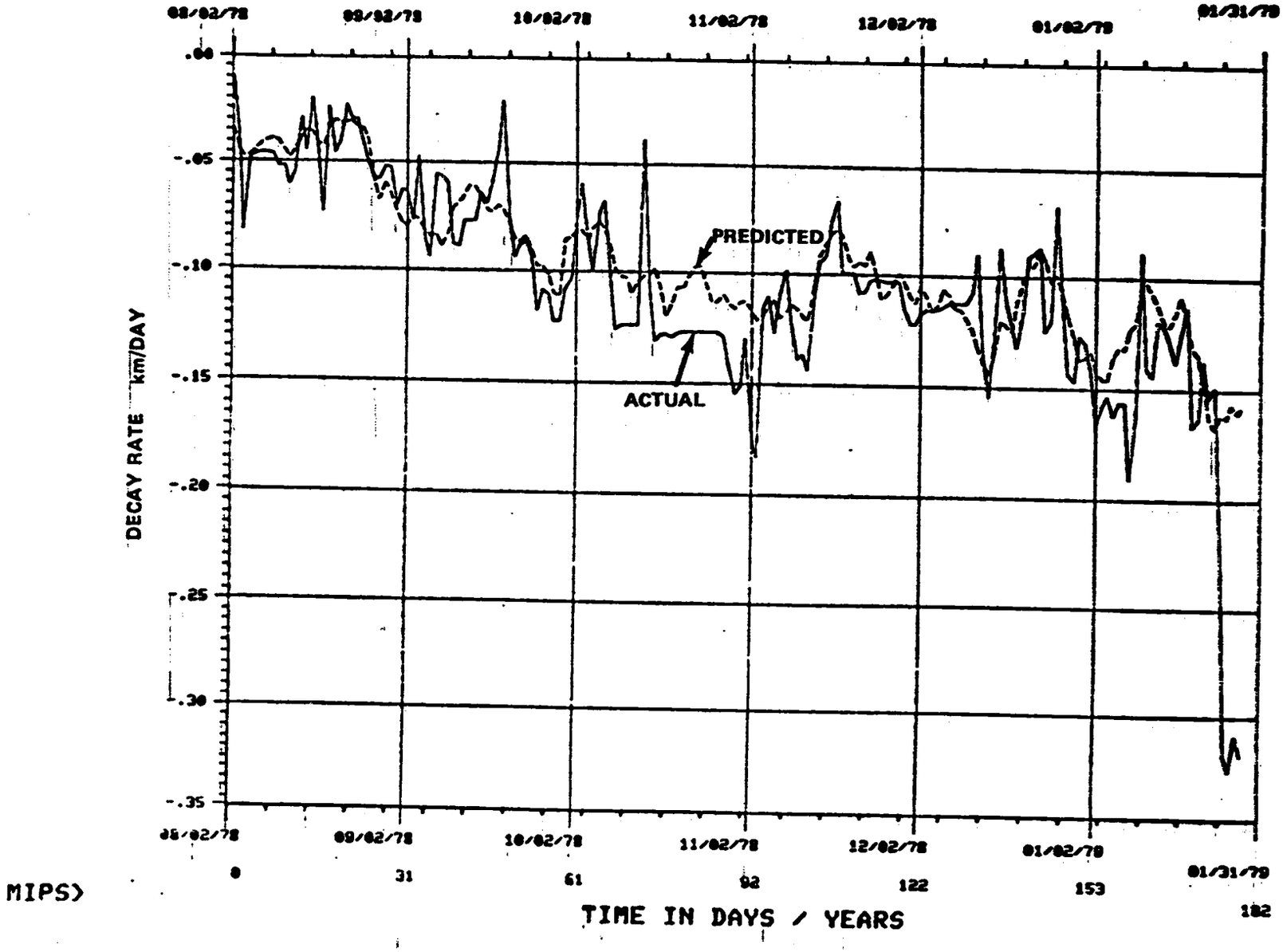

MIPS)

FIGURE 8-13 PREDICTED AND ACTUAL DECAY RATES

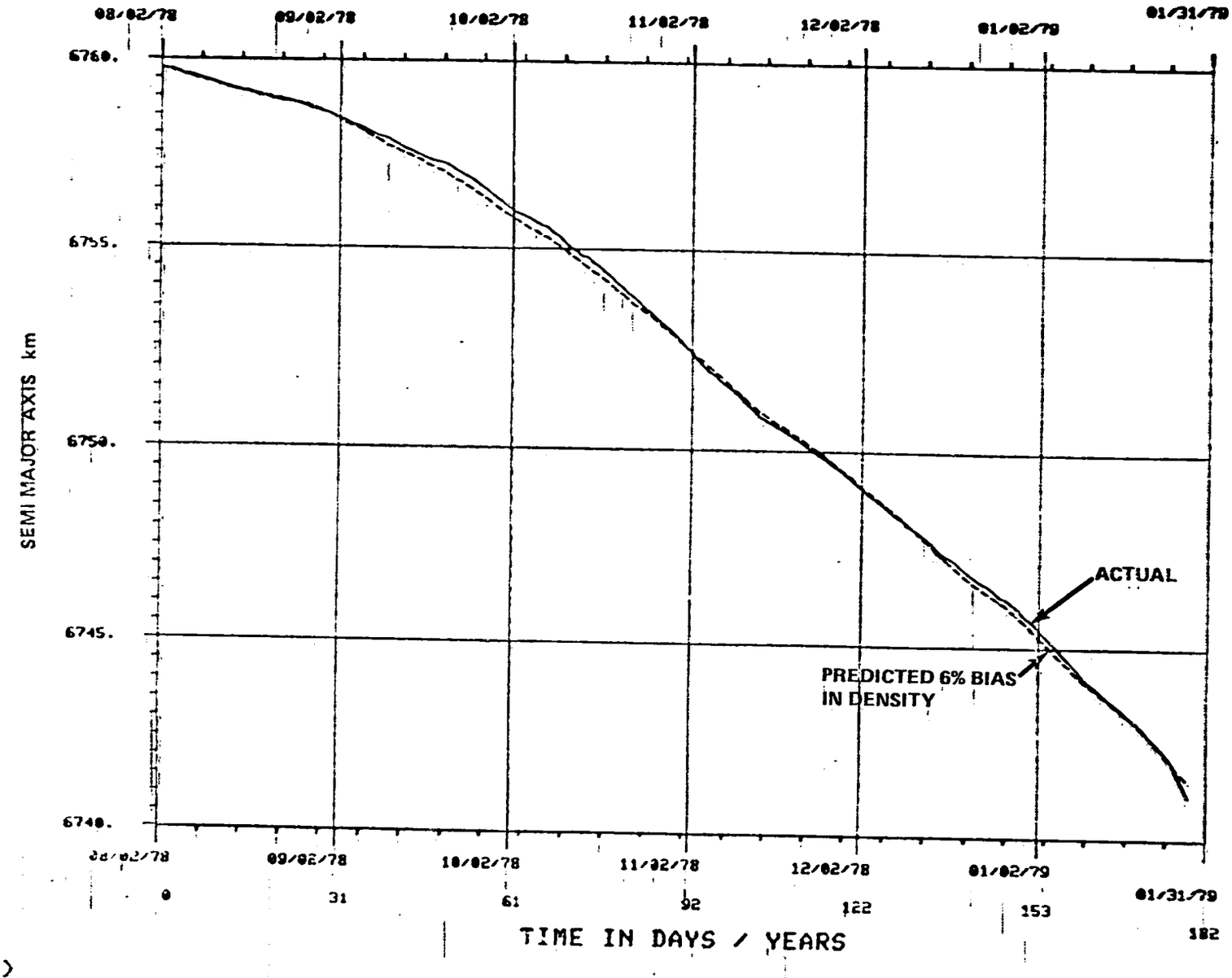

MIPS)

NOTE: EARTH RADIUS IS ~ 6378

FIGURE 8-14 PREDICTED AND ACTUAL DECAY RATES

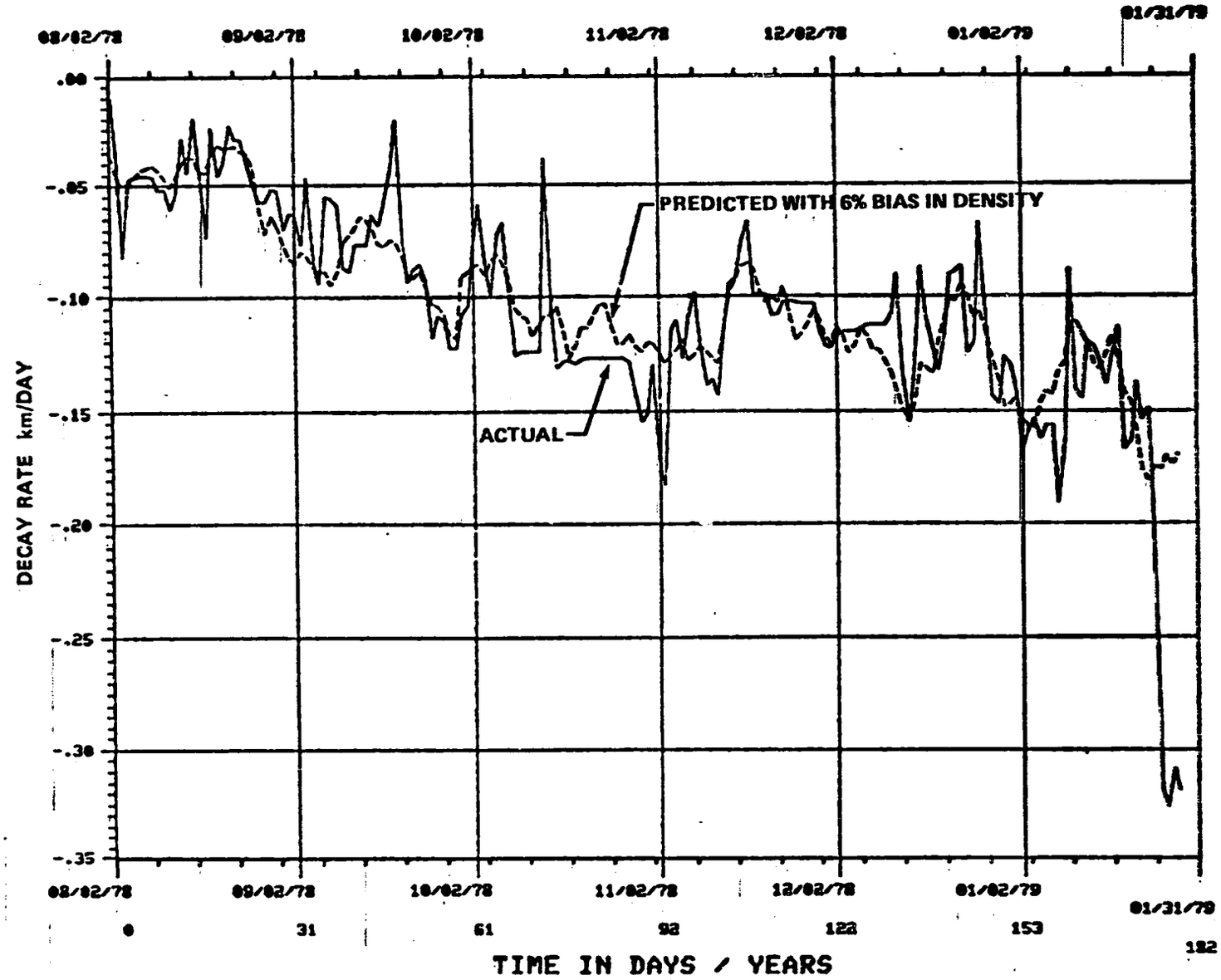

MIPS>

FIGURE 8-15 PREDICTED AND ACTUAL DECAY RATES

TABLE 8-1 LIFETIME PREDICTIONS WHILE IN EOVV

VECTOR DATE	DATE OF MSFC SOLAR ACTIVITY PREDICTION	PREDICTED DATE TO REACH 150 NMI		PREDICTED DATE TO REACH IMPACT	
		NOM *	+2σ	NOM *	+2σ
7-4-78	July 78	4-13-80	11-6-79	6-26-80	1-3-80
7-25-78	August 78	3-28-80	11-4-79	6-18-80	1-1-80
8-21-78	September 78	4-13-80	11-22-79	6-27-80	1-22-80
9-6-78	September 78	4-10-80	11-23-79	6-24-80	1-23-80
9-29-78	September 78	4-9-80	11-25-79	6-23-80	1-25-80
9-29-78	October 78	4-5-80	12-2-79	6-18-80	2-3-80
10-27-78	October 78	3-31-80	12-4-79	6-12-80	2-4-80
11-2-78	November 78	3-8-80	11-24-79	5-16-80	1-24-80
11-27-78	November 78	3-3-80	11-25-80	5-11-80	1-25-80
12-3-78	December 78	2-22-80	11-5-80	4-30-80	1-23-80
1-1-79	December 78	2-18-80	11-16-80	4-26-80	1-24-80
1-1-79	January 79	2-9-80	11-20-79	4-17-80	1-18-80

* SOLAR ACTIVITY PROBABILITY LEVELS
NOMINAL = 50% ___ . _
+2σ = 97.7%

8.6 SKYLAB ORBITAL DECAY JANUARY 25, THROUGH JUNE 21, 1979

Prior to the decision in December of 1978 to terminate efforts to attempt a controlled reboost or deorbit of Skylab with an orbital retrieval system, every effort possible was made to keep Skylab in orbit as long as possible. After this decision Skylab was placed in the SI control attitude, on January 25, 1979, and attention was then directed to the remaining orbital lifetime considering the SI attitude.

Precise derivation of the ballistic coefficient (BC) for this attitude was necessary. Since the SI attitude places the plane of the solar arrays perpendicular to the Earth/sun line, Skylab's orientation relative to the velocity vector and the resulting BC were continually changing. It was necessary to take this into account in predicting the ballistic coefficient. Knowing that the long axis of the vehicle (X-axis) was essentially in the orbit plane and that the vehicle roll angle was a function of the beta angle (see Figure 8-16), it was possible to derive a time history of BC as a function of beta which was later verified to be within a few percent of the observed values. The range of these BC's was between 140 and 220 (see Figure 8-17). Figure 8-18 shows the beta angle history for this time period.

During the time Skylab was in SI attitude several uncertainties compounded the task of predicting Skylab's lifetime. First, to what minimum altitude could Skylab be controlled in the SI attitude? Second, in what attitude could Skylab be controlled to a lower attitude? Third, what would be the ballistic coefficient for this attitude? Finally, when would the attitude change occur? In order to make the best possible lifetime prediction for Skylab these questions had to be answered. These questions were eventually answered and are discussed in Section 8-7 of this document. In the meantime lifetime predictions were made assuming the vehicle's SI attitude was held until 150 nm altitude with tumbling occurring from 150 nm to impact. This strategy provided consistent lifetime predictions until the above questions were answered as well as a data base of lifetime predictions to evaluate daily solar activity effects upon Skylab's decay. Table 8-1a shows the results of using this BC.

Figures 8-19 and 8-20 show the predicted and actual altitude and the predicted and actual decay rates of Skylab during the SI period. This comparison was based upon the solar activity data shown in Figure 8-3 and the ballistic coefficient history shown in Figure 8-17. The actual and predicted decay did not compare very well. As in the EOVV period this is attributed in part to the density modeling during periods of very active solar activity. Also, other contributing factors could have been

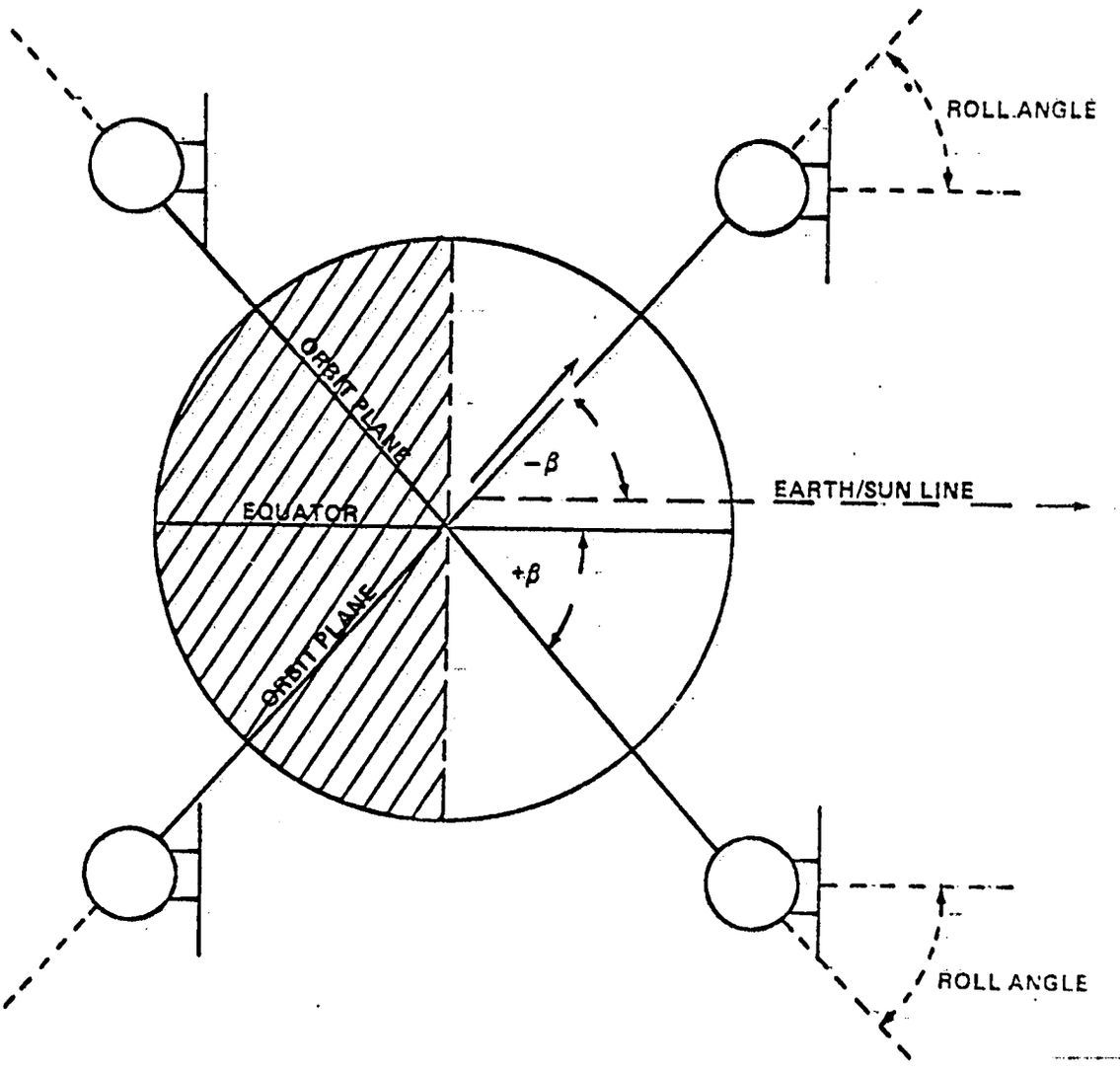

SOLAR INERTIAL ORIENTATION / EARTH SUN LINE

FIGURE 8-16

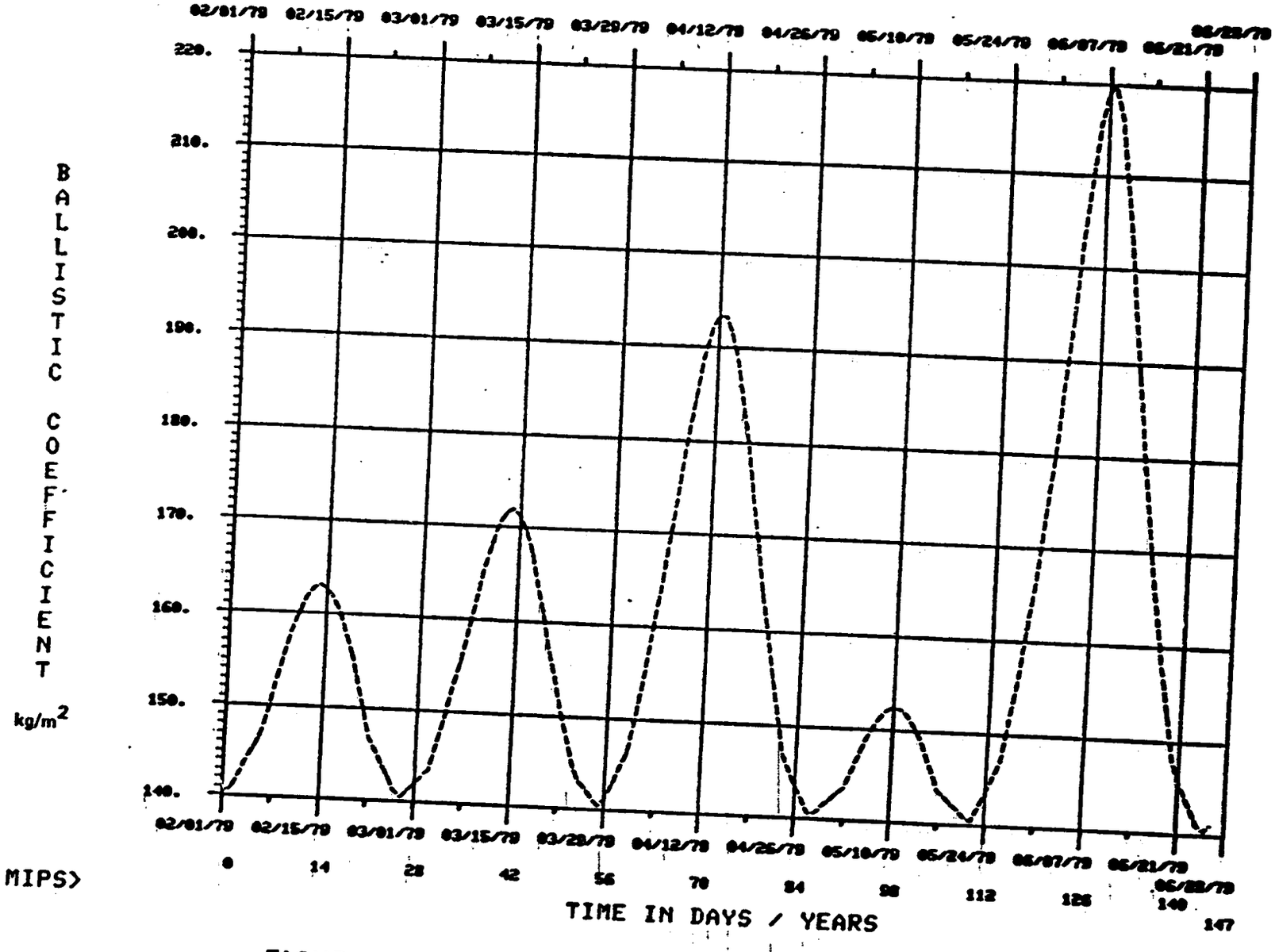

FIGURE 8-17 BALLISTIC COEFFICIENT VS DATE DURING SI ATTITUDE

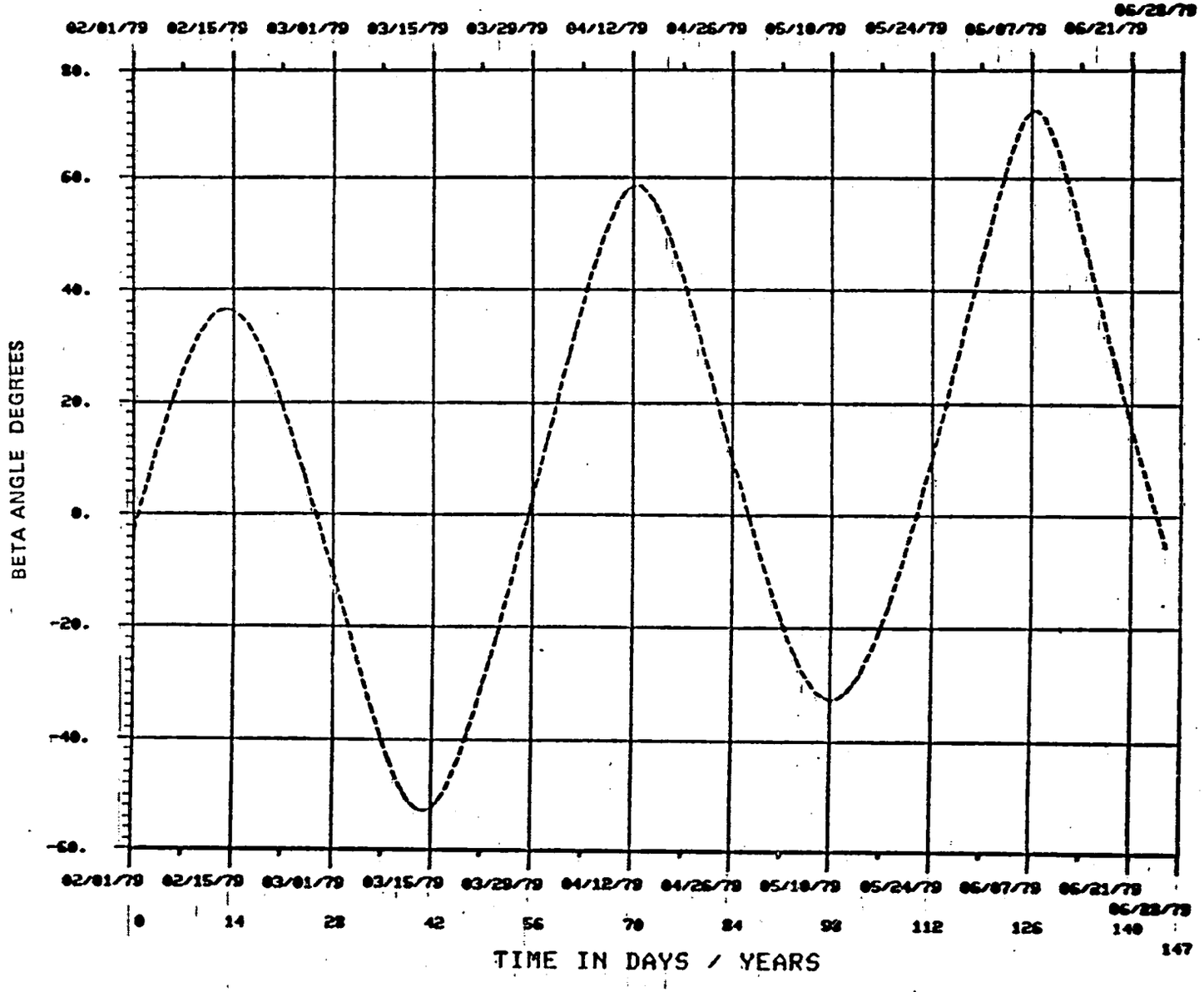

FIGURE 8-18 BETA ANGLE VS DATE

MIPS>

TABLE 8-1A PREDICTED IMPACT DATES USING SI AND TUMBLE BC

Vector Date	Impact Date
1/25/79	8/12/79
2/1/79	8/1/79
2/12/79	7/28/79
2/22/79	7/24/79
2/28/79	7/20/79
3/1/79	7/12/79
3/16/79	7/10/79
4/2/79	7/4/79
4/16/79	7/3/79
5/1/79	7/3/79
5/15/79	7/5/79
5/25/79	7/8/79
5/29/79	7/8/79
5/30/79	7/9/79
5/31/79	7/9/79
6/4/79	7/10/79
6/5/79	7/10/79
6/6/79	7/11/79
6/7/79	7/11/79
6/8/79	7/11/79
6/11/79	7/12/79
6/12/79	7/12/79
6/13/79	7/12/79
6/14/79	7/12/79
6/15/79	7/13/79
6/18/79	7/13/79
6/19/79	7/13/79
6/20/79	7/13/79
6/21/79	7/13/79
6/22/79	7/13/79

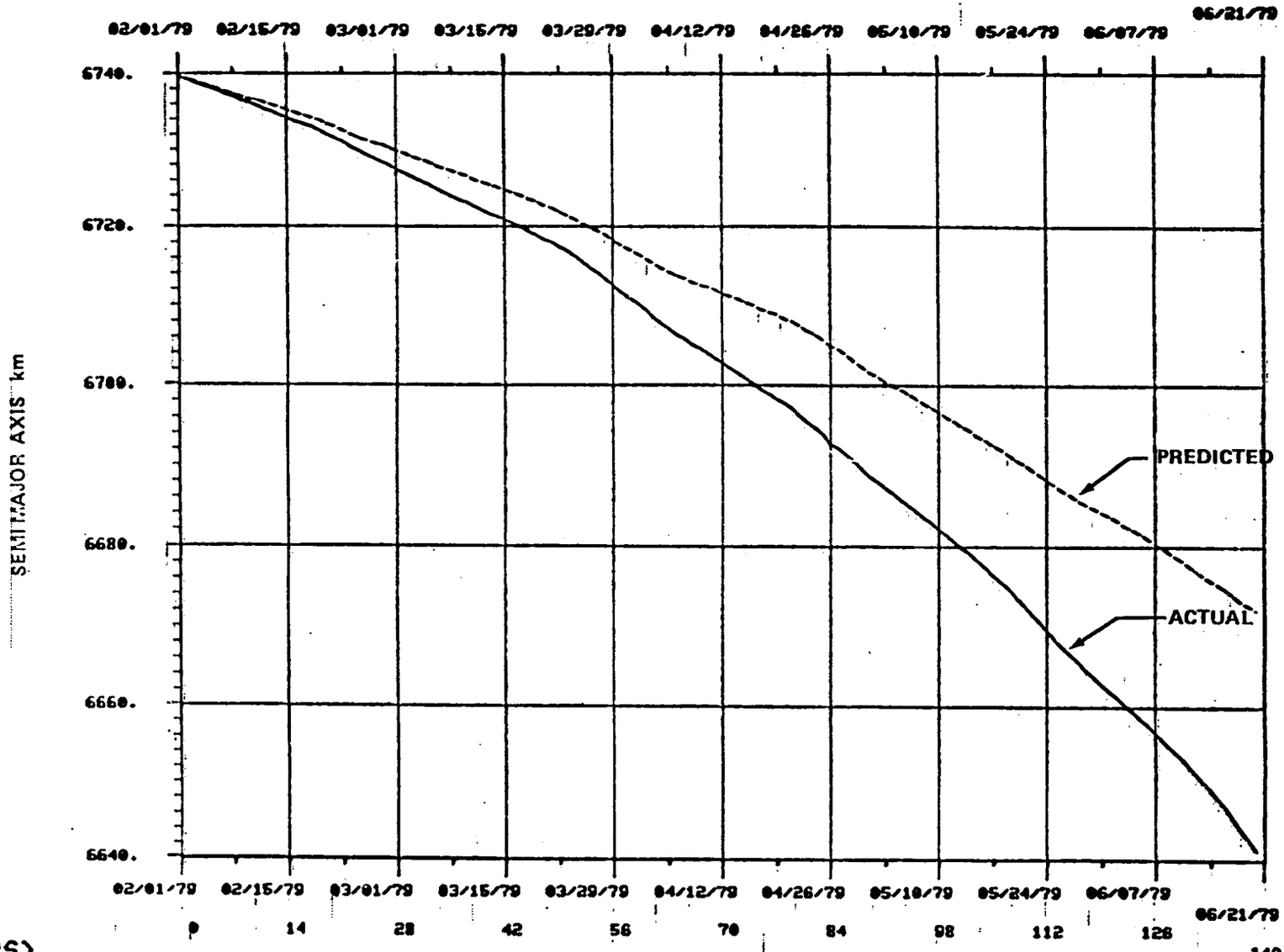

NOTE: EARTH RADIUS IS ~6378 km

FIGURE 8-19 PREDICTED AND ACTUAL DECAY DURING SI ATTITUDE

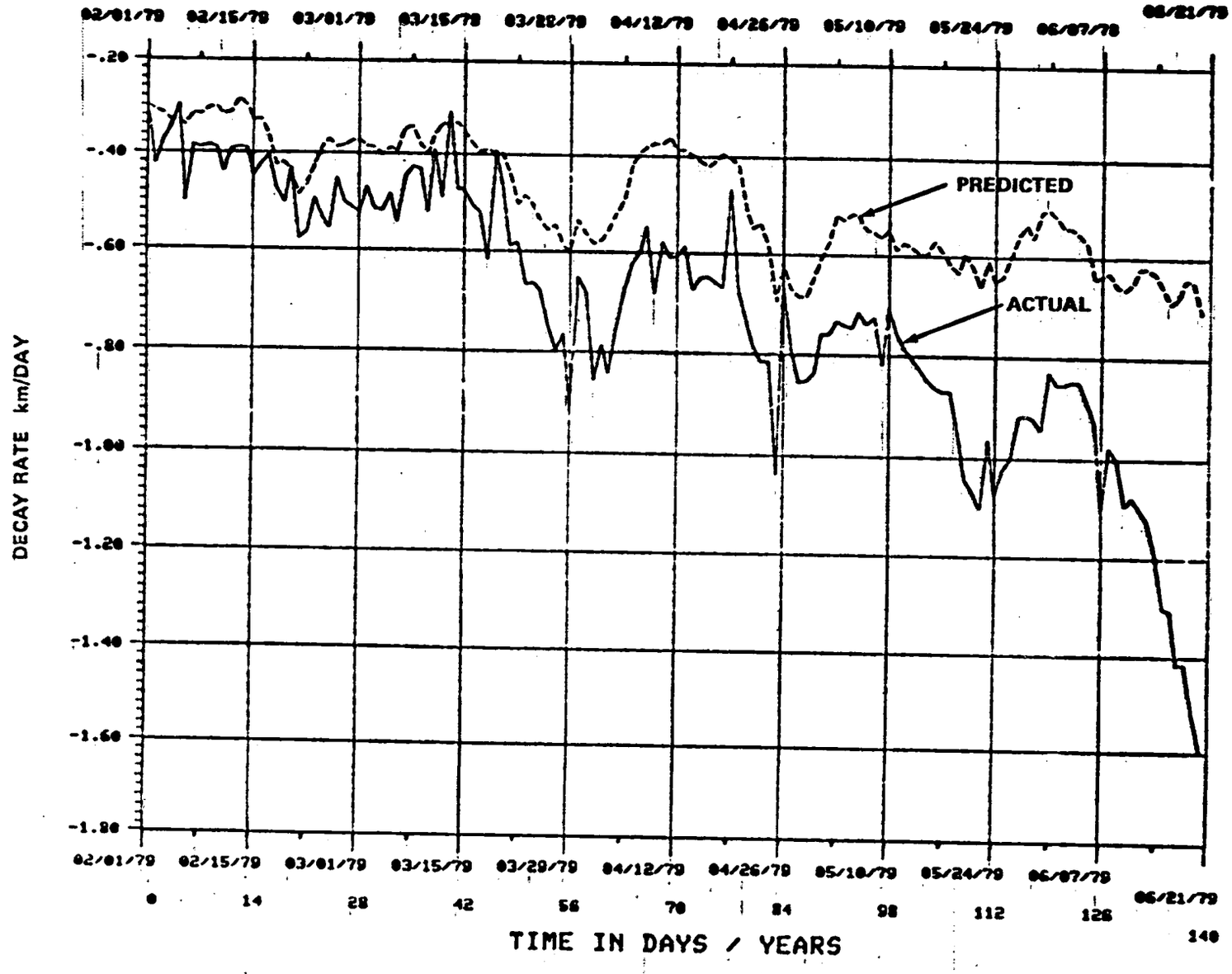

MIPS>

FIGURE 8-20 PREDICTED AND ACTUAL DECAY RATES DURING SI ATTITUDE

uncertainties in the aerodynamic and solar activity data. When the lifetime was calculated using a plus 18% bias in atmospheric density, the decay more closely approximted the observed decay as can be seen in Figures 8-21 and 8-22.

The density bias used in the calculated decay to provide for a closer match in decay is not a constant, but seems to be a function of the magnitude of the solar activity variations and other factors, e.g. aerodynamic data, attitude, etc. Comparison of the actual and predicted decay was made for the last month of SI (May 25 to June 20). When the decay was calculated with a plus 4% density bias it closely approximated the observed data as can be seen in Figures 8-26 and 8-27. This comparison was based upon the solar activity data shown in Figure 8-3 and the ballistic coefficient history shown in Figure 8-24.

8.7 SKYLAB ORBITAL DECAY JUNE 21, 1979 TO IMPACT

Development of the TEA control mode (Section 2.1.3 and 3.1.2) resulted from a decision to try to control the impact of Skylab to a particular orbit, one which would be characterized by a low population density. There were essentially two constraints which determined when the TEA control scheme could be used. One of these depended upon the sun angle on the solar arrays. The other constraint was the minimum altitude (140nm) at which Skylab could still be controlled in the SI attitude.

It thus became necessary to accurately predict both the beta angle and the altitude of Skylab such that a time (window) could be picked where sufficient power would be available during the total time Skylab would be in the high drag attitude (T121P). It was also necessary for the window to open before Skylab's altitude fell below the SI control threshold. Figure 8-23 shows the beta angle and altitude that were acceptable for the T121P control. As can be seen, June 19, 1979 to June 24, 1979 satisfied both the power and altitude constraints for entering T121P. Based upon predictions of altitude and beta angle, June 20, 1979 was selected as the date to go to the new attitude, which corresponded to an altitude of 142 nm. It was now necessary to derive a BC for the T121P attitude. Initial estimates were predicted by dynamics and control simulations of the vehicle in its operating environment. Final values were determined by methods developed by observing the orbital decay behavior. This method compared the decay rate of the vehicle for various BC's to that BC which gave the best fit of the actual decay rate. The method was modified by checking other satellite decay rates in order to be assured that atmospheric model variations and other factors were accounted for in the calculation of BC.

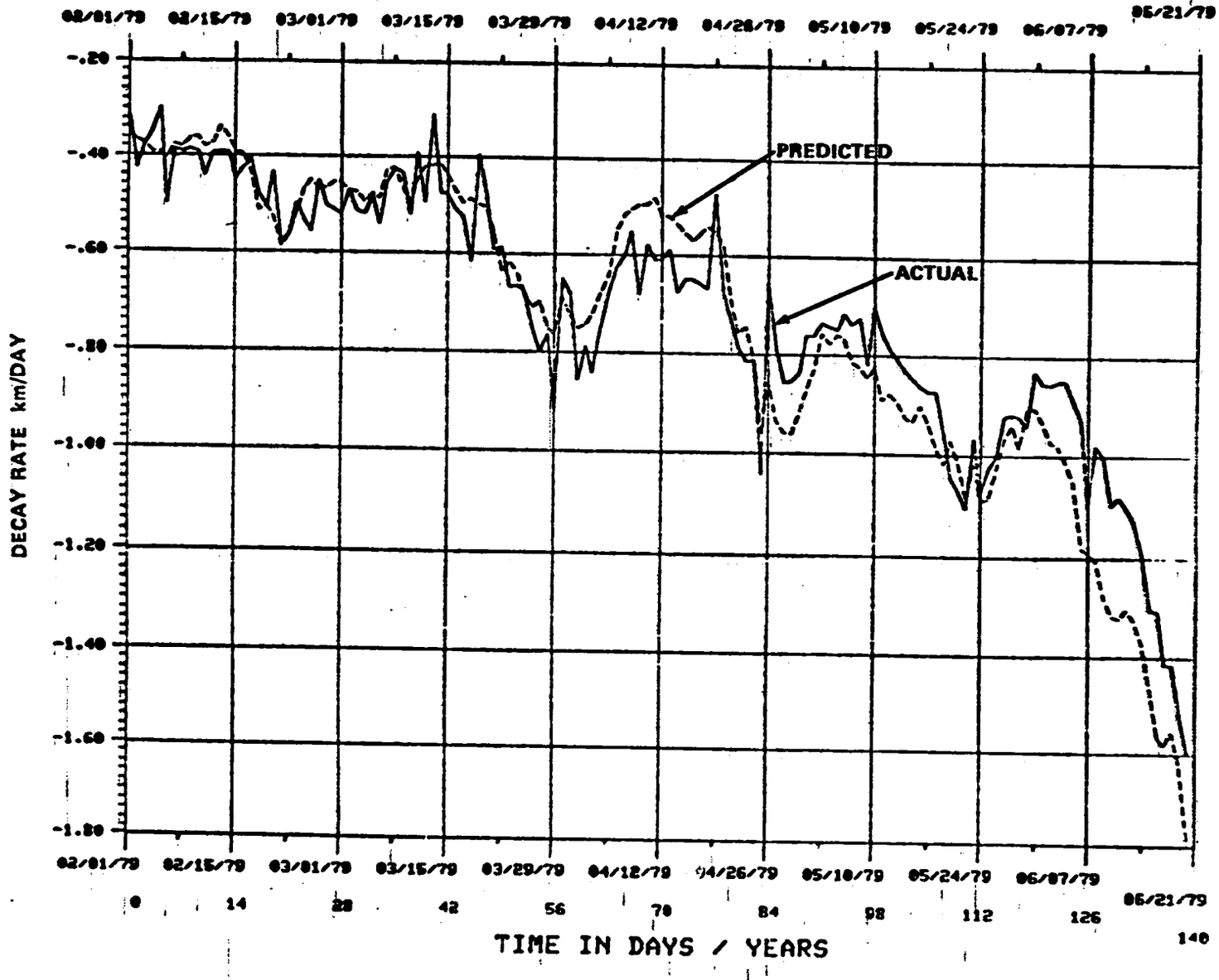

FIGURE 8-21 PREDICTED AND ACTUAL DECAY RATES DURING SI ATTITUDE

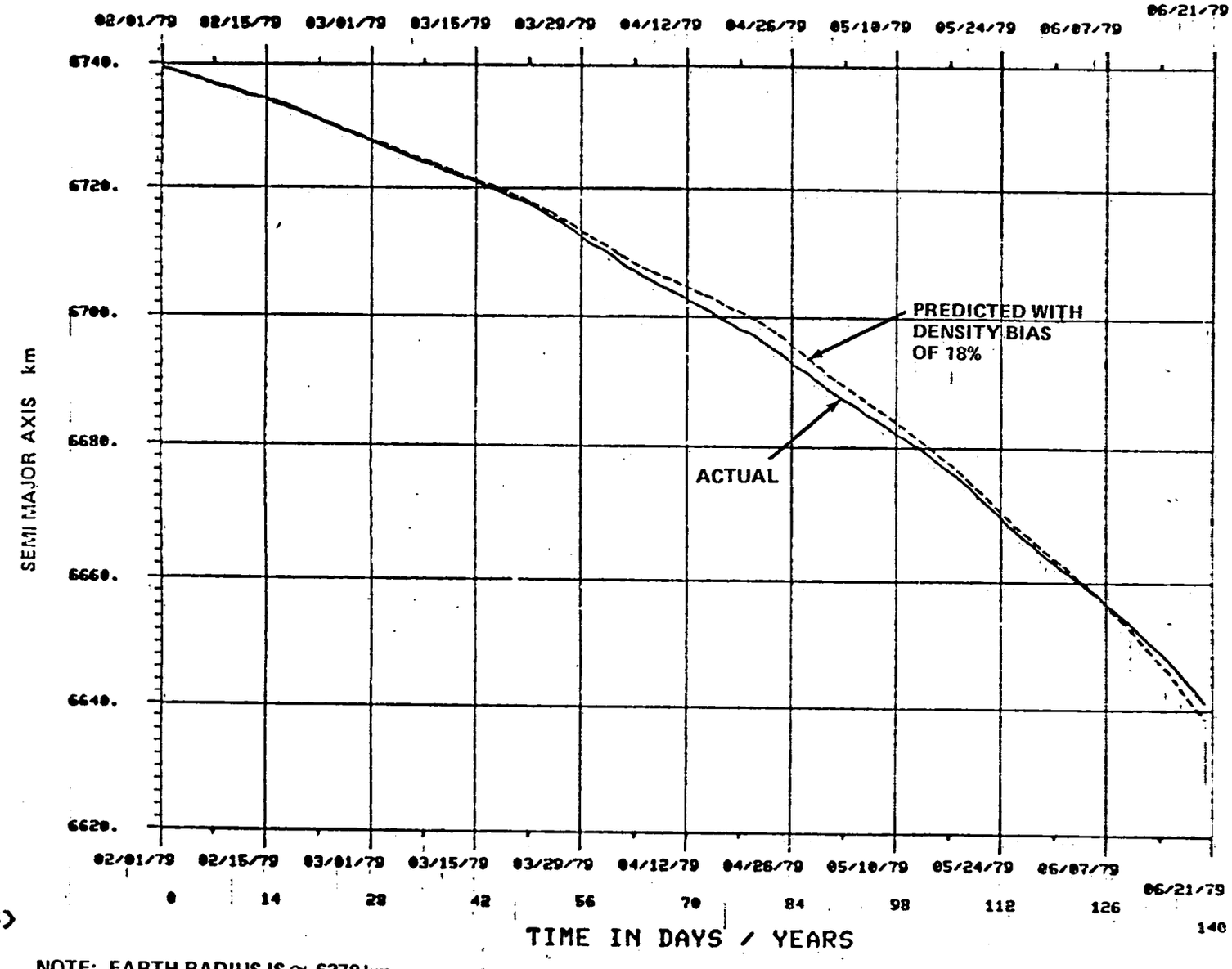

MIPS>

NOTE: EARTH RADIUS IS ~ 6378 km

FIGURE 8-22 ACTUAL AND PREDICTED DECAY RATES DURING SI ATTITUDE

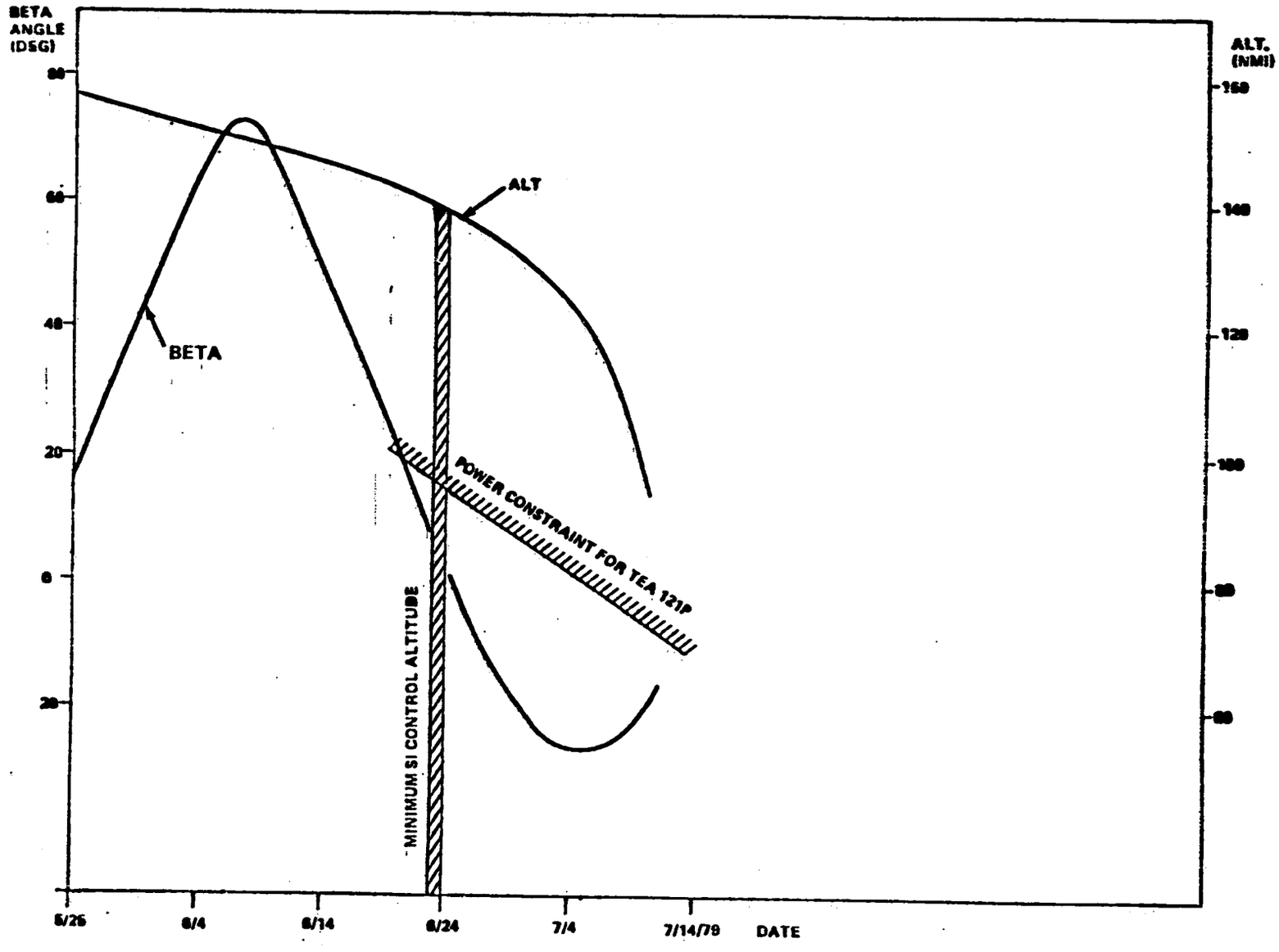

FIGURE 8-23 CONSTRAINTS FOR TEA ATTITUDE

Figures 8-24 and 8-25 show plots of the resulting BC's for a representative period of time for both the SI attitude and the T121P attitude respectively. Figure 8-26 shows the predicted and actual decay of Skylab during the final month of the SI attitude where decay is determined using the predicted BC's. Figure 8-27 shows that a 4% density bias is required to match the actual decay curve. Again, this 4% density bias may include uncertainties in the aerodynamic data and the solar activity data. Similarly, figures 8-28 and 8-29 show that a 3% density bias is required to match predicted decay with actual decay for the T121P attitude. As can be seen, the predeicted and observed decay curves were quite close in terms of a daily average. Lifetime predictions for this scenerio (i.e., SI until June 21, 1979, T121P until 80 n.m., a tumble thereafter) are shown in Table 8-2. The T121P configuration was maintained until 7:45 GMT on July 11, 1979, when the maneuver to tumble was initiated.

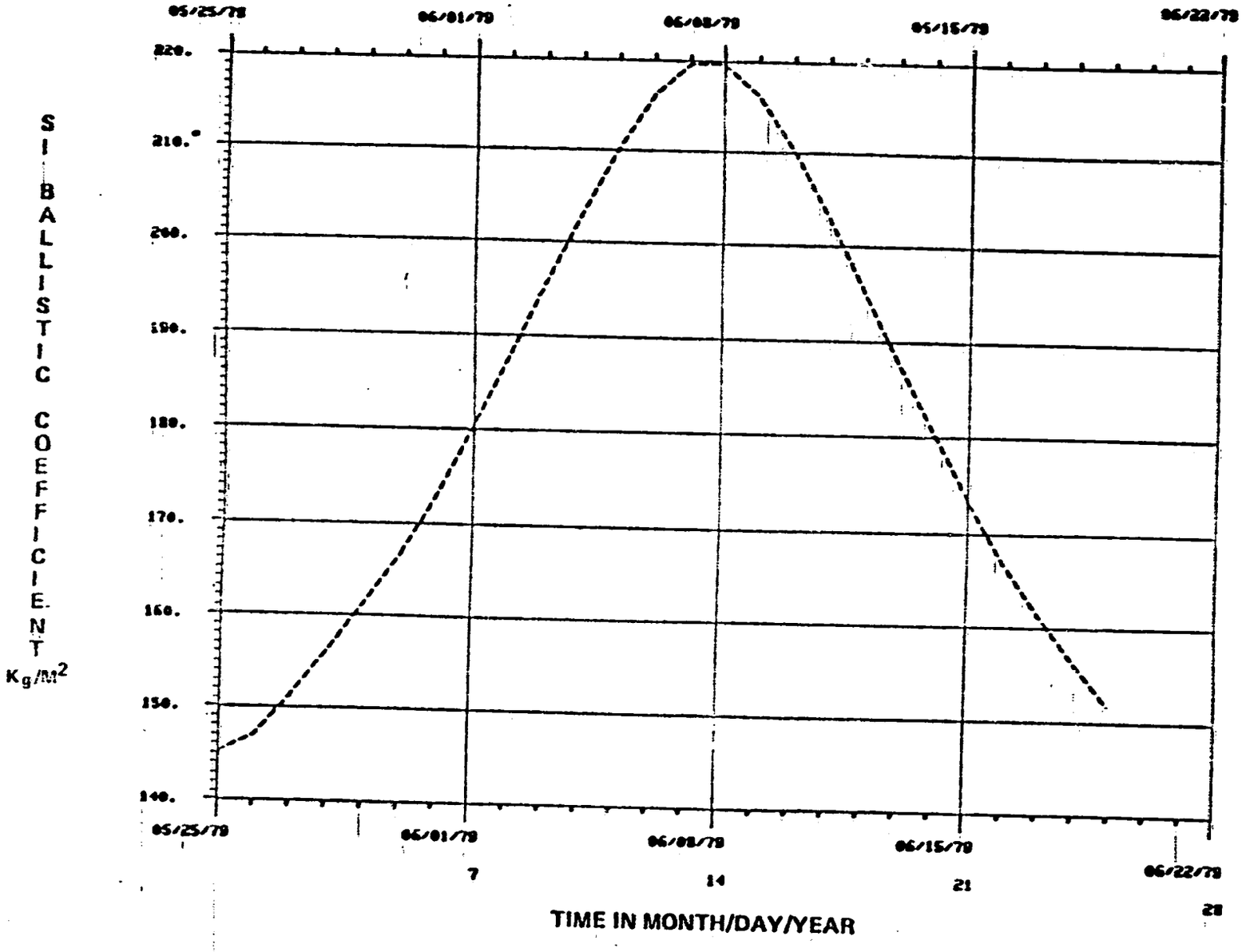

FIGURE 8-24 SI BALLISTIC CIEFFICIENT VS DATE

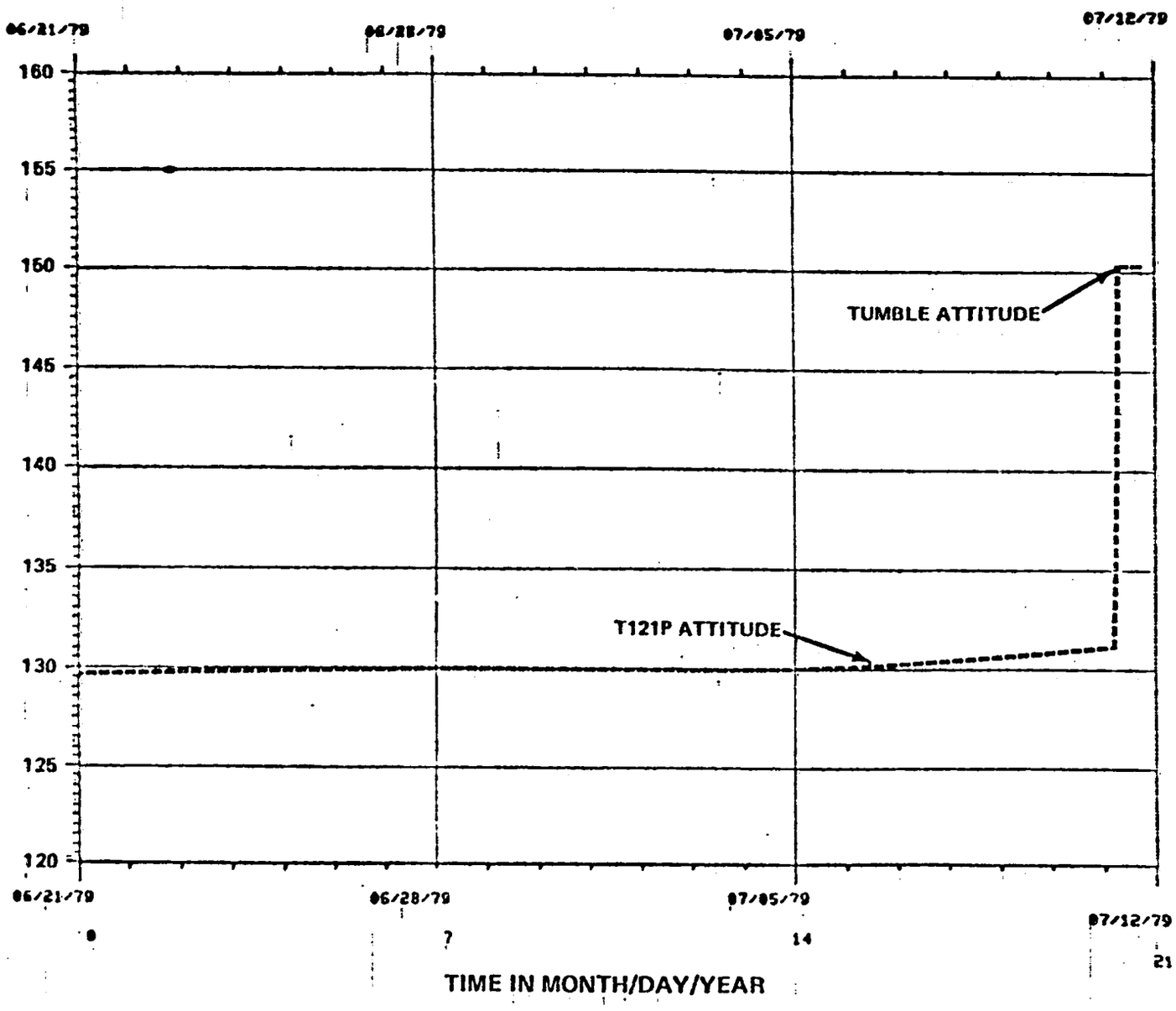

FIGURE 8-25
T121 BALLISTIC COEFFICIENT VS DATE

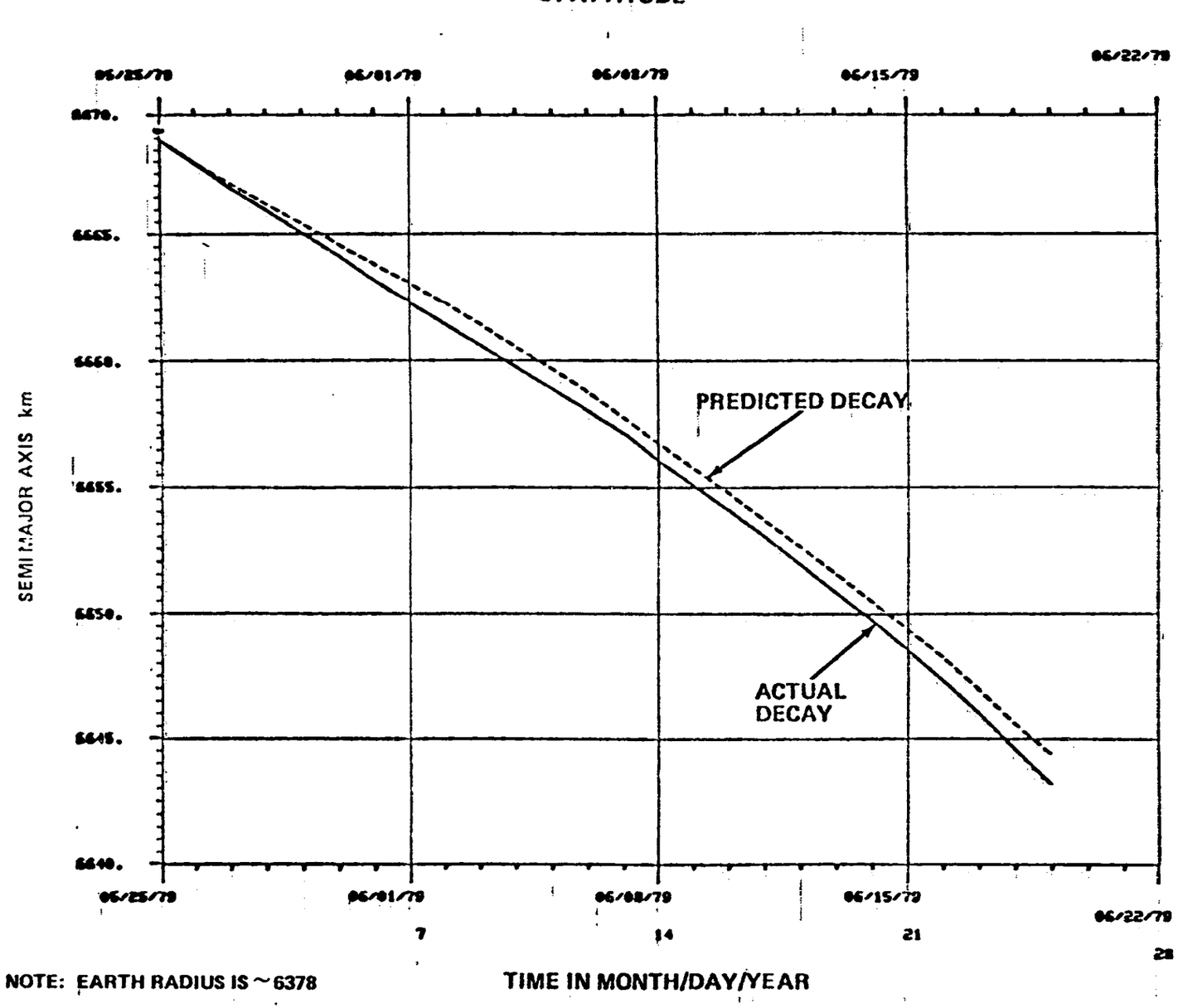

FIGURE 8-26 PREDICTED AND ACTUAL DECAY

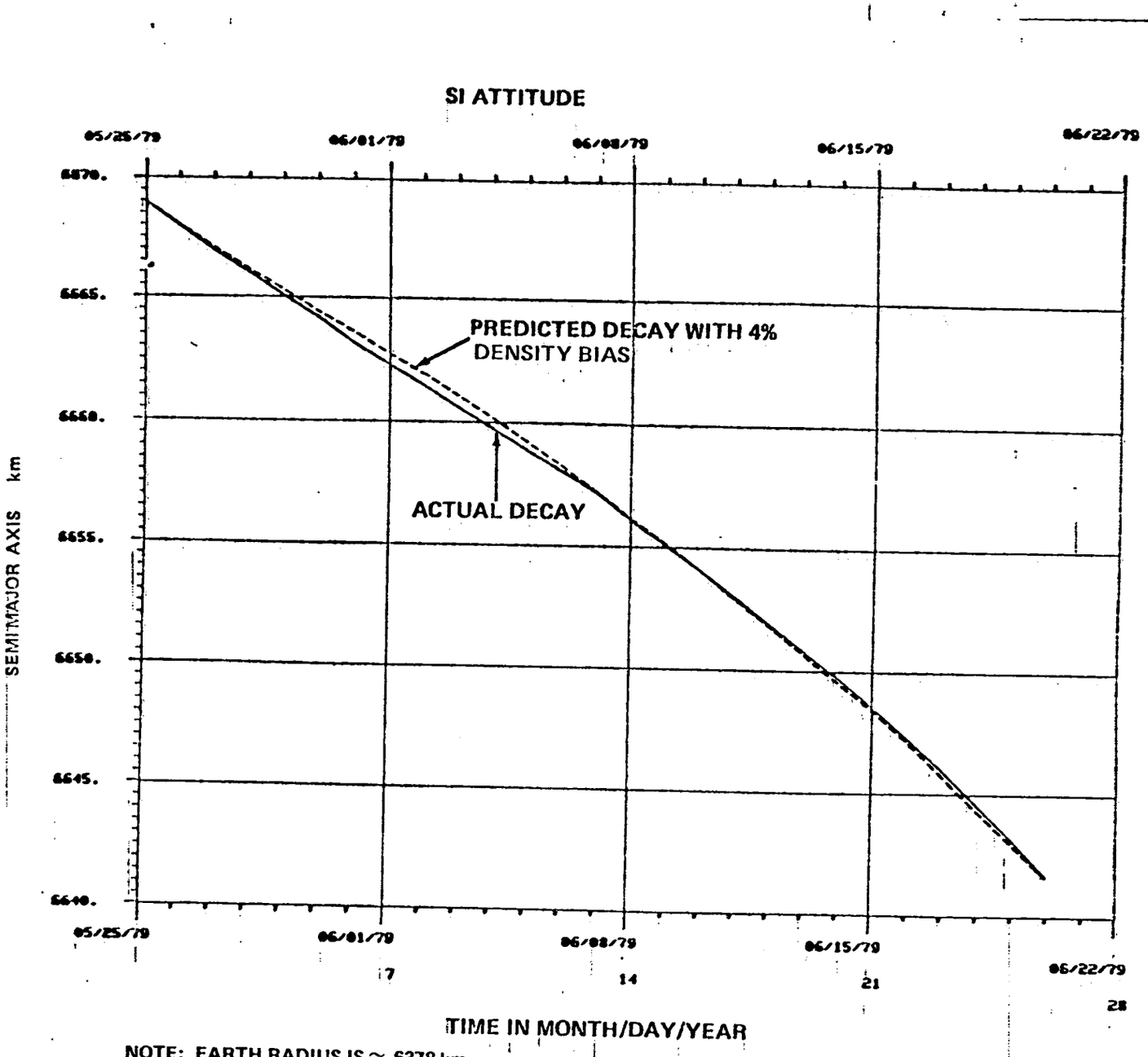

NOTE: EARTH RADIUS IS ~ 6378 km

FIGURE 8-27
PREDICTED AND ACTUAL DECAY

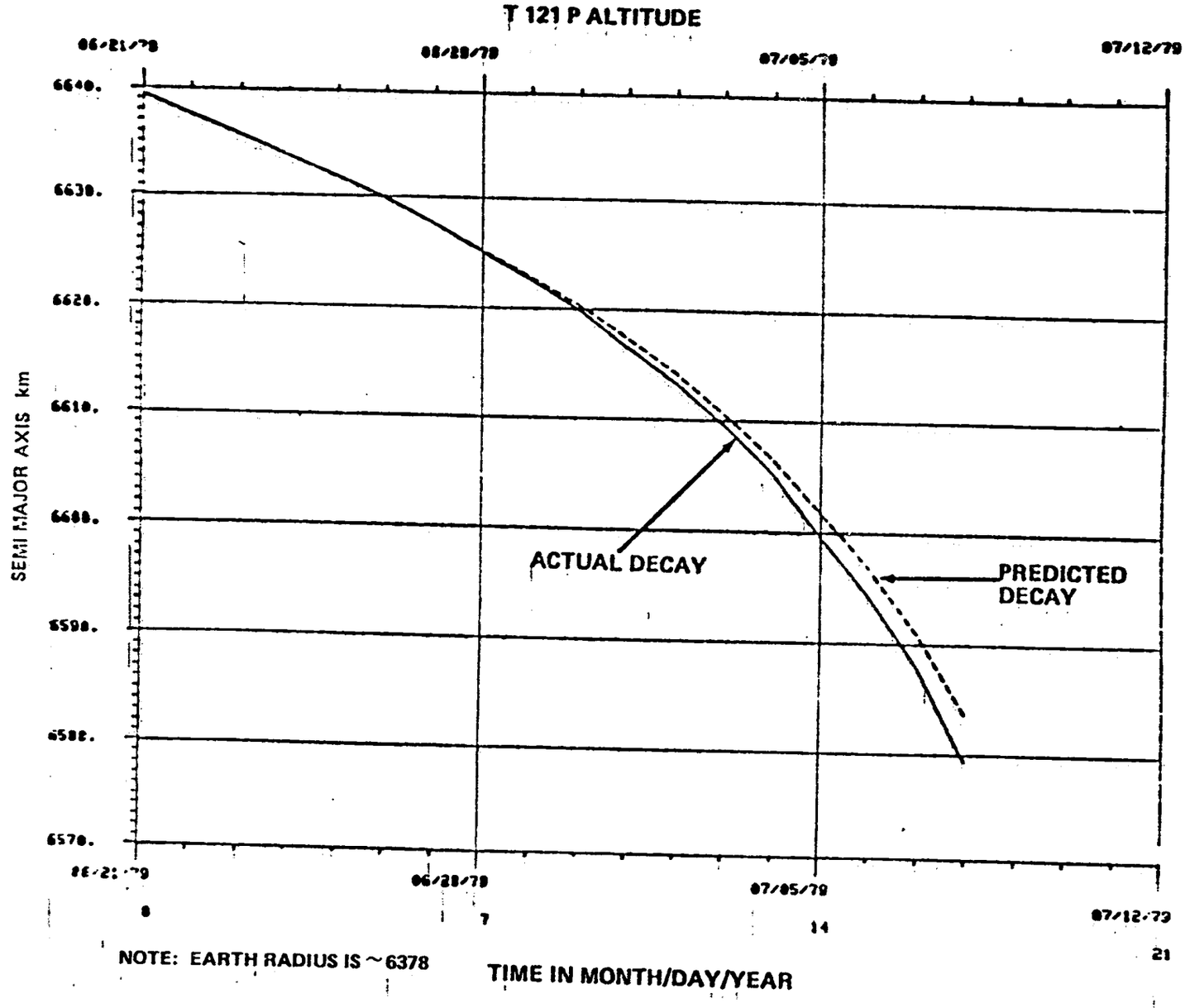

FIGURE 8-28
PREDICTED AND ACTUAL DECAY

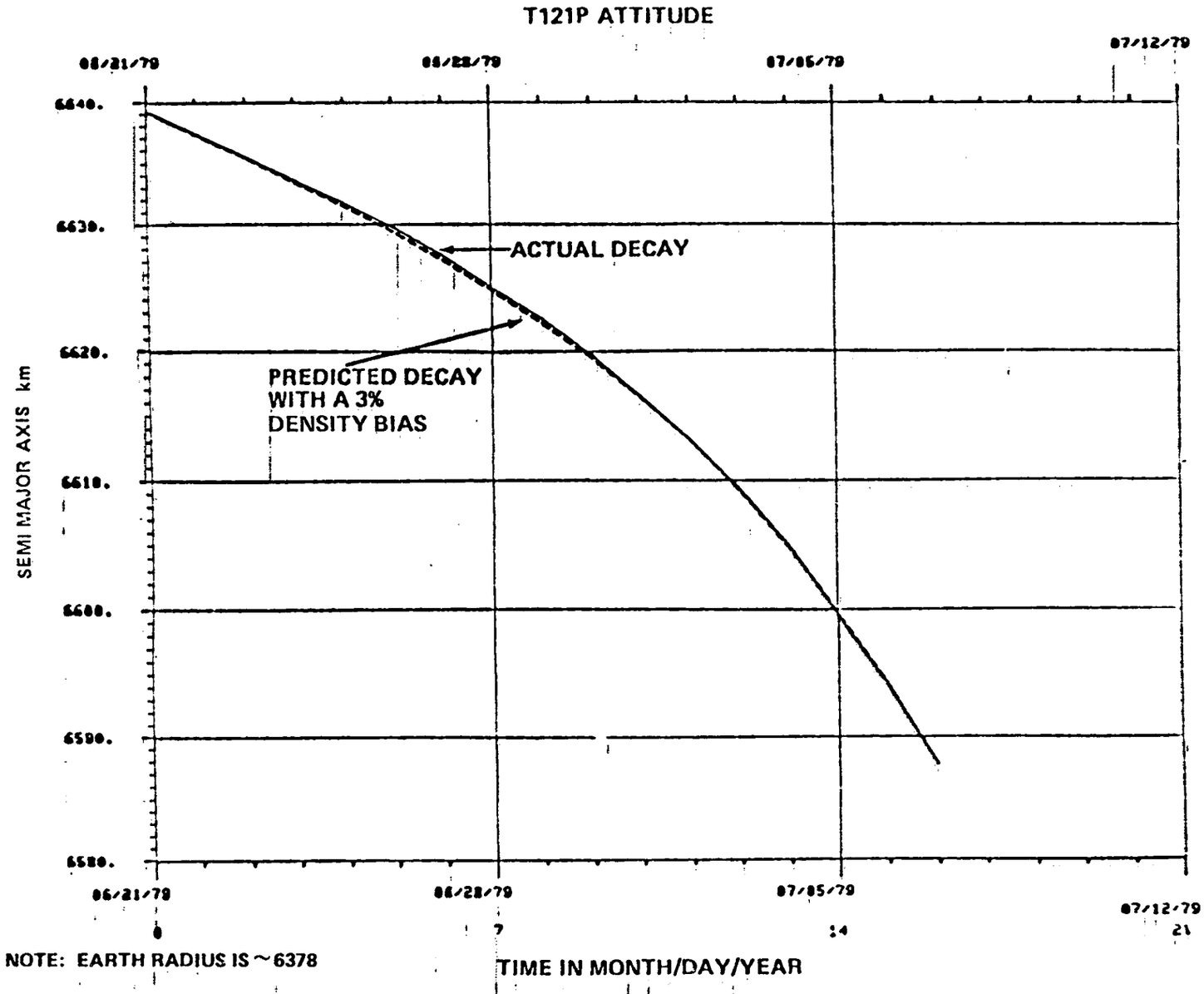

FIGURE 8-29 PREDICTED AND ACTUAL DECAY

TABLE 8-2 PREDICTED IMPACT DATES USING SI, 121P AND TUMBLE BC

Vector Date	Impact Date
5/25/79	7/09/79
5/29/79	7/09/79
5/30/79	7/10/79
5/31/79	7/10/79
6/04/79	7/10/79
6/05/79	7/10/79
6/06/79	7/10/79
6/07/79	7/10/79
6/08/79	7/10/79
6/11/79	7/10/79
6/12/79	7/10/79
6/13/79	7/09/79
6/14/79	7/09/79
6/15/79	7/09/79
6/18/79	7/09/79
6/19/79	7/10/79
6/20/79	7/10/79
6/21/79	7/10/79
6/22/79	7/10/79

9.0 SKYLAB REENTRY

9.1 DRAG MODULATION

With the decision to discontinue the effort to extend Skylab's orbital lifetime, a scheme had to be developed to maintain vehicle control in varying attitudes as a function of altitude, since lower altitudes resulted in a different aerodynamic drag effect on the vehicle thereby control stability. Also by changing the vehicles attitude its orbital decay rate could be increased or decreased as necessary to insure that the reentry of Skylab occured on an orbit characterized by a low population density. This provided several options that could be excercised. For example; (1) if it was desired to extend vehicle lifetime a multiple number of revolutions, the vehicle could be maneuvered from the high drag TEA attitude to the low drag TEA attitude reducing the drag approximately 50% (holding the low drag attitude for 12 revolutions resulted in a lifetime extension of approximately 6 revolutions); (2) a maneuver to effect a tumble during the terminal phase of decay (below about 85 n.m. to 75 n.m.) reduced the drag by approximately 15% for a lifetime extension of up to one revolution and (3) continued control in a high drag attitude in conjunction with a tumble (approximately 70 n.m.) reduced orbital lifetime by up to one revolution. In the actual mission, option (2) was successfully executed at about 81 n.m.

9.1.1 Procedures

The procedures used in real time were: first, determine the predicted longitude of the ascending node, time, and impact position of the reentry orbit; second, estimate the uncertainty in this impact point and time and the associated population hazard; and third, apply previously established mission rules to help establish a NASA headquarters "veto" or approval of any proposed maneuver. Decisions were to be based largely on the initial values of the population hazard, on the predicted revolution of impact and the reduction of that hazard afforded by implementing a maneuver to alter the aerodynamic drag on the vehicle and thus shift the revolution of impact. Ground rules for implementing the maneuver were: (1) if the predicted revolution of reentry was such that a substantial reduction of risk to the world population occurred the planned maneuver would be implemented unless vetoed within a preset time; (2) if the predicted reentry orbit population hazard was low but the predicted impact point (and its associated footprint) endangered a populated area, approval was required to implement a maneuver

to shift the impact footprint. Technically, the procedures varied slightly depending on the maneuver selected. For the low drag attitude multiple revolution shift maneuver, the plan was to determine the number of revolutions required to reduce the population hazard without danger of shifting the impact revolution to one of high population density. With this accomplished, it was then desirable to place the predicted impact point over the maximum amount of water on the impact revolution such that the nominal center of the footprint (heavy pieces at the front end of the footprint) was centered in water. This established the preliminary maneuver time and duration. Final calculations precisely determined the maneuver time and duration. A final recommendation was then to be made to implement the maneuver which would be done automatically unless overruled by NASA Headquarters. For the tumble maneuver, only a small specified population area was to be protected by shifting the predicted impact point and its nominal footprint to an ocean impact. To implement this plan required NASA headquarter's approval. In the actual situation, this was the procedure used.

The decision criteria for determining what data should be used to plan and implement the final maneuver went as follows. Based on historical NORAD statistical data, the state vector which appeared to correlate most solidly with the actual determination of final impact was the T-24 hour vector. Less satisfactory fits resulted with the T-12 hour vector. With the data available from Skylab decay history since 1974, the vehicle drag coefficients and associated ballistic terms for the uncontrolled tumble, End-On-Velocity-Vector, solar inertial and TEA attitudes were determined. Also based on the results of a simulation performed during the decay of object #5644, the significance of the phenomena of transition from free molecular to continuous aerodynamics was established.

The impact time results from the T-18 and T-12 hour vectors as compared to the T-24 hour vector established an uncertainty of impact of $\pm$25 min ($\pm$1/4 revolution). Based on these results, the time to initiate the tumble was selected to place the impact point within the $\pm$1/4 revolution uncertainty in the south Atlantic based on the T-24 hour vector. The time selected was 7:45 GMT July 11, 1979.

9.1.2 Results

Table 9-1 shows a summary of the projected times, latitude and longitude of impact (approximately to end of the footprint) from 72 hours prior to impact until 1 hour prior to impact. Figure 9-1 shows the population hazard versus the longitude of the ascending node for the revolution of impact. To evaluate this

TABLE 9-1 ALL DATA IS FOR IMPACTS ON JULY 11, 1979, D.O.Y. = 192

MSFC CALCULATIONS

Time of Estimate (hours)	Time Decay (GMT)	LAT (deg)	LONG (deg)
T-72	15:06:51	37.0 S	139.5 E
T-48	13:53:20	4.5 N	201.1 E
T-42	13:55:01	10.0 N	205.3 E
T-36	15:06:49	37.8 S	138.2 E
T-30	14:49:50	40.3 S	47.9 E
T-24	15:27:30	23.2 N	194.3 E
T-18	15:52:15	34.6 N	311.8 E
T-12	15:50:12	39.5 N	304.1 E
T-9	16:31:28	44.2 S	102.7 E
T-7	16:33:03	41.0 S	110.0 E
T-6	16:35:04	36.4 S	118.1 E
T-4	16:37:39	29.6 S	127.2 E
T-2	16:42:16	16.1 S	140.4 E
T-1	16:52:44	16.7 N	166.2 E

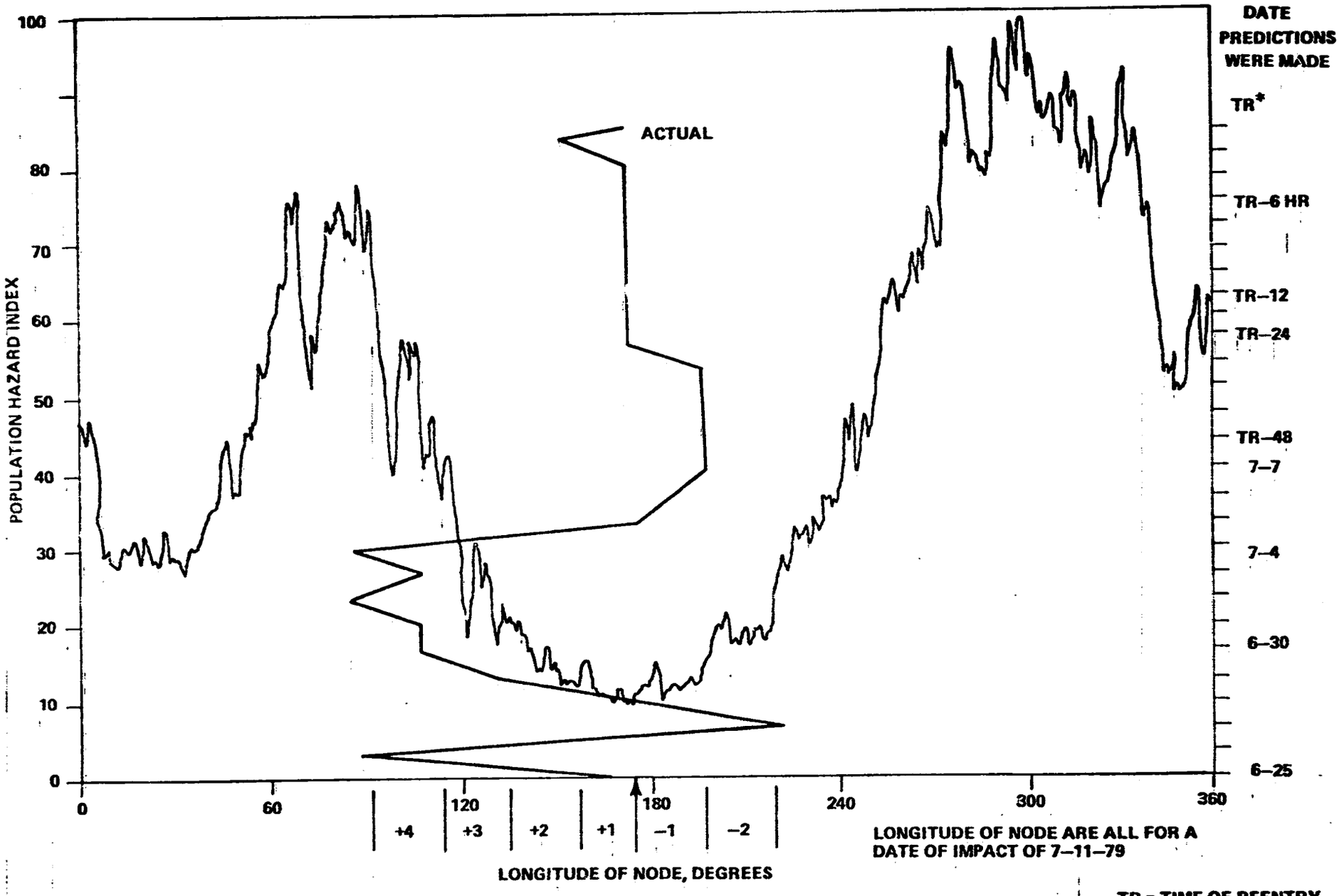

FIGURE 9-1 POPULATION HAZARD (AND PREDICTED LONGITUDE OF ASCENDING NODES)

data, note that a 22.2 degree delta in node results in a shift of one revolution or about 88 minutes. On the right is shown the date that the predictions were made starting with June 25, 1979. All cases predicted the impact revolution to be on July 11, 1979 but varied from +4 to -2 revolutions until the predictions made on July 5 and subsequent at which time they were within ±1 revolution. The impact prediction was essentially on the correct revolution from T-24 hours on. This corresponded to the "best" possible revolution of impact denoted by a low hazard index. The hazard index is the ratio of the total population beneath a certain orbit to that lying beneath the revolution of maximum population.

Figure 9-2 shows the impact predictions based on the baseline 75 n.m. tumble and the predictions that resulted from the decision to tumble early (81 n.m.) for the T-24 hour, T-18 hour, and T-12 hour vectors. As shown in figure 9-2, the predicted impact points for the baseline 75 n.m. tumble (with uncertainty) trended toward the U.S. and Canada. These data points are indicated by circles and spread from the Pacific Ocean (10 min from the west coast) to points just off the east coast (about 5 min from the east coast). Taking into account the debris footprint (3500 n.m. behind these points), this indicated a relatively large population area had a high probability of being impacted by Skylab debris. After the planned maneuver, the impact area (shown by dots) was shifted to the Indian Ocean (T-24, T-18,T-12) with a slight probability of an Australian impact. Additionally, the population density over that portion of Australia was very low indicating that if an overshoot occurred there would be very little risk to the population.

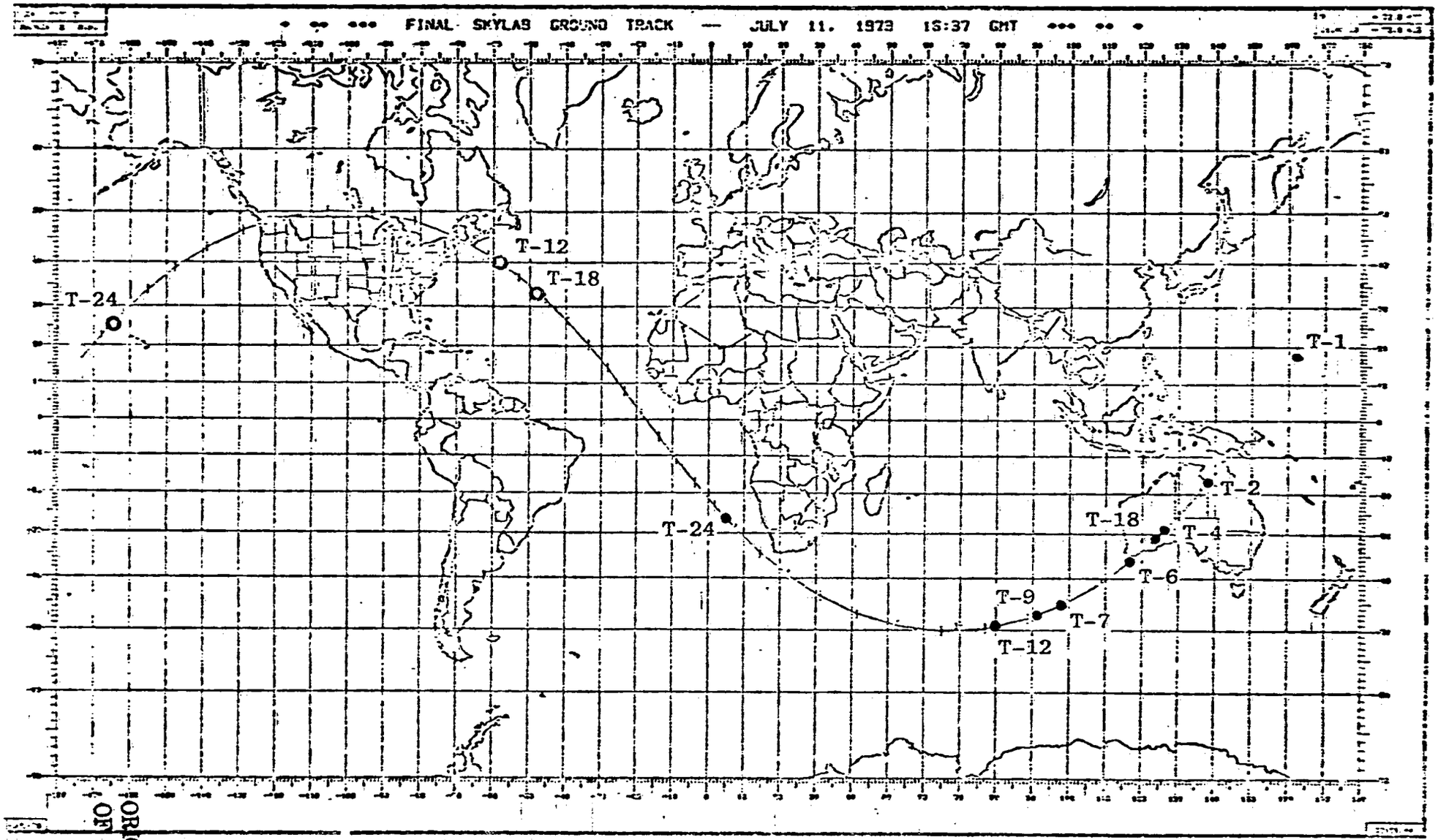

FIGURE 9-2
MAP OF REAL TIME RESULTS OF IMPACT PREDICTION

o Predictions Assuming Tumble at 75 nmi (Induced Tumble at 11:35 GMT) Before Decision To Tumble at 8:00 GMT

● Predictions After Decision to Tumble at 8 hrs GMT (81 nmi)

9.2 POST FLIGHT ANALYSIS

9.2.1 Reconstruction Procedures

Data has been analyzed to reconstruct a best estimate of what actually occurred based on observations after the decision was made to tumble at 81 n.m. and what possibly would have occured if the tumble had been postponed until the 75 n.m. altitude had been reached. The reconstruction procedure for Skylab decay was complex due to the extreme sensitivity that very small deviations in the observed data has on moving the impact point by a large amount. The data (and uncertainty) and sources used for this analysis were as follows:

o Actual Solar Data (±25%)	NOAA
o State Vectors Based on Tracking (+2 n.m.)	NORAD
o Special Altitude/Time Observations	NORAD
o Range/Elevation, Telemetry (±2 n.m)	Ascension Tracking Site
o Time of Tumble	NASA
o Predicted Aerodynamics and Breakup Sequence	NASA

Small uncertainties were associated with the preceding data. For example, the actual solar data was an estimate by NOAA of the final solar data which was not available at the time the analysis was done. If the data changed by 5% a three to five minute change in the impact time could occur. Another example would be to consider the state vector as being off slightly (2 n.m.) in altitude then up to a 10 minute variation in impact time could occur, similarly with the special observation and range/elevation data. Further in the case of the T-24 hour prediction, a 1% variation in predicted aerodynamics or breakup altitude could easily change the impact point by up to 10 minutes. Finally, it was impossible to separate these errors; therefore, no single data base will give the same impact points

when run from each of the different state vectors. The analysis was based on the following assumptions;

- Use of estimated solar data
- The altitude history as observed should fit reasonably well with the reconstructed predictions.
- All orbital workshop (OWS) solar array system (SAS) arrays were intact at Bermuda.
- The OWS SAS arrays were broken before Acquisition of Signal at Ascension.

The Skylab breakup scenerio was as follows:

- The OWS SAS array (aerodynamically) off at 62 n.m.
- The ATM separates from the remaining OWS at 54 n.m.
- ATM SAS arrays separate from the vehicle between 54 to 50 n.m.
- ATM and OWS break up at 42 n.m.

9.2.2 Results

An analysis was conducted to determine the drag and related BC of each of the attitude configuration "nominal" impact points required to match the observed data. First, however, the effect of the revised breakup sequence was evaluated. Figure 9-3 depicts the rationale for this analysis. The upper portion is the timeline showing the times when the NORAD vectors were obtained. There are three attitude configurations which had to be considered: high drag T121P, tumble, and breakup. Any time/impact predictions based on vectors from T-24 to T-9 required BC's for all three configurations. However, from T-7 to T-1 , only tumble and breakup needed to be considered. The T-7 hour case was selected and the effect of the revised breakup sequence was determined, this moved the impact point uprange. The tumble drag coefficient was varied to adjust the T-7 hour impact point to the actual impact point. This required a reduction in the tumble drag coefficient of about 4%. To check the breakup sequence further, these results were used for the sequence and the drag coefficient assumptions for each element. The results of these cases are shown in Figure 9-4 denoted by solid dots. As expected, these two cases moved closer to each other than had been estimated from real time results (Figure 9-2). The T-7 hour vector moved downrange from the Indian Ocean to close to the actual impact point, and the T-1 hour vector moved uprange from an impact north of the equator to the northeast tip of Australia. This indicated that the revised estimate of the tumble drag coefficient and the revised breakup sequence fit quite well.

Having dealt with the tumble and breakup sequence, all that remained was to adjust the T121P high drag coefficient. Using the T-12 hour vector, the drag coefficient was reduced by 1/2%. These results are shown in Figure 9-4 again resulting in a impact extremely close to the actual impact point for the T-12 hour vector and comparing favorably with all other vectors. The effects of these analysis can be compared with the real time results shown in Figure 9-2. Since the T-7 hour vector prediction provided the best correlation of the analysis to the observed data, the baseline impact point was derived with the T-7 hour vector resulting in the following:

Time of Impact - 16:37:28 GMT
Latitude - 30 Deg South
Longitude - 132 Deg East

NORAD VECTOR DESIGNATIONS

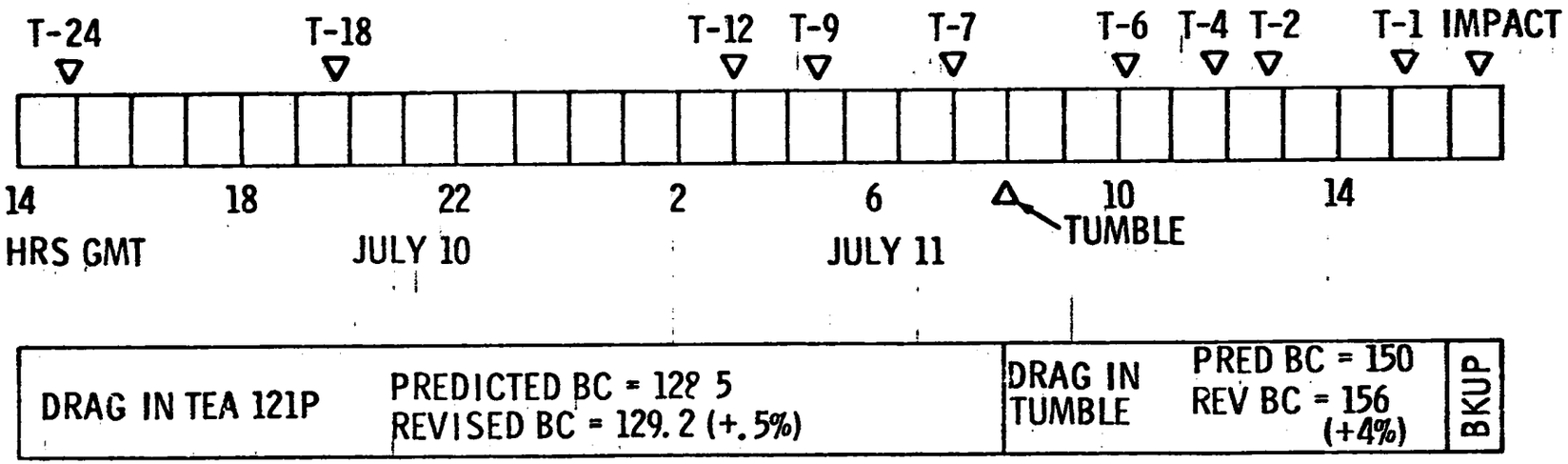

DRAG CONFIGURATIONS

FIGURE 9-3
DRAG/ATTITUDE TIMELINE

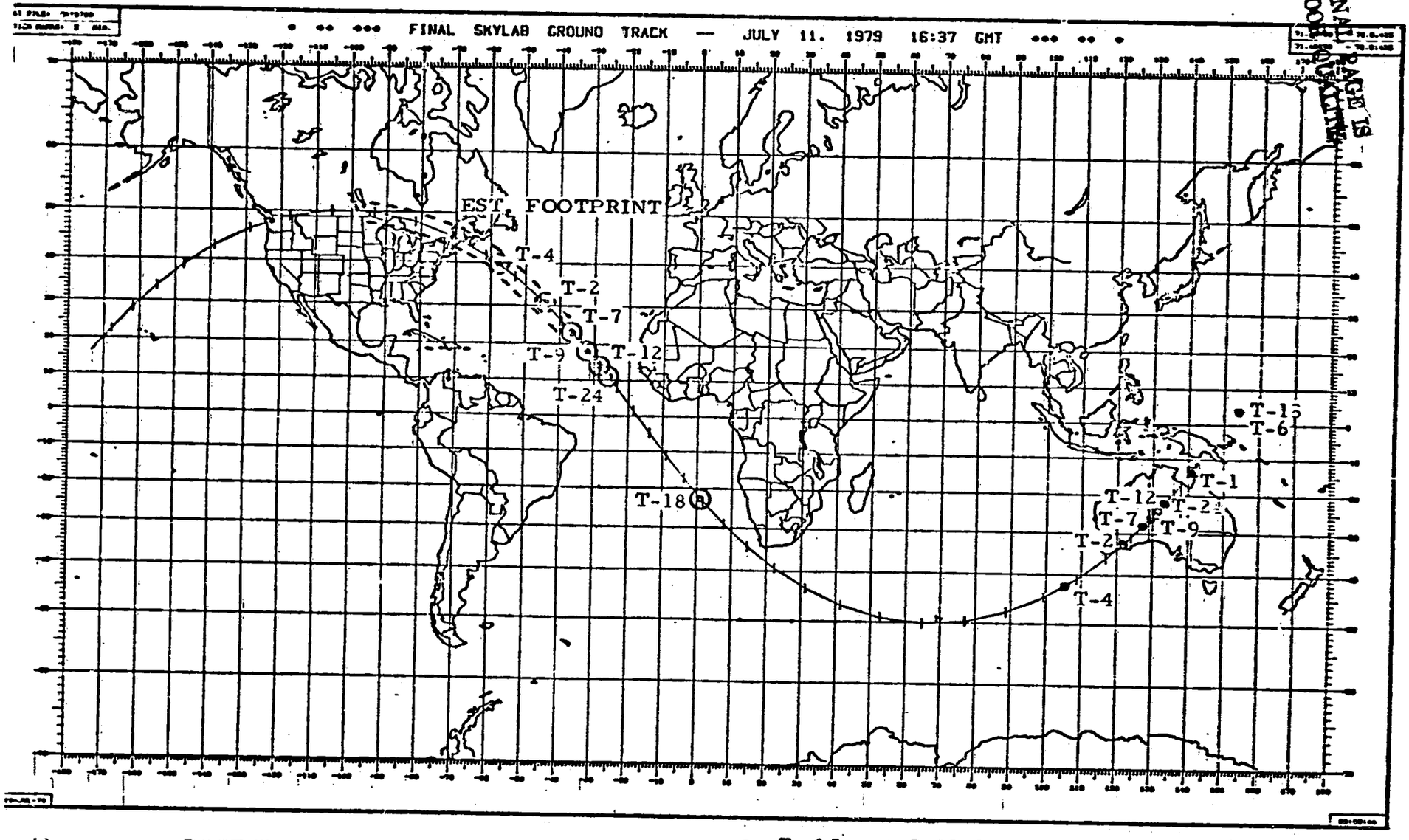

POST FLIGHT RECONSTRUCTION
FIGURE 9-4
MAP OF POST FLIGHT RESULTS RECONSTRUCTED IMPACTS

● Tumble at 8:00 GMT (81 nmi)
⊖ Tumble at 11:35 GMT (75 nmi)
⊛ Estimated Reconstruction at 11:35 GMT (75 nmi)

As is seen from Figure 9-4 denoted by solid dots, the entire set of reconstructed predictions fall within a quarter revolution of each other. The altitude fit is shown in Figure 9-5 for three vectors, T-24, T-12, and T-9. The data was very close to the observed altitude.

The last set of data generated shows where the impact points would have been for the T-24, T-12, and T-9 state vectors if the baseline 75 n.m. (11:35 GMT) tumble had been initiated. These results are shown as clear circles on the ground track in Figure 9-4. These reconstructions of the planned 75 n.m. tumble now appear to center about a latitude of approximately 18 degrees north. Also shown are estimates of where the T-2, T-4 hour impact predicitons would have been. As can be seen the predictions are as far uprange as about 46 degrees north latitude. With the extrapolation of the debris footprint this shows that a significant probability of a United States/Canadian impact still existed after the reconstruction. The reconstructed T-7 hour impact prediction and the estimated T-2 and T-4 hour cases all show significant amounts of debris in the United States and Canada. These results are all well within the estimated uncertainty of + 1/4 of a revolution. The primary cause of Skylab impacting down range from the nominal impact point was due to the less than expected drag experienced by the vehicle (4% less) during its tumble phase. The lack of this knowledge resulted in the planned time to tumble being earlier than required. In real time it was felt that drag predictions should be accurate to within +5%. In the actual case the drag was predicted to be within 4% of what it actually was. Based on real time data, the decision to tumble at 81 n.m. in leiu of waiting until 75 n.m. was correct when the accuracy of the data used in making the decision was considered.

9.3 IMPACT FOOTPRINT ANALYSIS

Figures 9-6 and 9-7 show preliminary results of the footprint analysis of Skylab debris. This analysis was based on the following data:

1. Special Pert Vector at T-2 hr.
2. Altitude at Ascension overflight = 57 n.m. (elevation, range derived)
3. OWS arrays still attached but aerodynamically off (i.e. folded back or dangling at 62 n.m.; all arrays off at 54 n.m.)
4. Special altitude observations by NORAD
5. Location of pieces in Australia

    a. Oxygen Tanks at 31.15 degrees South, 125.3 degrees East.

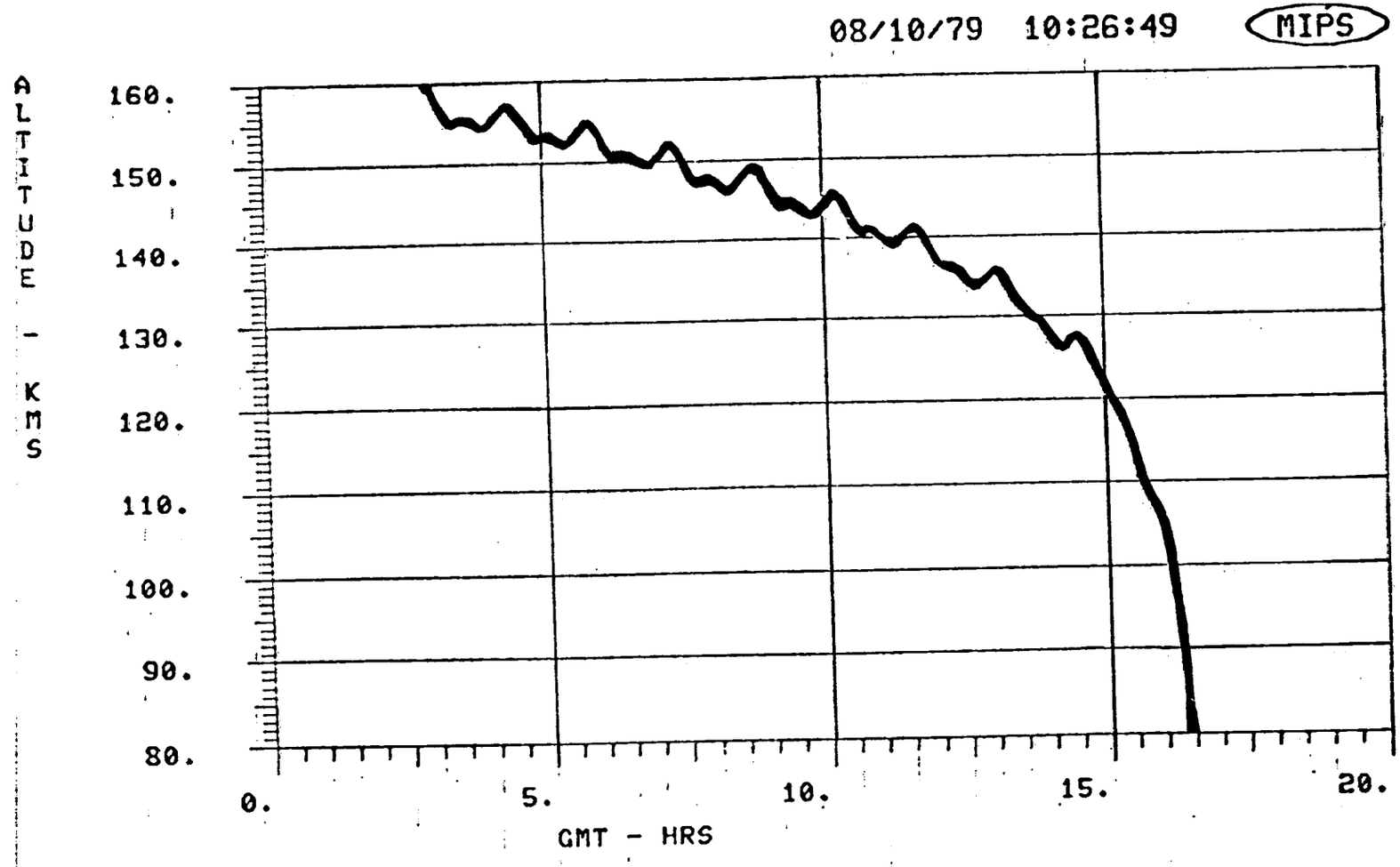

o VECTOPS AT T-24, T-12, T-9,

FIGURE 9-5 RECONSTRUCTED ALTITUDE PROFILE

b. Water Tanks at 33.8 degrees South, 122.05 degrees East
c. Heat Exchangers at 33.75 degrees South, 122.1 degrees East

As shown in Figure 9-6, this footprint extends from 46.9 degrees South 94.4 degrees east to 26.0 degrees South, 131.2 degrees East (about 2140 n.m.). Figure 9-7 provides additional detail of the footprint showing the location of pieces which were found and identifying where major elements are predicted to be located. The OWS/Cluster and AM pieces are centered around 32 degrees South, 124 degrees East, and the ATM pieces are predicted to be centered around 28.5 degrees South, 128.5 degrees East. The observed impact footprint compared favorably to that predicted at the T-2 and T-4 hour impact predictions times and was within ±1/4 orbit of all predictions made from 18 hours to one hour prior to impact.

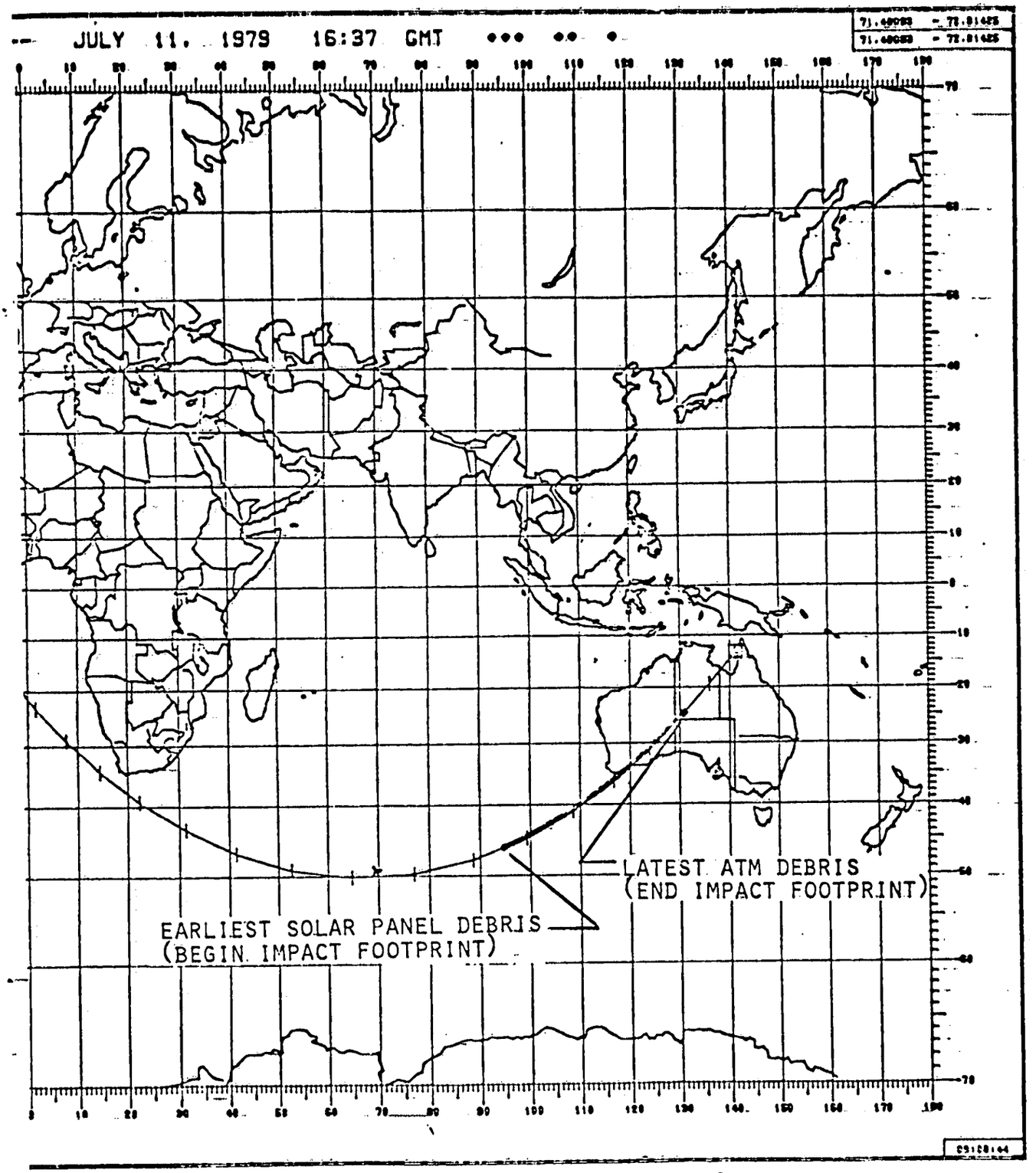

46.9°S, 94.4°E TO 26°S, 131.1°E

2140 NMI (2450 STATUTE MI)

ARRAYS OFF AT 54 NMI

MAP OF FOOTPRINT

FIGURE 9-6

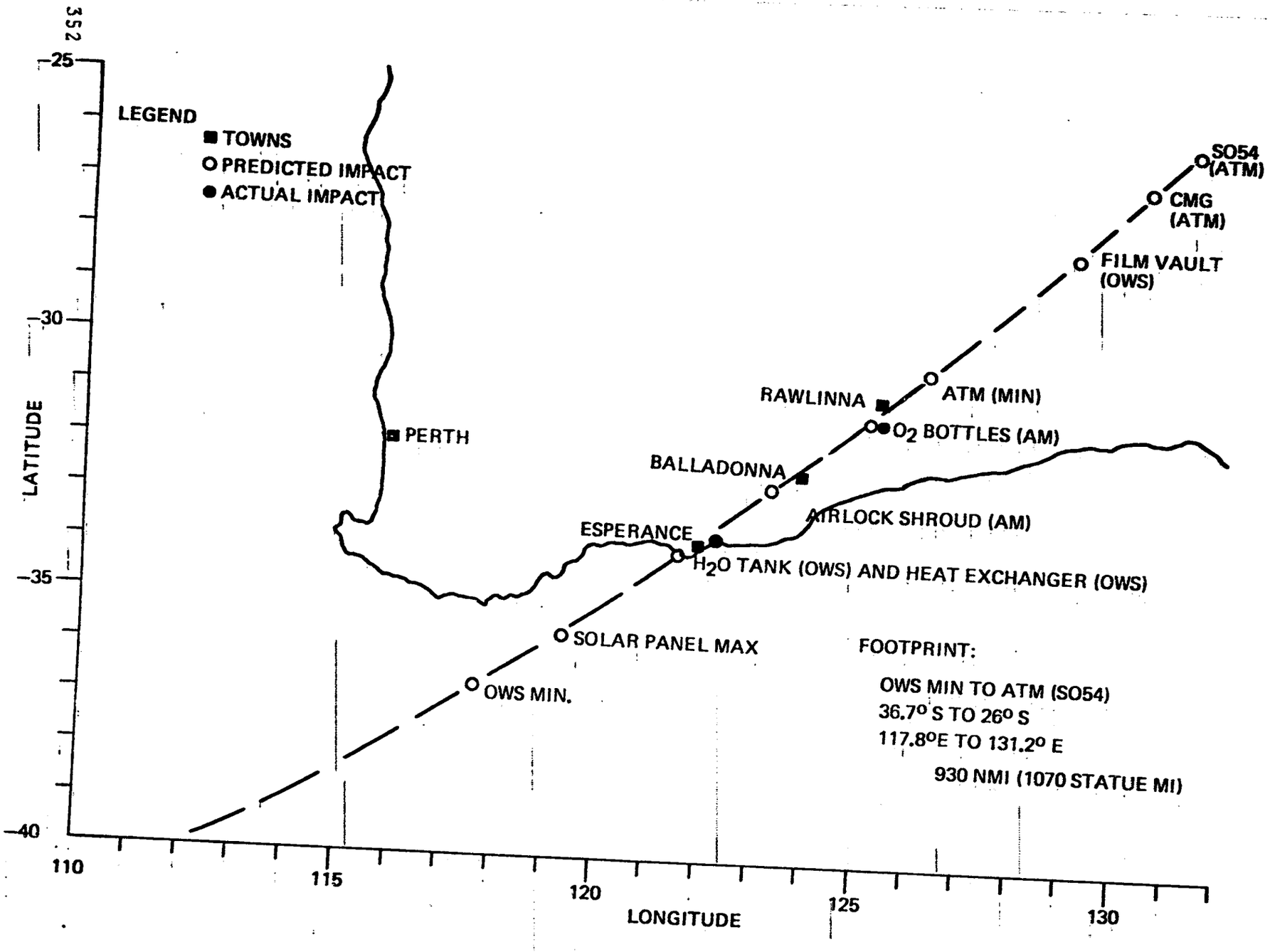

FIGURE 9-7 DETAILED MAP OF FOOTPRINT

10.0 MISSION OPERATIONS

10.1 INTRODUCTION

Skylab systems needed constant attention if the reactivation mission was to be successful. In order to accomplish this, frequent communication with the vehicle was necessary in order to check the status of onboard systems, and to reconfigure and/or modify their operation as required. In order to accomplish this, a mission control center was established at the L. B. Johnson Space Center (JSC) in Houston, Texas, and a mission support center at the Marshall Space Flight Center in Huntsville, Alabama.

In addition, since mission support computer programs at MSFC were already predicting Skylab's decay, which essentially involved predicting orbital parameters, it was logical that this capability be extended to provide mission operation tracking site coverage and navigation update data to flight controllers at both MSFC and JSC.

10.2 OPERATION

The JSC operation center was manned 24 hours per day, seven days a week, from June 1978 until splashdown July 11, 1979. The MSFC support center was manned in a similar manner except for a period from the February 1, 1979, to May 13, 1979, when the vehicle was under SI control and only normal working hour support was required from MSFC.

Each operation center had CRT displays of pre-selected data on special formats. Two consoles monitored guidance and navigation data at JSC while one console monitored this data at MSFC. The data was hardcopied off the displays and used to determine the health of the various systems. In addition, the displayed data contained ATMDC command data such that computer commands could be checked in realtime before being executed into the computer software. Figures 10-1, 10-2, 10-3, and 10-4 are typical guidance control and navigation data displays. In addition to these displays, JSC had one console to monitor vehicle power and one console to monitor the vehicle command and telemetry system, while MSFC had one console whose prime responsibility was to monitor both the power and communication systems of Skylab. Typical CRT displays of this data are shown in figures 10-5 and 10-6.

```
31-OCT-78 13:14:26  AM/ATM BLOCKS          50/    567  AM/ATM/ATMDC  / /    ACN
  GYRO  X        Y        Z        MODE   RSDP GMT 304:13:14:23.24          DIR
RT 1 -0.0041  0.0509  0.0107    SI       MT A/B  39:19:12:59.53    1        0
RT 2 -0.0042  0.0517  0.0105    EP         TGMT 140: 1:49:33.25    2      101
RT 3 -0.0042  0.0510  0.0107    ZLV *  TIME REL  39:19:13: 0.00    3        0
WARN          CS GN    FN GN *  STBY   MAN TIME      0:10: 0      4    64020
                                AH T   ELP MAN TIME  0:10: 0      6        0
INT1  -3.886 -14.064  28.827    AH C                          QVA ELEMENT 7      210
INT2  -3.719 -14.064  28.771          CMD WORDS      1  0.0002E-5    DOR
INT3  -3.914 -14.148  28.827        CURRENT 07777    2 -0.0009E-5  1 100000
RGBCON1     401 RGBCON2    1     SWD   WD 1    0     3 -0.0007E-5  2    452
  CMG     2       3           ADDR 0096  WD 2  226    4 -0.9994E-5  3  64104
BRG 1T  105      78             LOC 01C7  WD 3    0                  4  51410
BRG 2T  104      75     IA TEMP          WD 4 2004     QVI ELEMENT 5     52
PHSE A 1.052 1.052    1   83           CNTR 0006    1 -0.0088E-5  6  40000
PHSE B 1.068 1.080    2   82        ILL  ILL  UND DC 2  0.1077E-5  7      0
PHSE C 1.065 1.089    3   61         DATA MODE CMD REJ 3  0.0238E-5    SW
WH SPD   8849         ALRT       ERR                  4  0.9940E-5  1 103300
IGA        -4   -24   WARN       TMID  140: 1: 3: 7.50             2  55500
OGA        23    18   SHTDN EN   DMID      1:32: 2.50  S/O MODE    3   4200
      CMBCON  170161              LAMBDA Y  251.37      AUTO *      4  10050
CMG MOM     CMG RM   2     3        ETA Y  324.64       PRI *      5   1000
 X    -3     RCIT     0     0  SINE ETA X -.28646       SEC   NU ZE   -3.94
 Y    41     GSDT     0     0        RHO   69.74       ATEMP   88    ALERT
 Z    13     VREF      18  10.05  GAMMA Y  217.36       WTEMP   52    6666
13:13:37 141 MESSAGE BLOCK COUNT EQUALS 2 - BLOCK DISCARDED
I/A COMMANDS: ENTER NEW DISPLAY FORMAT NUMBER OR ZERO TO TERMINATE.  -1 -
```

FIGURE 10-1 GUIDANCE AND CONTROL DISPLAY FORMAT 1

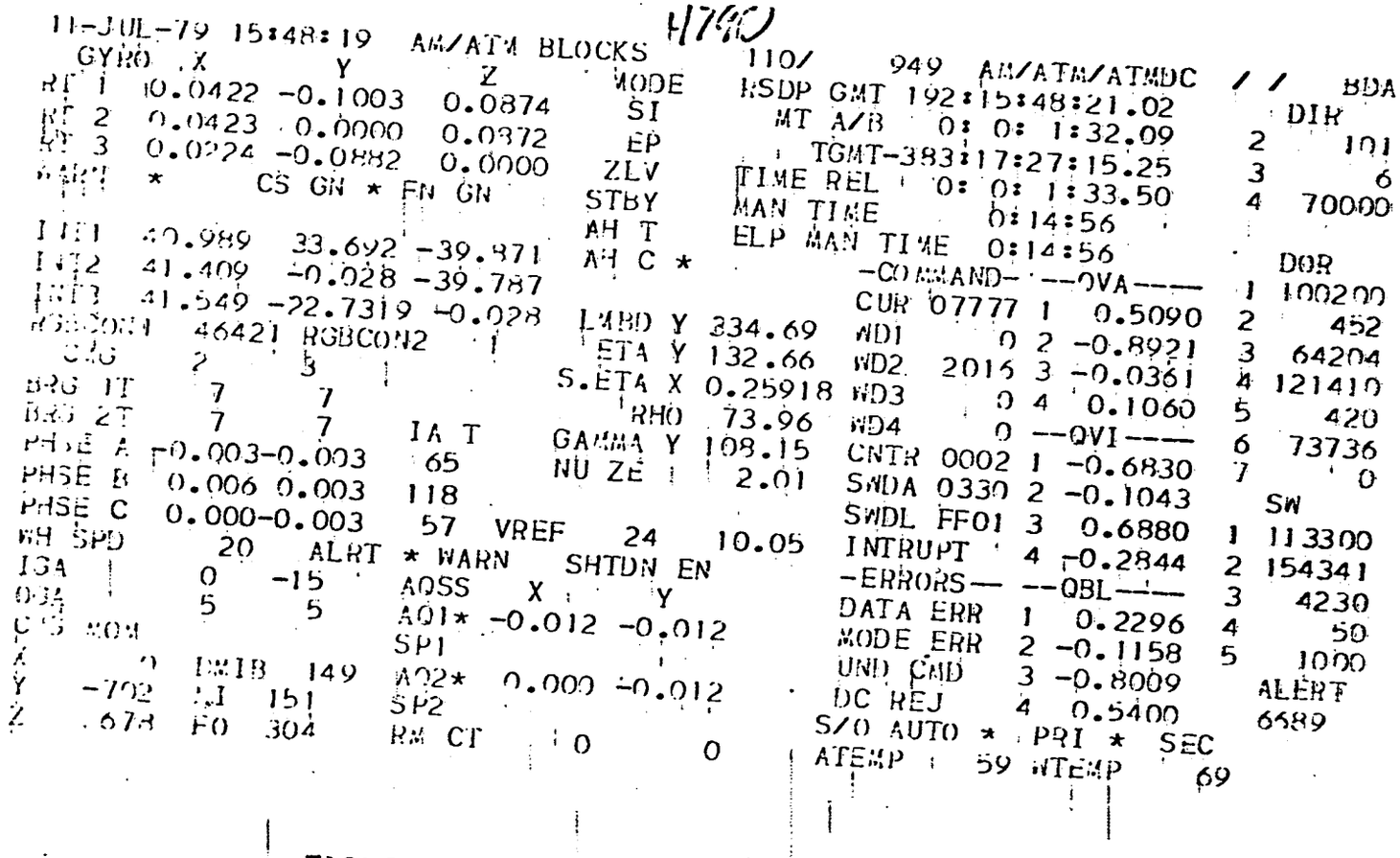

FIGURE 10-2 GUIDANCE AND CONTROL DISPLAY FORMAT 2

14-2

```
31-OCT-78 21:13:13   AM/ATM BLOCKS      72/     996  AM/ATM/ATMDC  / /   BDA
                                  GNS/ASCO 3      RSDP TIME  304:21:13:10.75

ETL11 EZ 0.01562500                    DELTA 04  0.9999396801
   21    2.32812500
   31 EX 0.0625000                          EA  -0.00781250

ETL12 EX 0.01562500                         ER  -0.01171875
   22    2.62500000
   32 EZ 0.0351562                     ETA ZM   -2.6367187 DEG

ETL13 -EZ 0.02343750                   ETA XN  -27.82286072 DEG
   23    2.31250000
   33 EX 0.0351562                          YN  -1.88415527 DEG

ETL14 -EX 0.04687500                        ZN   0.7910154 DEG
   24    2.62890625                  DELTA 01  -0.0012207031
   34 -EZ 0.0468750                  DELTA 02  -0.0006713867
                                     DELTA 03  -0.0008544922
CMG 2 OGR DC -0.137                CMG 2 IGR DC -0.021
    3 OGR DC  0.041                    3 IGR DC  0.171
ETA YC       0.07141108            ETA Y     0.52185017
ETN          2.50000000
```

FIGURE 10-3 EOVV CONTROL DISPLAY FORMAT 3

4238

```
31-MAY-79 21:10:59   AM/ATM BLOCKS      184/    1972  AM/ATM/ATMDC  / D@  ACN
                     TEA CONTROL PARAMETERS           RSDP GMT 151:21:10:56.48
               X            Y            Z                 TMID 352:  8:23:53.50
DELTA E     -0.000000    0.000000     0.000000             DMID        1:30:14.25
DELTA EP    -0.000000    0.000000     0.000000             TGMT 352:  9:47:58.00
                                                              DELTA T  TEA   -56
DELTA PH     0.873047    0.849365     0.000000
DELTA TH     0.000000    0.000000     0.873047             BUS 11  0
                                                      TEMP      12  0   -COMMAND-
ETSF        -0.546875    0.671875     0.585937          1   81  21  0   CUR 07777
                                                        5   23  22  0   WD1   1014
CMG MOM        -18          22           20             9   12  31  0   WD2   1003
                                                       13   43  32  0   WD3   1013
          -----CMG 2---    -----CMG 3---               17   68  41  0   WD4   2024
IGA IGR    28   0.0068     24   0.0068                 21   18  42  0   CNTR  0006
OGA OGR     6  -0.0137     11   0.0068        PRESS 1  226  51  0   SWDA  0096
WH SPD   8798                                       2  225  52  0   SWDL  01C7
          DMIB    0   MIB   2633  JET 123456  TEMP  1  117  61  0  INTRUPT  *0
                      F0    302                     2  -48  62  0   -ERRORS--
                                                                    DATA ERR
OBL  -0.0407104  -0.3272705   0.9414062   0.0615234                 MODE ERR
QVA   0.0021362   0.0217285  -0.0123901  -0.9996923                 UND CMD
QVI   0.0021362   0.0216674  -0.0123291  -0.9996923                 DC REJ
```

FIGURE 10-4 TEA CONTROL DISPLAY FORMAT 4

```
23-MAR-79 16:43:45  AM/ATM BLOCKS 3673    60      628  AM/ATM/ATMDC  / /  ***ACN
GMT    82:16:43:4316:43:24       EGIL/INCO
--BUS  20:12:32:31MPS--  ---SAS VOLTS--  ----BAT VOLTS---  --CBRM REG AMPS---
REG 1  29.3 REG 1  -0.2 1    69  5   70 1  24.9  5  39.5 1   2.7   10   3.2
REG 2  25  1REG 2  51 -1.0  76.66    1.6  41.-0.5  3  372     35   11   0.5
AM 1   29  0AM 1    5  6.6  -0.57    3.0  27.-0.5  2  374     25   12 -51.7
AM 2    0.54AM 2   12.6 50  .7 508   0.1  27.-0.5  2 -65      15   13 -50.2
EPS 1   0.01EPS 1   1.7 ---SAS AMPS--0.5---BA 1.2PS-  346  1  39   14   6.4
EPS 2   0.13EPS 2   1  9.5  -2.15  3 1.3  -0. 1.5  -  407     37   15   0.9
XFR 1   0.38XFR 1  15 39.2  39.16  2 1.5  -0. 0.1  -  338     -8   16.-48.6
XFR 2  35CLSXFR 2  17  9.7  10.17  221.5  -9. 0.1  -  389     -7   18 -41.8
ATM 1  29CLSATM 1   6. 0.1 137.38  5.9 4  -9. 5.3  -9.7        37
APCS 1 29CLSATM 2   1.8 ----------AMPS-------CBRM BAT--------VOLTS------
TM 1   29CLS---TEMPS---  1   0.1 8   -0.1 13  -0.1    1 34.4 8  34.6 13 34.5
                         1  0   0 FWD                 -3
-------AM---------       2  5   0     AFT              9              COMPUTER ENA
D1/S     PRI                -DCS-AVP-RCDR-                           CSTR THRM ENA
  D2 ON  SEC            1  -78              -5 DSIU    6                 TLM INH
STUB     CRDU VAL      2  -90              -3 ASAP    11                PWR INH
-TEMP--      40620                                                      ACS INH
 A2  20   --DCS--      ---------K198----------                  --SW SELECTOR--
                                                                  1 2 3
A10  56   1/1 -97     -ENBL-   ---DATA----  ER      ZERO IND 1 0 0
B10  -1    /2 -96              111111111111        REG TEST 0 0 0
C10  -1   2/1 -99.     1234-D  111987654321
           /2 -99          C  210
16:42:40 141 MESSAGE BLOCK COUNT EQUALS 2 - BLOCK DISCARDED
I/A COMMANDS: ENTER NEW DISPLAY FORMAT NUMBER OR ZERO TO TERMINATE.  -  -C
```

FIGURE 10-5 ELECTRICAL/COMMUNICATIONS DISPLAY FORMAT 1

```
26-MAR-79 14:07:56  AM/ATM BLOCKS 3685                44/     612  AM/ATM/ATMDC  /  /    GDS
GMT  85:14: 7:51                    EGIL/INCO
--BUS VOLTS--BUS AMPS--  ---SAS VOLTS---  ----BAT VOLTS---  --CBRM REG AMPS---
REG 1   29.3 REG 1  -1.0 1    94  5   94 1   24.9  5  39.0 1    2.9   10   4.1
REG 2   29.4 REG 2  53.4 2    94  6   81 2   40.0  6  42.8 2    3.1   11  14.3
AM 1    29.4 AM 1    5.4 3    94  7   81 3   38.8  7  42.6 4    0.0   12  13.6
AM 2    29.6 AM 2   13.0 4    94  8   94 4   39.6  8  37.2 5    0.1   13   2.5
EPS 1   29.1 EPS 1   1.7 ---SAS AMPS---  ----BAT AMPS----  6   15.3   14   3.0
EPS 2   29.1 EPS 2   1.6 1  50.0  5  3.0 1  -0.1  5  -0.1 7    2.3   15   0.0
XFR 1   29.5 XFR 1  16.1 2   3.3  6 10.3 2  -0.1  6   9.9 8    2.7   16   0.0
XFR 2   29.6 XFR 2  18.5 3   3.8  7 12.6 3  -0.1  7  10.0 9    3.4   18   4.4
ATM 1   29.3 ATM 1   8.0 4   2.1  8  2.7 4  -0.1  8  -0.1
APCS 1  29.4 ATM 2   6.6 ----------AMPS-------CBRM BAT--------VOLTS-------
TM 1    29.1 ---TEMPS---  1  15.6 8   15.4 13  15.1   1 35.7 8  36.0 13 35.9
LOG 1   23.6 CONV 2   77 2  10.8 9   15.2 14  15.4   2 34.8 9  35.7 14 35.7
EXP 1   23.6 REG 6    90 4  -0.1 10 -20.8P -0.10.2   4 16.2 10 36.1 15 16.3
ATM 2   29.2 REG 4    96 6 -21.0 11 -21.0 16  10.2   6 16.2 11 16.2 16 16.2
APCS 2  29.1 BAT 6    76 7  15.1 12 -21.0 18  13.5   7 35.7 12 16.1 18 35.3
-----------------AM-----------------------------------------ATM-------
    PWR  -1-DCS-2- VAL  --ANT----TEMP--  INC REF --ANT---INPUT- -TEMP-
PRI ON    -97   -99     D1/S     A2  60 1  0   0                    -4
SEC ON    -96   -70       D2 ON A10  54 2  5   0                    -3
            CRDU VAL STUB    B10  -1    -DCS-AVP-RCDR-   ----TEMP----
COAX 2              44224    C10  54 1  -78     RCD      0 DSIU    0
TR  17:20:36:24  K198  00000  7777     2  -79              0 ASAP    2
14:07:19 131 ACQUISITION STATUS BLOCK ENCOUNTERED
I/A COMMANDS: ENTER NEW DISPLAY FORMAT NUMBER OR ZERO TO TERMINATE.  -  -
```

FIGURE 10-6 ELECTRICAL/COMMUNICATIONS DISPLAY FORMAT 2

All commands to the vehicle originated at JSC and were sent verbally via one of the JSC flight controllers to a spacecraft command encoder (SCE) operator at one of the ground tracking stations. The SCE operator loaded and transmitted the commands to the vehicle in accordance with directions from the flight controllers. This command loop was monitored at MSFC in order that support personnel were able to keep aware of the various actions being telemetered to the vehicle.

The primary voice loop for data transfer and system operations discussion between JSC and MSFC was the Huntsville Operations Support Center (HOSC) voice loop. It was on this loop that the results of analysis of the various systems were passed on to JSC. In addition, this loop provided a means where planning and realtime emergency actions could be discussed prior to implementation.

10.3 OPERATIONAL SUPPORT

Operational support consisted of the generation and interpretation of data required to keep the Skylab functional. The availability of the various tracking stations, together with predicted acquisition of signal (AOS) and loss of signal (LOS) were generated for every Skylab orbit.

10.3.1 Tracking Station Coverage

A computer program was developed to produce a station coverage and orbital parameter chart commonly known as a circle chart, an example of which is shown in figure 10-7. A circle chart was produced for each of Skylab's orbits which contained at least one station pass. These charts were used in scheduling stations for navigation updates, power management, control parameter updates, and any other ground support functions which required communication with Skylab. Between twelve and fourteen thousand of these charts were produced during the Skylab reactivation mission.

Station coverage was especially important during attempts to change Skylab's attitude since these changes were initiated and monitored from the tracking stations. Also the various Skylab attitudes required constant monitoring and adjustments to keep the vehicle under control and the electrical power system adequately charged. For this reason a total of five tracking stations were used to give a minimum coverage of one station pass per orbit (figure 10-8). The stations which were used were Ascension, Bermuda, Goldstone, Madrid, and Santiago, Chile.

CIRCLE CHART

STATION ACQUISITION PERIODS FOR SKYLAB

TIME OF NORAD ELEMENT SET 11:42:31 GMT
7- 1-79

DATE	7- 2-79 (FIRST AOS)
ORBIT NUMBER	2
DAY NUMBER	183
BETA ANGLE	-24.7610 DEG

1 REV DELTA TIME	01:29:17.22	
ORBITAL MIDNIGHT	00:38:18.39	GMT
ORBITAL SUNRISE	00:56:19.68	
NIGHT TO DAY TERM	01:00:37.84	
ORBITAL NOON	01:22:57.30	
DAY TO NIGHT TERM	01:45:16.70	
ORBITAL SUNSET	01:49:34.22	
SI DUMP MIDNIGHT	02:04:40.07	
SUN SENSOR UPDATE	01:20:01.46	

STA	AOS	LOS	MAX ELV
GDS	01:36:30	01:43:11	9.6
AGO	01:56:40	02:04:41	56.7

TS2	00:57:42	TS6	01:42:20

EOVV SAMPLE TIMES

1 -	01:00:37
2 -	01:22:57
3 -	01:45:16
4 -	00:38:18

NOTE - ER SAMPLE VALID ONLY BETWEEN SAMPLE POINTS 1 & 2.

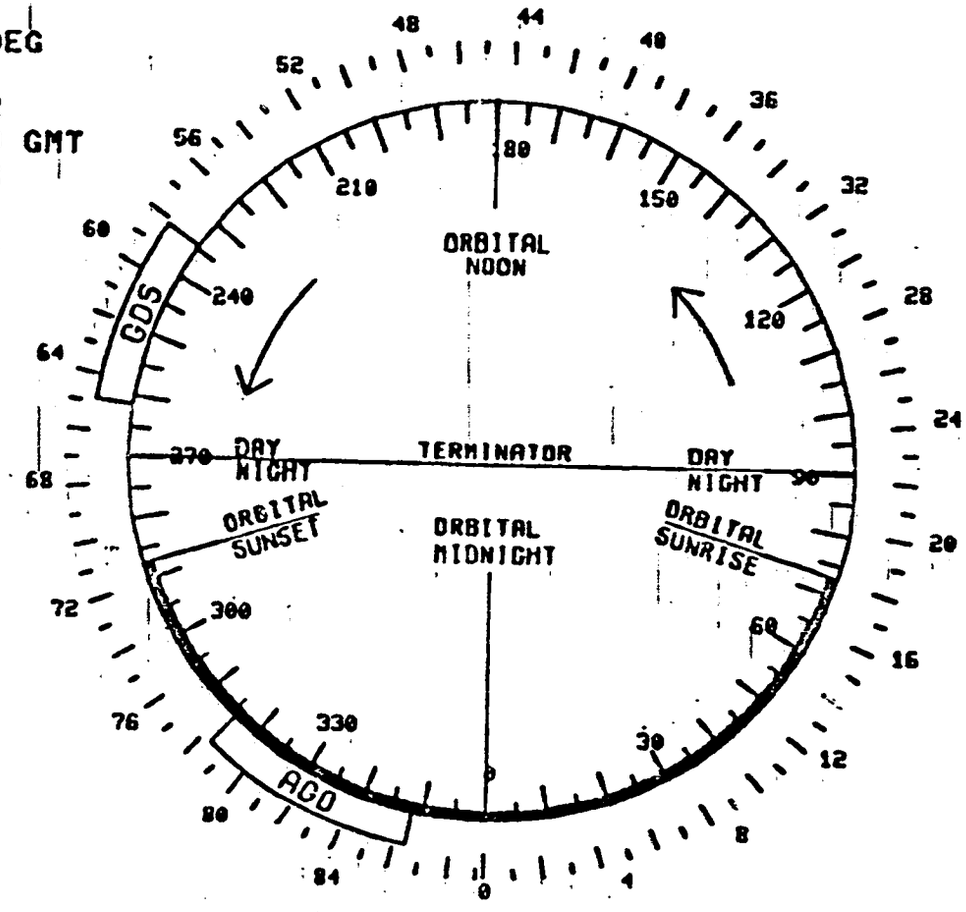

PROVIDED BY MSFC
SYS ANAL & INTEG LAB
MISSION ANAL DIV, EL-25

FIGURE 10-7 TYPICAL CIRCLE CHART

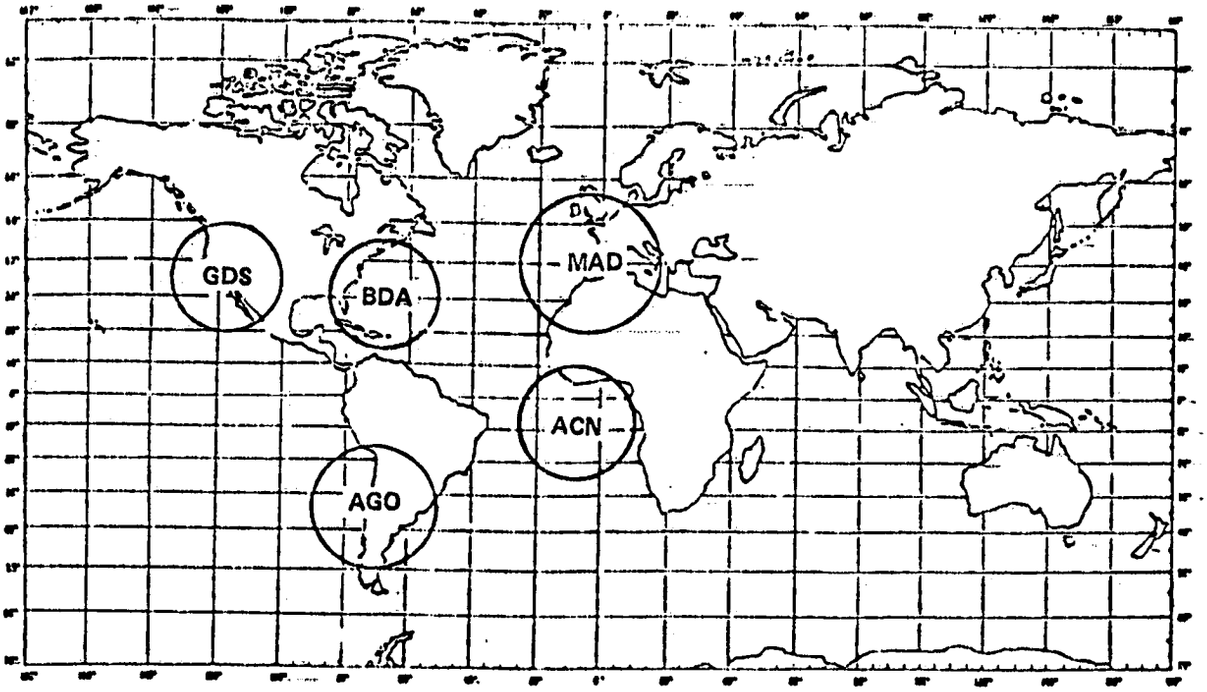

FIGURE 10-8 SKYLAB REACTIVATION MISSION STDN GROUND STATION COVERAGE

10.3.2 Navigation Updates

Navigation data was continually being generated and updated based on vehicle state vector information received from the North American Air Defense Command (NORAD). Updates were produced at specified times during critical mission periods and on an as needed basis at other times. A navigation update for Skylab meant that the actual time of orbital midnight (TMID) was being updated. This was required because orbital drag shifted TMID which was not modeled by the onboard computer. The actual TMID was required to maintain correct vehicle attitude. Techniques of biasing the orbital period were developed which allowed the navigation update to be done at reasonable time intervals. This was especially important near the end of the mission when navigation updates would have been needed every couple of orbits which would become difficult since station coverage was deteriorating rapidly due to Skylab's low orbital altitude.

Once it was determined that a navigation update was needed, a site was picked using the circle charts at which the update would be sent to the onboard computer. A Skylab tracking vector from NORAD was then projected forward in time to the midpoint of the pass over the chosen site. Figure 10-9 shows the data which was sent to the flight controllers at JSC who converted it to a form to be uplinked to the onboard computer. The flight controllers calculated a new TMID and a correction (DMID) to the onboard TMID and the DMID was actually uplinked to the computer.

10.3.3 Control Scheme and Power System Management Updates

Control scheme parameter updates were generated on off-line computers at MSFC and sent to JSC for implementation in the vehicle. Finally, power system data was carefully plotted for the various Skylab attitudes, and discussions between MSFC and JSC led to agreed upon battery, solar array, and voltage regulator configurations of the two vehicle power systems. Detailed system operational problems are discussed elsewhere in this document under their particular system section.

NAVIGATION UPDATE DATA

1. TIME OF NAV UPDATE: YR 79 MO 7 DY 2
   DAY 183 HR 02 MIN 00 SEC .00
2. SITE:AGO
3. AXIS 6617471.2
   ECCEN .00046094
   INCL 50.028511
4. ARG PER 253.73219
   RAN 28.28863
   MA 327.62411

   X -3044251.5
   Y -4825181.1
   Z -3347686.1
   XDOT 6290.7694
   YDOT -866.9284
   ZDOT -4467.2398

5. TMID BEFORE NAV UPDATE: DAY 183 HR 00 MIN 38 SEC 18.51
6. TMID AFTER NAV UPDATE: 183 : 02 : 07 : 35.28
7. TMID:
8. DMID:
9. GMT BEFORE PROPAGATION: 182 : 11 : 42 : 31.59
10. GMT AFTER PROPAGATION: 183 : 02 : 00 : .00
11. ATMDC ZERO SET:

FIGURE 10-9
TYPICAL NAVIGATION UPDATE

11.0 SUMMARY AND CONCLUSIONS

11.1 Conclusions

The performance of Skylab systems exceeded all expectations during the primary Skylab Mission and particularly during the Skylab Reactivation Mission. When Skylab reentry occurred on July 11, 1979, the Skylab systems had successfully supported 15960 hours (665 days) of powered flight operations of which 9432 hours (393 days) followed a 4 year and 30 day period of passive on-orbit storage. During both the primary and reactivation missions, many Skylab system were required to operate in modes never intended by its designers and to accomplish tasks dictated by unforeseen events.

The Skylab Reactivation Mission offered NASA a unique opportunity to evaluate complex power generation, mechanical, computer and environmental control systems after having been in a space environment for over six years. Further, these systems were in orbital storage for over four of the six years in a uncontrolled space environment before being reactivated in March of 1978. System degradation was determined to be minimal.

After Skylab control was regained in June of 1978 at an altitude of 218 nautical miles, it was essentially maintained under control to approximately 80 nautical miles before the vehicle was allowed to tumble. This permitted an opportunity to compare the predicted aerodynamic environment through which the vehicle transcended (218 n.m. to 80 n.m.) with the observed aerodynamics. Very little data of this type was available prior to the time of the Skylab transition. It is felt that this data will significantly increase the impact prediction accuracy of future space objects.

Finally, unique control schemes were developed (EOVV and TEA) which enabled Skylab to fly through the gravity gradient/aerodynamic torque transition region. Torque equilibrium points were discovered where gravity gradient and aerodynamic torques balanced. At these points very little vehicle control authority was required to maintain control. Moreover, vehicle orientations at these points were such that one could choose attitudes exhibiting high or low vehicle drag characteristics. By modulating between these orientations the rate of vehicle descent could be increased or decreased forcing it into an impact orbit which was characterized by a low population density.

REFERENCES

1. IBM Corporation, "Apollo Telescope Mount Digital Computer (ATMDC) Program Definition Document (PDD) Part I", IBM No. 70-207-0002, 10 May 1973.

2. GNS/ASCO, Skylab Reactivation Mission Rules, 22 May 1978.

3. IBM Corporation, "Design and Operational Assessment of Skylab ATMDC/WCIU Flight Hardware and Software," IBM No. 74W-00103, 9 May 1974.

4. Marshall Space Flight Center, "MSFC Skylab Attitude and Pointing Control System Mission Evaluation," NASA TM X-64817, July, 1974.

5. Marshall Space Flight Center, "MSFC Skylab Thruster Attitude Control System," NASA TM X-64852, July, 1974.

6. IBM Corporation, "Workshop System Simulator Description Document," IBM No. K10-70-141.

7. Marshall Space Flight Center, "Skylab Thermal and Environmental Control System Mission Evaluation Report," NASA TM X-64822, June 1974.

8. Marshall Space Flight Center, "Skylab Apollo Telescope Mount Summary Mission Report," NASA TM X-64815, June 1974.

9. Marshall Space Flight Center, "Skylab Appollo Telescope Mount Final Technical Report," NASA TM X-64811, June 1974.

10. Martin Marietta, ASTP/Skylab Alternate Mission, ED-2002-1735, June 1974.

11. Marshall Space Flight Center, "Skylab Electrical Power Systems Mission Evaluation Report," NASA TM X-64818, June 1974.

12. Marshall Space Flight Center, "Skylab Instrumentation and Communication System Mission Evaluation Report, NASA TM X-64819, June 1974.

13. Glaese, J.R. and Kennel, H.F., "Low Drag Attitude Control For Skylab Orbital Lifetime Extension," NASA TM (to be published) December 1979.

14. Glaese, J.R. and Kennel, H.F., "Torque Equilibrium Control For Skylab Reentry," NASA TM 78252, November 1979.

References (continued)

15. Kennel, H.F., "Angular Momentum Desaturation For Skylab Using Gravity Gradient Torques," NASA TM X-64628, December 7, 1971.

16. Marshall Space Flight Center, "Skylab Thermal and Environmental Control System Mission Evaluation," NASA TM X-64822, June 1974.

17. IBM Corporation, "Workshop System Simulator User's Manual," IBM No. 71-K10-046, 15 April 1971.

18. Glaese, J.R. and Kennel, H.F. "Torque Equilibrium Control For Skylab Reentry," NASA TM 78252, December 1979.

19. Garber, T.B., "Influence of Constant Disturbing Torques On the Motion of Gravity-Gradient Stabilized Satellites," AIAA Journal, Vol. 1, April 1963, pp. 968-969.

20. Nurre, G.S., "Effects of Aerodynamic Torque On an Asymmetric, Gravity-Stabilized Satellite," NASA TM X-53688, January 2, 1968.

21. Sperling, H.J., "Efeect of Gravitional and Aerodynamic Torques on a Rigid Skylab-Type Satellite," NASA TM X-64865, June 1, 1974.

22. Pack, H., "Vibration Data for the Skylab Cluster Less Command Service Module," NASA S&E-AERO-DD-8-71, Feb. 11, 1971.

23. Gyrofl, R. A., "Orbital Aerodynamic Data for the Updated Skylab I In-Orbit Configuration," Northrup Services Memo M-9230-73-197, July 11, 1973.

24. Pringle, R., "Bounds on the Librations of a Symmetrical Satellite," AIAA Journal, 1964, pp.908-912.

25. Meirovitch, L. and Wallace, F.B., "On the Effect of Aerodynamic and Gravity Gradient Torques on the Attitude Stability of Satellites," AIAA Journal, 1966, pp. 2196-2202.

26. Cochran, J.E., "Effects of Gravity-Gradient Torque On the Totational Motion of A Triaxial Satellite in a Precessing Elliptical Orbit," Celestial Mechanics, Vol.6, 1972, pp. 126-150.

27. Pringle, R., "Effect of Perturbed Orbital Motion on a Spinning Symmetrical Satellite," Journal of Spacecraft and Rockets, Vol. 11, 1974, pp. 451-455.

References (continued)

28. Thomson, W.T., "Spin Stabilization of Attitude Against Gravity Torque," Journal Astronautical Science, Vol. 9, 1962, pp.31-33.

29. Auelmann, R. R., "Regions of Libration for a Symmetriical Satellite," AIAA Journal, 1963, pp. 1445-1447.

30. Likins, P.W., "Stability of a Symmetrical Satellite in Attitudes Fixed In An Orbiting Reference Frame," Journal of Astronautical Sciences, Vol. XII, 1965, pp. 18-24.

31. Beletskii, V.N., "Motion of an Artificial Satellite About Its Center of Mass," TT F-425, NASA, 1966.

32. NASA Space Vehicle Design Criteria (1973): Models of Earth's Atmosphere (90 to 2500 km). NASA SP-8021, National Aeronautics and Space Administration, Washington, D.C.

33. Greenwood, D.T., "Principles of Dynamics," Prentice Hall, Inc., Englewood Cliffs, New Jersey, 1965, Chapter 8.

APPROVAL

SKYLAB REACTIVATION MISSION REPORT

by Systems Analysis and Integration Laboratory

The information in this report has been reviewed for technical content. Review of any information concerning Department of Defense or nuclear energy activities or programs has been made by the MSFC Security Classification Officer. This report, in its entirety, has been determined to be unclassified.

Herman E. Thomason
Director, Systems Analysis
and Integration Laboratory

U.S. GOVERNMENT PRINTING OFFICE: 1980 - 640-247/425 REGION NO. 4